Synthesis and characterisation of novel polymeric materials via living romp

Mason, Craig

SYNTHESIS AND CHARACTERISATION OF NOVEL POLYMERIC MATERIALS VIA LIVING ROMP

Craig Mason

A thesis submitted for the degree of Doctor of Philosophy at the University of Durham

September 2003

Abstract

A new series of dendronised monomers of different generations possessing different chemical structures has been designed, synthesised and characterised. Dendrons were initially synthesised in a stepwise manner from t-butanol, CDI and 1-[N, N-bis(2-hydroxyethyl)amino]-2-propanol (**HEAP**) and were then coupled to norbornene derivatives for the provision of dendronised monomers. In particular, mono- and di-substituted first generation and di-substituted second generation polycarbonate dendronised monomers containing t-butyl terminal groups have been synthesised. Two di-substituted second generation polyurethane dendronised monomers containing t-butyl and 4-heptyl terminal groups were also successfully synthesised.

Dendronised polymers have been synthesised from the NMR scale ring opening metathesis polymerisations of mono- and di-substituted first generation polycarbonate dendronised monomers along with a di-substituted second generation polycarbonate dendronised monomer, using varying ratios of monomer to initiator. It was found that the polymerisations were well-defined and that di-block copolymer products could be obtained due to the living nature of the systems.

Molecular modelling studies have been performed using the CAChe® 3.2 program on the di-substituted second generation polycarbonate dendronised monomer and on a dendronised polymer up to a degree of polymerisation of 16. It was found that low DP oligomers of the second generation polycarbonate dendronised monomer had an approximately spherical shape, which tended towards cylindrical as the DP increased. The polymer at a DP of 16 had dimensions of approximately 10 nm diameter by 4 nm thickness. AFM images were also obtained using a scanning probe microscope MultiMode^{TM} Nanoscope IV. The structures were found to be pancake shaped with dimensions of between 30-50 nm diameter and 3-6 nm thickness, which was approximately a factor of 3 greater than the dimensions calculated by molecular modelling. This discrepancy in size between the modelling studies and the AFM results is thought to arise from the effect that structure-solvent and structure-substrate interactions have on the overall conformation of the dendronised polymer when imaging by AFM.

Acknowledgements

I would first of all like to thank the people who have helped me to get to where I am today. These include teachers at Clyde Valley High School, who taught me the basics of core subjects that I still use today. Special thanks go to my English teacher Mrs Hope and my chemistry teachers Mr Deans and Mr Carrol.

I would like to thank the staff at Strathclyde University for helping me through my undergraduate degree and for teaching the subject of chemistry at a very high standard. I would also like to thank the University for giving me the opportunity to carry out an Industrial Placement in Belgium for one year, which not only improved my skills as a chemist but also broadened my life experiences at the same time. Special thanks go to Berend Eling (ICI) and Prof. Sherrington of Strathclyde University for developing me as a chemist and showing me how to successfully complete chemistry projects.

For my time at Durham, I would first of all like to thank Jim for further developing my skills as a chemist and for teaching me the many things that go hand-in-hand with being a chemist. Many thanks also go to Ezat for his supervision and for initially spending a lot of time with me in the laboratory teaching me all the techniques that I required throughout my PhD. I am also very grateful to Mark Wilson for helping me with the computer modelling studies. I would like to acknowledge all the support staff in Durham University: Alan Kenwright, Ian McKeag and Catherine Heffernan for the NMR service, Douglas Carswell and Lian Hutchings for SEC chromatograms, David Parker for MALDI-TOF analysis, Jaroslava Dostal for elemental analysis and Michael Jones for MS spectra. I would also like to thank the people in the IRC for making it such a friendly environment to work in.

Last but not least, I would like to thank my Mum, Dad and Brother for always being there for me no matter what, my Nanna for giving me all the encouragement and insight into life that I could possibly wish for, and to my other relatives for shaping me into what I am today. Finally, I would like to thank Jane, for making my life so enjoyable.

Memorandum

The work reported in this thesis has been carried out at the Interdisciplinary Research Centre in Polymer Science and Technology, Department of Chemistry, Durham University between October 2000 and September 2003. This work has not been submitted for any other degree either in Durham or elsewhere and is the original work of the author except where acknowledged by means of appropriate reference.

Statement of Copyright

Financial Support

I gratefully acknowledge the Engineering and Physical Sciences Research Council (EPSRC) and the Interdisciplinary Research Centre (IRC) for their generous funding.

Contents

Chapter 4: Molecular Modelling and AFM Studies

Chapter 5: Experimental

Abbreviations

approx.	approximate or approximately
br	broad
C_6H_{14}	hexane
$CDCl_3$	deuterated chloroform
CDI	1,1' carbonyl diimidazole
CD_3OD	deuterated methanol
$(CD_3)_2SO$	deuterated dimethylsulfoxide
cf.	compare
CH_2Cl_2	dichloromethane
d	doublet
dd	doublet of doublets
δ	chemical shift
Da	Daltons
DSC	differential scanning calorimetry
e.g.	for example
ES	electrospray
EtOAc	ethyl acetate
g	gram
G	generation
GPC	gel permeation chromatography
HEAP	1-[N,N-bis(2-hydroxyethyl)amino]-2-propanol
Hz	Hertz
i.e.	that is
J	coupling constant
KOH	potassium hydroxide
L	litre
NMR	nuclear magnetic resonance
m	multiplet
M	molar
MALDI-TOF	matrix-assisted laser-desorption ionisation – time of flight
mg	milligram

mL	millilitre
MS	mass spectrometry
M_w	molecular weight
m/z	mass to charge ratio
PAMAM	polyamidoamine
q	quartet
s	singlet
t	triplet
T_g	glass transition temperature

Chapter 1

Introduction

1.1 Overview

This thesis reports a study of the synthesis and characterisation of polymers carrying dendritic substituents. This chapter reviews the background science associated with the project. First, the syntheses of the two main types of macromolecule encountered in this area will be discussed briefly. This will provide background information concerning the dendrons whose synthesis and use will be described in chapter 2. The work to be reported relies heavily on the selectivity of reactions involving the coupling agent, 1,1'-carbonyl diimidazole (CDI), which will be described and exemplified. Following on from this will be a review of ring opening metathesis polymerisation (ROMP) and the development of initiators associated with the process. Finally, the emerging field of dendronised polymers will be highlighted with the main synthetic achievements being documented.

1.2 Dendrimers

1.2.1 Dendritic Macromolecules

Dendrimers and hyperbranched polymers are two classes of branched macromolecules that have attracted a lot of interest recently.[1] Dendrimers are usually defined as perfectly branched, monodisperse macromolecules, whereas their hyperbranched counterparts are irregularly branched structures that have varying degrees of branching and are polydisperse in size and structure.[2] Monomers of the type, AB_x, where x is greater than or equal to two, are used to form these structures, but the synthetic approach is different in the two cases.[3] Dendrimers are typically synthesised by a stepwise, repetitive sequence of a few reactions, often coupled with purification procedures, whereas hyperbranched polymers are prepared by a one-step polymerisation of an AB_x monomer. However, the more laborious and time-

consuming synthetic route required for dendrimers is rewarded as they often exhibit unique properties and can be created with predetermined, specific structures.[4-6]

The structure of a dendrimer has three distinct regions – the core, interior branching units and the terminal groups – these are shown in the two-dimensional schematic of *Figure 1.1*. The number of layers within a dendrimer is commonly described as the generation (G) of the structure; for example, the dendrimer shown is of the third generation.

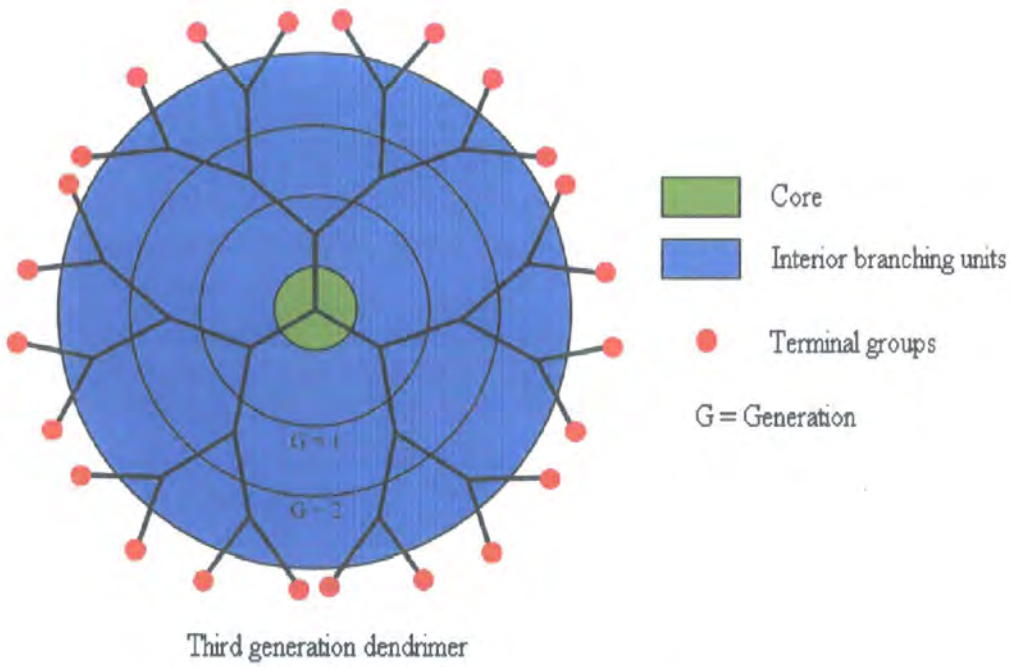

Figure 1.1 Schematic of a dendrimer

1.2.2 Synthesis of Dendrons and Dendrimers

Dendrimers are usually synthesised using a repetitive sequence of two reactions, comprising the addition of a monomer corresponding to a structural increase of one generation, followed by the deprotection/activation of functional groups. The activation of the groups allows repetition of the two reactions generating dendritic molecules of the next generation.

Two main synthetic strategies have been extensively employed in the synthesis of dendrimers over the past three decades.[2] The strategies differ in the direction in which the molecules are constructed and are termed accordingly as either the divergent route or the convergent route. The divergent route builds up the dendrimer, layer by layer, starting from a multifunctional core molecule diverging out

towards the periphery as shown in *Figure 1.2.* In the first step, an AB_x monomer (x = 2 in this case) containing protected B groups (B_p) reacts with a trifunctional core to yield a first generation dendrimer containing unreactive end groups. In the second step, deprotection or activation of these end groups forms a first generation dendrimer that is able to add the next layer. Repetition of these two steps results in the preparation of a second generation dendrimer with activated end groups.

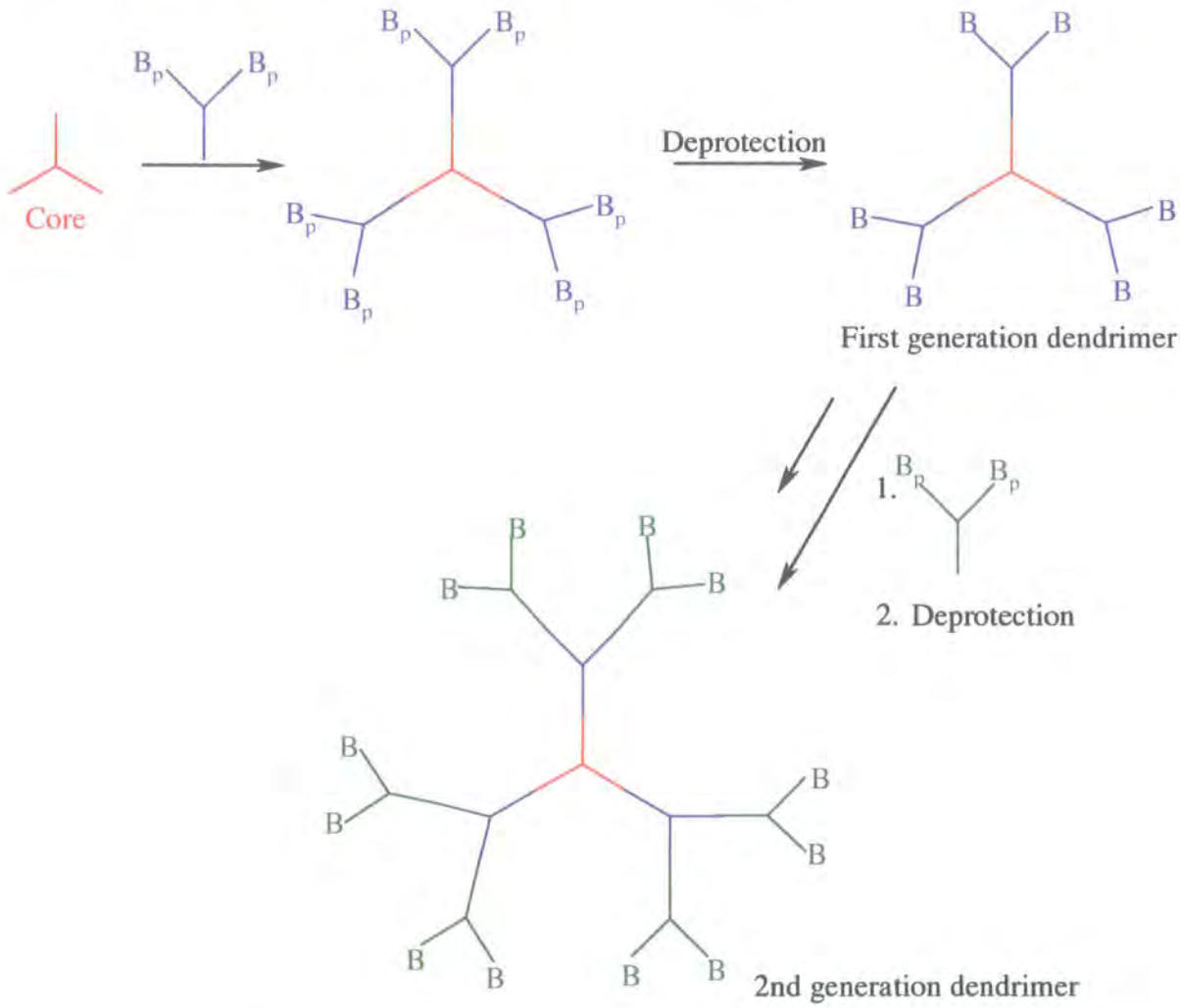

Figure 1.2 Schematic of the divergent route

The earliest example in the literature of the repetitive concept of dendrimer synthesis was reported by Vögtle *et al.* and was achieved using the divergent route, see *Figure 1.3.*[7] The first stage of the reaction involved the Michael addition of a primary amine to acrylonitrile resulting in the formation of a branch point. The terminal groups were then activated by reduction of the nitrile groups to primary

amine functions. The repetition of this sequence of reactions yielded a structure of the second generation, however, low yields in the reduction step hindered further development of the series. In subsequent work carried out by other researchers, the problems with the reduction have been solved and structures, termed poly(propylene imine) (PPI) dendrimers, are now commercially available up to the fifth generation.[8-9] Another well-known series of dendrimers, which are commercially available and synthesised divergently, are the polyamidoamine dendrimers (PAMAMs).[10]

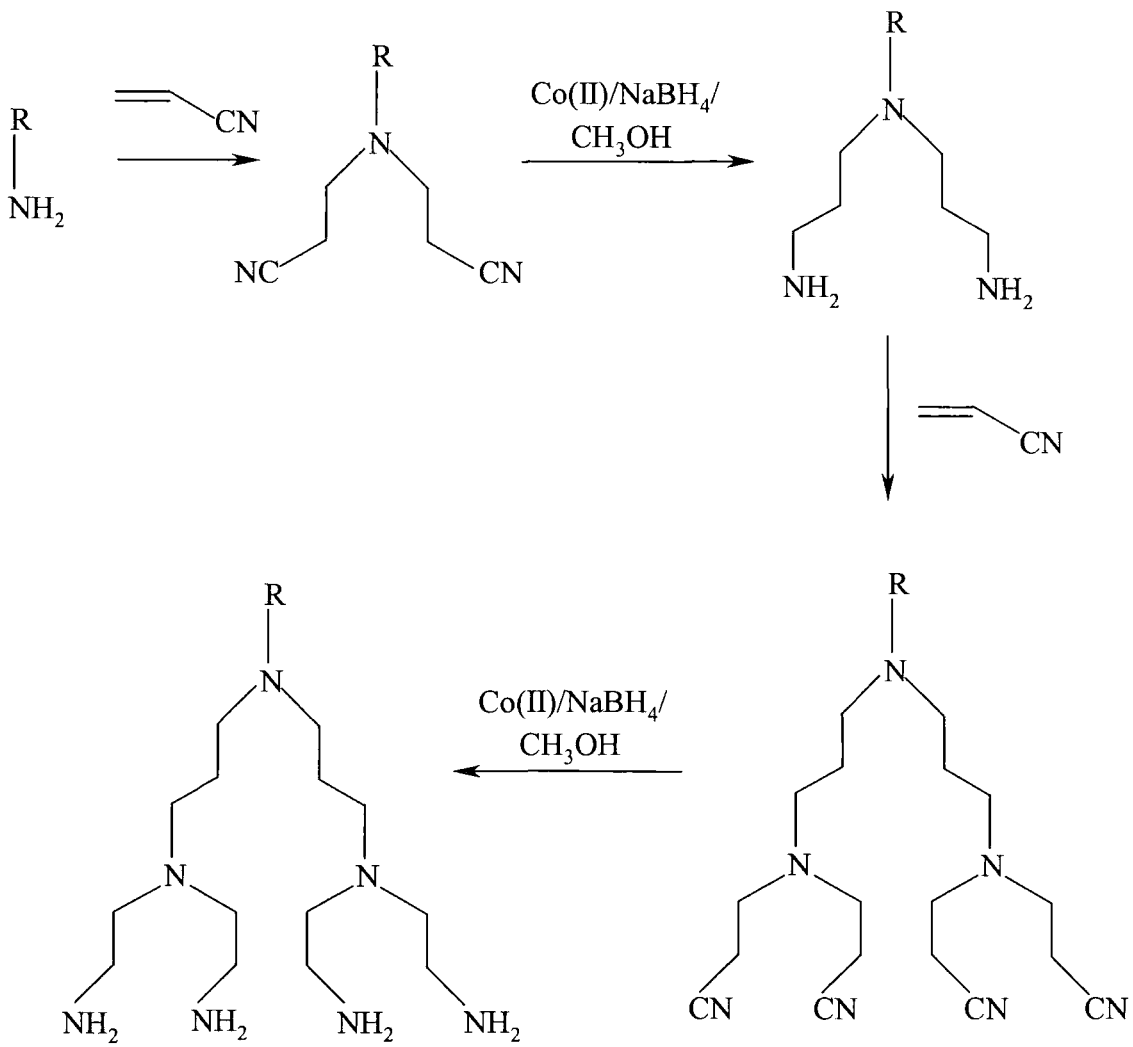

Figure 1.3 First example in the synthesis of a dendritic molecule via the divergent approach

By following the divergent synthetic strategy, dendrimers of high generations have been prepared. For example, the synthesis of the PAMAM series has reportedly been successful up to the tenth generation dendrimer.[11] However, due to the fact that

the number of reactions required on each molecule increases exponentially for successive generations, incomplete formation of branches becomes a problem at higher generations. The result is imperfect macromolecules and impurities from side reactions such as cyclisation. Therefore, dendrimers of high generations are likely to contain defects and have some degree of polydispersity.

The *convergent* route to dendrimer synthesis varies in that the macromolecule is assembled by starting at the periphery of the structure and then moving inwards towards the core. This is achieved by the construction of dendrons or dendritic wedges, which can be coupled to a multifunctional core molecule to produce dendrimers of differing generations. The convergent procedure is outlined schematically for the synthesis of a second generation dendrimer in *Figure 1.4.*

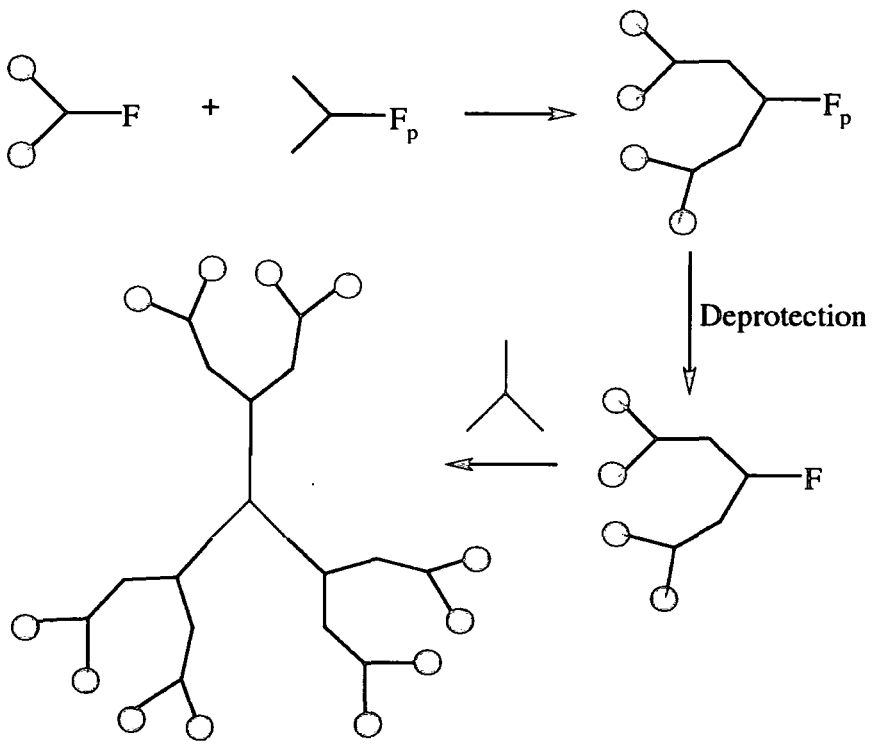

Figure 1.4 Schematic of the convergent route

The apex of a dendron is often referred to as the 'focal point' and the function at this position can be either protected (F_p) or reactive (F) depending on the stage in the synthesis. The first step in the scheme represents the addition of the branched monomer, which contains a protected focal point (F_p) to the first generation dendron

with a reactive focal point (F). This yields a second generation structure with a protected focal point and after deprotection, the dendron can be coupled to a multifunctional core to produce a second generation dendrimer.

Hawker and Fréchet first introduced the convergent synthetic route, synthesising a series of poly(benzyl ether) dendrimers. The synthesis of the first generation dendrimer is outlined in *Figure 1.5*.[12,13] 3,5-Dihydroxybenzyl alcohol, **1**, was used as an AB_2 monomer in the synthesis of the dendrons. The first step consists of a Williamson ether synthesis between benzyl bromide and the phenolic hydroxyl groups. The primary alcohol function at the focal point was then activated by conversion to a benzylic bromide function. These two steps were repeated to prepare higher generation dendrons (up to G = 6). Alternatively, the dendron can be coupled to a multifunctional core resulting in the formation of a first generation dendrimer.

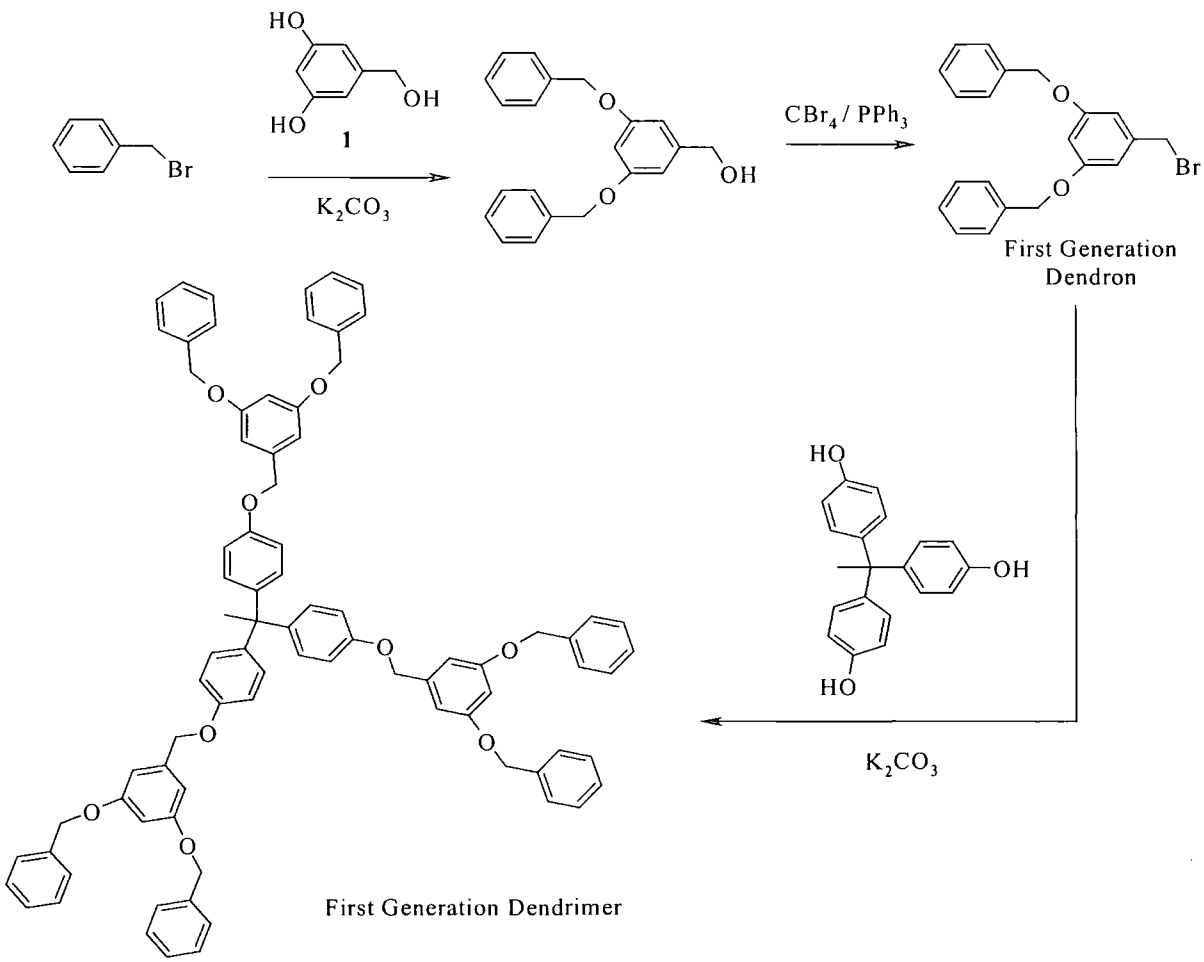

Figure 1.5 Synthesis of a first generation poly(benzyl ether) dendrimer[12]

A similar series of poly(benzyl ester) dendrimers was also synthesised using the convergent route and the dendrimers were isolated up to the fifth generation.[5] The major drawback of this method has been the difficulty in synthesising higher generation structures due to the steric demands involved in coupling two (or more) large molecules to functions in close proximity on the same branching unit or core. However, the small number of reactions required for each generational increase and the ability to remove any impurities by chromatographic techniques has enabled the isolation of dendrimers that are more precisely monodisperse than those isolated via the divergent route.

As has been described, the main problems associated with dendrimers/dendrons are their time-consuming and often difficult preparation. The protection/deprotection strategies required only add to the synthetic burden. In order to reduce the number of steps required in dendrimer synthesis, Rannard and Davies have used the selectivity of 1,1'-carbonyl diimidazole (CDI) chemistry. With CDI, the protection/deprotection step is circumvented providing a shorter route to dendritic architectures. The chemistry of CDI is highlighted in section 1.3.

1.2.3 Properties of Dendrimers

1.2.3.1 Intrinsic Viscosity

Although the dendrons synthesised in this work were coupled to a monomer with the aim of producing dendronised polymers, rather than to a core, it seems appropriate to highlight the special properties that dendrimers can possess. Intrinsic viscosity (η) is the solution viscosity at infinite dilution and is proportional to the volume of the polymer divided by its mass.[14] In the plot of log η vs log M, linear and branched polymers show an increase in intrinsic viscosity with molecular weight, see *Figure 1.6*. However, this is not the case for several series of dendrimers where it has been observed that the graph of log η vs log M passes through a maximum and intrinsic viscosity decreases with increasing molecular weight past the maximum, see *Figure 1.6*. The reason for this may be explained by considering the volume and mass change with increasing generation of spherical dendrimers. The volume of the dendrimer is proportional to the cube of its radius and grows with each additional generation whereas the mass doubles for each generational increase; consequently, at high generations, the mass term dominates resulting in a decrease in the intrinsic

viscosity. With the poly(benzyl ether) dendrimer series it was found that the intrinsic viscosity maximum occurred at the third generation.[4]

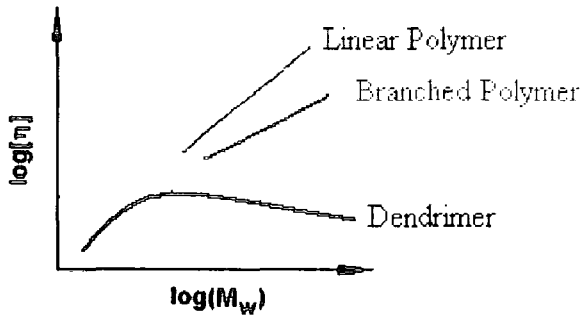

Figure 1.6 Graph of log (intrinsic viscosity) versus molecular weight

1.2.3.2 Solubility

In a study of branched and linear polyesters with comparable structures, the solubility of the dendrimer in tetrahydrofuran (1.05 g mol^{-1}) was found to be significantly greater than that of its linear analogue (0.05 g mol^{-1}).[15] A hyperbranched polymer constructed using the same aromatic building block also had an enhanced solubility (0.70 g mol^{-1}) compared with the linear polyester but was less soluble than the dendrimer. The highly branched and spherical topology of a dendrimer and the large number of chain ends per molecule were believed to be the factors that caused this difference in solubility.

1.3 1,1'-Carbonyl Diimidazole (CDI)

1.3.1 Introduction

1,1'-Carbonyl diimidazole (CDI) has been used for a large number of coupling reactions both in small molecule synthesis and in the formation of peptides and the preparation of polymers.[16,17] CDI is an analogue of phosgene, but has characteristics that make it more favourable to use; for example, CDI is a white crystalline solid, which enhances ease of handling, whereas phosgene is a toxic gas. Also, the by-product of CDI reactions is imidazole, a crystalline solid, which can be removed easily by filtration and/or aqueous work-up. In the equivalent phosgene reactions hydrogen chloride gas is generated.

CDI is versatile in that it has the ability to react with a combination of various acids, alcohols and amines in a two-stage reaction to create five different functional groups, namely, ester, amide, carbonate, urethane and urea groups, *Figure 1.7.*

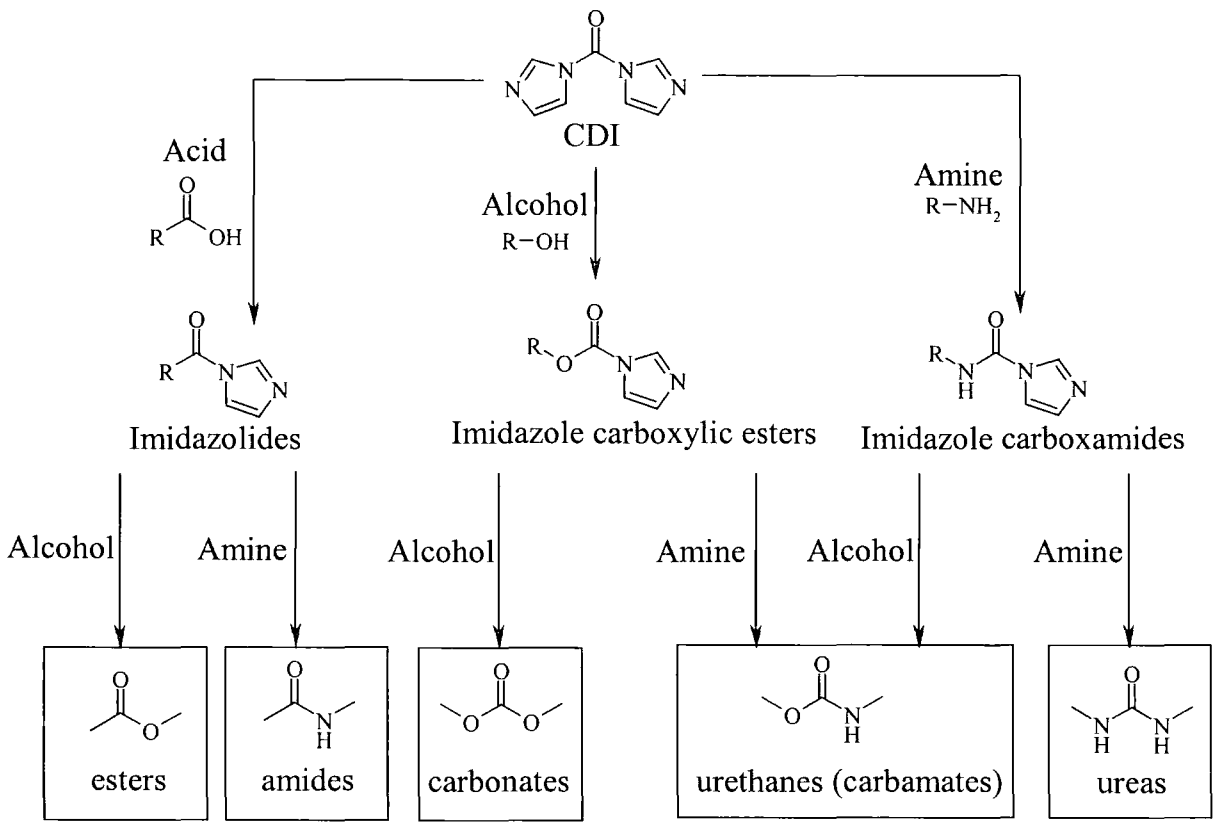

Figure 1.7 The potential reactions of CDI with acids, alcohols and amines

As shown, monosubstituted intermediates are formed when only one of the imidazole rings is displaced. In such a way, imidazolides, imidazole carboxylic esters and imidazole carboxamides are prepared from CDI reactions with acids, alcohols and amines, respectively. In this thesis, these intermediates will often be referred to as 'CDI adducts' or 'adducts'. Staab recognised that it was unnecessary to separate these intermediates from the imidazole produced and used them *in situ.*[16] However, he did not provide any evidence that the intermediates reacted selectively with alcohols and amines. Recent investigations by Rannard et. al have shown that the success of the reaction between the intermediates and acids, alcohols or amines depends on whether the functional group is primary (1°), secondary (2°) or tertiary (3°) in nature.[18]

1.3.2 Selectivity of CDI in Carbonates

The synthesis of dendrons containing both carbonate and urethane functional groups will be described in this thesis. There are certain rules that govern reactions of CDI and CDI adducts, *Figure 1.8.* The rules are listed below for the formation of carbonates case.

a) Under certain reaction conditions a primary alcohol undergoes a disubstitution reaction with CDI, resulting in the formation of a symmetrical carbonate **4**. However, if an excess of CDI is used, at room temperature with no base present, the intermediate adduct **1** can be isolated in a yield of 94%.

b) Secondary and tertiary alcohols react with CDI in a 1:1 ratio to give the corresponding adducts, **2** and **3** respectively. Even if the alcohols are used as the reaction solvent, no second addition is observed.

c) Adducts of primary, secondary and tertiary alcohols, **1**, **2** and **3**, react selectively with primary alcohols, under base catalysis and at a reaction temperature of 60°C, to give **4**, **5**, and **6** respectively.[20]

d) No reaction is observed between all three adducts and secondary and tertiary alcohols.

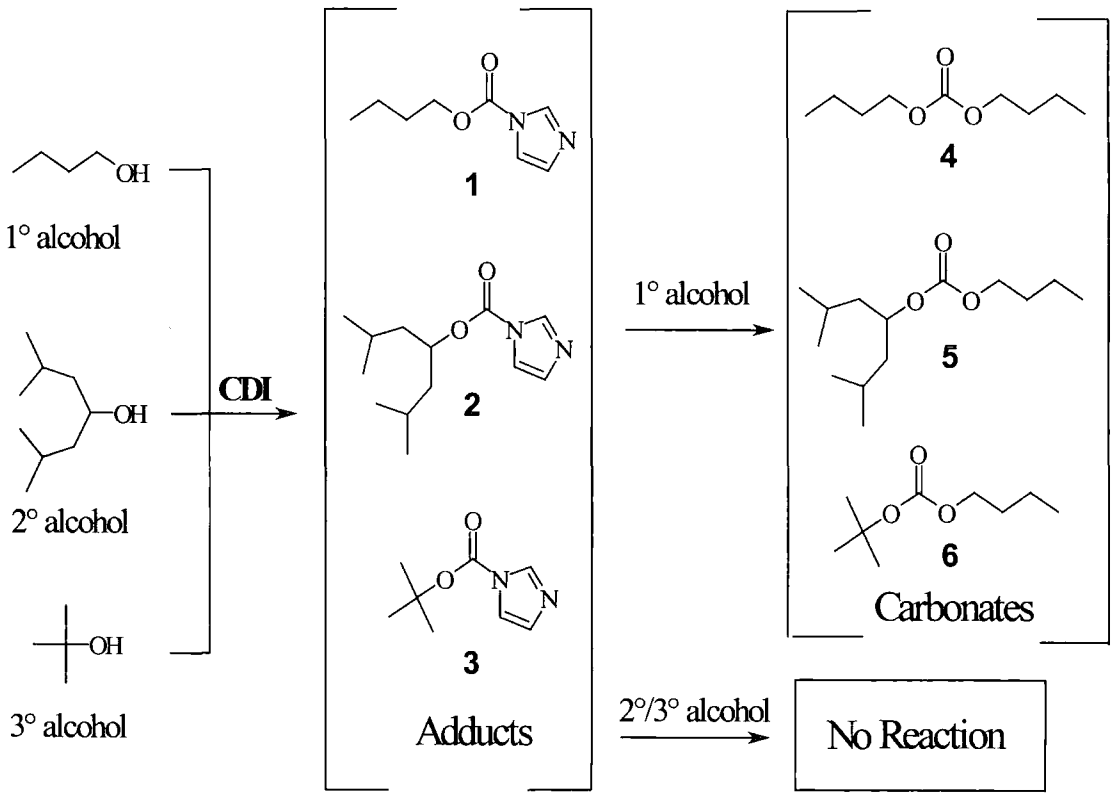

Figure 1.8 Selective reactions of CDI and CDI adducts with alcohols

It has been found, however, that there are exceptions to the rules.[20] The secondary alcohol adduct, **2**, was found to react as predicted with the primary site of 1,4-pentanediol to form predominantly (80%) carbonate **7**, *Figure 1.9*. However, there was evidence of a reaction occurring at the secondary site (20%), to form carbonate **8**. Despite this, the selection rules applied in the reaction of tertiary alcohol adduct **3**, *Figure 1.8*, with 1,4-pentanediol and no evidence was found of a reaction at the secondary site in this case.

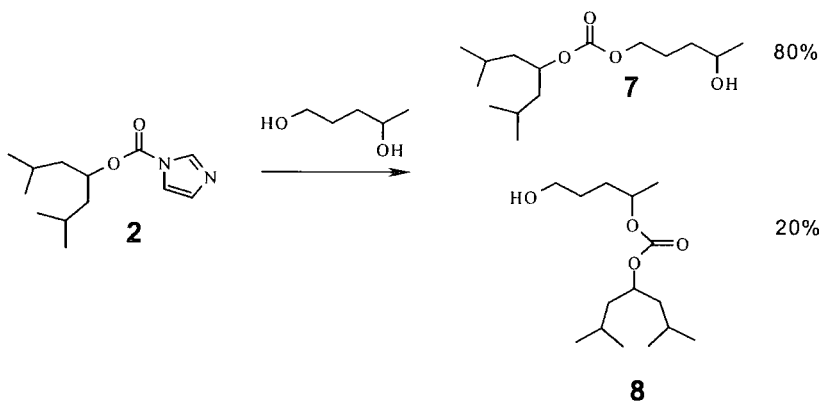

Figure 1.9 Carbonate formation not following the selection rules

Bertolini *et al.* have studied the selectivity of such reactions during the preparation of asymmetric carbonates, *Figure 1.10*.[21] The experiments involved the addition of CDI to an equimolar mixture of a primary and a secondary alcohol, **9** and **10**, followed by the addition of a different primary alcohol **13**, under base catalysis.

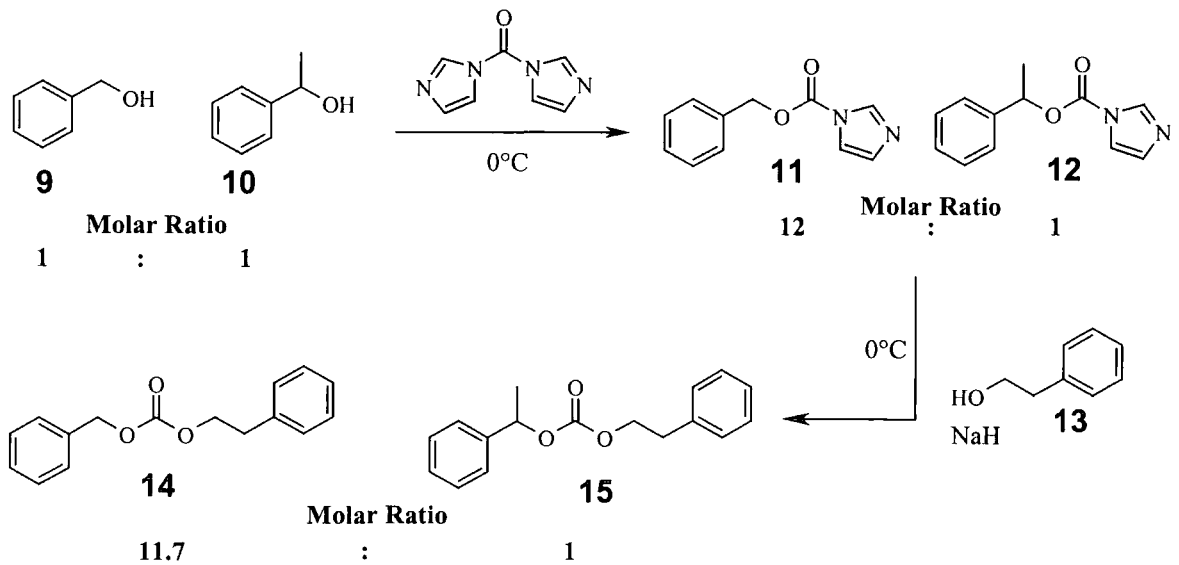

Figure 1.10 Synthesis of asymmetric carbonates by Bertolini et al.

In the first stage, the primary alcohol adduct **11** was formed preferentially in a ratio of 12:1, over the secondary alcohol adduct **12**. Subsequent addition of a different primary alcohol **13** and base to the mixture produced predominantly carbonate **14**, rather than carbonate **15**. The overall yield of the reaction was moderate (46%) due to residual alcohols **9** and **10** reacting with the adducts formed in the first step producing carbonates **16** and **17**, *Figure 1.11*. However, the yield was significantly improved when intermediates **11** and **12** were isolated.

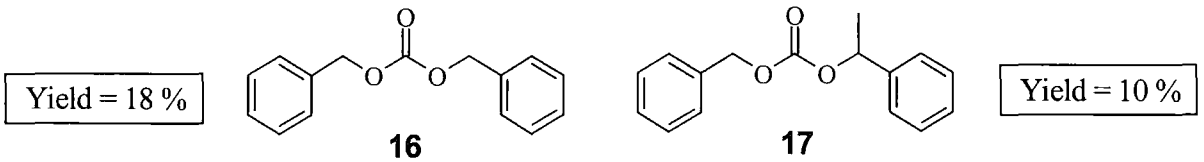

Figure 1.11 Side products isolated in the one-pot reaction

1.3.3 Selectivity of CDI in Urethane Synthesis

One strategy for synthesising a urethane link is by the reaction of an alcohol with CDI, followed by the reaction of the intermediate with an amine. Urethane formation follows selection rules similar to those for carbonates;[22,23] for example, primary amines will react with the adducts of primary, secondary and tertiary alcohols. However, secondary or tertiary amines will not react with any of the adducts formed, whereas in carbonate synthesis the secondary alcohol will sometimes react. This regioselective urethane formation can be demonstrated by the reaction of triamine **18** with adducts **2** or **3**, as a reaction only occurs at the primary sites, to give **19** and **20**, respectively. There is no evidence of a reaction occurring at the secondary site, *Figure 1.12*.

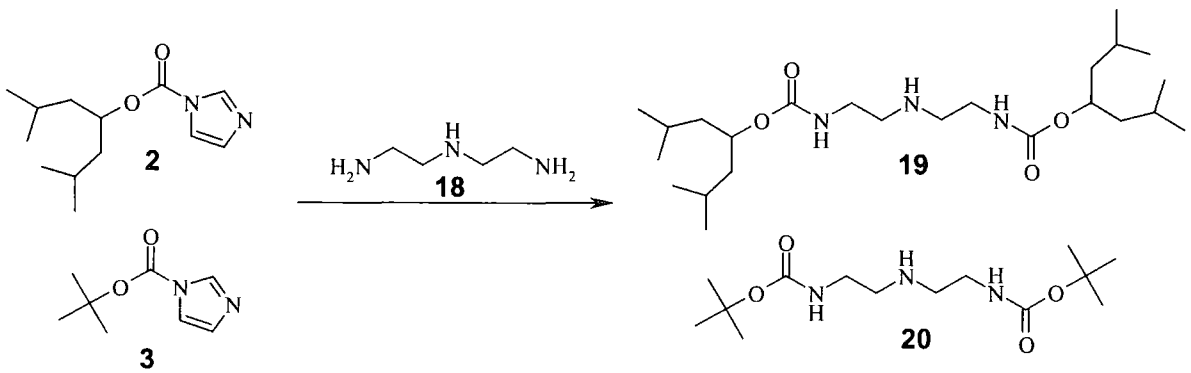

Figure 1.12 Regioselective reactions of CDI adducts with a multifunctional amine

1.3.4 Uses of CDI in Dendrimer Synthesis

Polycarbonate dendrimers have been synthesised by exploiting the selective reactions of CDI.[23] The commercially available branching unit 1-[N, N-bis(2-hydroxyethyl)amino]-2-propanol (**HEAP**) was used in the synthesis of the second generation dendron **21**, *Figure 1.13*. It was found that when toluene was used as the reaction solvent, the imidazole by-product and CDI were only partially soluble in the solvent when cold, enabling easy removal via filtration. Also, these workers were able to prepare polyamide dendrimers, the largest being a third generation structure with a molecular weight of 3999 Da.

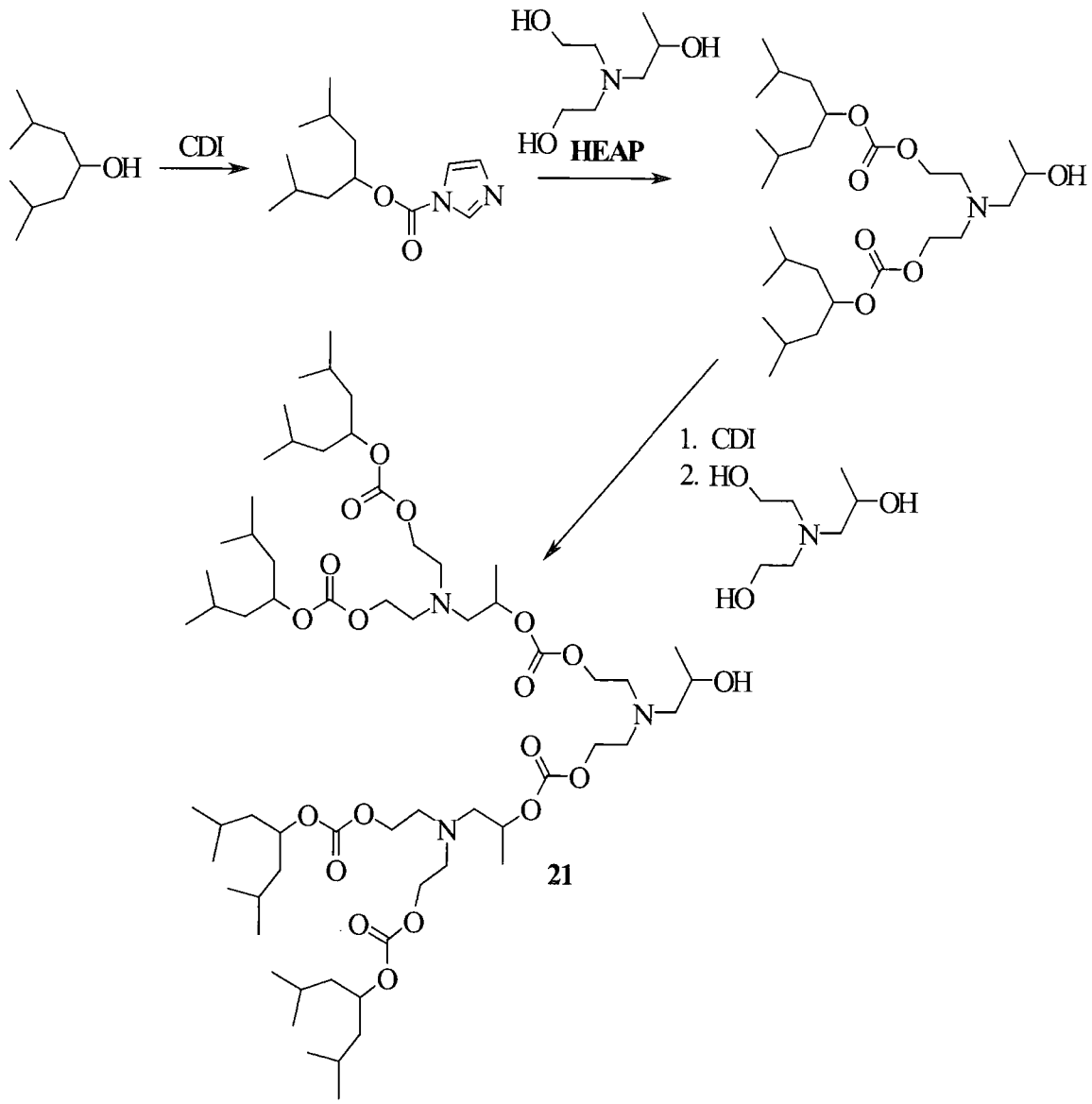

Figure 1.13 Synthesis of a second generation polycarbonate dendron

1.3.5 Summary of CDI Reactions

The regioselective reactions of CDI have been shown to be effective in the synthesis of small molecules and macromolecules, circumventing the need for the use of protecting groups. This attribute, together with the relatively high yielding nature of the reactions, makes CDI an attractive choice of coupling agent in the synthesis of dendrimers.

1.4 Ring Opening Metathesis Polymerisation

1.4.1 Definition and Historical Background

Olefin metathesis is a catalytically induced bond reorganisation process and involves exchange of carbon-carbon double bonds. For an acyclic olefin, this leads to exchange of alkylidene units. The reaction was first reported by Banks and Bailey in 1964 and termed 'olefin disproportionation', *Figure 1.14*.[24]

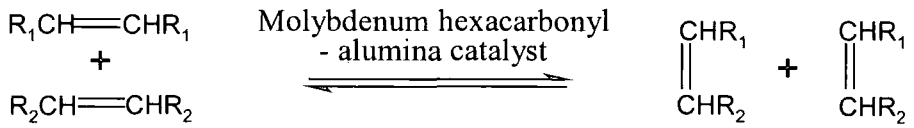

Figure 1.14 General reaction scheme for the metathesis of an acyclic olefin

For cyclic or polycyclic olefins, which are the type dealt with in this thesis, the metathesis reaction leads to ring scission and the formation of an unsaturated linear polymer, *Figure 1.15*.

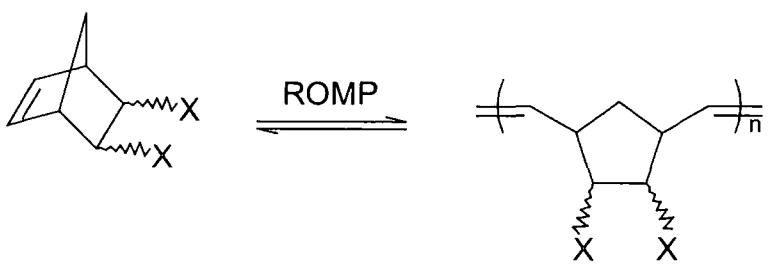

Figure 1.15 General reaction scheme for the metathesis of a bicyclic olefin

The first example of olefin metathesis involving a bicyclic olefin (in fact only recognised as such some years later) was reported by Anderson and Merkling in a

DuPont patent in 1955.[25] They successfully polymerised norbornene using a mixture of titanium tetrachloride and ethylmagnesium bromide to initiate the process. Calderon *et al.* recognised that disproportionation of acyclic olefins and ring opening polymerisations of cyclic olefins are examples of one and the same chemical reaction. They gave these types of reactions the name 'Olefin Metathesis'.[26-29]

1.4.2 The Mechanism of Olefin Metathesis and Ring Opening Metathesis Polymerisation

According to the 'pair-wise' mechanism postulated by Bradshaw, it was thought that two double bonds came together in the vicinity of the transition metal site and that the orbitals of the transition metal overlapped with those of the double bonds in such a way as to allow exchange to occur via a weakly held cyclobutane type complex.[30] This pair wise mechanism has now been abandoned in favour of one proposed by Herrison and Chauvin in which the propagating species alternates between a metal-carbene complex and a metallocyclobutane, *Figure 1.16*.[31]

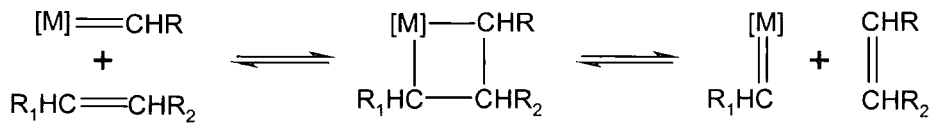

Figure 1.16 Herrison and Chauvin's mechanism of olefin metathesis

The process involves reversible [2+2] cycloaddition of the olefinic carbon-carbon double bond to a metal carbene species to form a metallocyclobutane, which then opens either non-productively (degeneratively) to regenerate the original reaction mixture or productively to form a new olefin and a new metal carbene, *Figure 1.17*.

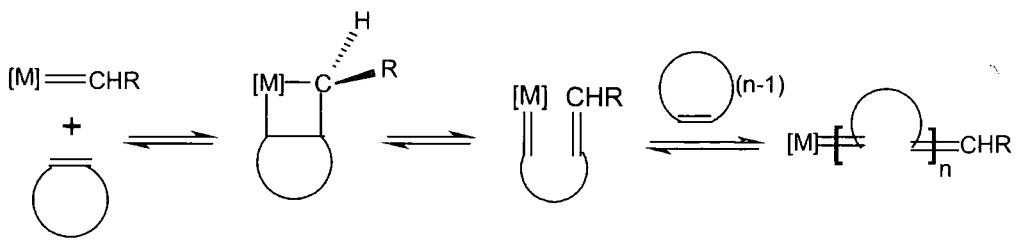

Figure 1.17 Mechanistic pathway for ring opening metathesis polymerisation

All of the above steps are reversible, so the outcome of the metathesis of acyclic alkenes and ring opening polymerisation depends on reaction conditions, such as temperature, concentration, reaction duration, the nature of the olefin and the nature of the propagating polymer chain end.

1.4.3 Living Polymerisation

A living polymerisation is a chain polymerisation that proceeds in the absence of the kinetic steps of termination or chain transfer. Thus once total conversion of the monomer has been attained, the growing polymer chain end still remains active. Some of the important features of living polymerisation are that the polymerisation proceeds until all of the monomer has been consumed and further addition of monomer results in continued polymerisation. The number average molecular weight (M_n) is a linear function of conversion and thus the molecular weight can be controlled by the stoichiometry of the reaction. The polymers produced have narrow molecular weight distributions and block co-polymers can be prepared by sequential monomer addition. The initiation, propagation and termination steps for the ring opening metathesis polymerisation of a substituted norbornene are shown in *Figure 1.18.*

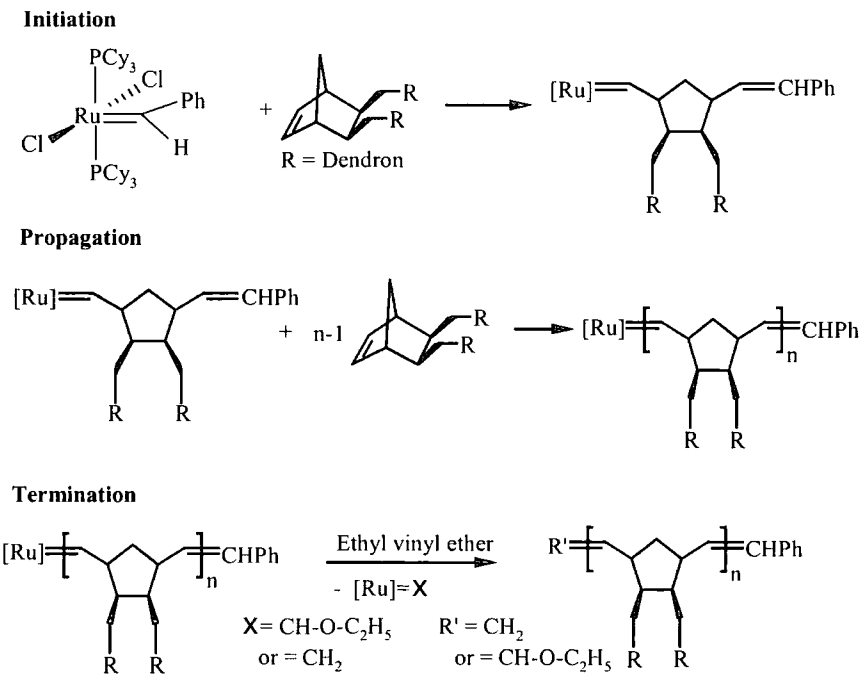

Figure 1.18 Initiation, propagation and termination steps in ring opening metathesis polymerisation

In the first step, the initiating species is formed via a [2 + 2] cycloaddition reaction between the ruthenium carbene and the olefin followed by ring opening to generate a chain end ruthenium carbene. In the propagation step, n equivalents of monomer are inserted into the reactive chain end by repetition of the same steps. Finally, the polymerisation may be terminated by the addition of ethyl vinyl ether, which undergoes cross metathesis with the chain end ruthenium carbene, predominantly capping the chain with a CH_2 unit.

1.4.4 Metathesis Initiators

In general the catalysts for olefin metathesis and ring-opening metathesis polymerisation are based on transition metals of groups IV to IX of the Periodic Table. However, Mo, W, Re and Ru compounds have been shown to be the most effective catalysts. Metathesis catalysts can be divided into two major categories; namely, the ill-defined dual component systems, known as 'classical initiators', and single component 'well-defined initiators'. The well-defined initiators include transition metal carbenes and metallocyclobutanes, both of which were predicted by Chauvin. For the sake of completeness, this section includes a brief description of classical initiators but the bulk of the section is devoted to well-defined initiators. In particular, the well-defined ruthenium carbene initiators will be discussed, since they are of specific interest to the work in this report.

1.4.4.1 Classical Initiators

Catalysts for a classical initiating system can be either homogeneous or heterogeneous and always contain a transition metal compound. Many of the commonly used catalyst systems are based on the chlorides, oxides or oxychlorides of Mo, W or Re. Although these compounds are sometimes effective by themselves, more commonly they require activation by a co-catalyst, which is usually an organometallic compound or a Lewis acid. In some cases a third component called a promoter, is used as well. These promoters often contain oxygen; examples include O_2, EtOH and PhOH. Some typical homogeneous catalyst systems are $WCl_6/EtAlCl_2/EtOH$, $WOCl_4/Me_4Sn$ and $ReCl_5/Et_3Al/O_2$. Examples of heterogeneous supported catalyst systems include MoO_3/Al_2O_3, WO_3/SiO_2 and Re_2O_7/Al_2O_3. Due to their low cost and simple preparation, these systems have an important place in commercial applications of olefin metathesis.

Some of the disadvantages of classical initiators are that the precise nature of the active site at the metal centre is not known, nor are the number of metal centres that are active in the reaction or the number of types of active centre, the system is ill defined. There is a lack of control of molecular weight and molecular weight distribution due to the occurrence of intra- and/or intermolecular reactions. The utility of the catalysts is also limited by the harsh conditions that are required, rendering them incompatible with most functional groups.

1.4.4.2 Well-Defined Initiators

Greater control over the reactivity of ROMP initiators became possible with the use of well-defined alkylidene complexes. These well-defined initiators allow, in favourable cases, the synthesis of polymers with narrow molecular weight distributions (M_w/M_n <1.01) and control over tacticity. The first isolated metal carbene species, the Fischer carbene, was described in 1964, *Figure 1.19*.[32] It was a heteroatom stabilised complex and was shown to be reactive in olefin metathesis. It was found to react with highly strained olefins such as cyclobutene and norbornene derivatives. The diphenyl complex, first synthesised by Casey and Burkhardt in 1973, was not stabilised by a heteroatom (*Figure 1.19*) and was much more reactive, initiating the polymerisation of less strained olefins.[33] Although they were active well-defined initiators, they did not give living polymerisations.

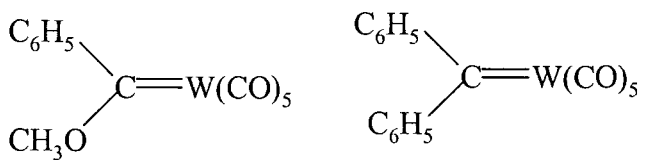

Fischer carbene Casey carbene

Figure 1.19 Metal carbenes used to initiate metathesis

Grubbs and co-workers were the first to isolate well-defined metallacyclobutane complexes that were active as metathesis catalysts. The reaction of Tebbe reagent with various olefins in the presence of nitrogen bases resulted in the formation of titanacyclobutane complexes. It has been shown that these titanacycles readily exchange with olefins via a rate determining loss of olefin from the titanacyclobutane ring to generate the transition metal methylidene species

$Cp_2Ti=CH_2$ which is active in metathesis.[34,35] These titanacyclobutane complexes, *Figure 1.20,* provided the first example of a living polymerisation of a cycloolefin when Gilliom and Grubbs reported their use to initiate the polymerisation of norbornene.[36]

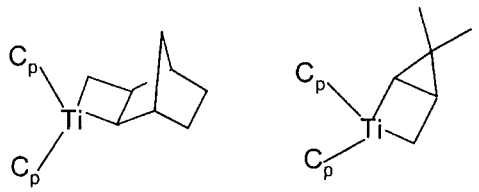

Figure 1.20 Grubbs' well-defined titanacyclobutane initiators

In this case, the polymerisation proceeds without termination or chain transfer to give polynorbornene with a narrow molecular weight distribution. However, there are some drawbacks associated with this initiator system in that titanacyclobutanes require a temperature of 50°C in order to ring-open even norbornenes and they are very reactive toward functionalities owing to the highly electrophilic nature of the metal centre. This high reactivity makes them difficult to prepare and handle.

Schrock and co-workers introduced well-defined tungsten and molybdenum initiators with bulky alkoxide and arylimido ligands of the type $M(CHR)(NAr)(OR')_2$, *Figure 1.21.*[37-42]

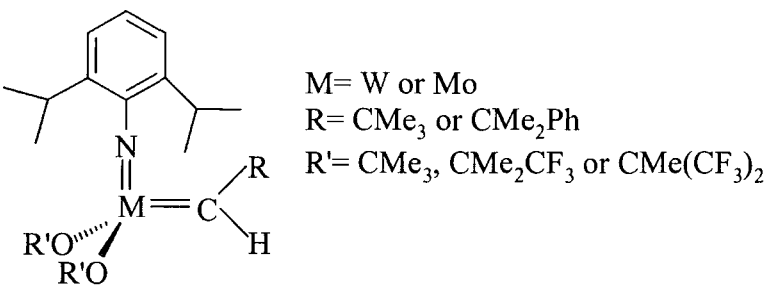

Figure 1.21 Well-defined Schrock initiators

The four co-ordination of these complexes allows a relatively small substrate to attack the metal to give a five co-ordinate intermediate metallocyclobutane complex. The bulky alkoxide groups and the imido ligand prevent intermolecular reactions, which could result in inactive complexes or decomposition of the catalyst. Substitution of the methyl groups on the alkoxides with the more electronegative

trifluoromethyl groups makes the complex more active since the trifluoro groups draw electron density away from the metal centre. This makes the metal centre of the complex more electrophilic and a better acceptor for the incoming olefin.[43] This effect is demonstrated by the observation that when OR is $O(C(CH_3)(CF_3)_2)$ the tungsten complex will readily metathesise acyclic olefins, whereas when OR is OBu^t it does not react with acyclic olefins.

The Mo catalyst reacts rapidly with both terminal and internal olefins and performs ROMP of low-strain monomers, as well as ring-closing of sterically demanding and electron-poor substrates. However, this catalyst and others based on the early transition metals are limited by the high oxophilicity of the metal centres, which renders them extremely sensitive to oxygen and moisture. As a result of this, they are limited by moderate to poor functional group tolerance reducing the number of potential substrates.[43]

1.4.4.3 Ruthenium Carbene Initiators

It was realised from the results of the molybdenum catalyst that the key to improved functional group tolerance was in the development of a catalyst that reacts preferentially with olefins in the presence of heteroatom functionalities. Due to the advent of single-component catalysts, the relationships between structure and reactivity were more clearly defined. This led to the observation that selectivity of catalysts towards olefins increases with the use of late transition metals.[44] This trend is illustrated for titanium, tungsten, molybdenum, and ruthenium in the table shown in *Figure 1.22* where the groups appearing below **olefins** in each column are tolerated by well defined catalysts based on the metal at the top of the column.

Titanium	Tungsten	Molybdenum	Ruthenium
Acids	Acids	Acids	**Olefins**
Alcohols, Water	Alcohols, Water	Alcohols, Water	Acids
Aldehydes	Aldehydes	Aldehydes	Alcohols, Water
Ketones	Ketones	**Olefins**	Aldehydes
Esters, Amides	**Olefins**	Ketones	Ketones
Olefins	Esters, Amides	Esters, Amides	Esters, Amides

Figure 1.22 Functional group tolerance of early and late olefin metathesis catalysts

Titanium is more strongly disposed to olefinate ketones and esters, which has been shown to be useful in organic synthesis. Molybdenum catalysts on the other hand are more reactive toward olefins, although they also react with aldehydes and other polar or protic groups. Farthest to the right, ruthenium reacts preferentially with carbon-carbon double bonds over most other species, which makes these catalysts unusually stable toward alcohols, amides, aldehydes, and carboxylic acids. It is therefore possible to increase the functional group tolerance of an olefin metathesis catalyst by focusing on a later transition metal, such as ruthenium.

Despite this selectivity, ruthenium was not initially considered as a suitable candidate for metathesis reactions. The main reason for this was the low metathesis activity of ruthenium salts coupled with a limited understanding of how to achieve functional group tolerance. In the early 1980's when ruthenium catalysts were re-examined, it was found that $RuCl_3$(hydrate) had very long initiation periods under strictly anhydrous conditions. However, water was found to be not only compatible with the catalyst system, but also beneficial to the initiation process; indeed, the polymerisation could be conducted in aqueous solution.[45,46]

After testing other ruthenium complexes, such as $Ru(H_2O)_6$(tos) (tos = p-toluenesulfonate), it was found that the initiation rates could be further reduced to a few minutes.[47] This catalyst was able to ROMP functionalised norbornene derivatives obtaining polymers in greater yields, higher molecular weights and lower polydispersities than most other catalysts at that time. However, the initiation process remained unclear, but observations had led to the belief that ruthenium alkylidene was the active species. Although no ruthenium alkylidene species at that time could perform olefin metathesis, the success of other alkylidene catalysts led to attempts being made to find a ruthenium equivalent.

A major breakthrough occurred when the methodology for the synthesis of tungsten alkylidenes, in which 3,3-disubstituted cyclopropenes were used as the carbene precursors, was applied to the synthesis of a ruthenium catalyst. Reaction of 3,3-diphenylcyclopropene with either $RuCl_2(PPh_3)_3$ or $RuCl_2(PPh_3)_4$ produces the vinylalkylidene complex $(Cl)_2Ru(=CHCH=CPh_2)(PPh_3)_2$ (**22**), which was synthesised by Grubbs and co-worker in 1992, *Figure 1.23*.[48] Norbornene, in the presence or absence of water or ethanol, and other highly strained cyclic olefins such as cyclobutene and cyclooctene were readily polymerised by this initiator in a living

fashion. More significantly, during the ROMP of norbornene a propagating alkylidene species could be observed using ^{1}H NMR spectroscopy.

However, it is inactive for the polymerisation of less-strained cyclic olefins and for acyclic metathesis.[49-50] In an attempt to overcome this problem, the ligand environment was modified in a systematic way in order to extend the activity to low-strain monomers. It was found that the exchange of triphenylphosphine (PPh_3) ligands with tricyclohexylphosphines (PCy_3) resulted in a much more active catalyst, compound **23**, *Figure 1.23*.[51] In particular, the larger and more basic the phosphine, the higher the metathesis activity. It was found that this catalyst was air stable as a solid and retained its activity even when exposed to water, alcohol or acids. The PCy_3 derivative catalyses the ROMP of both high and low strained cyclic olefins as well as the metathesis of acyclic olefins at room temperature. However, the polydispersities of the low strained systems were high (~2.5).

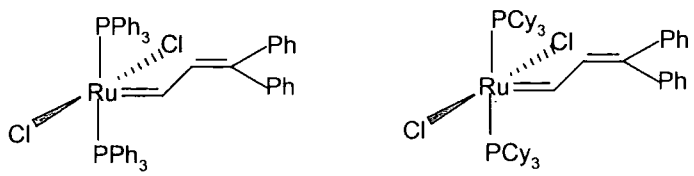

22 **23**

Figure 1.23 Well-defined vinylalkylidene ruthenium initiators

In 1995, Grubbs and co-workers reported the use of diazoalkanes as an alternative carbene source to provide air-stable ruthenium benzylidene complexes, **24** and **25**, in high yield, *Figure 1.24*.[51,52] Diazoalkanes were utilised due to their stability and ease of synthesis.[53] These catalysts display greater metathesis activity, compared to the vinylalkylidene complex, due to faster initiation. Catalyst **25** is able to perform the ROMP of highly strained monomers including functionalised norbornenes in a living fashion giving narrow molecular weight distributions.

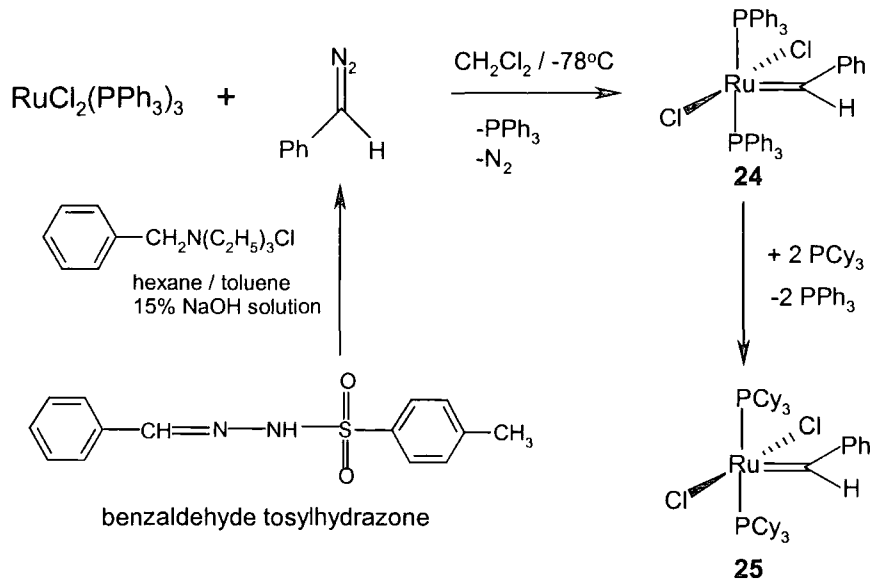

Figure 1.24 Synthesis of air-stable ruthenium benzylidene complexes

Recently, Grubbs *et al.* in an attempt to increase the utility of the ruthenium family of complexes by increasing their activity, prepared ruthenium-based complexes coordinated with 1,3-dimesitylimidazol-2-ylidene ligands (IMes), **26a** and **26b**, *Figure 1.25*.[54] These complexes exhibited a high ring-closing metathesis activity similar to that of Schrock's molybdenum complex and displayed dramatically improved thermal stability and inertness towards oxygen and moisture when compared to **25**.

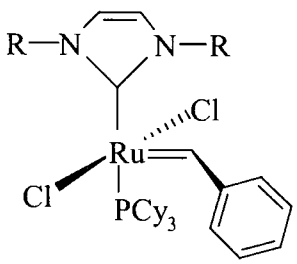

26a: R = ^{i}Pr or Cy
26b: R = mesityl (Mes)

Figure 1.25 Ruthenium complex bearing the unsaturated IMes ligand

They also prepared the related ligands, **27a-27c**, containing a saturated ring, which they believed might be more basic than the unsaturated analogues, *Figure 1.26*.

They postulated that this higher basicity should in turn translate into an increased activity of the desired catalysts.

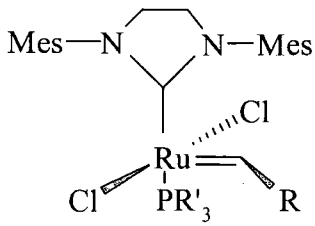

27a: R=Ph, R'=Cy
27b: R=$CH(CH_3)_2$, R'=C_y
27c: R=$CH(CH_3)_2$, R'=Cp

Figure 1.26 Ruthenium complex bearing the saturated IMes ligand

Indeed, it was found that these saturated complexes display catalytic activity in ring closing metathesis (RCM) and cross-metathesis (CM) that not only exceeds that of the unsaturated complexes, but also begins to rival that of Schrock's molybdenum complex, while maintaining the functional group compatibility of **25**.[55-57] More interestingly, it was found that both the saturated and unsaturated ruthenium complexes bearing the IMes ligands were more active than the molybdenum complex in ROMP.[58] It is believed that the role of the IMes ligand is twofold: being a better donor than PCy_3, catalyst performance is enhanced, and its more sterically demanding presence helps prevent (or slow) bimolecular carbene decomposition.

The relative activities of the various catalysts in the ROMP of the low-strain cyclic olefin cis, cis-cycloocta-1,5-diene (COD) was determined. It was found that at 20°C, the polymerisation rate of COD when initiated with **27a** was significantly higher than when initiated with the molybdenum complex at 20°C. In addition, the saturated N-heterocyclic carbene ligand displayed increased activity in ROMP relative to its unsaturated analogue **26b**.

However, close examination of the ROMP of various low-strain cyclic olefins revealed that complex **27a** does not form well-defined polymeric structures. For example, it was found that the polydispersity indices (PDIs) of the resulting polymers were high and that secondary metathesis isomerisations were occurring. In addition, ^1H NMR spectroscopy indicated that less than 5% of the complex initiated before the

ROMP of the monomer was complete. Therefore, with complex **27a**, the rate of propagation is a lot greater than the rate of initiation resulting in polymers possessing high molecular weights and PDI's.

It is also important to note that the widespread use of **27a** has been limited due to its relatively difficult preparation. The initial syntheses utilised free carbenes as shown in *Figure 1.27*.[59] However, these are extremely air and moisture sensitive, which is inconvenient for large scale preparations. The free carbenes once generated, can be directly trapped by the parent ruthenium benzylidene complex **25**, but the isolation of the new catalyst requires air-free, anhydrous conditions and multiple purifications to remove the free phosphine generated in the synthesis. The purifications are required due to the fact that an excess of free phosphine inhibits productive metathesis using such complexes, since the first step in the process is loss of the phosphane ligand.

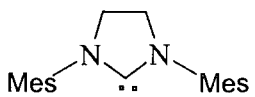

Figure 1.27 The free carbenes used in the synthesis of the ruthenium complexes containing the IMes ligand

In order to solve this problem, Grubbs *et al.* synthesised complexes as protected forms of the free carbenes.[60] These complexes contain alkoxide or trichloromethyl groups which can eliminate alcohol or chloroform to unmask the carbene to coordinate to the metal centre. The desirable properties of the complexes are that they are easy to synthesise, are air stable which makes them easier to handle and the latent carbene is readily released in solution.

In this project, the aim is to synthesise well-defined polymeric structures. It would seem from the literature that such structures are not possible via the saturated ruthenium complex containing the IMes ligand, **27a**. As a consequence of this, it was decided that the Grubbs benzylidene initiator, **25**, would be an ideal candidate for the ROMP reactions carried out in this work.

1.4.5 Detailed Mechanistic Studies

Initially, two limiting mechanisms were proposed for the ligand substitution of phosphine with olefinic substrate, *Figure 1.28*.[61] It was postulated that substitution could take place in an associative or dissociative fashion. The associative pathway, **[A]**, involves initial binding of olefin to form a coordinatively saturated 18- electron intermediate, while the dissociative substitution pathway, **[B]**, proceeds by initial loss of PCy_3 to generate a 14-electron intermediate, **28**.[62]

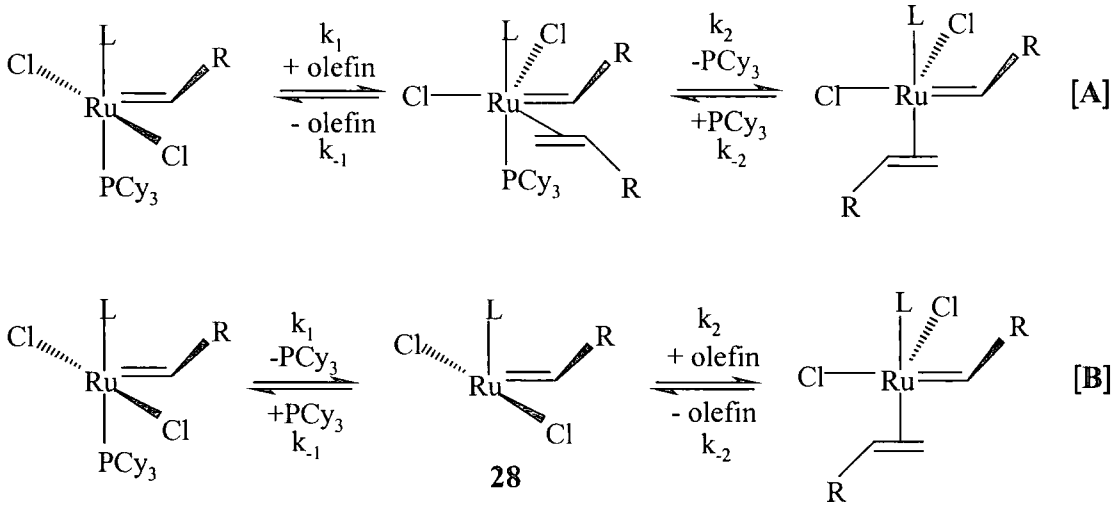

Figure 1.28 Proposed mechanisms for the ligand substitution of phosphine with olefinic substrate

Initially, the associative mechanism was proposed as it was thought that the 18-electron intermediate would be preferred over the 14-electron intermediate. However, early studies could not distinguish between the two pathways as it was difficult to investigate the ligand displacement directly in solution due to the fact that the ruthenium-olefin adduct could not be observed by spectroscopic methods. As a result of this, it was decided to study the exchange of free and bound phosphine as a potential model system in various catalysts using ^{31}P NMR spectroscopy, *Figure 1.29*.

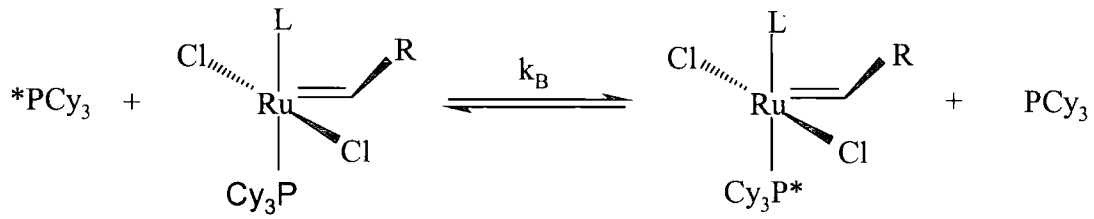

Figure 1.29 ^{31}P NMR spectroscopy study on the exchange rates of free and bound phosphine

It was found, for $X_2(PR_3)_2Ru=CHR'$ type catalysts, that the rate of phosphine exchange is much faster ($\sim 10^4$) than the rate of reaction with olefin. However, with the IMes ligand in place, a decrease in the phosphine exchange rate of over 2 orders of magnitude was found. These results were surprising as they showed an *inverse* relationship between phosphine exchange rate and olefin metathesis activity. This was compounded by the fact that the sterically bulky and highly basic IMes ligand was originally designed to accelerate the phosphine dissociation event.

It was found from thermodynamic data and the exchange rate constant as a function of phosphine concentration that the reaction follows a dissociative mechanism. The intermediate, **28** (*Figure 1.28*), has never been observed by NMR spectroscopy suggesting that the equilibrium for phosphine dissociation lies very much towards the 16 electron starting material. From the results, it was realised that the activity of catalysts **25** and **27a** is not only related to the rate-determining phosphine dissociation step, but also to the ratio of k_{-1} to k_2 which determines whether the catalyst binds olefin or returns to its original resting state.

The kinetic data showed that although the IMes carbene initiator does not lose phosphine efficiently, a small amount of initiated 14-electron species is capable of cycling through multiple olefin metathesis reactions before it is deactivated by the rebinding of PCy_3. On the other hand, initiator **25**, containing two tricyclohexylphosphine ligands loses phosphine relatively rapidly, but the rebinding of phosphine is competitive with olefin coordination and as such, the highly active 14-electron intermediate undergoes relatively few turnovers before being trapped by free PCy_3. Therefore the reason for the high activity of the IMes initiator, which had previously been attributed to its ability to promote phosphine dissociation, instead appears to be due to its improved selectivity for binding π–olefinic substrates in the presence of σ–donating free phosphine.

1.4.6 Thermodynamic Aspects of Ring Opening Metathesis Polymerisation

For any reaction to occur the change in Gibbs Free Energy (ΔG) must be ≤ 0. This change is expressed as a function of the enthalpy change (ΔH), the entropy change (ΔS) and the absolute temperature (T, Kelvin scale), *equation 1*.

$$\Delta G = \Delta H - T\Delta S \qquad (1)$$

For polymerisations the entropy is always negative since the monomers are combined with each other into macromolecules resulting in a reduction of their freedom. This makes the entropy term ($-T\Delta S$) positive, and for a favourable reaction, the change in enthalpy has to be larger than the $T\Delta S$ component. The temperature where $\Delta G=0$, namely $T=\Delta H/\Delta S$, is called the ceiling temperature, and above this temperature, the polymerisation reaction cannot take place.

In general the most favourable conditions for ring opening metathesis polymerisation of cycloalkenes are high monomer concentration, low temperature and high pressure. The enthalpy change is dependent on the ring strain. Therefore, for three and four membered rings, which are strained due to the deformation of the normal bond angles, and rings containing eight or more carbon atoms which are strained due to torsional or transannular effects, the enthalpy change is high (i.e. negative) and polymerisations go to completion at normal temperatures and monomer concentrations. For monomers with low ring strain, that is 5, 6 and 7 membered rings, the reaction entropy is a major determining factor, since the reaction enthalpy is low. However, in the case of the norbornene ring system, despite being composed of only five and six membered rings, the strain energy (100 kJ/mol) is comparable to that of cyclopropane (115 kJ/mol). The main reasons for this high strain energy are distortions of the bond angles around the bridging CH_2 group and the alkene unit, and eclipsing of the ring hydrogens due to the six-membered ring being confined to a boat conformation as shown in *Figure 1.30*:

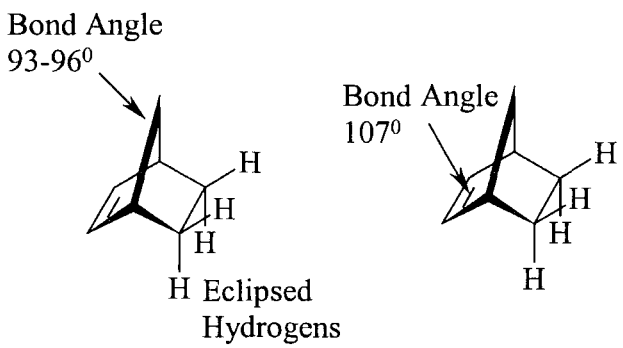

Figure 1.30 The distorted bond angles and eclipsing of the ring hydrogens that leads to the high strain energy of norbornene

If any of the carbon-carbon bonds within a norbornene unit is broken, most of the strain energy is released, and one way in which this can be achieved is by ring-opening metathesis polymerisation (ROMP) using a suitable initiator. Also, another significant advantage of norbornene derivatives as monomers for ROMP is that they have a greatly reduced tendency to undergo secondary metathesis (back biting) with the vinylene units in the polymer backbone due to the steric hindrance of approach to the olefinic moiety resulting from the branching at the alpha carbons.

The ΔG of polymerisation may also be sensitive to structural factors such as the nature of substituents and their position on the ring. Specifically, in ROMP, substituents on a given carbon usually have an unfavourable effect on ΔG, either making ΔG less negative or changing the sign from negative to positive.

1.4.7 Microstructure of Polymer Chains

The way that the monomer unit is incorporated into the polymer chain determines the microstructure, that is the frequency and distribution of the isomeric repeat units, of the resulting polymer.[63-66] The three main factors that define the microstructure of polymers obtained by ring opening metathesis polymerisation are: -

1. Cis/trans vinylene ratios and distribution,
2. Tacticity effects, and
3. Head/head, head/tail and tail/tail frequency and distribution.

1.4.7.1. Cis/Trans Vinylene Ratios and Distribution

The backbone of polymers prepared by ROMP contain unsaturated bonds that can be cis or trans, the ratio of which can be determined by high resolution NMR, *Figure 1.31*. The catalyst system, concentration, solvent and temperature primarily determine the proportion of cis and trans in a particular polymer. The nature of the monomer may also affect the outcome. In practise it has proved possible, through the use of a specific catalyst, to prepare polymers with cis/trans distributions varying form all cis to all trans.

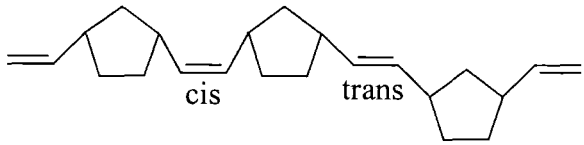

Figure 1.31 Cis/Trans double bonds in polynorbornene

1.4.7.2. Tacticity Effects

Monomers such as symmetrically substituted norbornenes do not have chiral centres but can be polymerised to give polymers with repeat units containing chiral centres. There is the possibility of two centres adjacent to the double bond having the same chiralities resulting in a meso dyad or different chiralities, giving a racemic dyad. Sequences of racemic dyads produce syndiotactic polymers and sequences of meso dyads give isotactic polymers. Polymers with a random distribution of meso and racemic dyads are known as atactic. Due to the possibility of cis or trans geometry, four regular microstructural arrangements are possible as shown in *Figure 1.32.*

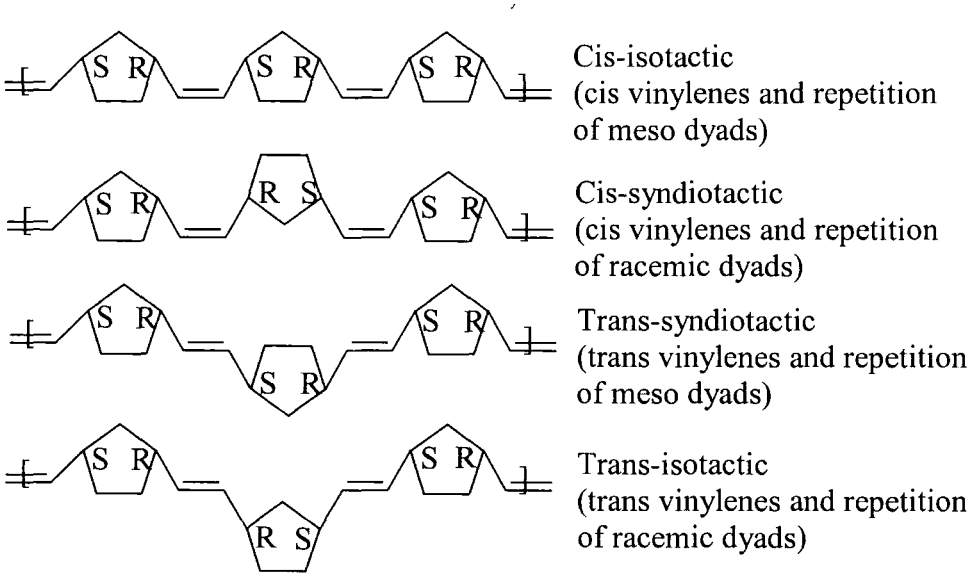

Figure 1.32 Tacticity effects in polynorbornene

1.4.7.3. Head/Head, Head/Tail and Tail/Tail Frequency and Distribution

In the case of unsymmetrically substituted monomers such as 5-substituted norbornene, polymers can form with head-head (HH), head-tail (HT) or tail-tail (TT) structures, *Figure 1.33.* A combination of all the microstructural possibilities leads to

16 ways in which a substituted norbornene can be incorporated into the polymer backbone.

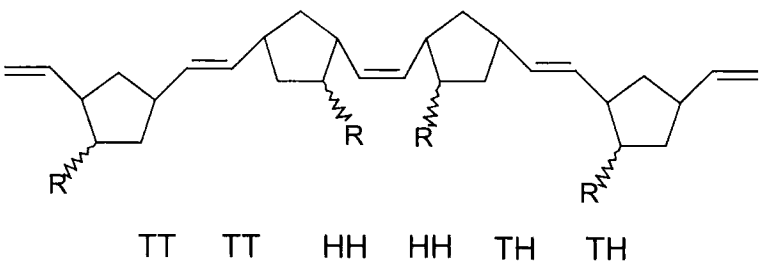

Figure 1.33 Head/tail effects in a polymer synthesised from an unsymmetrically substituted monomer

1.4.8 Summary of Ring Opening Metathesis Polymerisation

From an accumulation of years of research activity, the possibility to use well-defined initiators in the ROMP of both high and low strain substituted monomers now exists. The initiators are not only stable in numerous hostile conditions, but can produce polymers of high molecular weight having narrow molecular weight distributions. Due to the ease of use and advantages of such systems, it was decided to use ring opening as the polymerisation method in the synthesis of dendronised polymers, which is the topic of discussion in the next section.

1.5 Survey of Novel Topologies

1.5.1. Dendronised Polymers – Definition and Role

Dendronised polymers are formally like comb polymers, but are so unique that they are normally not referred to as such. Their uniqueness stems from the effects of factors such as dendron size, the distance between the dendrons, the backbone flexibility or rigidity, together with several interactions (e.g. dendron/dendron, dendron/backbone, solvent/dendron).[67,68] The term dendron designates a dendrimer segment. In this work, the dendrons were not attached to a central core unit to form a dendrimer, but were attached to a monomer unit forming a dendronised monomer. The aforementioned factors result in a slower decrease in density in going from the interior to the exterior than in comb polymers where the linkages are linear chains. This density profile in turn leads to new and interesting properties.

One critical issue is the influence on the shape of the polymer depending on the substitution of dendrons. It has been demonstrated that factors such as the dendron's structure, size and attachment density along the polymer backbone can alter the conformation in polystyrene and polyacrylate from random coil to fully stretched linear. Hence, a flexible polymer can be converted to a rigid rod via substitution with large dendrons. This stiffening of the polymer backbone is due to the steric repulsion between adjacent dendrons and hence the shape is being controlled by the implementation of steric strain. The effect is so profound that a macromolecule can turn into a molecular cylinder with defined dimensions as a result of the densely packed dendritic layer around the polymer backbone, *Figure 1.34*. The length of the cylinder is determined by the degree of polymerisation and the diameter is generally two times the dendron extension.

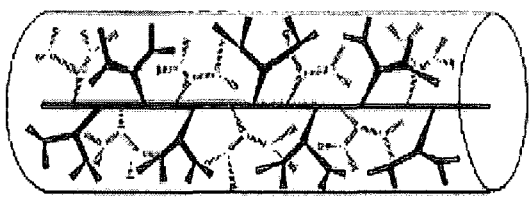

Figure 1.34 Representation of a denronised polymer with an extended backbone due to the effects of the densely packed dendrons

These cylindrical objects are of importance due to their pronounced rigidity and surface characteristics. The diameter of such objects is in the scale of a few nanometers rather than a few angstroms for that of conventional polymers and as such, the rigidity is so high that the persistence length is not on the order of 10nm, but may exceed 50nm. Thus, despite the polymers still being single stranded, they can possess an exceptionally high bending modulus. This leads to the potential use of dendritic rods as constructions on the nanometer scale.

In order for potential uses to be realised, it is necessary to isolate and manipulate individual rods to determine their dimensions. It has been possible thus far to adsorb individual molecules onto atomically flat surfaces. The effects of high modulus are to align these rods in large, ordered, two dimensional arrays where the individual rods are packed parallel to each other. However, the rods synthesised so far have had a length distribution. These large, parallel ordered, nanometer-scale objects

on surfaces are potentially interesting for a number of applications, namely as polarisers, polarised emitters, or orientating surfaces in liquid crystal displays.

Dendrons can also be designed to provide an attractive interaction between each other, leading to shape control. In order for an attractive interaction to take place the dendrons must possess mesogenic properties and be loosely attached to the backbone enabling optimum packing to be determined. Supramolecular organisation/self-assembly of dendrons can lead to columnar or spherical superstructures, the structure formed depending on directional and attractive interactions between such wedge shaped molecules and the size and shape of the dendrons.

1.5.2. Synthesis of Dendronised Polymers

There are two distinct synthetic routes currently used to synthesise dendronised polymers, *Figure 1.35*. In the first route, route A, a sequence of dendrons is attached either divergently or convergently to the anchor groups of a particular polymer. In route B, monomers with dendronised units already attached are subjected to polymerisation. Both routes have associated problems that become more critical with increasing steric demand of the dendrons. The main problem with route A is that it is difficult to achieve complete coverage of dendrons onto the polymer backbone anchor groups. This is due to steric hindrance, especially when large dendrons are to be attached, as existing dendrons may block other unchanged anchor groups on the backbone. A large excess of dendron is often used to try and resolve this problem, however, the purification of the product becomes more difficult as a result.

Steric hindrance also plays a major part in the problems associated with route B. If during the polymerisation process, the steric hindrance of the incoming monomer to the chain end is too high, the process may slow or stop altogether. This has the effect of limiting the molecular weight of the dendronised polymer and is most pronounced with increasing generation of dendron. From the literature,[69,70] it can be deduced that route A to dendronised polymers is inferior due to the fact that no group has been able to achieve complete coverage of the polymer backbone using dendrons with a generation greater than two. In addition to this, the polymeric backbones used did not have very high molecular weights. Due to the mechanism of route B, it is

guaranteed that the polymers will have total coverage of dendrons attached to the anchor groups. As a result of this, the route has proven more successful as one example of both a generation three and four substituted polymer have been synthesised. To date, most dendrons have consisted of the benzyl ether type where the terminal phenyl rings are either unsubstituted or have between one and three long alkoxy or flouroalkoxy chains.

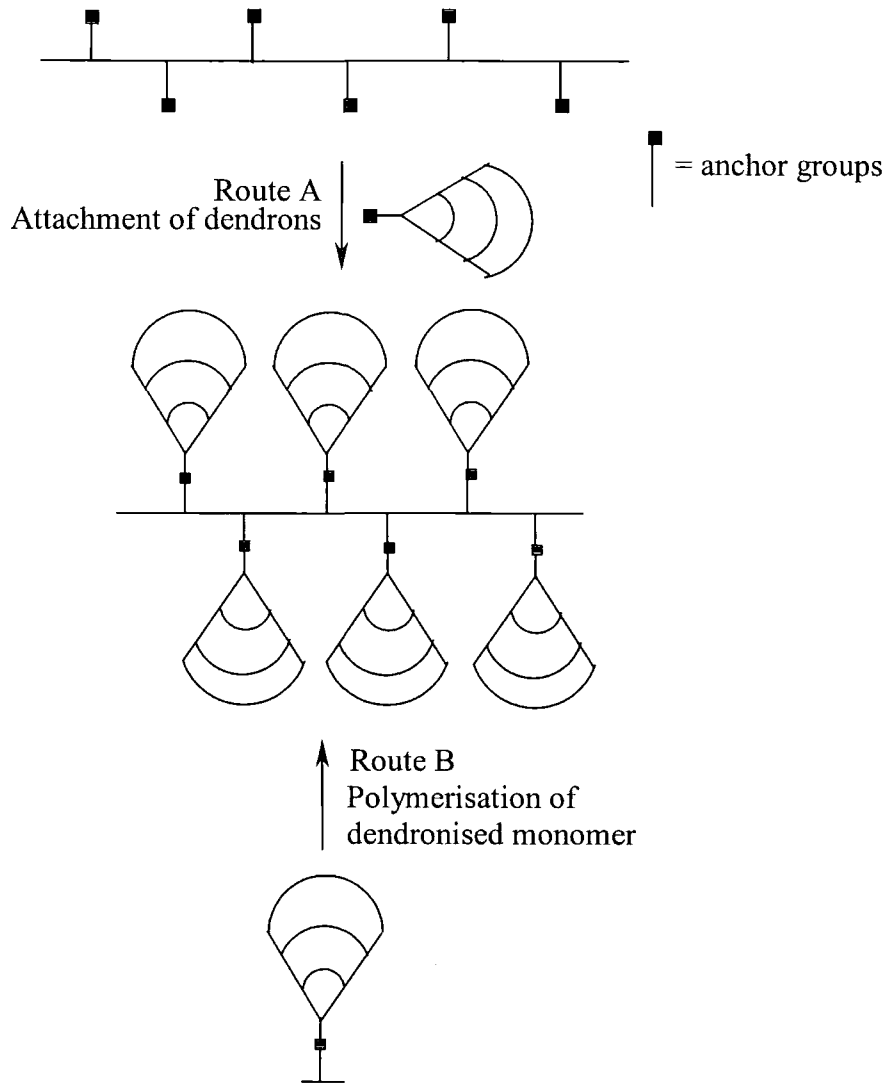

Figure 1.35 The two main synthetic routes to dendronised polymers

1.5.3 Dendronised Polymers via Living ROMP

Percec *et al.* have synthesised a variety of dendronised monomers and polymerised them via ROMP, using Grubbs benzylidene initiator, to form

dendronised oligomers and polymers having a narrow molecular weight distribution. Specifically, the polybenzylether monomer **29**, *Figure 1.36*, was synthesised and it was found that both the monomer and polymers self-assembled into disklike and cylindrical supramolecular structures forming columnar hexagonal liquid crystalline phases.[71] These phases were characterised by Differential Scanning Calorimetry (DSC) and thermal optical polarised microscopy and the shape of the supramolecular architectures was determined via X-ray diffraction experiments.

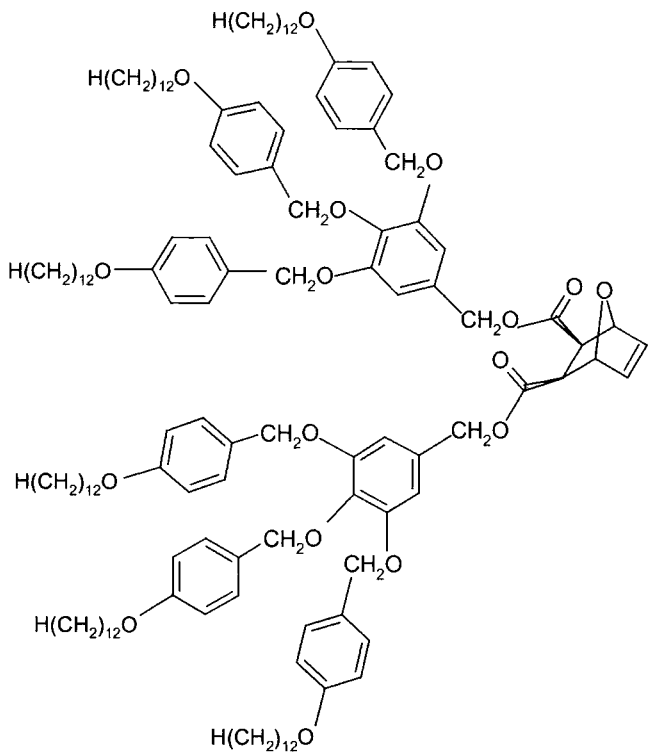

29

Figure 1.36 Exo, exo substituted norbornene derivative containing polybenzylether dendrons[71]

The DSC data indicated the existence of various regimes depending on the degree of polymerisation. In the liquid crystalline phase, two monomer units self-assemble into disklike supramolecular dimers, which represent the stratum of the column, *Figure 1.37*. As the degree of polymerisation increases, rigid three-dimensional cylindrical shapes are formed and finally, once a DP in the region of 26 to 64 is reached, the polymer becomes rod-like. It was also noted that when smaller dendrons were attached to the monomer unit, it required three monomer units to produce a disklike supramolecular architecture.

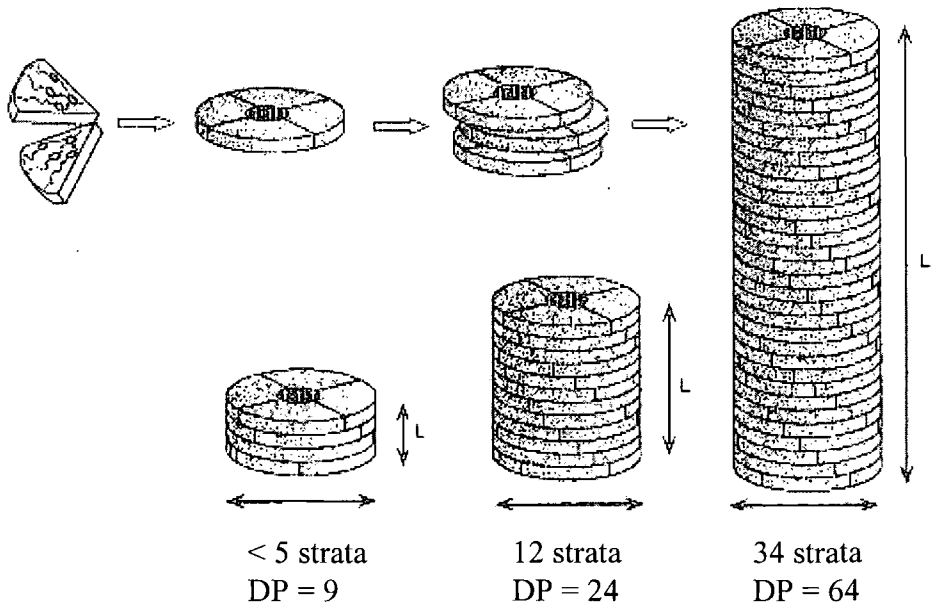

Figure 1.37 Formation of supramolecular columns

From this example, it can be deduced there is a distinct correlation between the polymer architecture and the DP and that the overall structure of the resultant polymer is dependent on the nature of the dendrons attached to the polymer backbone.

In another study by Percec *et al.* it was found that monomer **30,** when polymerised by radical polymerisation, produced a polymer that self-assembled into a tubular supramolecular structure which exhibited hexagonal phases, *Figure 1.38.*[72] However, when a second-generation dendron was used, it was found by scanning force microscopy, that the dendronised polymer's shape changed from spherical to cylindrical as the degree of polymerisation increased. This was accompanied by the backbone conformation going from random-coil to extended. This correlation between polymer conformation and DP is opposite to that seen in most synthetic and natural macromolecules, which usually switch from extended to random coil with increasing DP. As a result of this relationship, there exists the possibility for molecular engineering of polymer shapes and properties and it also demonstrates the impact that the dendron has on the overall shape of the dendronised polymer.

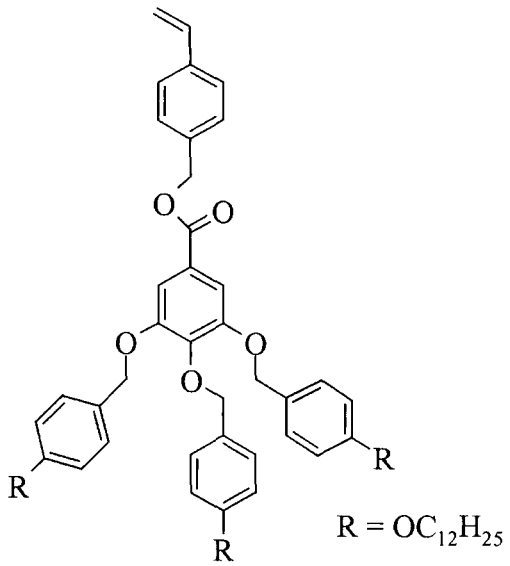

30

*Figure 1.38 Monomer **30** which formed polymers with liquid crystalline phases*

1.6 Summary of Novel Topologies

High molecular weight dendronised polymers are synthetically possible. It has been shown that a correlation exists between the dendron structure and the overall polymer architecture providing researchers with the possibility of synthesising novel architectures with predetermined properties and dimensions.

1.7 Objectives of the Project Reported in this Thesis

The objectives of this work were to synthesise various dendronised monomers, containing dendrons of differing shape and chemical structure, and to then polymerise the monomers using ROMP for the preparation of dendronised polymers. These polymers would then be characterised by a number of methods to deduce the correlation between the dendron structure and the overall polymer architecture.

1.8 References

1. Fréchet, J. M. J. *Synthesis and Properties of Dendrimers and Hyperbranched Polymers*, in *Comprehensive Polymer Science*, Wiley: New York, 2nd Suppl. **1996**, p 71.

2. Newkome, G. R.; Moorefield, C. N.; Vögtle, F. *Dendritic Molecules: Concepts, Syntheses and Applications*; VCH: Weinheim. **1996**.

3. Hult, A.; Johansson, M.; Malmstrom, E. *Adv. Polym. Sci.* **1999**, *143*, 1.

4. Mourey, T. M.; Turner, S. R.; Rubinstein, M.; Fréchet, J. M. J.; Hawker, C. J.; Wooley, K. L. *Macromolecules* **1992**, *25*, 2401.

5. Hawker, C. J.; Fréchet, J. M. J. *J. Am. Chem. Soc.* **1992**, *114*, 8405.

6. Wooley, K. L.; Hawker, C. J.; Fréchet, J. M. J. *J. Chem. Soc. Perkin Trans. 1* **1991**, 1059.

7. Vögtle, F.; Wehner, W.; Buhleier, E. *Synthesis* **1978**, 155.

8. Worner, C.; Mullhaupt, R. *Angew. Chem. Int. Ed. Engl.* **1993**, *32*, 1306.

9. de Brabander-van den Berg, E. M. M.; Meijer, E. W. *Angew. Chem. Int. Ed. Engl.* **1993**, *32*, 1308.

10. Tomalia, D. A.; Baker, H.; Dewald, J.; Hall, M.; Kallos, G.; Martin, S.; Roeck, J.; Ryder, J.; Smith, P. *Poly. Jour.* **1985**, *17*, 117.

11. Tomalia, D. A.; Naylor, A. M. *Angew. Chem. Int. Ed. Engl.* **1990**, *29*, 138.

12. Hawker, C. J.; Fréchet, J. M. J. *J. Am. Chem. Soc.* **1990**, *112*, 7638.

13. Hawker, C. J.; Fréchet, J. M. J. *J. Chem. Soc., Chem. Commun.* **1990**, *15*, 1010.

14. Strobl, G. *The Physics of Polymers*, 1 ed.; Springer: Berlin, **1996**, p. 293.

15. Wooley, K. L.; Fréchet, J. M. J.; Hawker, C. J. *Polymer* **1994**, *35*, 4489.

16. Staab, H. A. *Angew. Chem. Int. Ed. Engl.* **1962**, *1*, 351.

17. Breuilles, P.; Kaspar, K.; Uguen, D. *Tet. Lett.* **1995**, *36*, 8011.

18. Rannard, S.; Davis, N. *Abstr. Pap. Am. Chem. Soc. 214* **1997**, *144-PMSE Part 2*, 63.

19. Rannard, S. P.; Davis, M. J. *J. Am. Chem. Soc.* **2000**, *122*, 11729.

20. Rannard, S. P.; Davis, N. *Org. Lett. 1* **1999**, *6*, 933.

21. Bertolini, G.; Pavich, G.; Vergani, B. *J. Org. Chem.* **1998**, *63*, 6031.

22. Rannard, S. P.; Davis, N. *Org. Lett.* **2000**, *2*, 2117.

23. Rannard, S. P.; Davis, N.; McFarland, H. *Polym. Int.* **2000**, *39*, 1002.

24. Banks, R. L.; Bailey, G. C. *Ind. Eng. Chem. Prod. Res. Dev.* **1964**, *3*, 170.

25. Anderson, A. W.; Merckling, N. G. *U.S. Patent 2721 189. Chem. Abstr.* **1955**, *50*, 3008i.

26. Calderon, N. *Chem. Eng. News.* **1967**, *45*, 51.

27. Calderon, N.; Chen H. Y.; Scott, K. W. *Tetrahedron Lett.* **1967**, *31-40*, 3327.

28. Calderon, N.; Ofstead, E. A.; Judy, W. A. *J. Polym. Sci. Part A-1*, **1967**, *5*, 2209.

29. Calderon, N.; Ofstead, E. A.; Ward, J. P.; Scott, K. W. *J. Am. Chem. Soc.* **1968**, *90*, 4133.

30. Bradshaw, C. P. C.; Howmann, E. J.; Turner, L. *J. Catal.* **1967**, *7*, 269.

31. Herrison, J. L.; Chauvin, Y. *Makromol. Chem.* **1971**, *141*, 161.

32. Fischer, E. O.; Maasbol, A. *Angew. Chem. Inter. Ed.* **1964**, *3*, 580.

33. Casey, C. P.; Burkhardt, T. S. *J. Am. Chem. Soc.* **1973**, *95*, 5833.

34. Howard, T. R.; Lee, J. B.; Grubbs, R. H. *J. Am. Chem. Soc.* **1980**, *102*, 6876.

35. Straus, P. A.; Grubbs, R. H. *Organometallics* **1982**, *1*, 1658.

36. Gilliom, L. R.; Grubbs, R. H. *J. Am. Chem. Soc.* **1986**, *108*, 733.

37. Schavarien, C. J.; Dewan, J. C.; Schrock, R. R. *J. Am. Chem. Soc.* **1986**, *108*, 2771.

38. Murdzek, J. S.; Schrock, R. R. *Organometallics* **1987**, *6*, 1373.

39. Schrock, R. R.; Feldman, J.; Cannizzo, L. F.; Grubbs, R. H. *Macromolecules* **1987**, *20*, 1169.

40. Schrock, R. R.; DePue, R. T.; Feldman, J.; Schavarien, C. J.; Dewan, J. C.; Liu, A. H. *J. Am. Chem. Soc.* **1988**, *110*, 1423.

41. Schrock, R. R.; Murdzek, J. S.; Bazan, G. C.; Robbins, J.; DiMare, M.; O'Regan, M. *J. Am. Chem. Soc.* **1990**, *112*, 3875.

42. Schrock, R. R.; DePue, R. T.; Feldman, J.; Yap, K. B.; Yang, D. C.; Davis, W. M.; Park, L.; DiMare, M.; Schofield, M.; Anhaus, J.; Walborsky, E.; Evitt, E.; Kruger, C.; Betz, P. *Organometallics* **1990**, *9*, 2262.

43. Schrock, R. R. *Acc. Chem. Res.* **1990**, *23*, *158*.

44. Grubbs. R. H.; Trnka. T. M. *Acc. Chem. Res.* **2001**, *34*, 18.

45. Novak, B. M.; Grubbs, R. H. *J. Am. Chem. Soc.* **1988**, *110*, 7542.

46. Lu, S. Y.; Quayle, P.; Heatley, F.; Booth, C.; Yeates, S. G.; Padget, J. C. *Macromolecules* **1992**, *25*, 2692.

47. Hillmyer, M. A.; Lepetit, C.; McGrath, D. V.; Novak, B. M.; Grubbs, R. H. *Macromolecules* **1992**, *25*, 3345.

48. Wu, Z.; Benedicto, A. D.; Grubbs, R. H. *Macromolecules* **1993**, *26*, 4975,

49. Nguyen, S. T.; Grubbs R. H.; Ziller, J. W. *J. Am. Chem. Soc.* **1993**, *115*, 9858.

50. Fu, G. C.; Nguyen, S. T.; Grubbs, R. H. *J. Am. Chem. Soc.* **1993**, *115*, 9856.

51. Schwab, P.; Grubbs R. H.; Ziller, J. W. *J. Am. Chem. Soc.* **1996**, *118*, 100.

52. Lynn, D. M.; Kanaoka, S.; Grubbs, R. H. *J. Am. Chem. Soc.* **1996**, *118*, 784.

53. Yates, P. *J. Am. Chem. Soc.* **1952**, *74*, 5376.

54. Scholl, M.; Ding, S.; Lee, C. W.; Grubbs, R. H. *J. Org. Lett. 1* **1999**, *6*, 953.

55. Chatterjee, A. K.; Morgan, J. P.; Scholl, M.; Grubbs, R. H. *J. Am. Chem. Soc.* **2000**, *122*, 3783.

56. Ackermann, L.; Fustner, J.; Weskamp, J.; Kohl, F. J.; Herrmann, W. A. *Tetrahedron Lett.* **1999**, *40*, 4787.

57. Chatterjee, A. K.; Grubbs, R. H. *Org. Lett. 1*, **1999**, 1751.

58. Bielawski, C. W.; Grubbs, R. H. *Angew. Chem. Int. Ed.* **2000**, *39*, 16.

59. Arduengo, A. J. *J. Am. Chem. Soc.* **1997**, *119*, 12742.

60. Trnka, T. M.; Morgan, J. P.; Sanford, M. S.; Wilhelm, T. E.; Scholl, M.; Choi, T. L.; Ding, S.; Day, M. W.; Grubbs, R. H. *J. Am. Chem. Soc.* **2003**, *125*, 2546.

61. Sanford, M. S.; Ulman, M.; Grubbs, R. H. *J. Am. Chem. Soc.* **2001**, *123*, 749.

62. Sanford, M. S.; Love, J. A; Grubbs, R. H. *J. Am. Chem. Soc.* **2001**, *123*, 6543.

63. Hamilton, J. G.; Ivin, K. J.; Rooney, J. J. *J. Mol. Catal.* **1985**, *28*, 255.

64. Steinhäusler, T.; Stelzer, F.; Zenkl, E. *Polymer* **1994**, *35*, 616.

65. Sunaga, T.; Ivin, K. J.; Hofmeister, G. E.; Oskam, J. H.; Schrock, R. R. *Macromolecules* **1994**, *27*, 4043.

66. Feast, W. J.; Gibson, V. C.; Ivin, K. J.; Kenwright, A. M.; Khosravi, E. *J. Mol. Catal.* **1994**, *90*, 87.

67. Rabe, J. P.; Schlüter, A. D. *Angew. Chem. Int. Ed.* **2000**, *39*, 864.

68. Frey, H. *Angew. Chem. Int. Ed.* **1998**, *37*, 2193.

69. Freundenberger, R.; Claussen, W.; Schlüter, A. D.; Wallmeier, H. *Polymer* **1994**, *35*, 4496.

70. Percec, V.; Heck, J.; Tomazos, D.; Falkenberg, F.; Blackwell, H.; Ungar, G. *J. Chem. Soc. Perkin Trans.* **1993**, 2799.

71. Percec, V.; Schlueter, D. *Macromolecules* **1997**, *30*, 5783.

72. Percec, V.; Ahn, H.; Ungar, G.; Yeardley, D. J. P.; Moller, M.; Sheiko, S. S. *Nature* **1998**, *391*, 161.

Chapter 2

Synthesis and Characterisation of Monomers, Dendrons and Novel Dendronised Monomers

2.1 Introduction

The aim of the project was to synthesise dendronised monomers containing various dendritic structures and to polymerise them via ROMP for the provision of dendronised polymers. Analysis of the polymers by a number of characterisation methods, including AFM to determine their shape and size, would then reveal the effect of the dendron structure on the overall polymer architecture and organisation.

The first task in the synthesis of dendronised monomers was to prepare a series of monomer derivatives using the Diels-Alder reaction. Functional group conversion reactions were then performed on the monomer derivatives to obtain the desired functionalities to be used as attachment points for the dendrons. Dendrons containing different chemical structures and generations were then synthesised using the selectivity of 1,1'-carbonyl diimidazole (CDI). The dendrons were then coupled to the monomer derivatives, resulting in the synthesis of dendronised monomers.

The design, synthesis and characterisation of monomers, dendrons and a novel series of dendronised monomers will be described in this chapter. A code by which the dendrons and dendronised monomers are to be identified will also be explained. The use of ROMP in the preparation of dendronised polymers will be discussed in chapter 3, with molecular modelling and AFM studies being addressed in chapter 4.

2.2 The Diels-Alder Cycloaddition Reaction

A typical Diels-Alder reaction involves 1,4-addition of a dienophile to a 1,3-diene to give a six membered ring, as shown in *Figure 2.1*.[1,2,3]

Figure 2.1 The Diels-Alder reaction between a conjugated diene and dienophile, where X denotes an electron withdrawing group

The reaction mechanism involves a pericyclic process, which takes place in a single step by a cyclic redistribution of bonding electrons. The two reactants join together in a concerted fashion through a cyclic transition state in which two new σ-bonds form at the expense of two π-bonds in the starting material. So when X represents an electron-withdrawing group, as in *Figure 2.1*, the rate of reaction increases with respect to that of a simple alkene and it decreases when X represents an electron-donating group. The diene must adopt a cis conformation in order that carbons 1 and 4 of the diene are close enough to react through a cyclic transition state; five membered ring dienes are particularly favoured due to the fact that they are rigidly fixed in the correct cis geometry.

One of the most useful features of a Diels-Alder reaction is that the stereochemistry of the starting dienophile is maintained during the reaction and a single product isomer, sometimes a racemate, results. However, when dealing with bicyclic structures, there are two possible ways in which addition can take place. The larger side of the dienophile may be under the ring (*endo* addition), or the reverse (*exo* addition) depending on the reaction conditions, *Figure 2.2*.

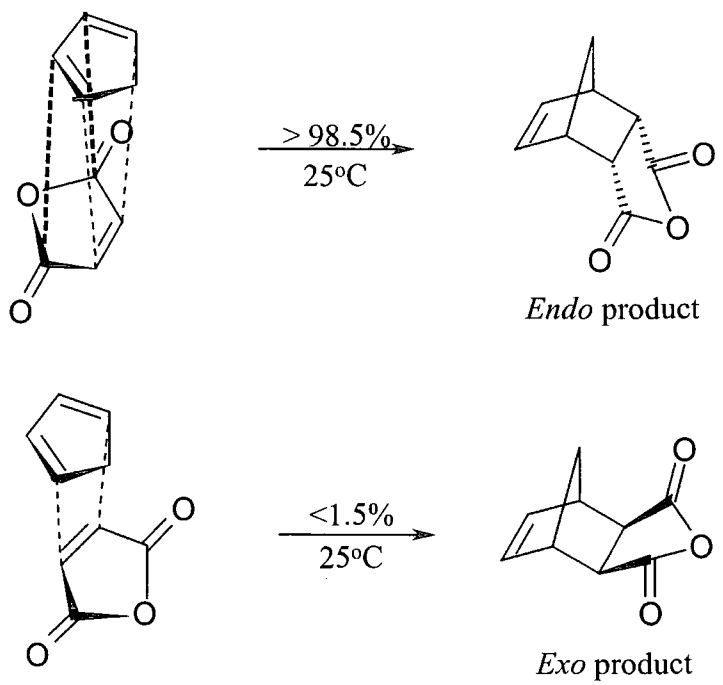

Figure 2.2 Representation of the orientation of the reactants in the approach to the transition state and the products of the Diels-Alder cycloaddition reaction between cyclopentadiene and maleic anhydride

When the reaction is under moderate temperature conditions, the addition is predominantly *endo*, the kinetically favoured product. This is usually attributed to the fact that in this case the dienophile is added so as to give a maximum of 'secondary overlap' of π-molecular orbitals in the transition state. Higher reaction temperatures and longer reaction times favour the thermodynamic product, the *exo* isomer. However, the endo product is invariably the kinetic product whether or not there is the possibility of secondary overlap of π-molecular orbitals, for example, cyclopentene gives the *endo* isomer as the kinetic product in reactions with cyclopentadiene.

2.3 Synthesis and Characterisation of Norbornene Derivatives

Norbornene derivatives have been successfully synthesised and characterised through the use of the Diels-Alder reaction. Subsequent functional group conversion has led to the acquisition of monomers to which dendrons can be attached.

2.3.1 Synthesis and Characterisation of Norbornene-5-*exo*-methanol

Three separate reactions were required in order to synthesise norbornene-5-*exo*-methanol, *Figure 2.3*. Norbornene-5-carboxylic acid was obtained as a mixture of *exo* and *endo* isomers from the reaction of dicyclopentadiene with acrylic acid, using a small amount of hydroquinone to prevent the radical induced polymerisation or oligomerisation of the acid, at 160°C.[4] The crude product was distilled to remove excess acrylic acid and a ratio of approximately 50/50 *endo*/*exo* norbornene-5-carboxylic acid was determined by analysis of the ^{1}H NMR spectrum.

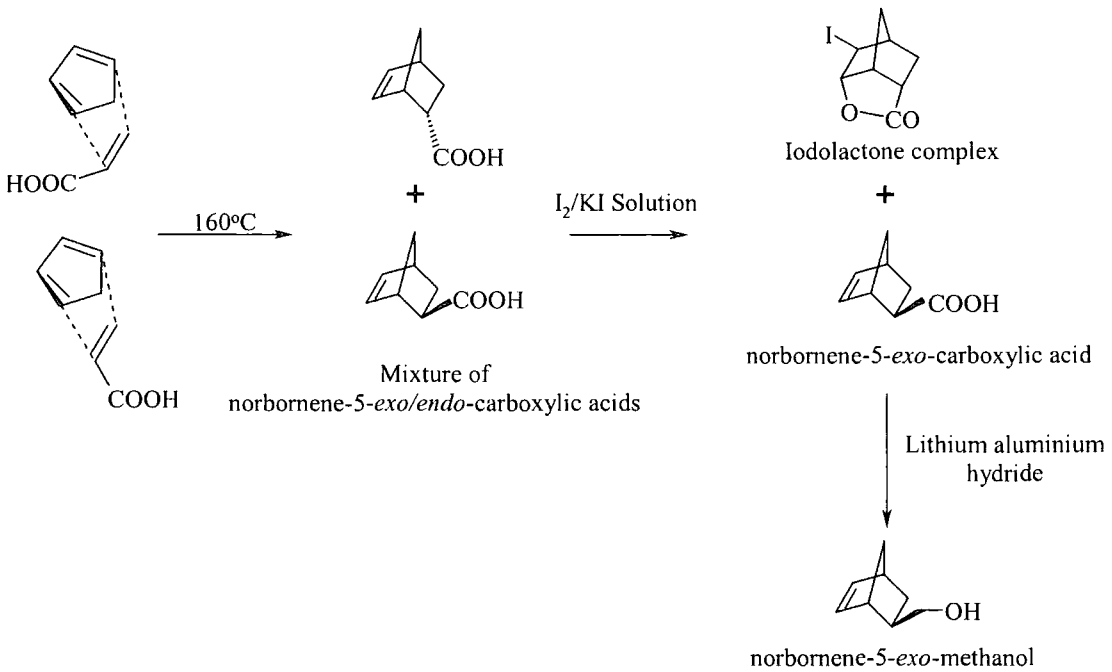

Figure 2.3 The synthetic stages involved in the synthesis of norbornene-5-exo-methanol

The vinylic hydrogens have different chemical shifts depending on whether the isomer of the acid is *endo* or *exo*. The vinylic hydrogens of the *exo* isomer have very similar chemical shifts of 6.14 and 6.10 ppm, whereas in the *endo* isomer, the chemical shifts occur at 6.19 and 5.98 ppm, *Figure 2.4*. This can be explained by the fact that in the *endo* isomer, the vinylic hydrogens are in closer proximity to the carboxylic acid and experience a shielding effect.[5]

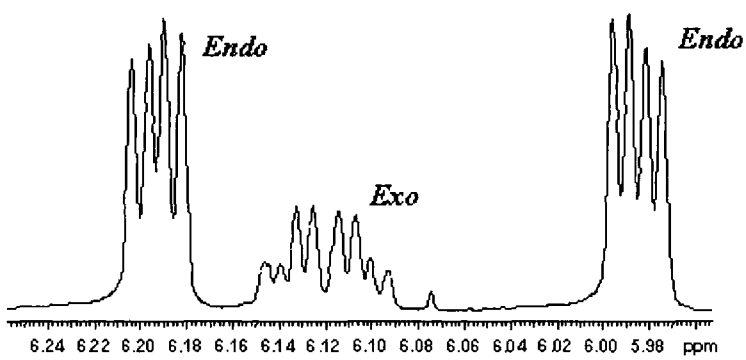

Figure 2.4 Region of the ^1H NMR spectrum of exo/endo 5-norbornene-2-carboxylic acid showing the vinylic hydrogen signals for the endo and exo isomers

Both molecules give pseudo AB quartets for the vinylic hydrogens, with each limb split by further coupling. The structure gives rise to a complex AA'BB'X non-first order splitting pattern in which the vinylic bridgehead and 7-anti hydrogens all interact and the apparent simplification into AB quartets is fortuitous and can be misleading.

Pure norbornene-5-*exo*-carboxylic acid was obtained through the removal of the *endo* isomer as the iodolactone, *Figure 2.5*.

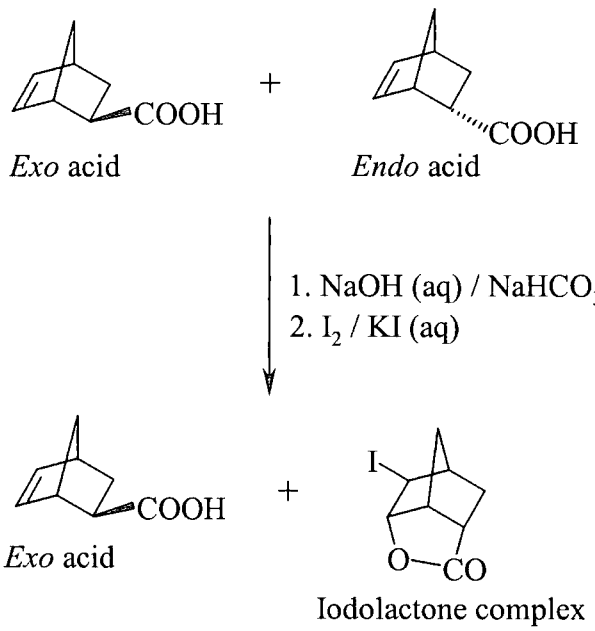

Figure 2.5 Conversion of the endo isomer to the iodolactone complex

The iodolactone was formed from the *endo* isomer when iodine was added to an aqueous solution of the mixed sodium salts, precipitated as a dark oil and was separated. The aqueous layer was then acidified, extracted with ether and washed with a solution of sodium thiosulphate to remove excess iodine. Several recrystallisations gave the *exo* isomer as a pale yellow solid. Analysis of the ^1H NMR spectrum showed that only the *exo* isomer remained, as the two signals corresponding to the *endo* isomer had totally disappeared. It was found that there was a poor correlation between the expected and found carbon elemental analysis values for the product. This was also found to be the case with the di-substituted acid derivative (section 2.3.2) and the mono-substituted alcohol derivative, discussed in this section. The poor correlations are thought to be due to the hygroscopic nature of these compounds, which made them difficult to dry. The calculated elemental analysis

value for carbon was always found to be higher than the experimental result obtained, which also indicated that there was water present in the sample. The elemental analysis results from the other norbornene monomer derivatives were found to have a good correlation with the expected values. The purity and structure of all the intermediates was, nevertheless, unambiguously established by ^{1}H and ^{13}C NMR spectroscopy and mass spectrometry, see Experimental section 5.2.1, pp 128. Further, the dendronised monomers required for this project, which were derived from these intermediates, were shown to be single compounds of the correct structure by spectroscopic and chromatographic analyses.

Norbornene-5-*exo*-methanol, *Figure 2.6,* was synthesised via the reduction of norbornene-5-*exo*-carboxylic acid using $LiAlH_4$ in dry diethyl ether.

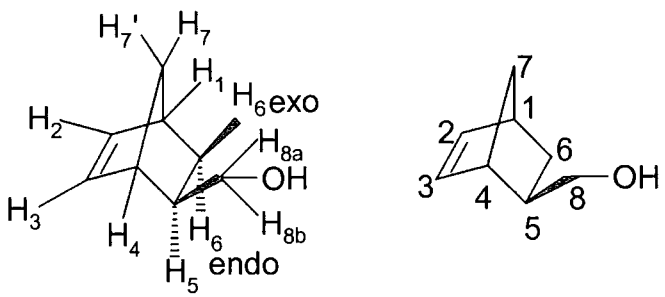

Figure 2.6 Structure of 5-norbornene-2-exo-methanol

After work-up, the alcohol was obtained as a colourless liquid. Analysis of the ^{1}H NMR spectrum of norbornene-5-*exo*-methanol shows that the vinylic hydrogens appear as two pseudo ABqs with further splittings analogous to the spectrum of the acid starting material. Norbornene-5-*exo*-methanol is chiral and, as a consequence, the hydrogens on C_8, C_6 and C_7 are not equivalent. As a result of this, the ^{1}H NMR spectrum shows two signals for H_{8a} and H_{8b} at 3.67 ppm and 3.51 ppm, *Figure 2.7.* Each hydrogen on C_8 couples to the other ($J_{8a,8b}$ ~ 10.6Hz) and, have different coupling constants to H_5 ($J_{8b,5}$ ~ 8.7Hz and $J_{8a,5}$ ~ 6.3Hz). Therefore, H_{8a} and H_{8b} are both represented by a doublet of doublets.

The signals for the hydrogens attached to C_6 appear at chemical shifts of 1.10 and 1.06 ppm. The hydrogens couple with each other ($J_{6exo,6endo}$ ~ 11.5Hz) and each hydrogen couples differently with H_5 and H_1. If the hydrogen is in the exo position,

($J_{6exo,5} \sim J_{6exo,1} \sim 4Hz$), the signal is seen as a doublet of triplets. The hydrogens on C_7 were difficult to interpret due to the fact they were superimposed on other signals.[6]

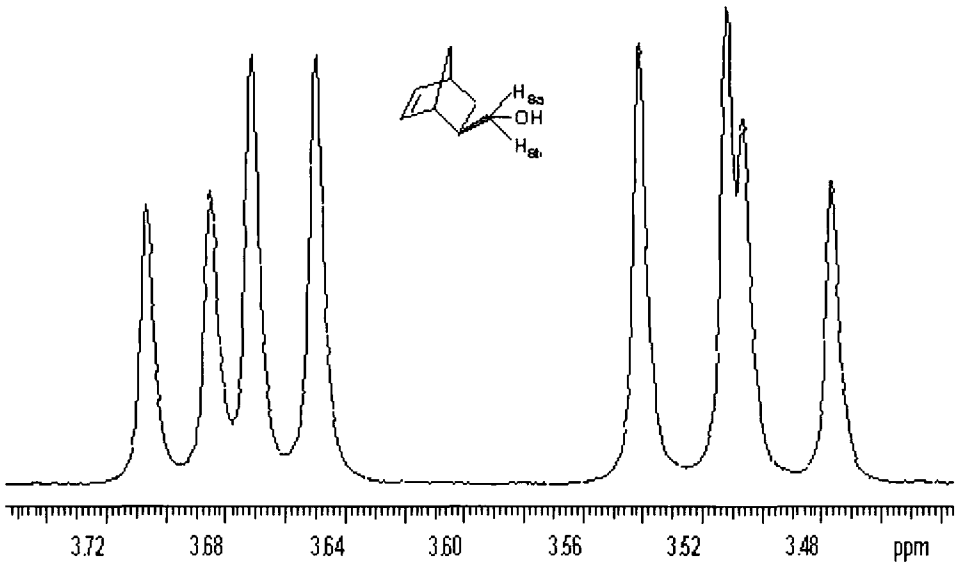

Figure 2.7 Region of the ^1H NMR spectrum of norbornene-5-exo-methanol showing diastereotopic protons H_{8a} and H_{8b}

2.3.2 Synthesis and Characterisation of Norbornene-5-*exo*, 6-*exo*-dimethanol

Three separate reactions were also required to synthesise norbornene-5-*exo*, 6-*exo*-dimethanol, *Figure 2.8*. The synthesis of norbornene-5, 6-dicarboxylic anhydride as a mixture of both *exo* and *endo* isomers (50/50 ratio), was performed by a Diels-Alder reaction between maleic anhydride and dicyclopentadiene at high temperature. A reaction temperature above 180°C was necessary in order to crack dicyclopentadiene into cyclopentadiene and to obtain as high as possible ratio of the thermodynamically favoured *exo* isomer. It was also found that, as expected, a longer reaction time resulted in increased formation of the *exo* isomer, the thermodynamic product. Despite these harsh conditions, multiple recrystallisations using acetone were required in order to produce pure *exo* isomer as a transparent, crystalline solid.

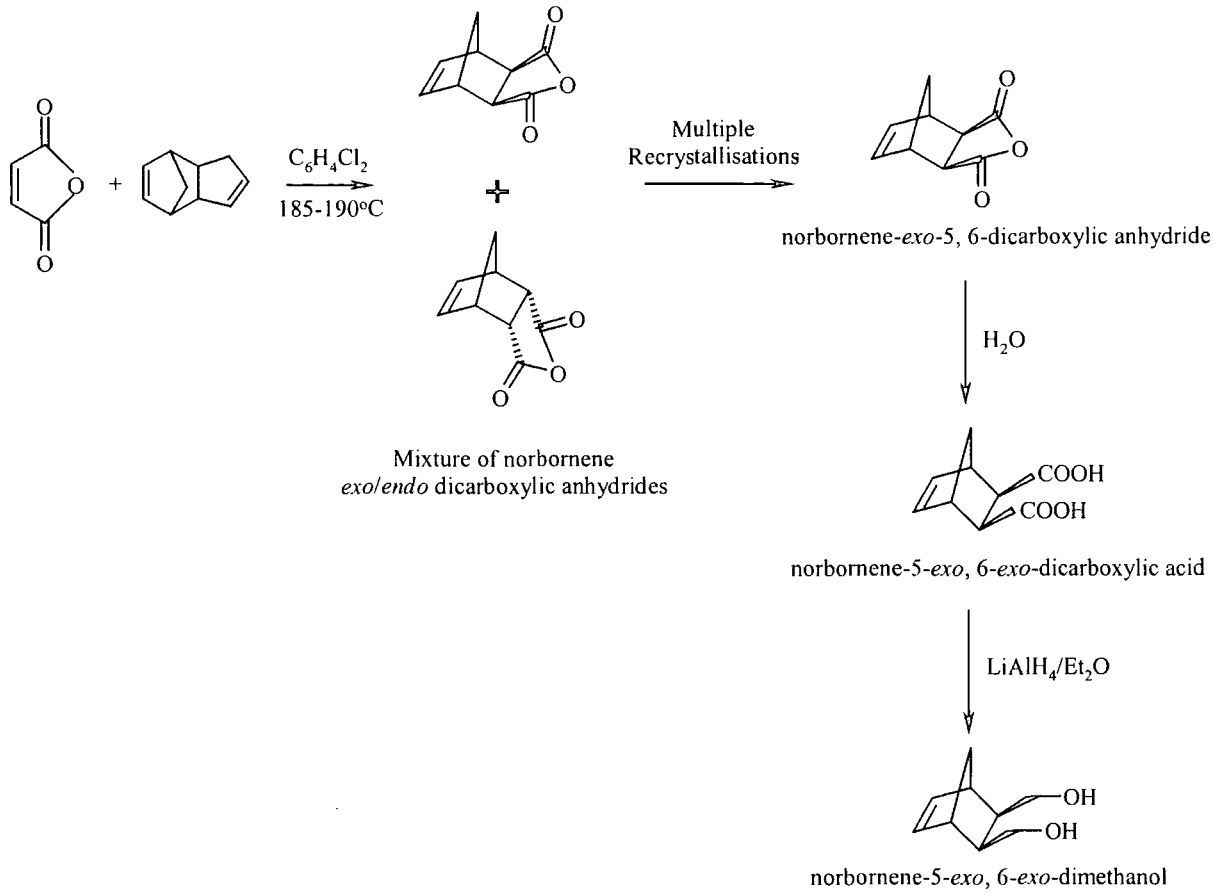

Figure 2.8 The synthetic stages involved in the synthesis of norbornene-5-exo, 6-exo dimethanol

The purity of the *exo* isomer was confirmed by analysis of the ^1H NMR spectrum, which showed that the signal corresponding to the *endo*-adduct at 6.29 ppm had totally disappeared, leaving only the *exo*-adduct signal at 6.38 ppm. Norbornene-*exo*-5, 6-dicarboxylic anhydride was hydrolysed to afford norbornene-5-*exo*, 6-*exo*-dicarboxylic acid. Evidence that the hydrolysis had taken place was obtained from analysis of the ^1H NMR spectra of both compounds. It can be seen from the spectrum, *Figure 2.9,* that the difference in chemical shifts for the AB quartet signals arising from H_7 and $H_{7'}$ is greater in the dicarboxylic acid than in the corresponding anhydride. The reason for this difference in chemical shifts is that the carbonyl groups of the acid have less restriction to their movement than in the corresponding anhydride, due to the rigid ring structure of the anhydride. This comparatively greater freedom of movement results in the carbonyl groups being in closer proximity to $H_{7,7'}$, leading to a larger interaction. Another feature of the spectrum that led to the belief

that norbornene-5-*exo*, 6-*exo*-dicarboxylic acid had formed is that the vinylic signal had shifted from 6.38 ppm for the anhydride to 6.24 ppm for the acid.

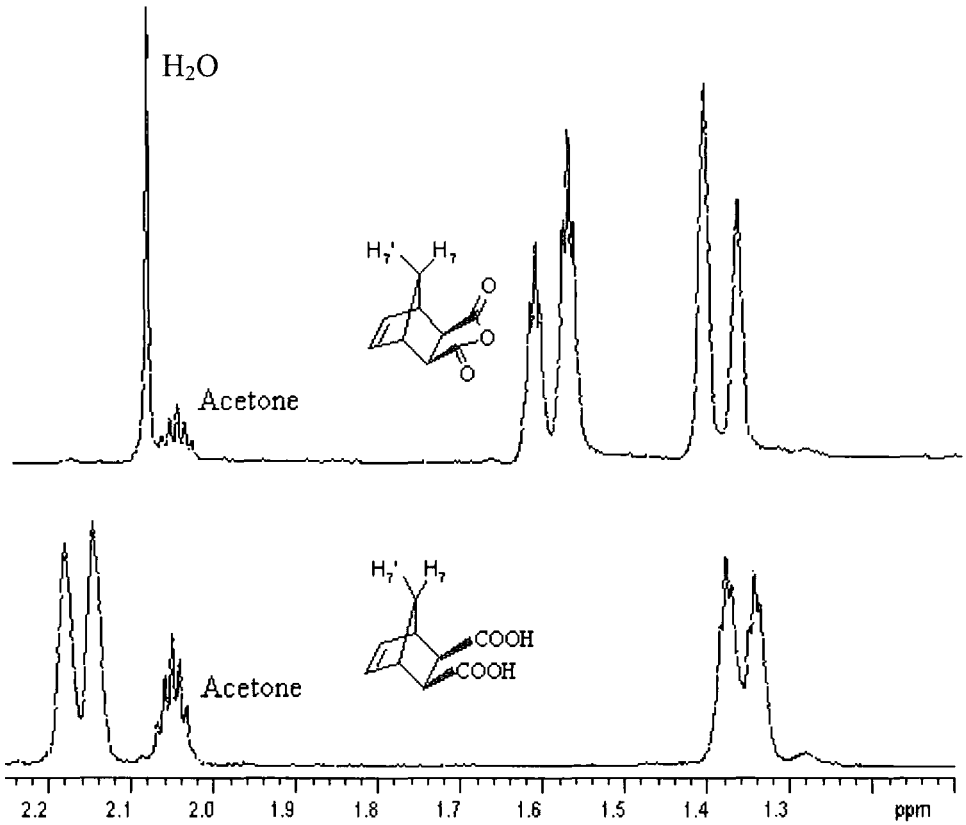

Figure 2.9 ^{1}H NMR spectra for norbornene-exo-5, 6-dicarboxylic anhydride, top, and norbornene-5-exo, 6-exo-dicarboxylic acid, bottom.

Norbornene-5-*exo*, 6-*exo*-dimethanol was prepared via the reduction of norbornene-5-*exo*, 6-*exo*-dicarboxylic acid using $LiAlH_4$ in dry diethyl ether. In the ^{1}H NMR spectrum of the product, a signal appeared at 3.51 ppm corresponding to the two hydrogens of the hydroxyl groups. This assignment was confirmed by performing a deuterium exchange reaction, which produced a new signal for HOD at around 4.6 ppm whilst removing the previous –OH signal. There was also a marked difference in the chemical shifts of H_7 and $H_{7'}$ for the diol as opposed to the diacid. The signals for these two hydrogens on the alcohol were closer together (1.33 and 1.26 ppm) than that of the equivalent hydrogens on the acid (2.15 and 1.34 ppm). The reason for this pronounced difference is thought to be due to the increased interaction

and shielding effect that the carbonyl groups are having on one of the bridging C_7 hydrogens.

2.3.3 Synthesis and Characterisation of Norbornene-5-*exo*, 6-*exo*-dicarbonyl chloride

Norbornene-5-*exo*, 6-*exo*-dicarbonyl chloride was synthesised from the reaction of norbornene-5-*exo*, 6-*exo*-dicarboxylic acid with oxalyl chloride. Analysis of the ^{1}H NMR spectrum of the product showed that the vinylic hydrogens of the acid (6.24 ppm) had totally disappeared and that a new signal corresponding to the vinylic hydrogens of the acid chloride was present at 6.37 ppm. Elemental analysis values also indicated that the acid chloride had formed, as the chlorine percentage of the product (32.04) found, was close to the expected value (32.37).

2.4 Synthesis and Characterisation of Dendrons

A series of dendrons of different generations possessing different chemical structures has been synthesised. Polycarbonate dendrons of the first and second generation, containing t-butyl terminal groups, have been synthesised in a stepwise manner from t-butanol, CDI and 1-[N, N-bis(2-hydroxyethyl)amino]-2-propanol (**HEAP**). Using precursors obtained in previous studies,[7] second generation polyurethane dendrons containing both t-butyl and 4-heptyl terminal groups have been synthesised. The synthesis of a second generation polyurethane dendron containing a benzhydryl terminal group was also attempted. Finally, a first generation polyamide dendron was synthesised with phenyl rings as terminal groups.

2.4.1 Nomenclature of Dendrons

The code used in this thesis to identify the polycarbonate and polyurethane dendrons is based on three parts. The first part describes the nature of the terminal groups, the second part indicates the number of generations and the third signifies the functionality at the focal point of the dendron, see table in *Figure 2.10.* Firstly, the three terminal groups are represented by letters; *t*-**B**utyl (**B**), 4-**H**eptyl (**H**) and **B**enz**H**ydryl (**BH**). The second part indicates the generation of the structure with the term G***x***, where ***x*** is the generation number. Finally, the functionalities at the focal points of the dendrons are represented by letters; secondary alc**OH**ol, (**OH**), and

IMidazole carboxylic ester group, (IM). Note, that polyurethane dendrons are denoted with the symbol (U) at the end of the code.

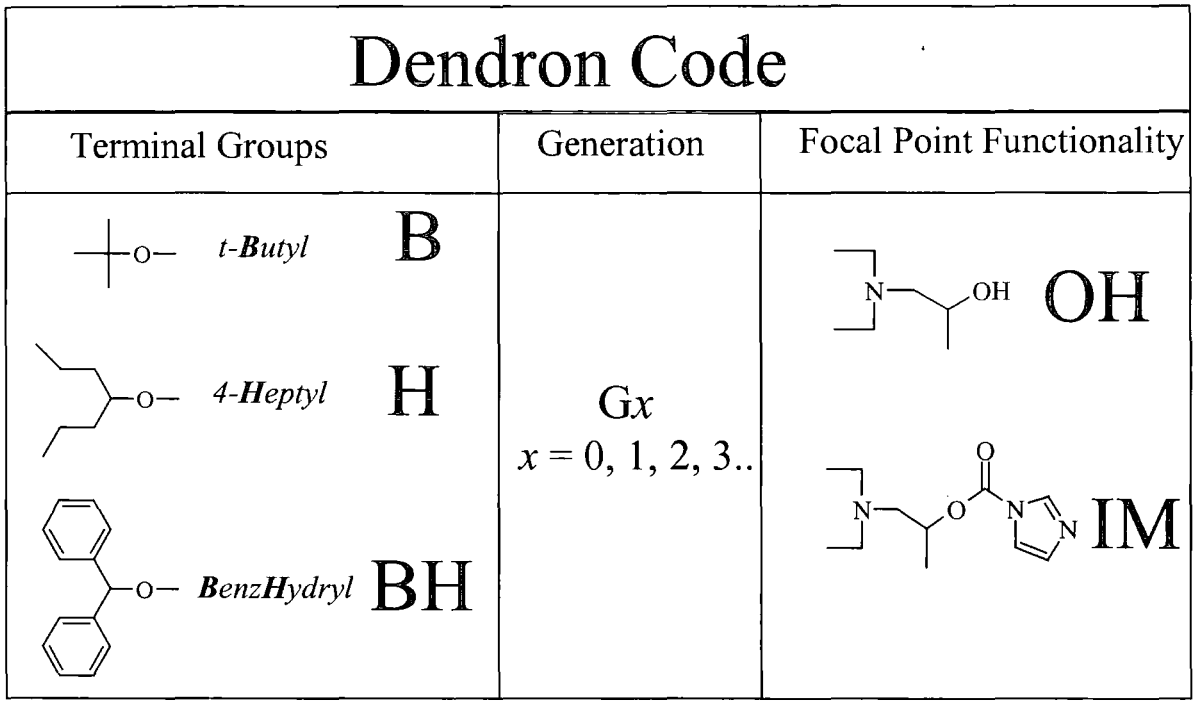

Figure 2.10 Identification code for polycarbonate and polyurethane dendrons

A first and second generation polycarbonate and polyurethane dendron, respectively, containing two different functionalities at the focal point, are shown with their corresponding codes in *Figure 2.11*.

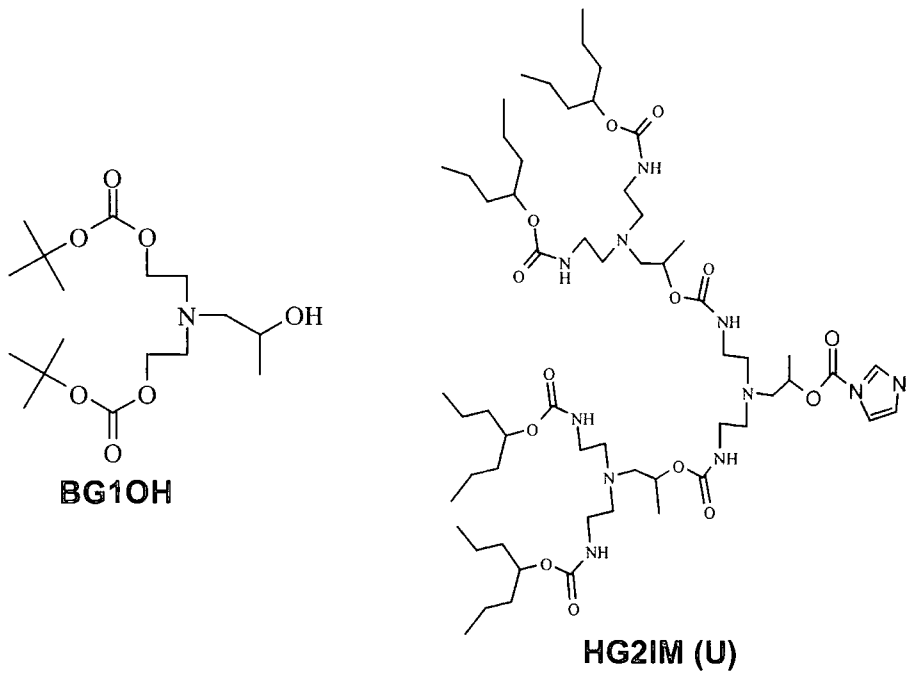

Figure 2.11 Identification codes for a first generation polycarbonate (left) and a second generation polyurethane dendron (right) containing different functionalities at the focal points

2.4.2 Synthesis of First Generation Polycarbonate Dendrons

The three synthetic steps required in the synthesis of the first generation polycarbonate dendron, **BG1IM**, containing an imidazole carboxylic ester group at the focal point are shown in *Figure 2.12*.

In the first step, despite the presence of the alcohol in excess, t-butanol reacted in an equimolar ratio with CDI, to give adduct **BG0IM**. An excess of the alcohol was necessary to ensure that no leftover CDI could react with **HEAP** in the subsequent step, producing unwanted side reactions. Toluene was used as the reaction solvent throughout as the imidazole by-product produced in each synthetic step has low solubility in this solvent. This resulted in the imidazole precipitating as the reaction mixture cooled, allowing easy removal. In the second step, 0.5 equivalents of **HEAP**, the branching unit containing two primary alcohol functions and one secondary alcohol function, was added to a solution of **BG0IM** under basic conditions (KOH). A reaction temperature of 85°C and a time of 3 days were required in order for the reaction to reach completion. Such harsh conditions were necessary due to the relatively low nucleophilicity and hence reduced reactivity of the primary alcohols. The addition of base was essential for the success of the reaction and the

concentration of the mixture was found to have an effect on the rate of the reaction. However, the optimum conditions were difficult to determine due to problems with the reproducibility of the reaction. The crude material formed was purified using silica gel chromatography, eluting with ethyl acetate and hexane in a ratio of 1:1, to give **BG1OH** as colourless oil in a yield of 46%. The calculated elemental analysis values for all the polycarbonate dendrons were found to be in good agreement with the expected values.

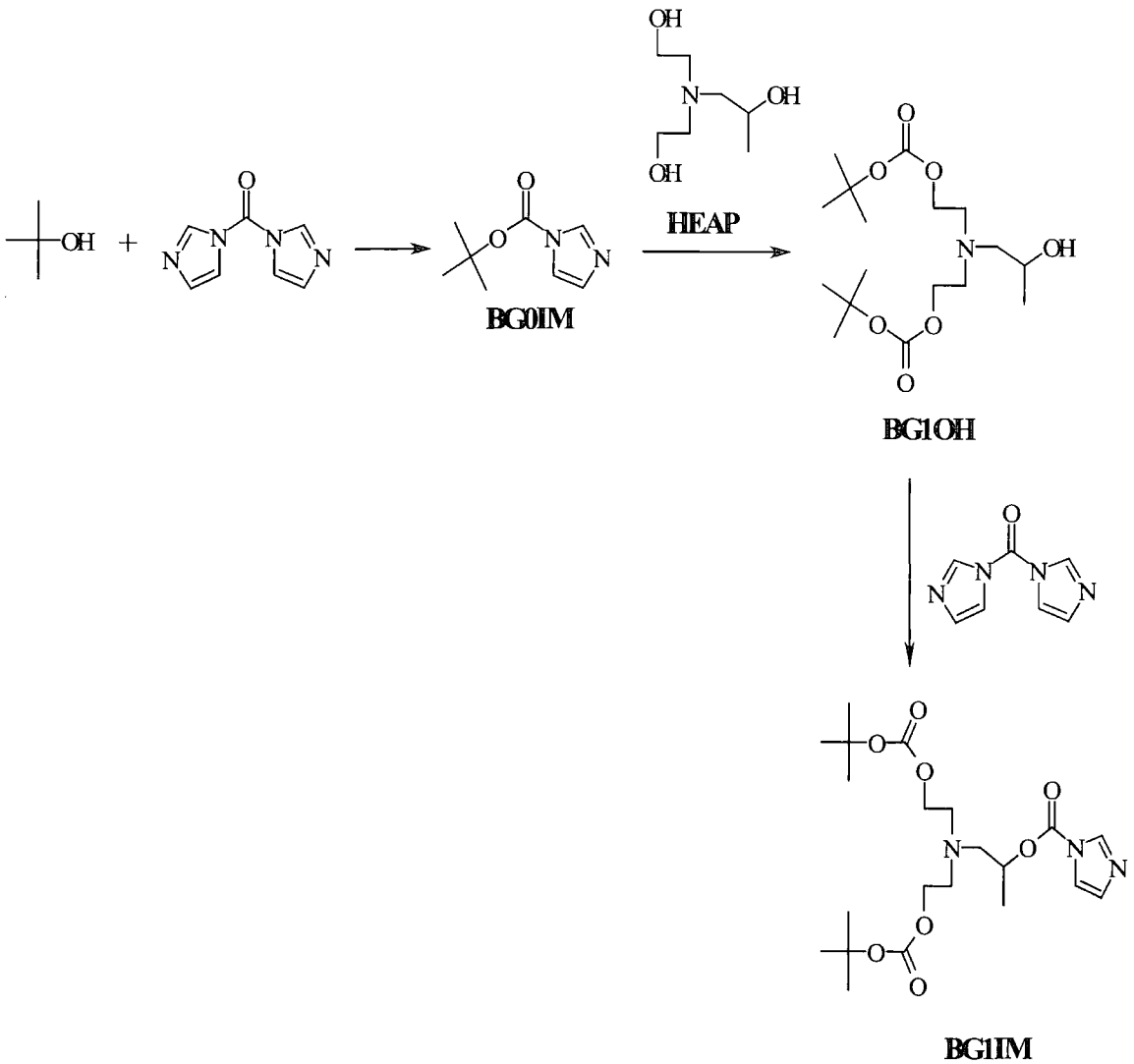

Figure 2.12 Synthetic steps involved in the synthesis of the first generation polycarbonate dendron **BG1IM**

^{1}H NMR spectroscopy was found to be useful in the assignment of **BG1OH**, however, the presence of diastereotopic hydrogens in the molecule complicated the

spectrum. For example, H_α and H_β of the methylene group adjacent to the chiral centre have chemical shifts that differ by 0.3 ppm and are seen as two doublets of doublets, *Figure 2.13*.

The hydrogens H_α and H_β of **BG1OH** appear as an AB quartet with a coupling constant of 13Hz, but each limb of the ABq couple to the hydrogen at the chiral centre with vastly different coupling constants of 10.4Hz and 2.8Hz. In **BG1OH**, there are three sets of diastereotopic hydrogens in total, with two pairs being present between the carbonate group and the tertiary amine function. However, the coupling pattern of these two pairs was complex, probably as a result of a non-first order interaction of all four hydrogens. The ^{13}C NMR spectrum of **BG1OH** contained eight signals, as expected.

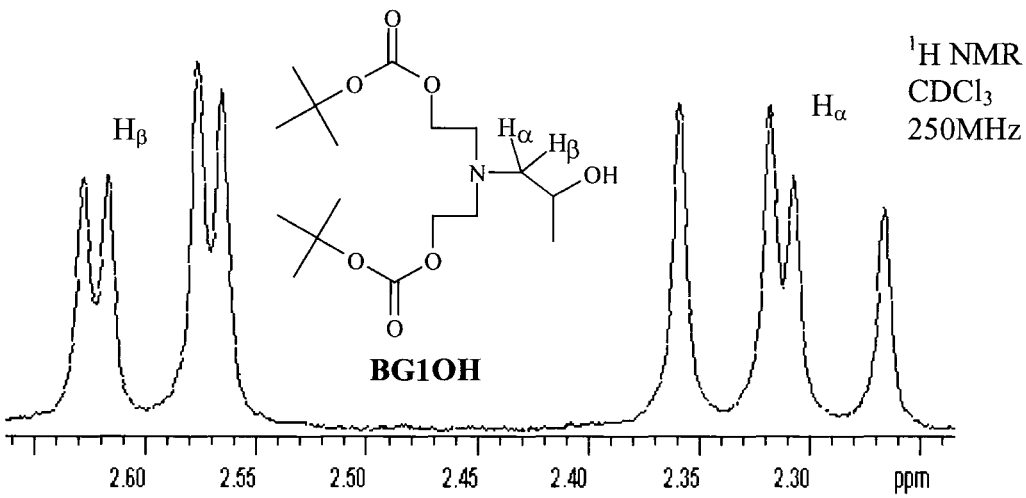

Figure 2.13 Region of ^1H NMR spectrum showing the diastereotopic hydrogens adjacent to the chiral centre of **BG1OH**

Purification of **BG1OH** was challenging as several side products were generated probably resulting from the high temperature, base catalysis and high concentration of the reagents. One of the side products, **1** (*Figure 2.14*), which was formed contrary to the selection rules for CDI reactions, was obtained in variable yields (~10%). This product was formed by reaction of the CDI adduct, **BG0IM**, at the secondary alcohol group of **HEAP** as well as at primary alcohol functions. The presence of **1** shows that the selectivity for reaction at primary sites in the presence of a secondary alcohol is not 100%, which is in agreement with work reported by

Rannard and Davis.[8] It is thought that the reason for the reduced selectivity is a result of the basic conditions and high temperature used in the reaction.

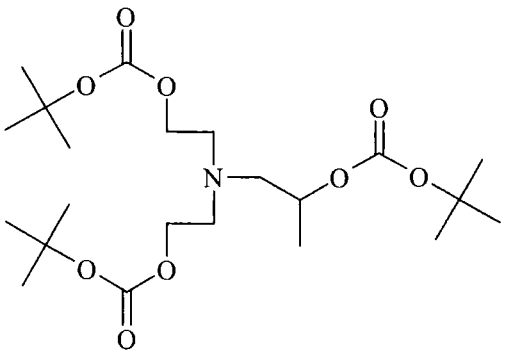

1

Figure 2.14 Side product, **1**, *isolated during the purification of* **BG1OH**

Evidence of formation of **1** was provided from the analysis of both ^{1}H NMR and ^{13}C NMR spectra. In particular, an extra signal in the ^{13}C NMR spectrum appeared which was assigned as the carbonyl formed from the reaction of the secondary alcohol group of **HEAP** with the CDI adduct, **BG0IM**. Also, the diastereotopic hydrogens in the ^{1}H NMR spectrum of **1** were different to those seen in **BG1OH**, as the two observed doublet of doublets now had identical ^{3}J couplings of 6.4Hz, *Figure 2.15*.

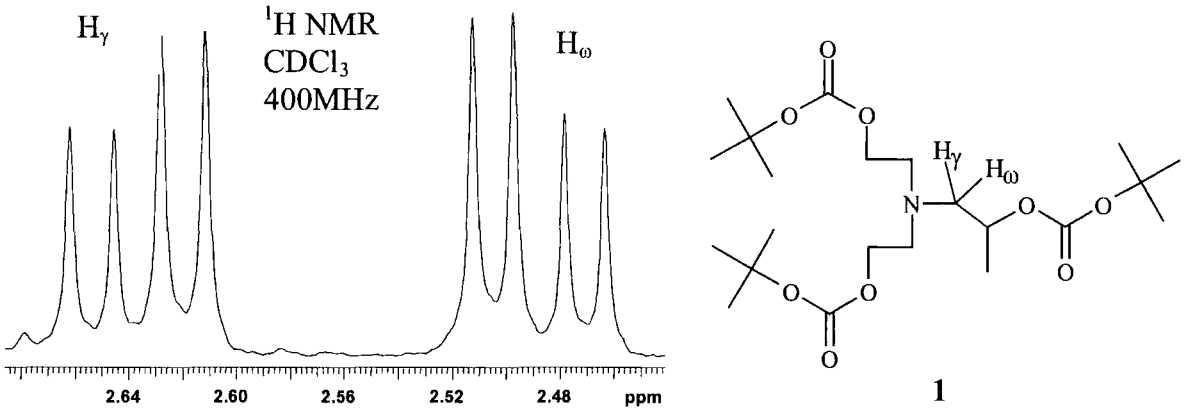

Figure 2.15 Region of ^{1}H *NMR spectrum showing the diastereotopic hydrogens adjacent to the chiral centre of* **1**

The reason that the coupling constants of the two diastereotopic hydrogens in **BG1OH** and **1** differ is thought to be due to the fact that the hydroxyl group at the focal point of **BG1OH** is hydrogen bonded to another part of the molecule. Such an

interaction would lead to the structure having a dominant conformation on the NMR timescale. One possible preferred conformation is that of a pseudo five membered ring formed by the hydrogen bonding of the hydroxyl group to the tertiary amine function, *Figure 2.16*. The existence of a dominant conformation results in different dihedral angles between each of the diastereotopic hydrogens and the hydrogen of the chiral centre. Since ^{3}J or vicinal coupling is dependent on the dihedral angle, the coupling constants for the two hydrogens are different. For the side product **1**, hydrogen bonding cannot occur and rotation around the carbon-carbon bonds in the molecule is less restricted, resulting in similar time-averaged vicinal coupling constants.

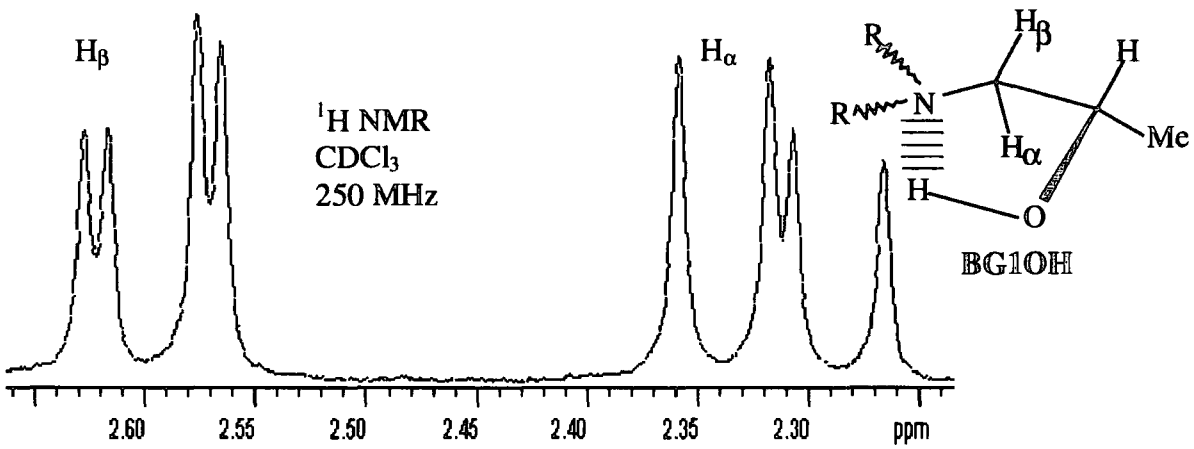

Figure 2.16 Region of ^{1}H NMR spectrum showing the diastereotopic hydrogens adjacent to the chiral centre of **BG1OH** *and a possible preferred conformer*

The third step in the synthesis of **BG1IM** involved the reaction of **BG1OH** with CDI, in which CDI was used in excess to ensure complete conversion of **BG1OH** to **BG1IM**. Analysis of the ^{1}H NMR spectrum provided evidence that the product had formed as the signal corresponding to the OH focal point of **BG1OH** totally disappeared and three new signals corresponding to the imidazole carboxylic ester functionality in **BG1IM** appeared in the product spectrum in the appropriate intensities.

2.4.3 Synthesis of Second Generation Polycarbonate Dendrons

The synthesis of **BG2IM**, a second generation dendron containing an imidazole carboxylic ester group as the focal point, was achieved in two steps from **BG1IM**, *Figure 2.17*. In the first reaction, a toluene solution of **BG1IM** and **HEAP** were stirred at a temperature of 75°C for 3 days in order for the reaction to reach completion.

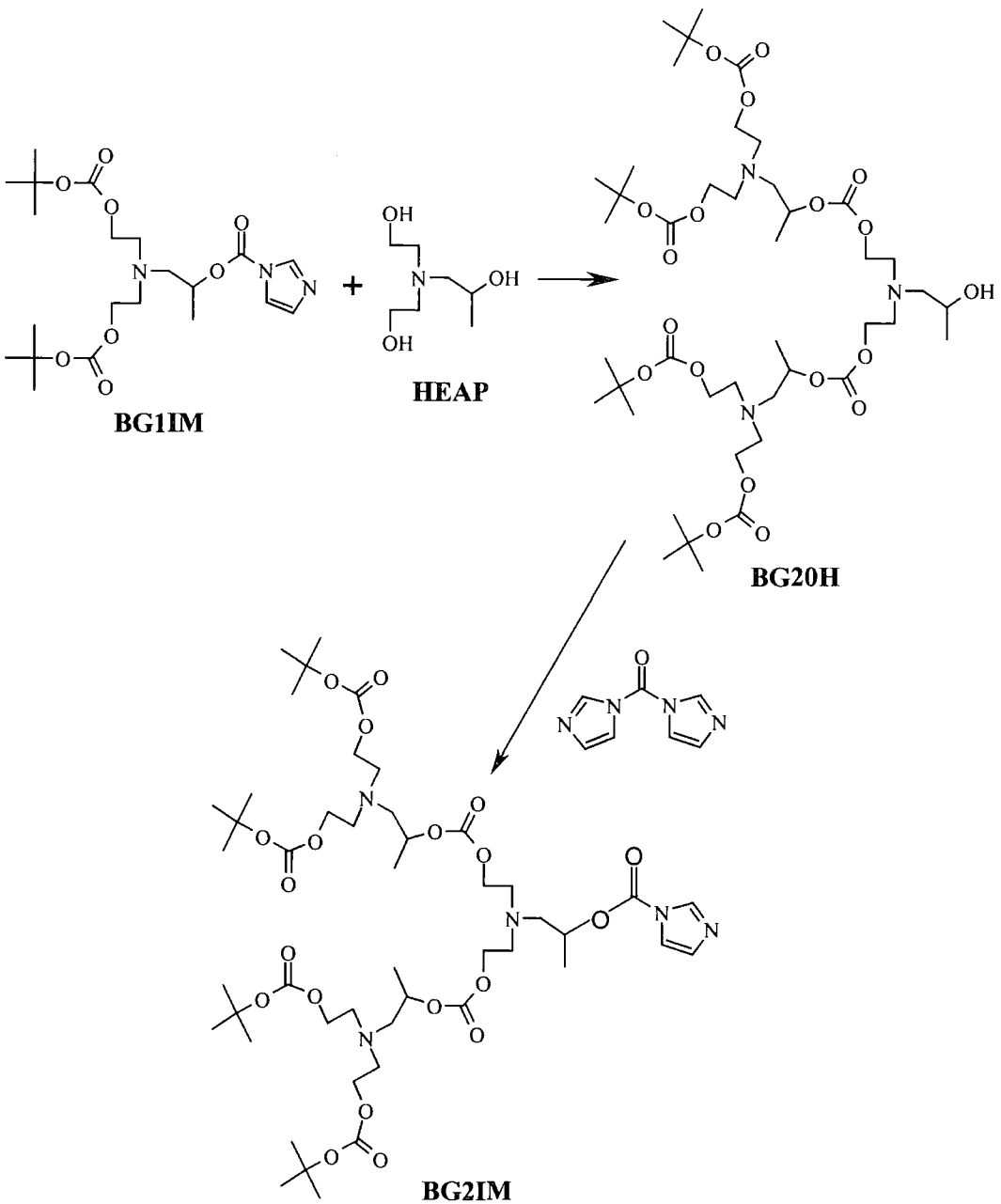

Figure 2.17 The synthetic steps involved in the formation of **BG2IM**

Purification of **BG2OH** proved problematic, due to the formation of a mixture of side products. In particular, the mono-substituted product, **2**, *Figure 2.18*, proved difficult to separate as it eluted very close to **BG2OH** when using silica gel chromatography. However, due to the fact that the molecular weight of **BG2OH** was approximately 400 Da greater than that of the mono-substituted product, **2**, it was decided to separate the two compounds using a Biobeads S-X column with toluene as the eluent. The beads used were neutral, porous styrene divinylbenzene copolymer beads with exclusion limits ranging from 400 to 14,000 Da.

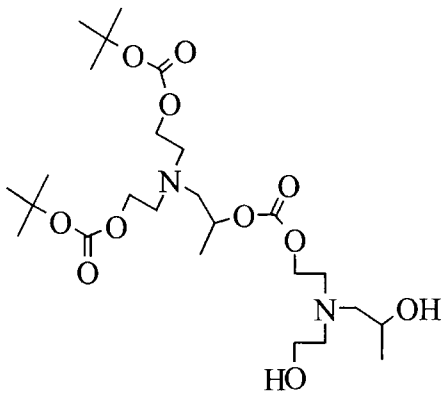

2

Figure 2.18 The mono-substituted compound formed as a by-product in the reaction of **BG1IM** *with* **HEAP**

The mechanism of separation involves gel permeation in which large compounds pass through the column relatively unhindered, whereas small compounds permeate the pores of the beads and hence take longer to pass through the column. Using the Biobeads method, it was possible to isolate pure **BG2OH**. However, there were drawbacks associated with the method, including low overall yield of product and low throughput as only 1 g of crude material could be purified per column, resulting in purification being very time-consuming.

^{1}H NMR spectroscopy was a useful technique in the characterisation of **BG2OH**. Two doublets at 1.2 and 1.04 ppm corresponding to the methyl group hydrogens, H_β and H_α respectively, were present in a ratio of 2:1 as expected, *Figure 2.19*. From this it could be deduced that the product had formed and no mono-substituted material was present. Another interesting feature of the spectrum was a large singlet at 1.41 ppm corresponding to the tertiary butyl hydrogens. Integration of

this signal with respect to the other two doublets gave a ratio of 12:2:1, which was in agreement with the expected ratio of t-butyl hydrogens:H_β:H_α in **BG2OH**. The ^{13}C NMR spectrum of **BG2OH** showed 14 resonances corresponding to the 14 different carbon environments in the molecule.

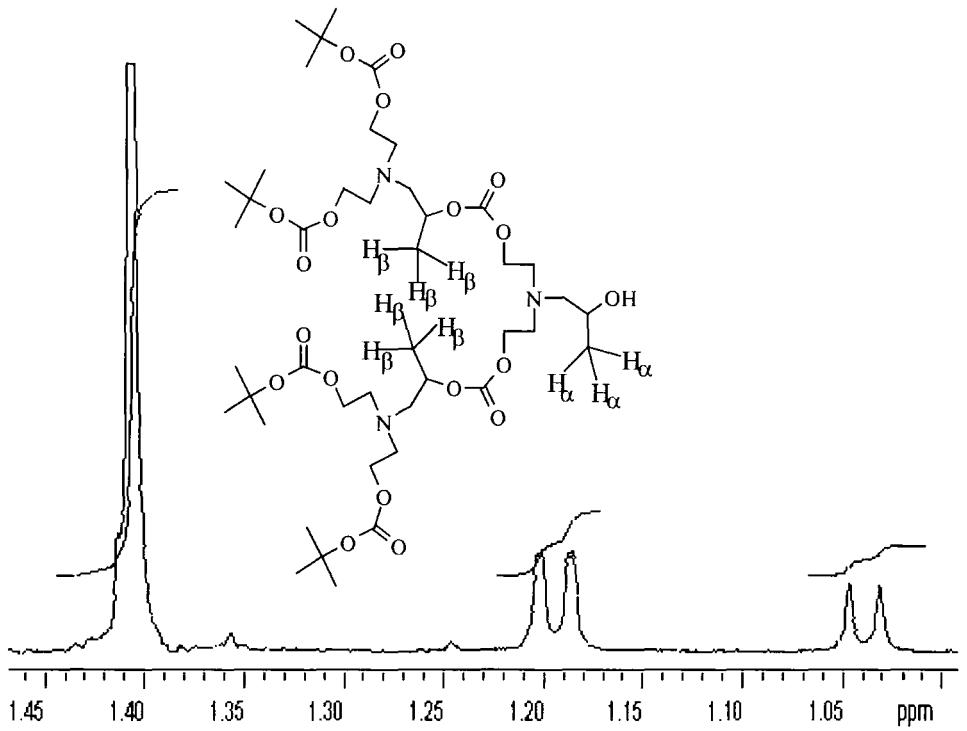

Figure 2.19 Region of ^1H NMR spectrum of **BG20H** *showing (from left to right) signals corresponding to the t-butyl hydrogens, H_β and H_α*

The GPC trace of **BG2OH** was obtained by conventional calibration against linear polystyrene standards, see *Figure 2.20.* The experimental molecular weight value (1250 Da) was found to be reasonably close to the calculated value (941 Da). The reason for the slight discrepancy between the experimental and calculated molecular weights is probably explained by the fact that the second generation dendron, **BG2OH**, is adopting a conformation dissimilar to that of a random coil polymer, making the calibration inappropriate. Despite this, it can be seen from the trace that **BG2OH** is pure as one single symmetrical peak with a computed PDI of 1.00 is present.

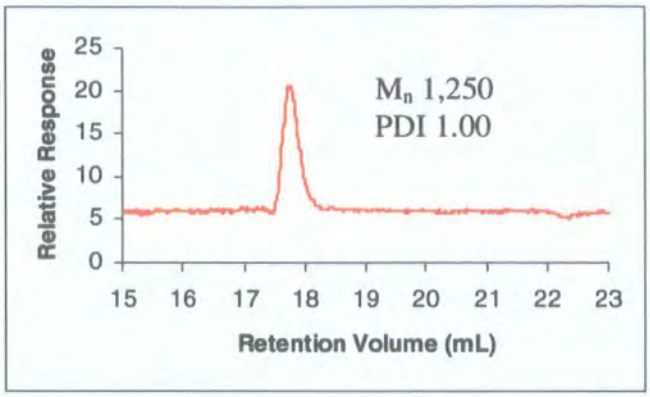

Figure 2.20 GPC trace of **BG2OH**

BG2OH was also analysed by electro spray mass spectrometry, see *Figure 2.21*. There are two main signals present in the spectrum at 942.5 and 965.5 Da, corresponding to $[M+H]^+$ and $[M+Na]^+$, respectively.

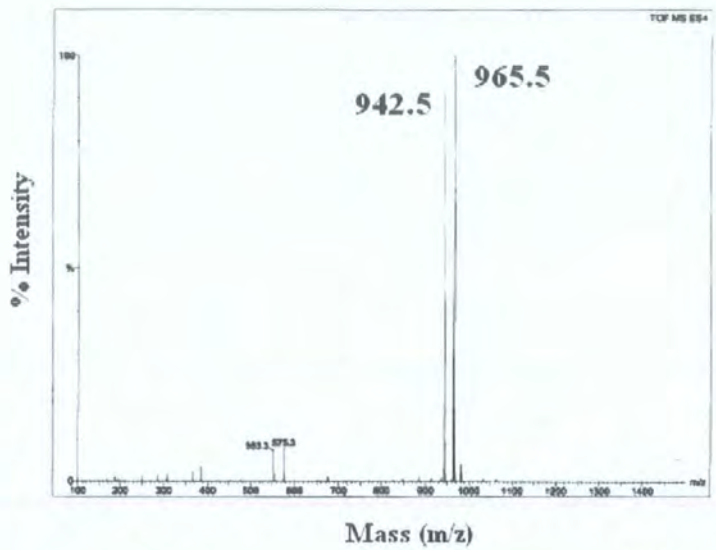

Figure 2.21 Electro spray mass spectrum of **BG2OH**

BG2OH was then reacted with 2 equivalents of CDI in toluene solution at a reaction temperature of 75°C for four hours in the presence of a catalytic amount of KOH to form **BG2IM**. Analysis of the ^{1}H NMR spectrum indicated the formation of **BG2IM,** as three new signals in the appropriate intensities corresponding to the imidazole ring appeared in the product spectrum. A new signal also appeared at 5.18 ppm in the spectrum of **BG2IM** corresponding to $\mathbf{H_x}$, *Figure 2.22*. The

corresponding signal in **BG2OH** (3.63 ppm), had disappeared, suggesting that all of **BG2OH** had been converted to the imidazole carboxylic ester functionality.

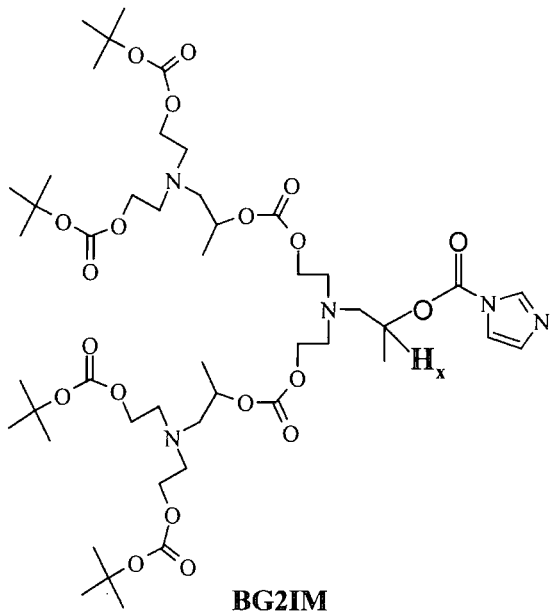

BG2IM

Figure 2.22 Structure of **BG2IM**

The electro spray mass spectrum of **BG2IM** was obtained, see *Figure 2.23*.

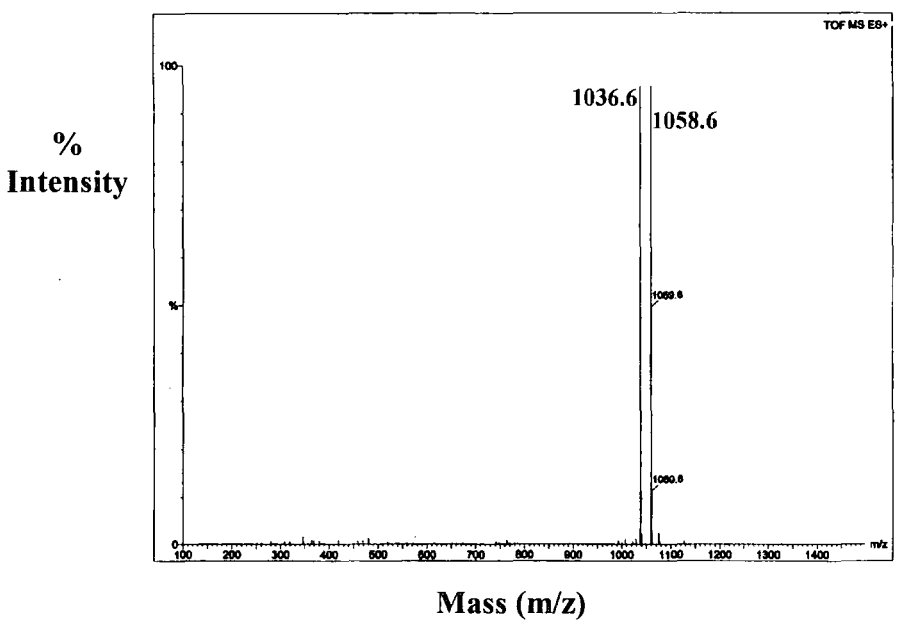

Figure 2.23 Electro spray mass spectrum of **BG2IM**

In the spectrum, there are two main signals present at 1036.6 and 1058.6 Da, which correspond to $[M+H]^+$ and $[M+Na]^+$, respectively.

2.4.4 Synthesis of Second Generation Polyurethane Dendrons

Two second generation polyurethane dendrons, **BG2IM (U)** and **HG2IM (U)**, have been synthesised, which contain t-butyl and 4-heptyl terminal groups, respectively, see page 53 for the branching structure. The polyurethane dendrons were synthesised using starting materials obtained from previous studies.[7] **BG2IM (U)** was synthesised from the reaction of **BG2OH (U)**, provided by Dr Stoddart, and CDI at a reaction temperature of 70°C for 5 hours. As with most reactions involving CDI, the overall yield was high (~80%) and after work-up, the material was obtained in high purity. The electro spray mass spectrum of **BG2IM (U)** showed two main signals present at 1031 and 1053 Da, corresponding to $[M+H]^+$ and $[M+Na]^+$, respectively, see *Figure 2.24*.

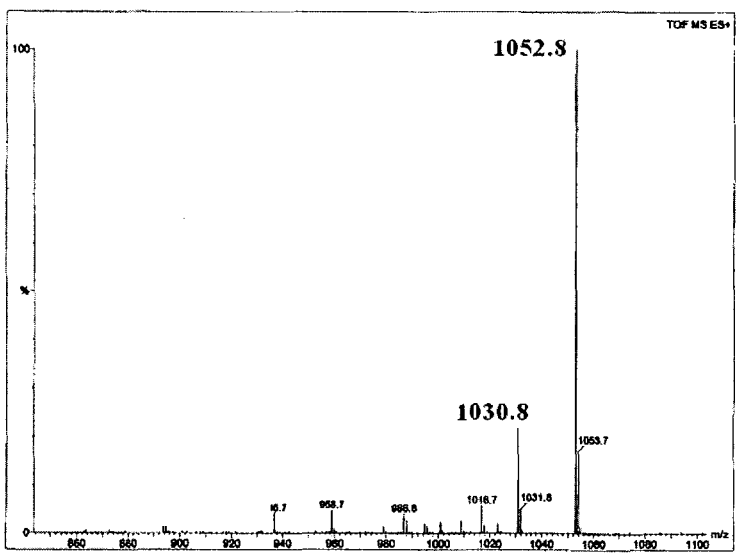

Figure 2.24 Electro spray mass spectrum of **BG2IM (U)**

The ^1H NMR spectrum of **BG2IM (U)** in chloroform-d gave broad signals that were difficult to assign. The reason for this broadening of resonances is probably due to hydrogen bonding within the dendron reducing the mobility of the molecules. It was found that protic NMR solvents (e.g. methanol) could break up the hydrogen bonding to some degree, enabling sharper signals to be obtained. In the ^{13}C NMR

spectrum of **BG2IM (U)**, the number of signals (18) was in accordance with the expected number. The elemental analysis results for carbon showed a poor correlation with the expected values. This was thought to be due to trapped water molecules, as a result of extensive hydrogen bonding within the polyurethane dendrons.

HG2IM (U) was obtained from the reaction of **HG2OH (U)** with CDI in toluene solution. The electro spray mass spectrum is shown in *Figure 2.25* and the structure on page 49, *Figure 2.11*. The main signal is present at 1221.8 Da , which corresponds to $[M+Na]^+$.

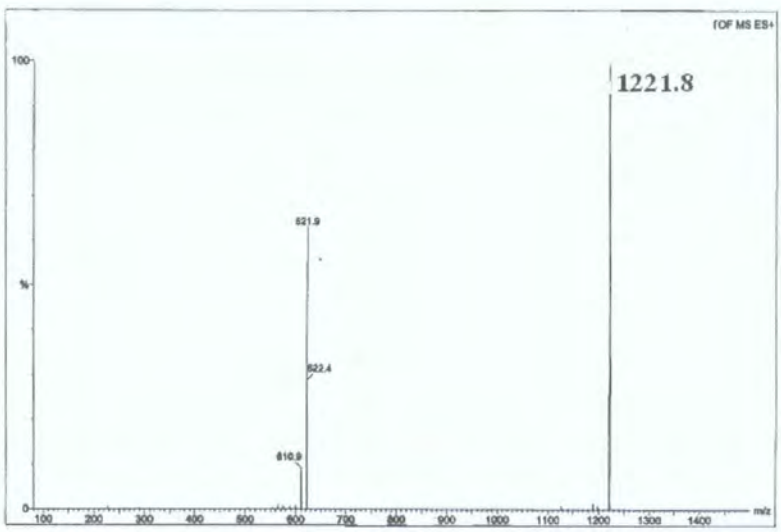

% Intensity

Mass (m/z)

Figure 2.25 Electro spray mass spectrum of **HG2IM (U)**

The synthesis of **BHG1IM (U)**, containing benzhydryl terminal groups, was performed from the reaction of **BHG1OH (U)**, which was provided by Dr Stoddart,[7] with CDI, see *Figure 2.26*.

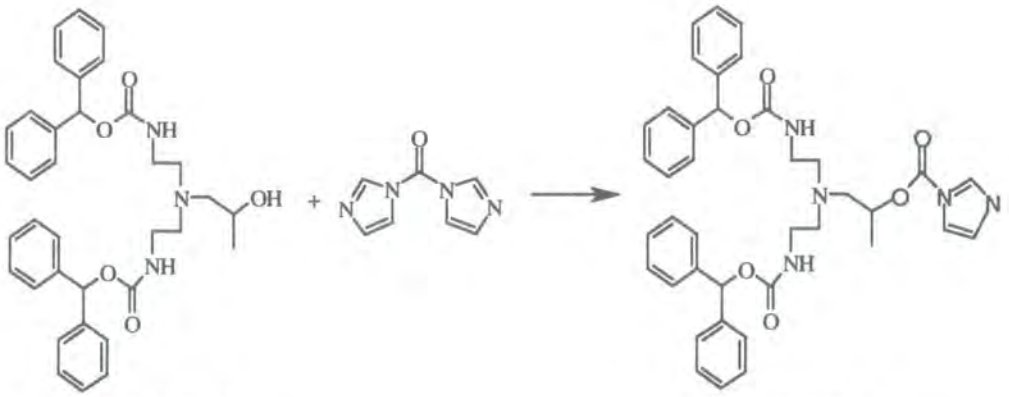

Figure 2.26 Synthesis of **BHG1IM (U)**

After the initial work-up, it was found that **BHG1IM (U)** was impure, a low molecular weight impurity being identified by GPC, see *Figure 2.27a.* Silica gel column chromatography was used to purify the crude material and had the effect of removing the impurity completely, see *Figure 2.27b.*

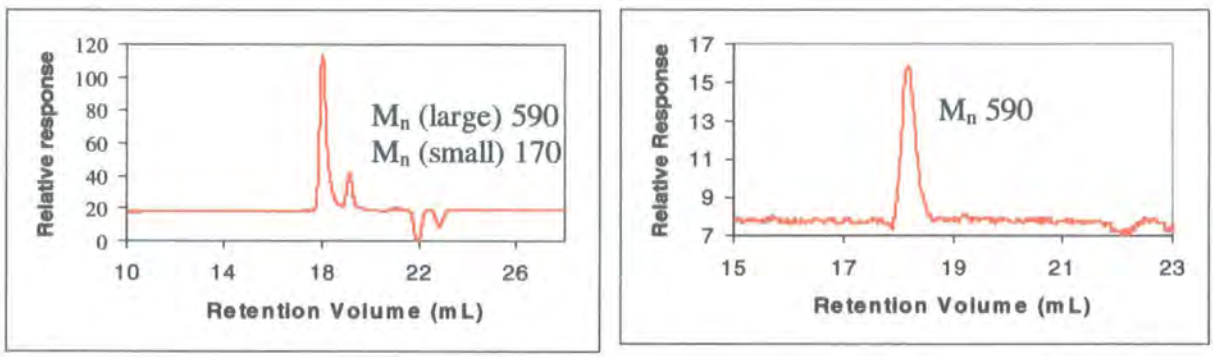

Figure 2.27 a) GPC trace of **BHG1IM (U)** *containing a low molecular weight impurity (left trace) b) GPC trace of pure* **BHG1IM (U)** *after purification by silica gel column chromatography (right trace)*

The reaction of **BHG1IM (U)** with **HEAP** in toluene solution was then attempted in order to synthesise **BHG2OH (U)**. However, difficulties were encountered when trying to purify **BHG2OH (U)**. In particular, after silica gel column chromatography of the crude material, it was apparent from GPC that the material still contained several impurities. As a result of this, a Biobeads column was used in an attempt to try and isolate pure **BHG2OH (U)**. Unfortunately, only lower

molecular weight fractions were isolated and then in low yield, one of which was thought to be the mono-substituted product. The reason why this reaction failed is still unknown, but the large bulk and stiff nature of the terminal groups may have played a part.

2.4.5 Synthesis of First Generation Polyamide Dendrons

The code used to identify the polyamide dendrons was based on two parts. The first part consists of the number of phenyl rings in the dendron and the second part, either **[NO_2]** or **[NH_2]**, refers to the functionality at the focal point of the dendron.

The synthetic steps involved in the synthesis of the first generation polyamide dendron, **[7]-NH_2**, are outlined in *Figure 2.28*. In the first step, 5-nitroisophthalic acid was reacted with phosphorus pentachloride to form 5-nitroisophthaloyl dichloride in moderate yield after recrystallisation. The elemental analysis values indicated that the material was pure as the experimental chlorine percentage value (28.7) was very close to that expected (28.6). Analysis of the ^1H NMR spectrum showed the presence of two signals each with a coupling constant of 1.5Hz and the ^{13}C NMR spectrum showed 5 distinct signals, as expected.

[3]-NO_2 was synthesised from the reaction of 5-nitroisophthaloyl dichloride with aniline in the presence of dry pyridine. Five signals were present in the ^1H NMR spectrum of **[3]-NO_2**, *Figure 2.29*. H_A and H_B both appeared as triplets, with a coupling constant of approximately 7.6Hz. The signal for H_C appeared as a doublet, again with a coupling constant of approximately 7.6Hz. The signals for H_D and H_E came very close together and could not be distinguished, although integration indicated that three hydrogens were present. Finally, the signal for the two -NH hydrogens was present at 10.75ppm.

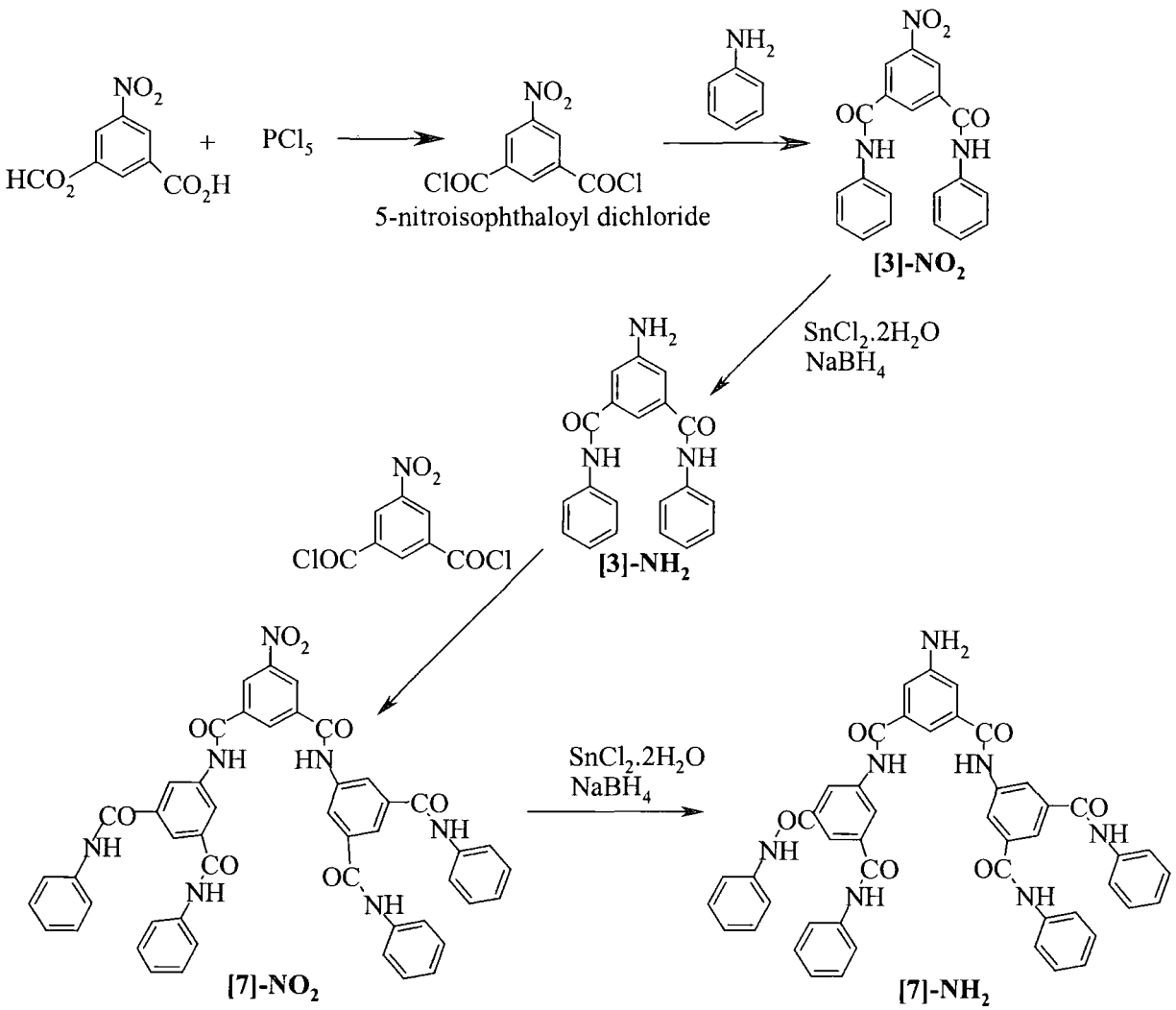

Figure 2.28 The synthetic steps involved in the synthesis of **[7]-NH_2**

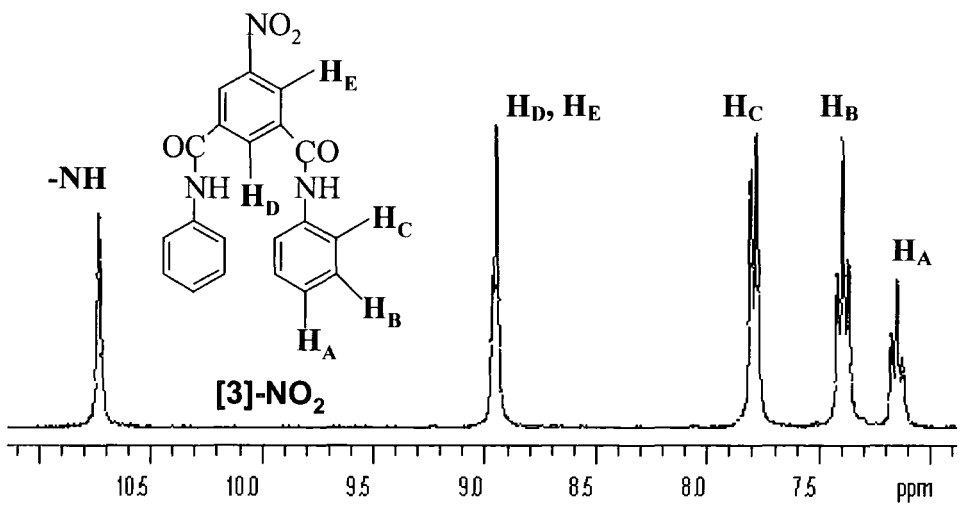

Figure 2.29 The ^1H NMR spectrum and structural assignment of **[3]-NO_2**

[3]-NO_2 was then reduced to **[3]-NH_2** using a mixture of tin chloride dihydrate and sodium borohydride in ethanol solution. The overall yield of the reaction was only ~30% with the product being obtained as a dark orange solid. The main feature in the ^1H NMR spectrum of **[3]-NH_2**, compared to that of **[3]-NO_2**, was the appearance of a new singlet at 5.6ppm corresponding to the hydrogens of the **–NH_2** focal point.

[7]-NO_2 was synthesised from the reaction of **[3]-NH_2** with 5-nitroisophthaloyl dichloride in dry pyridine for several hours. The mono-substituted by-product and **[3]-NH_2** present in the crude product, were removed by washing with methanol, in which **[7]-NO_2** was essentially insoluble. After filtration, pure **[7]-NO_2** was obtained, as can be seen from the GPC trace, *Figure 2.30*. The experimental molecular weight of 720 Da obtained from the GPC analysis was in close agreement to the expected value of 838 Da.

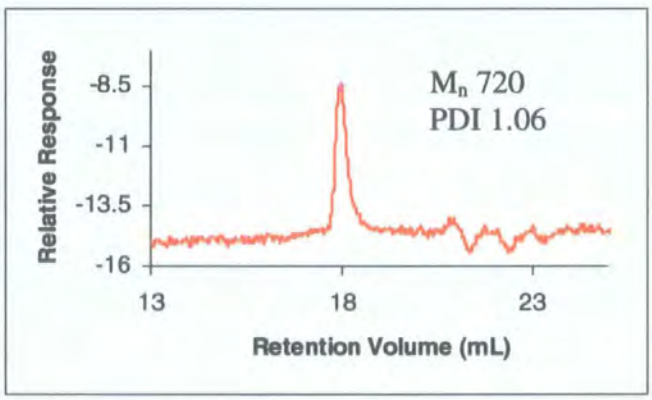

Figure 2.30 GPC trace of **[7]-NO_2**

The ^1H NMR spectrum of **[7]-NO_2** shows the presence of nine signals, see *Figure 2.31*. One of the key resonances is present at 10.49 ppm, which corresponds to the 4-NH signal, indicating the formation of the di-substituted dendron **[7]-NO_2**.

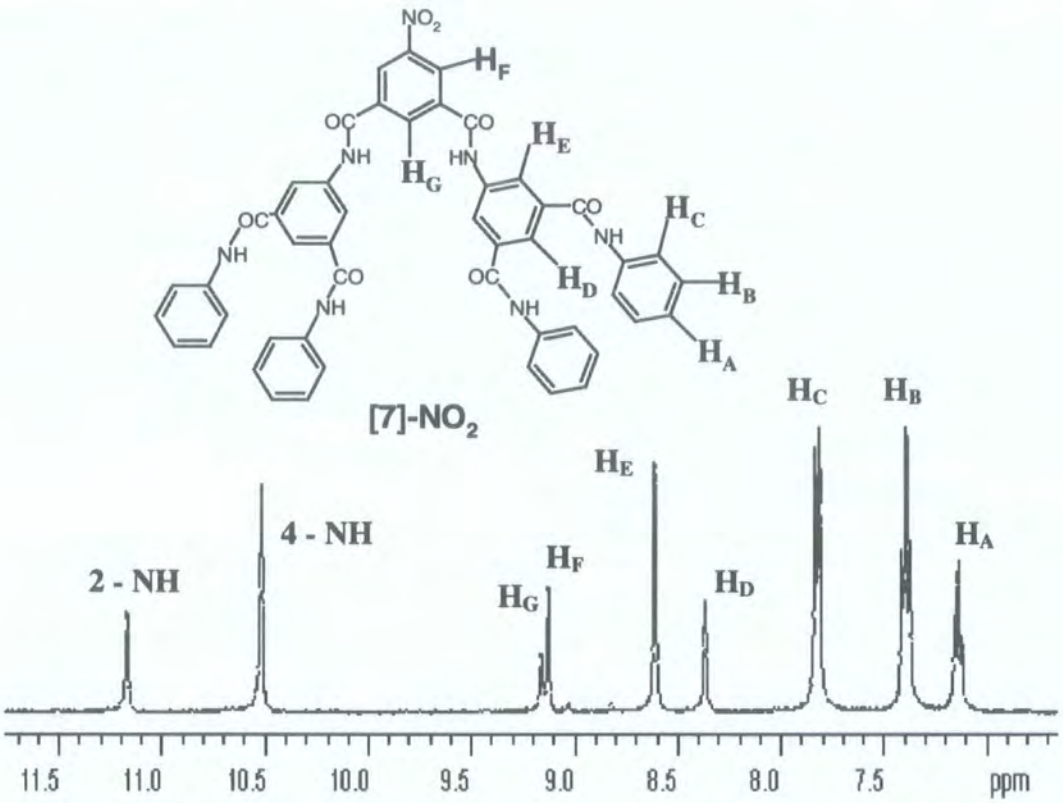

Figure 2.31 The ^{1}H NMR spectrum and structural assignment of **[7]-NO_2**

[7]-NO_2 was then reduced to **[7]-NH_2**, using a mixture of tin chloride dihydrate and sodium borohydride in methanol solution. GPC provided evidence of sample purity as the PDI of the sample was low (1.05) and the experimental molecular weight of 730 Da was in close agreement to the expected value of 807 Da, *Figure 2.32.*

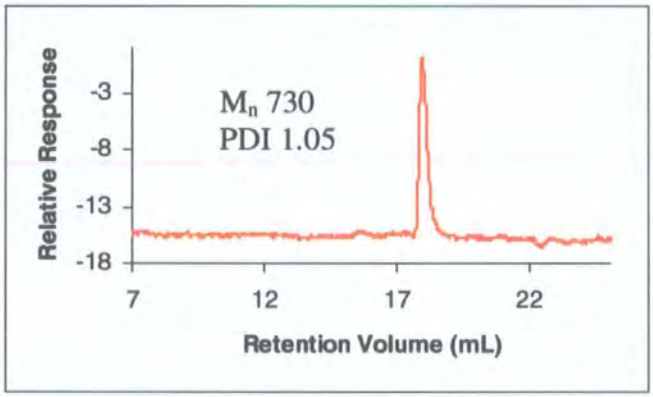

Figure 2.32 GPC trace of **[7]-NH_2**

The electro spray mass spectrum of **[7]-NH_2**, shows that the major signal is present at 807 Da, which corresponds to $[M]^+$, *Figure 2.33.* In electro spray mass spectrometry,

the ions are produced by catonisation, usually by addition of H^+, Na^+ or K^+, in this case the parent ion is detected at 807 Da, which is close to the expected value at 808 Da for $[M+H]^+$ and within the accuracy of the instrument calibration.

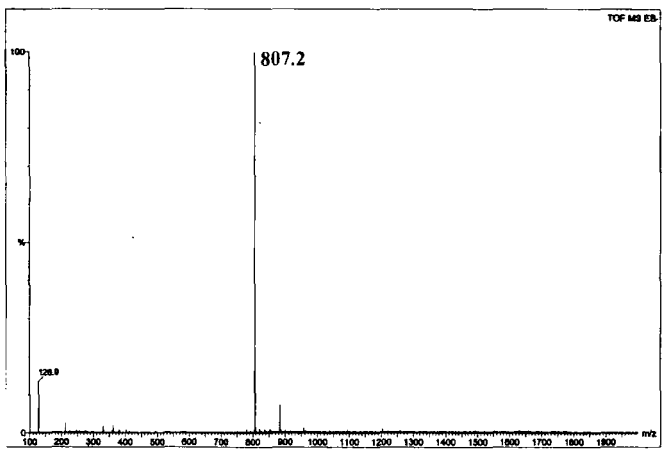

Figure 2.33 Electro spray mass spectrum of **[7]-NH_2**

2.5 Synthesis and Characterisation of Dendronised Monomers

A series of dendronised monomers, containing both mono- and di-substituted dendrons of different generation possessing different chemical structure, has been synthesised. In particular, a mono- and di-substituted first generation polycarbonate dendronised monomer was synthesised, along with a di-substituted second generation polycarbonate dendronised monomer. The polycarbonate dendronised monomers all contained t-butyl groups at the periphery. Using the dendrons described in section 2.4.4, di-substituted second generation polyurethane dendronised monomers, containing both t-butyl and 4-heptyl terminal groups, have also been synthesised. Finally, an attempt was made to synthesise the first generation di-substituted polyamide dendronised monomer with phenyl groups at the periphery.

2.5.1 Nomenclature of Dendronised Monomers

The code used in this thesis to identify dendronised monomers is based on five parts. The first part highlights that a dendronised monomer is the compound being discussed, the second part indicates the chemical structure of the dendron, the third part describes the nature of the terminal groups of the dendron, the fourth signifies the generation of the dendron and the fifth describes whether the norbornene is mono- or di-substituted. Firstly, letters **DM** represent dendronised monomers. Secondly, the

three chemical structures of the dendrons are represented by letters; PolyCarbonate (PC), PolyUrethane (PU) and PolyAmide (PA). Thirdly, the three terminal groups are represented by letters; t-Butyl (B), 4-Heptyl (H) and Phenyl (P). The fourth part is represented by number 1 or 2, indicating a first or second generation structure, respectively. Finally, the substitution of the norbornene unit is represented by letters; -Mono (M) and -Di (D), see table in *Figure 2.34*.

Dendronised Monomer Code

Dendronised monomer	Chemical Structure	Terminal Groups	Generation Number	Substitution
DM	carbonate links PC urethane links PU amide links PA	*t-Butyl* B *4-Heptyl* H *Phenyl* P	1, 2	Mono (M) Di (D)

Figure 2.34 Identification code for dendronised monomers

2.5.2 Synthesis of a Mono-Substituted First Generation Polycarbonate Dendronised Monomer (DMPCB1M)

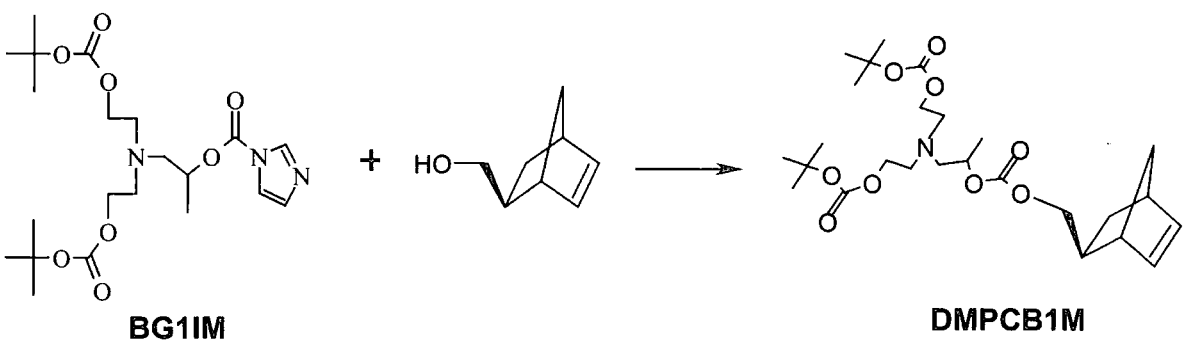

Figure 2.35 Coupling reaction used in the synthesis of **DMPCB1M**

DMPCB1M was synthesised from the coupling reaction of **BG1IM** with norbornene-5-*exo*-methanol in toluene solution at 95°C for three days, *Figure 2.35.* Analysis of the ^{1}H NMR spectrum of the mixture showed whether the reaction had reached completion, by monitoring the disappearance of the three hydrogens from the imidazole functionality of **BG1IM**. Signals corresponding to the hydrogens adjacent to the –OH functionality on norbornene-5-*exo*-methanol were also monitored, as their chemical shift changed when **DMPCB1M** formed. When all of **BG1IM** had reacted, and the aqueous work-up had been performed, the crude material was purified by silica gel chromatography, eluting with hexane and ethyl acetate (ratio 4:1), producing pure **DMPCB1M** in 66% yield. Analysis of the ^{1}H NMR and 2D COSY spectrum was useful in the determination of the structure of **DMPCB1M**. It was found by integration, that the ratio of vinylic protons to t-butyl hydrogens (2:18) was as expected, indicating the formation of the mono-substituted dendronised monomer. Analysis of the ^{13}C NMR spectrum showed the presence of 17 signals and the DEPT spectrum indicated the presence of 6 $-CH_2$ signals and a total of 8 –CH and CH_3 signals, as expected. The product was characterised by electro spray mass spectroscopy, which showed a signal at 513 Da, close to the expected value at 514 for $[M+H]^+$ and within the accuracy of the instrument calibration, *Figure 2.36.*

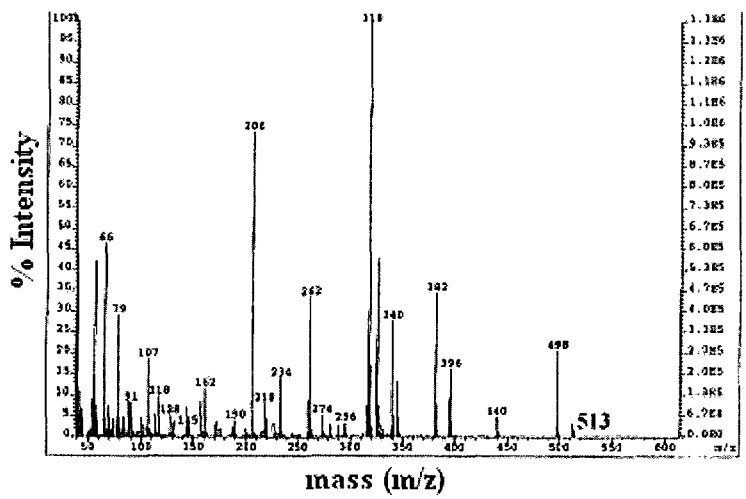

Figure 2.36 Electro spray mass spectrum of **DMPCB1M**

2.5.3 Synthesis of a Di-Substituted First Generation Polycarbonate Dendronised Monomer (DMPCB1D)

DMPCB1D was synthesised from the reaction of norbornene-5-*exo*, 6-*exo*-dimethanol with **BG1IM** in toluene solution at a reaction temperature of 90°C for five days, *Figure 2.37.*

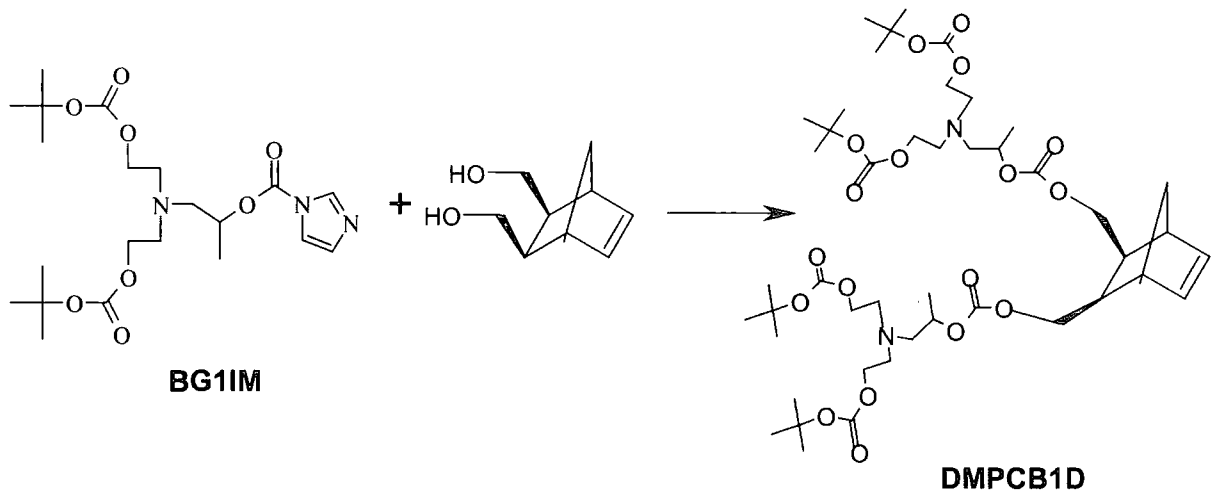

Figure 2.37 Coupling reaction used in the synthesis of **DMPCB1D**

The hydrogens from the imidazole functionality of **BG1IM** were monitored by ^{1}H NMR spectroscopy. When the reaction had gone to completion, the work-up was performed and the crude material was then purified by silica gel chromatography, eluting with hexane and ethyl acetate (ratio 1.5:1), to give pure **DMPCB1D** in 44% yield. Analysis of the GPC trace showed that the computed PDI of the sample was low (1.01) and the experimental molecular weight of 1,070 Da was in close agreement to the expected value of 933 Da, see *Figure 2.38.*

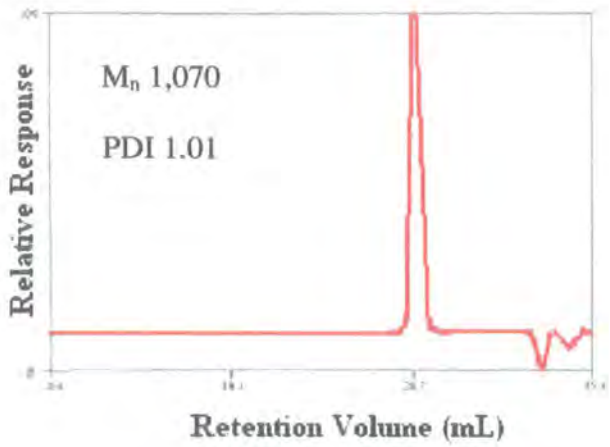

Figure 2.38 GPC trace of **DMPCB1D**

Analysis of the electro spray mass spectrum showed signals at 933.6 Da and 956.6 Da corresponding to $[M+H]^+$ and $[M + Na]^+$, respectively, within the calibration error. Analysis of the ^1H NMR spectrum of **DMPCB1D** indicated that the ratio of vinylic hydrogens (6.16 ppm) to t-butyl hydrogens (1.47 ppm) was in perfect agreement with that expected (2:36), providing good evidence that the di-substituted product had formed. The ^{13}C NMR spectrum gave 14 distinct signals, as expected.

2.5.4 Synthesis of a Di-Substituted Second Generation Polycarbonate Dendronised Monomer (DMPCB2D)

DMPCB2D was synthesised from the reaction of **BG2IM** with norbornene-5-*exo*, 6-*exo*-dimethanol in toluene solution at a reaction temperature of 75°C for 7 days. **BG2IM** was seen to have fully reacted by analysis of the ^1H NMR spectrum. Silica gel chromatography was initially used to purify the crude material, but pure **DMPCB2D** could not be isolated by this method, as the mono-substituted product eluted at the same time. The molecular weight of **DMPCB2D** (2090 Da) is more than 500 Da greater than the mono-substituted product (1511 Da) and as a result of this, a Biobeads S-X column was used to isolate pure **DMPCB2D** in low yield (24%), *Figure 2.39*. Elemental analysis, ^1H NMR and ^{13}C NMR spectroscopy, GPC, and MALDI-TOF were used to characterise **DMPCB2D**. The elemental analysis values for carbon (55.75%), hydrogen (8.10%) and nitrogen (3.86%) were all in good agreement with the expected values - carbon (55.73%), hydrogen (8.10%) and nitrogen (4.02%). The ^1H NMR spectrum contained broad unresolved resonances,

probably due to the size of the dendronised monomer and overlapping of signals. Also, the number of observed resonances in the ^{13}C NMR spectrum was lower than that expected, probably as a result of overlapping of signals corresponding to carbons in equivalent positions in successive layers of the structure. The GPC trace of **DMPCB2D**, *Figure 2.40a*, showed a single peak at 1,770 Da with a PDI of 1.01, which correlates reasonably with the expected molecular weight of 2090 Da. The MALDI-TOF spectrum, *Figure 2.40b*, showed signals at 2091.4 Da and 2113 Da, which correspond to $[M+H]^+$ and $[M+Na]^+$, respectively.

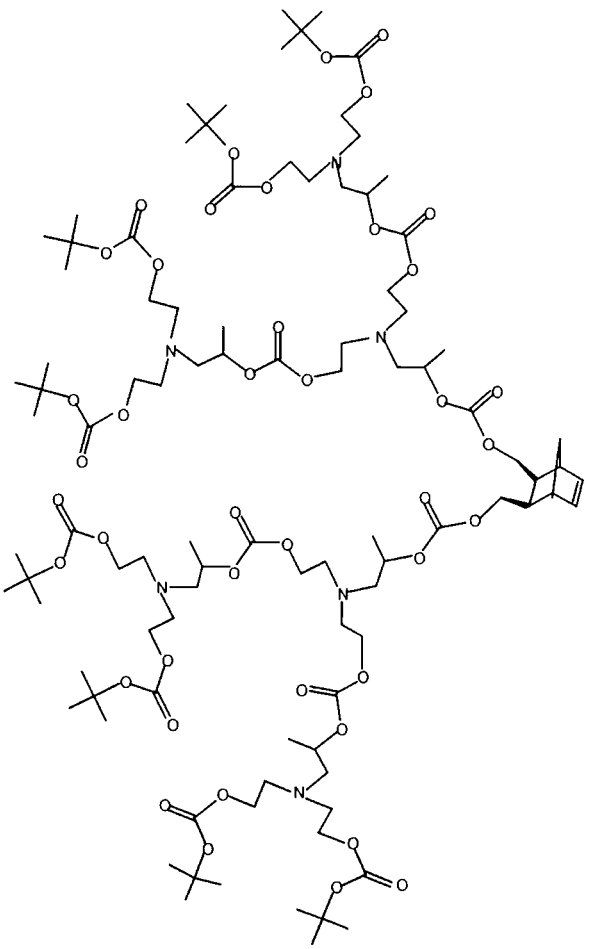

Figure 2.39 Structure of **DMPCB2D**

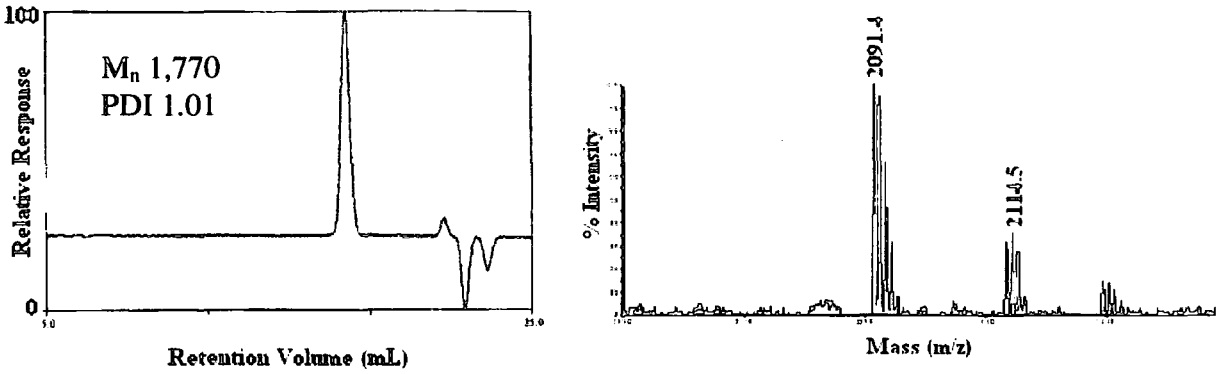

Figure 2.40 a) GPC trace of **DMPCB2D** *(left) b) Maldi-TOF spectrum of* **DMPCB2D** *(right)*

2.5.5 Synthesis of a Di-Substituted Second Generation Polyurethane Dendronised Monomer containing t-Butyl Terminal Groups (DMPUB2D)

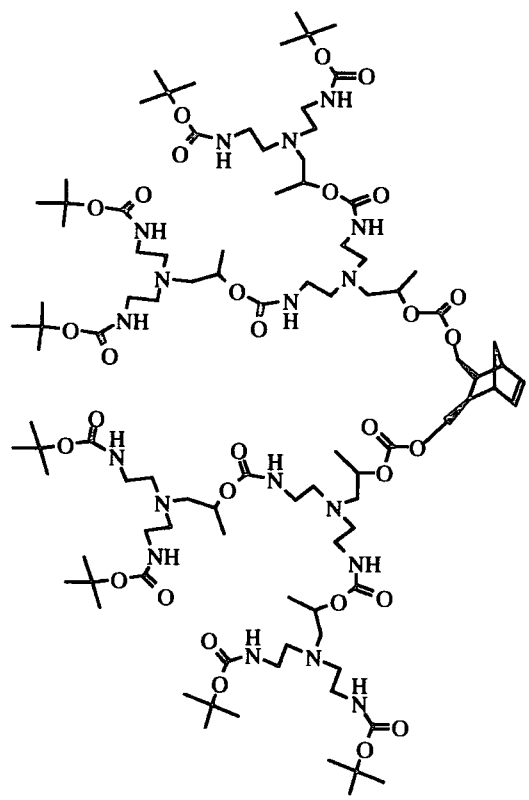

Figure 2.41 Structure of **DMPUB2D**

DMPUB2D, *Figure 2.41*, was synthesised from the reaction of **BG2IM (U)** with norbornene-5-*exo*, 6-*exo*-dimethanol in toluene solution at a reaction temperature

of 80°C for 7 days. The crude material was initially purified by flash column chromatography on silica, however, there were remaining impurities and it was found that a Biobeads S-X column was required to produce pure **DMPUB2D** in low yield (8.4%). The Biobeads column was again used to isolate the pure di-substituted product from the mono-substituted product. Elemental analysis, ^{1}H NMR spectroscopy, GPC, electro spray mass spectrometry and MALDI-TOF were used to characterise **DMPUB2D**. The elemental analysis values for carbon (55.52%), hydrogen (8.75%) and nitrogen (12.70%) were all in reasonable agreement with the expected values - carbon (56.05%), hydrogen (8.73%) and nitrogen (12.13%). The signals in the ^{1}H NMR spectrum were broad and unresolved. This is probably as a result of hydrogen bonding within the dendrons. It was found that, in this case, using protic NMR solvents, such as methanol, did not alleviate this problem. The GPC trace of **DMPUB2D** is shown in *Figure 2.42*. The trace shows the presence of a main signal with a molecular weight of 1,870 Da and a PDI of 1.03. However, it can be seen that there are two less intense lower molecular weight signals present. Electro spray and MALDI-TOF mass spectra were both obtained for **DMPUB2D**. However, neither method could detect a signal close to the molecular ion of the compound.

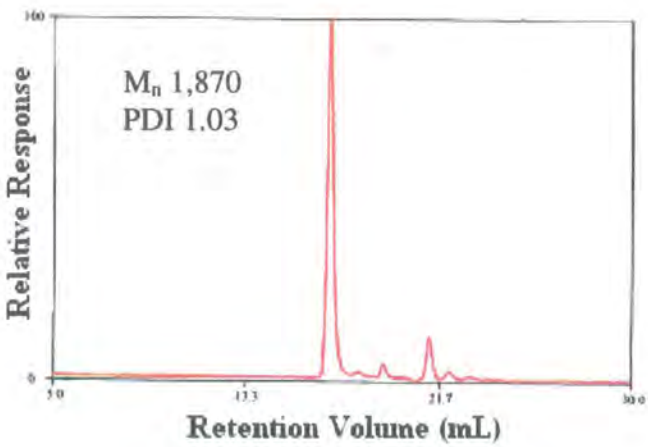

Figure 2.42 GPC trace of **DMPUB2D**

2.5.6 Synthesis of a Di-Substituted Second Generation Polyurethane Dendronised Monomer containing 4-Heptyl Terminal Groups (DMPUH2D)

DMPUH2D, *Figure 2.43*, was synthesised from the reaction of **HG2IM (U)** with norbornene-5-*exo*, 6-*exo*-dimethanol in toluene solution at a reaction temperature of 80°C for 7 days. The crude material was initially purified by flash column

chromatography on silica, eluting with hexane and ethyl acetate at a ratio of 1:1, and then further purified using a Biobeads S-X column to produce **DMPUH2D** in low yield (10%). Again, the ^{1}H NMR spectrum of **DMPUH2D** contained signals that were broad due to hydrogen bonding within the dendron structure and the number of observed resonances in the ^{13}C NMR spectrum was lower than expected.

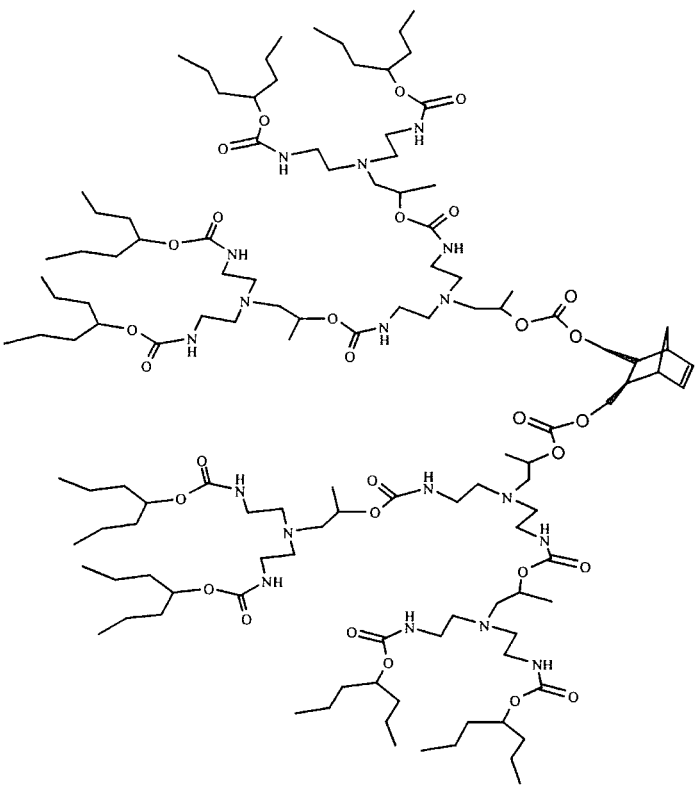

Figure 2.43 Structure of **DMPUH2D**

The GPC trace of **DMPUH2D** is shown in *Figure 2.44a*. The trace shows the presence of one signal with a molecular weight of 2,550 Da and a computed PDI of 1.00. The MALDI-TOF mass spectrum shows the presence of signals at 2415 and 2437 Da, corresponding to $[M+H]^+$ and $[M+Na]^+$, respectively, within the error of the measurement (*Figure 2.44b*). The inaccuracy in molecular weight is probably due to the instrument's calibration being slightly out.

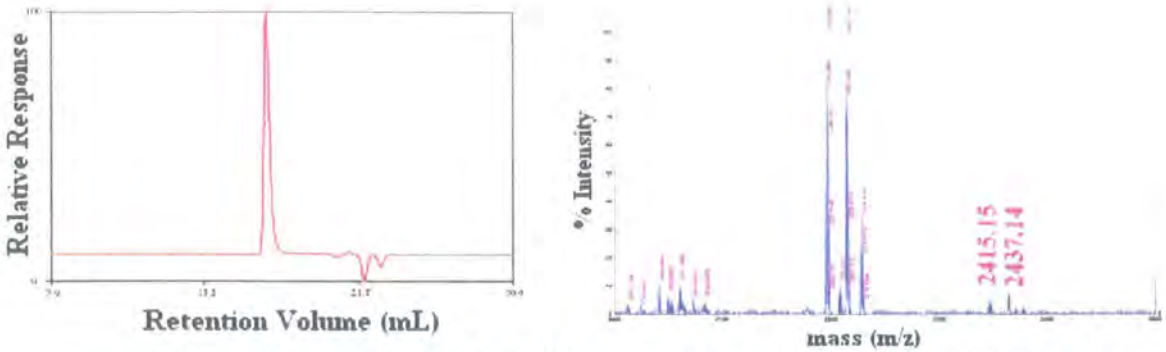

Figure 2.44 a) GPC trace of **DMPUH2D** *b) Maldi-TOF spectrum of* **DMPUH2D**

2.5.7 Attempted Synthesis of a Di-Substituted First Generation Polyamide Dendronised Monomer containing Phenyl Terminal Groups (DMPAP1D)

The synthesis of **DMPAP1D** was attempted via the reaction of **[7]-NH_2** with norbornene-5-*exo*, 6-*exo*-dicarbonyl chloride in toluene solution at a reaction temperature of 60°C. As the reaction between an acid chloride and an amine is generally rapid, it was expected that the reaction would go to completion relatively quickly. However, after 1 day, it was apparent by analysis of the ^{1}H NMR spectrum that not all of **[7]-NH_2** had reacted. The reaction was continued for another day, after which, the crude mixture was washed with a 10% HCl solution several times and then dried. The crude mixture was analysed by electro spray mass spectrometry to deduce whether any signals were present in the region between 1700 and 1800 Da, which would indicate the presence of **DMPAP1D**. Unfortunately, the mass spectrum only showed low intensity signals in the region between 800 and 1000 Da. The crude material was purified by flash chromatography, eluting with tetrahydrofuran and hexane in a ratio of 2:1. Two fractions were isolated from the column. The first fraction was analysed using ^{1}H NMR spectroscopy and electro spray mass spectrometry. Evidence from the ^{1}H NMR spectrum, aided with a 2D COSY spectrum, suggested that the first fraction from the column was the product of an intramolecular condensation reaction between a substituted amine and an acid chloride functionality, *Figure 2.45*. The first step in the synthesis of the intramolecular condensation product is the formation of the mono-substituted dendronised monomer. The nitrogen of the amide group attached to the norbornene derivative is then able to react at the carbonyl function of the remaining acid chloride functionality, eliminating chlorine in the process, to form the stable five membered cyclic diimide intramolecular condensation product, **3**.

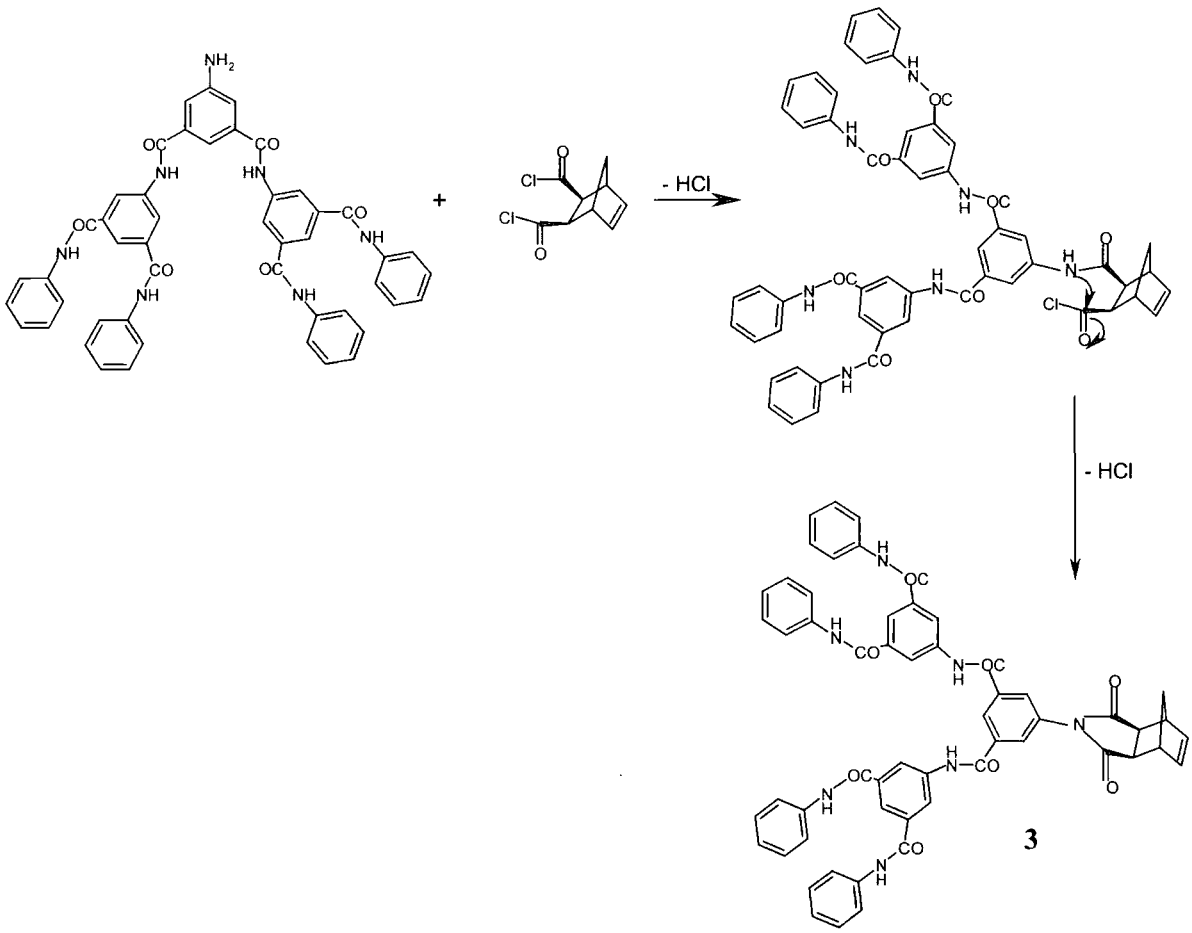

Figure 2.45 Formation of an intramolecular condensation product, **3**, *via the reaction between* **[7]-NH_2** *and* norbornene-5-*exo*, 6-*exo*-dicarbonyl chloride

By analysis of the ^{1}H NMR spectrum, it could be deduced that the first fraction was *not* the di-substituted dendronised monomer, see *Figure 2.46*. In particular, two signals were present in the region between 10 and 11 ppm, which could be integrated with respect to the well resolved olefinic hydrogens and were found to correspond to a total of six amide groups. This number of amide groups is in good agreement with the intramolecular condensation product, **3**. On the other hand, the ^{1}H NMR spectrum of the di-substituted dendronised monomer would have contained three different resonances in this region corresponding to a total of fourteen amide groups. The formation of the mono-substituted product was also ruled out, as there would have been three distinct signals present in the ^{1}H NMR spectrum in the region between 10 and 11ppm, corresponding to a total of seven amide groups.

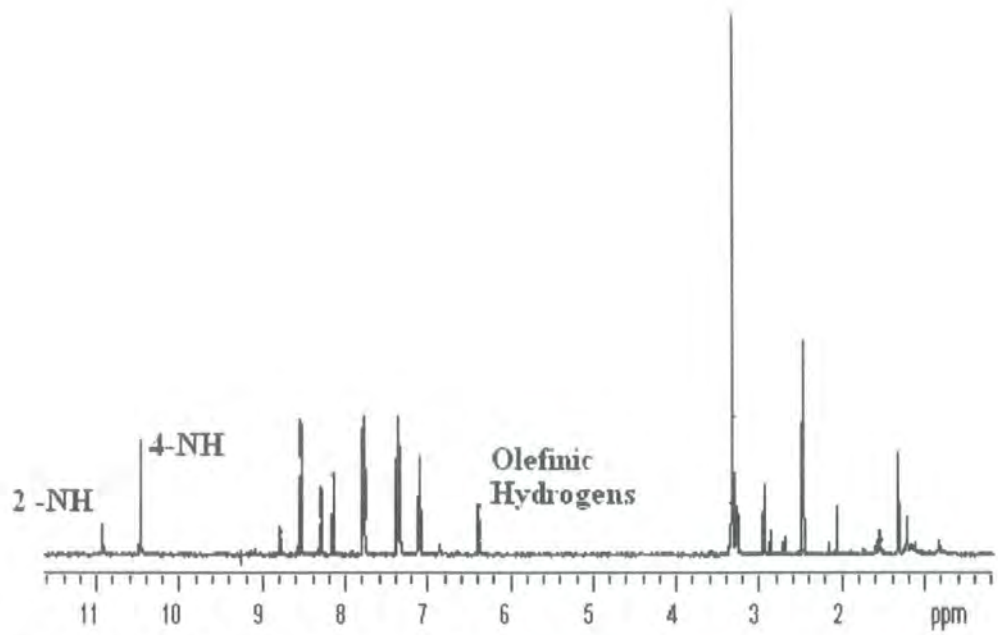

Figure 2.46 ^{1}H NMR spectrum of the intramolecular condensation product, **3**

Analysis of the MALDI-TOF spectrum of the first fraction showed that there were signals present at 977.25 and 993.21 Da, which correspond to $[M+ Na]^+$ and $[M+K]^+$, respectively, of the intramolecular product, **3**, see *Figure 2.47.*

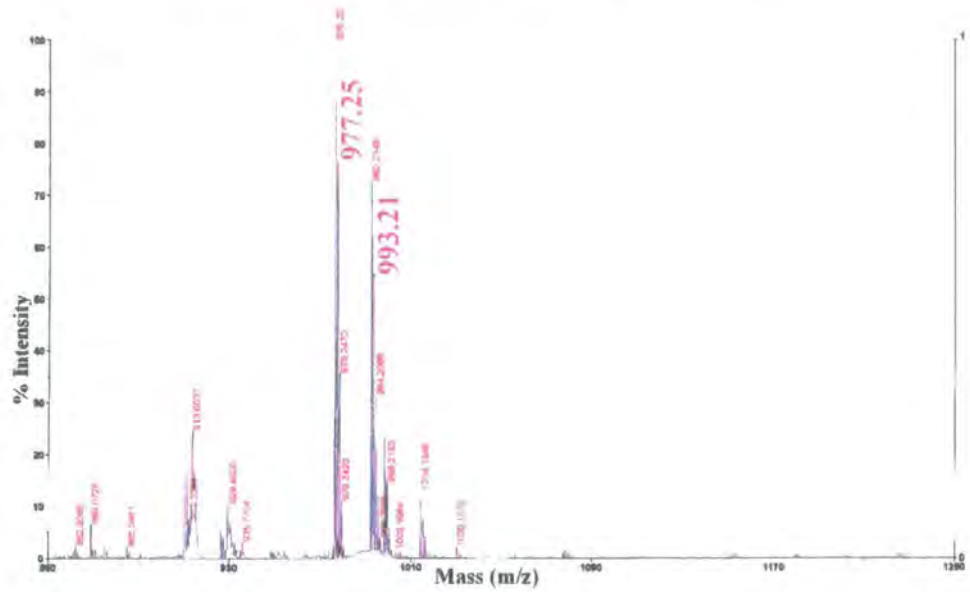

Figure 2.47 Maldi-TOF spectrum of intramolecular condensation product, **3**

From the characterisation of the reaction products, it can be unambiguously stated that the intramolecular condensation product, **3**, formed during the attempted synthesis of **DMPAP1D**.

Analysis of the ^{1}H NMR spectrum of the second fraction showed that there was no signal present corresponding to the olefin hydrogens of the norbornene derivative. As a result of this, it was thought that this fraction was an impurity of no relevance to the objective of the work and the material was discarded. All in all, this synthesis proved very demanding and in the end, not enough of the purified compound **3** was obtained for ROMP studies.

2.6 Conclusions

A series of dendronised monomers of different generations possessing different chemical structures has been synthesised. In particular, mono- and di-substituted first generation polycarbonate dendronised monomers have been synthesised and fully characterised, along with a di-substituted second generation polycarbonate dendronised monomer. Two di-substituted second generation polyurethane dendronised monomers containing t-butyl and 4-heptyl terminal groups were also successfully synthesised. Despite these successes, the attempted synthesis of a di-substituted first generation polyamide dendronised monomer was unsuccessful. Nonetheless, the range of dendronised monomers obtained was polymerised via ROMP to prepare dendronised polymers, the synthesis of which is described in chapter 3.

2.7 References

1. M^{c}Murray, J. *Organic Chemistry*, 2nd Ed.; Brooks and Cole: New York, **1996**, p 508.

2. Furniss, B. S.; Hannaford, P.; Smith, W. G.; Tatchell, A. R. *Vogel's Textbook of Practical Organic Chemistry,* 5th Ed.; Longman: London, **1989**.

3. Warren, S. *Organic Synthesis, The Disconnection Approach*, Wiley: Chichester, **1982**, p 132.

4. Roudabush, R. L.; Drummond, L. E. *US Patent 3641108 Eastman Kodak Co.*, **1976**.

5. Kemp, W. *NMR in Chemistry, a Multinuclear Introduction*, MacMillan Press, New York, **1986**, p 46.

6. Viera, M. P. New Water-Soluble Polymers for Surface Applications *Ph.D. Thesis, University of Durham*, **2000**.

7. Stoddart, A. Synthesis, Characterisation and Properties of Novel Dendrimers *Ph.D. Thesis, University of Durham*, **2002**.

8. Rannard, S. P.; Davis, N. *Org. Lett. 1* **1999**, *6*, 933.

Chapter 3

Synthesis of Dendronised Polymers via ROMP

3.1 Introduction

This chapter describes the synthesis of dendronised polymers of varying molecular weight via ring opening metathesis polymerisation (ROMP), using the well-defined ruthenium benzylidene initiator, $Cl_2Ru(=CHPh)(PCy_3)_2$. In particular, the NMR scale ROMP reactions of a mono-substituted and di-substituted first generation polycarbonate dendronised monomer using varying ratios of monomer to initiator will be discussed. A different monomer was subsequently added to these systems in order to deduce whether the reactions had remained living. A 1g scale ROMP reaction using a mono-substituted first generation polycarbonate dendronised monomer was also performed and the product characterisation results obtained will be described. The NMR scale ROMP reactions of a di-substituted second generation polycarbonate dendronised monomer using varying ratios of monomer to initiator were performed and a different monomer was subsequently added to test the living nature of these systems. The attempted ROMP of two di-substituted second generation polyurethane dendronised monomers, containing both t-butyl and 4-heptyl terminal groups, will also be described.

3.2 The NMR Scale Monitoring of ROMP reactions

NMR tubes were loaded with initiator, monomer and solvent and sealed under nitrogen in a glove box before rapid transfer (ca. 10 minutes) to the spectrometer. The initiation and propagation steps were probed directly by ^1H NMR spectroscopy, as the carbene signals for the initiating and propagating species were clearly distinguishable and well separated from all of the other hydrogen signals in the spectrum. Specifically, the disappearance of the signal corresponding to the alkylidene hydrogen ($\mathbf{H_a}$, 19.98 ppm) of the ruthenium initiator and the appearance of signals corresponding to the propagating alkylidene hydrogen ($\mathbf{H_p}$, ~19 ppm) can be monitored, see *Figure 3.1.* The signal corresponding to the vinylic hydrogens from the dendronised monomer ($\mathbf{H_v}$, 6.2 ppm) can also be monitored and when this signal has disappeared, it can be deduced that all of the monomer has reacted to form a

dendronised polymer. A different monomer can then be added to the polymerisation mixture to show whether the system has remained living. ^{1}H NMR spectroscopy can confirm the living nature of the system as the chemical shift of the signal representing $\mathbf{H_p}$ shifts, due to a change in its chemical environment when the second monomer is added. The addition of ethyl vinyl ether terminates the polymerisations, which predominantly leads to the capping of polymer chains with a CH_2 unit. All the polymers were precipitated using methanol.

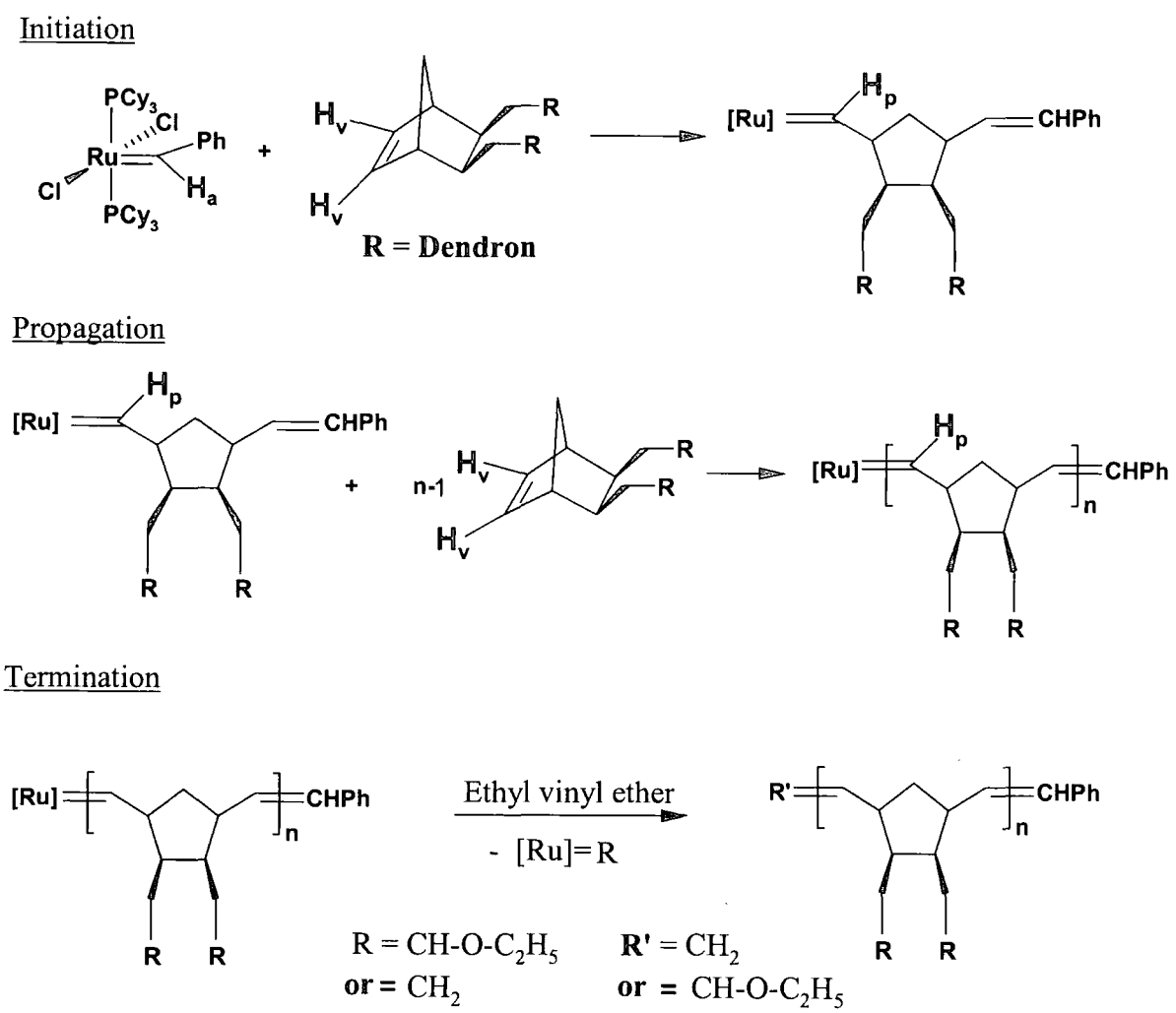

Figure 3.1 Initiating ($\mathbf{H_a}$) *and propagating* ($\mathbf{H_p}$) *alkylidene hydrogens and the vinylic hydrogens* ($\mathbf{H_v}$) *that can be monitored by* ^{1}*H NMR spectroscopy*

3.3 The NMR Scale Polymerisations of a Mono-Substituted First Generation Polycarbonate Dendronised Monomer (DMPCB1M)

Note: For the key to the name codes of the dendronised monomers, see chapter 2, section 2.5.1 and the bookmark card. The NMR scale polymerisations of **DMPCB1M,** at varying monomer to initiator molar ratios, have been investigated. In particular, ROMP reactions at a molar ratio of 10, 20 and 50 to 1 (monomer to initiator) were performed. For the 10:1 molar ratio system, the ^{1}H NMR spectra of both the ruthenium benzylidene initiator (Spectrum A) and **DMPCB1M** (Spectrum B) are shown in *Figure 3.2.* The alkylidene hydrogen of the ruthenium initiator $\mathbf{H_a}$ in dichloromethane-d can be seen at around 20.02 ppm (inset of Spectrum A). The disappearance of this signal during the polymerisation indicates that all of the initiator has been consumed. The signal corresponding to the vinylic hydrogens $\mathbf{H_v}$ of **DMPCB1M** (Spectrum B) in chloroform-d can be seen at approximately 6.02 ppm. Once this signal has disappeared, it can be deduced that all of the monomer has reacted and that the reaction has gone to completion. The ^{1}H NMR spectrum of the polymerisation mixture containing 10 molar equivalents of **DMPCB1M** in chloroform-d after one day is shown in Spectrum C of *Figure 3.2.* It can be seen that not all of the initiator has been consumed due to the presence of the signal corresponding to the alkylidene hydrogen of the ruthenium initiator $\mathbf{H_a}$ at 19.98 ppm. However, it can be deduced from the spectrum that all of the dendronised monomer has reacted due to the disappearance of the vinylic signal $\mathbf{H_v}$ at approximately 6.02 ppm. This suggests that in the case of the mono-substituted first generation polycarbonate dendronised monomer, the rate of propagation is significantly greater than the rate of initiation. This finding agrees with work reported, where systems involving both norbornene and mono-substituted norbornenes were found to have a greater rate of propagation than initiation.[1]

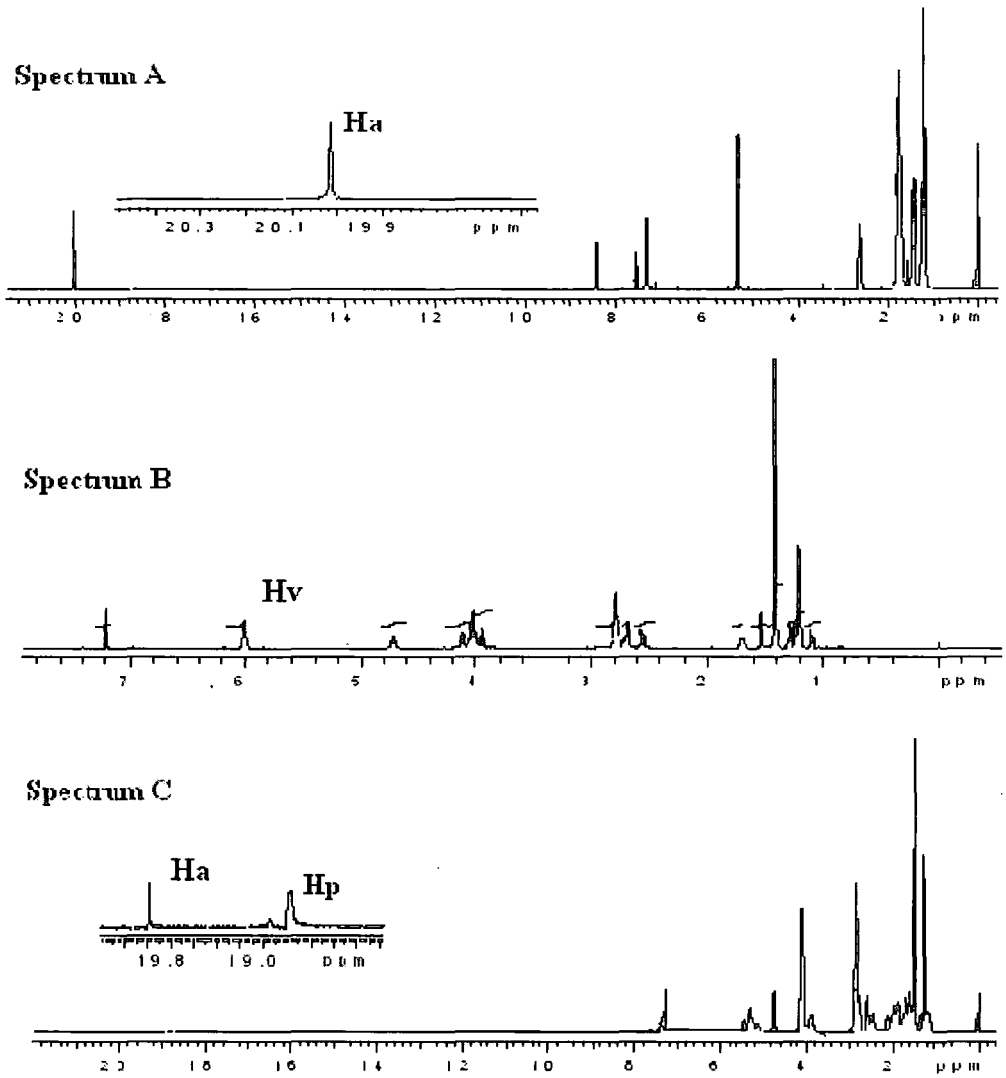

Figure 3.2 ^{1}H NMR spectra of the ruthenium benzylidene initiator in dichloromethane-d (Spectrum A), **DMPCB1M** *in chloroform-d* (Spectrum B) *and the polymerisation mixture in chloroform-d after one day containing* 10 *molar equivalents of* **DMPCB1M** (Spectrum C)

As can be seen from Spectrum C, there are two signals present at approximately 18.94 and 18.77 ppm, which correspond to the propagating alkylidene hydrogen, $\mathbf{H_p}$. The reason for the two signals being broad and unsymmetrical is probably due to the fact that the dendronised monomer, **DMPCB1M**, is mono-substituted and hence unsymmetrical. As a result of this, there exists the possibility of the dendronised monomer inserting in a head or tail fashion to the active site, leading to head-tail, tail-tail or head-head placements of repeat units in the polymer chain, *Figure 3.3.*[1] Another reason for the broad and unsymmetrical nature of the signals

could be due to the cis/trans effect, which is frequently seen in polymers synthesised by ROMP.[1] The presence of polymer could be detected by a broad signal at around 5.2 ppm, which corresponds to the unsaturated hydrogens of the polymer backbone, again the signal appears as a broad multiplet indicative of many vinyl hydrogen environments.

For the polymerisation reaction containing 20 molar equivalents of **DMPCB1M**, it was again found that initiator was present in the system after one day and that all of the dendronised monomer had reacted. The presence of the alkylidene hydrogen of the propagating species, H_p, could be detected at 18.95 and 18.77 ppm. Due to the fact there was insufficient dendronised monomer to react with all of the initiator in both the 10 and 20 molar equivalent polymerisations of **DMPCB1M**, it was decided to increase the molar ratio of dendronised monomer to 50.

The ^{1}H NMR spectrum corresponding to the polymerisation of 50 molar equivalents of **DMPCB1M** is shown in *Figure 3.4*. It can be deduced from the expanded inset of the alkylidene region of the spectrum that the signal corresponding to the alkylidene hydrogen of the ruthenium initiator H_a at approximately 20 ppm has disappeared after 1 day. The spectrum shows two broad signals at 18.88 ppm and 18.70 ppm corresponding to the hydrogens of the several propagating alkylidenes H_p. Also, the region at approximately 6.2 ppm indicates that all of the 50 molar equivalents of **DMPCB1M** have reacted. The broad signal at around 5.25 ppm corresponds to the unsaturated hydrogens of the polymer backbone.

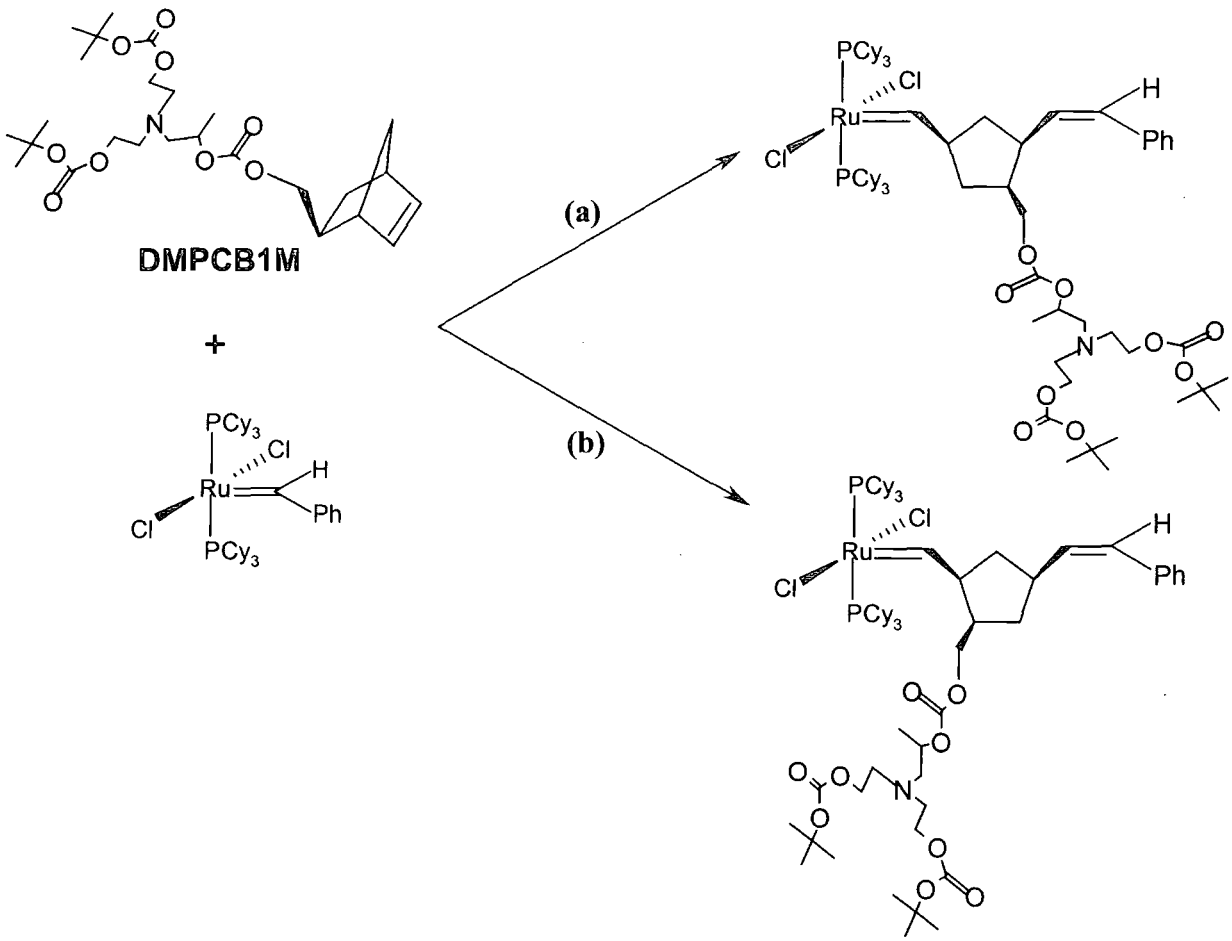

Figure 3.3 The products of the first insertions of **DMPCB1M** *into the ruthenium alkylidene initiator showing a) ruthenium tail insertion and b) ruthenium head insertion*

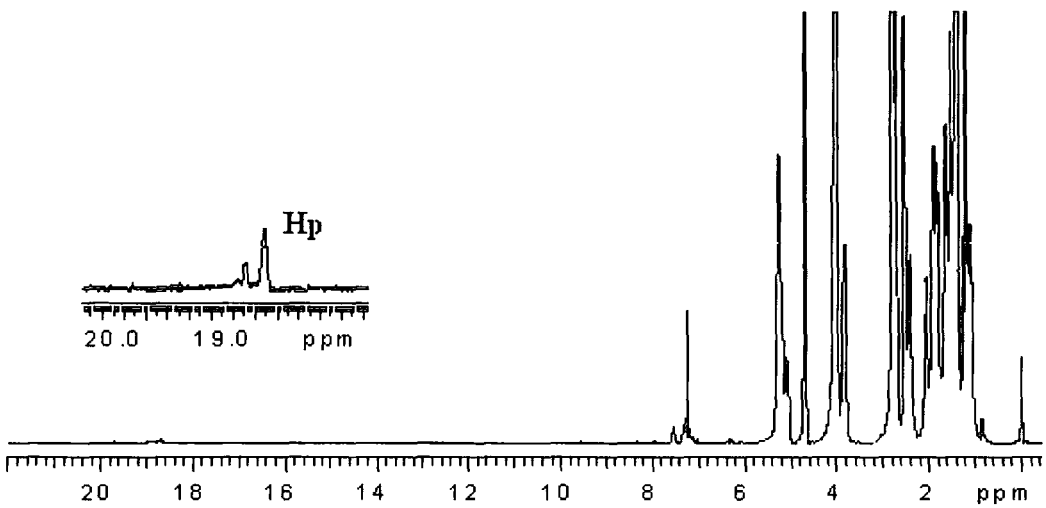

Figure 3.4 The ^{1}H NMR spectrum of the polymerisation of 50 molar equivalents of **DMPCB1M** *in chloroform-d after one day*

The ^{13}C NMR spectrum was also obtained for the 50 molar equivalents polymerisation of **DMPCB1M**, *Figure 3.5*. The spectrum shows a complex series of signals arising from vinylic carbons in the region between 130 and 135 ppm, which are probably due to a combination of cis/trans and head/tail sequence effects. The signals due to the cyclopentylene units between 30 and 50 ppm are similarly weak, broad and overlapping. The poor spectral resolution and signal to noise ratio for these sets of signals made it impossible to calculate the cis/trans vinylene ratio of the polymer or any of the details of microstructure. However, it has been reported that the well-defined ruthenium initiator used in these polymerisations gives a typical vinylene ratio close to 80/20 (trans/cis) and an essentially atactic statistical incorporation of monomer units, and the complexity of these spectra are consistent with such microstructures.[1]

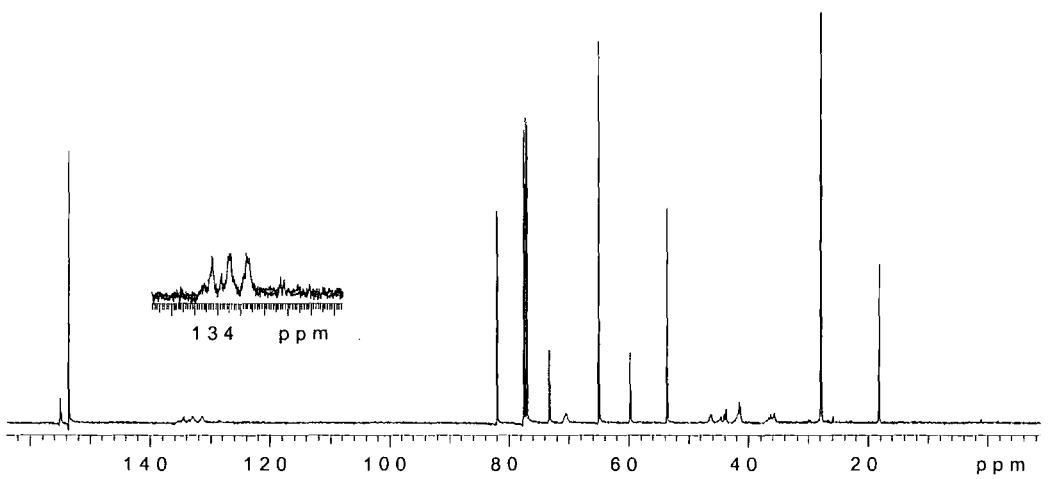

Figure 3.5 The ^{13}C NMR spectrum of the polymerisation of 50 *molar equivalents of* **DMPCB1M** *in chloroform-d*

3.3.1 The NMR Scale Synthesis of a Di-Block Copolymer containing DMPCB1M and Norbornene

Due to the fact that both the initiator and the monomer were completely consumed in the polymerisation of 50 molar equivalents of **DMPCB1M**, 50 molar equivalents of norbornene were added to the mixture in order to determine whether the system had remained living. It was found that when norbornene was added to the mixture, the signals corresponding to the hydrogen of the propagating alkylidene, $\mathbf{H_p}$, shifted from 18.88 and 18.70 ppm to 18.75 and 18.73 ppm, see *Figure 3.6*. The reason for this observed chemical shift in the propagating alkylidene, $\mathbf{H_p}$, is that when

norbornene is added to the system, H_p becomes adjacent to a cyclopentane ring containing *no* substituents, *Figure 3.7.* As a result of this observed chemical shift change, it can be deduced that the system is indeed living. Another observation from this reaction is that the two main peaks for the propagating alkylidene signals for the living **DMPCB1M** chains have different intensities, whereas for the propagating norbornene chains, the two signals are in roughly equal intensity. The propagating **DMPCB1M** is unsymmetrical and this observation implies a preference for head and tail insertion, although the data does not allow a decision on which is preferred.

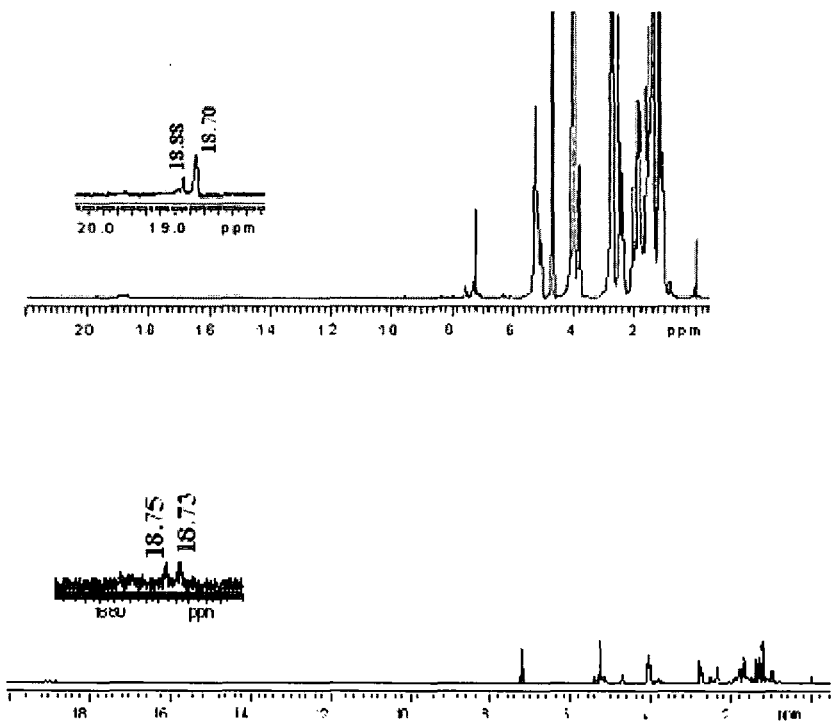

Figure 3.6 The ^1H NMR spectra of the polymerisation of 50 *molar equivalents of* **DMPCB1M** *(top spectrum) and the subsequent addition of* 50 *molar equivalents of norbornene (bottom spectrum) (both in chloroform-d)*

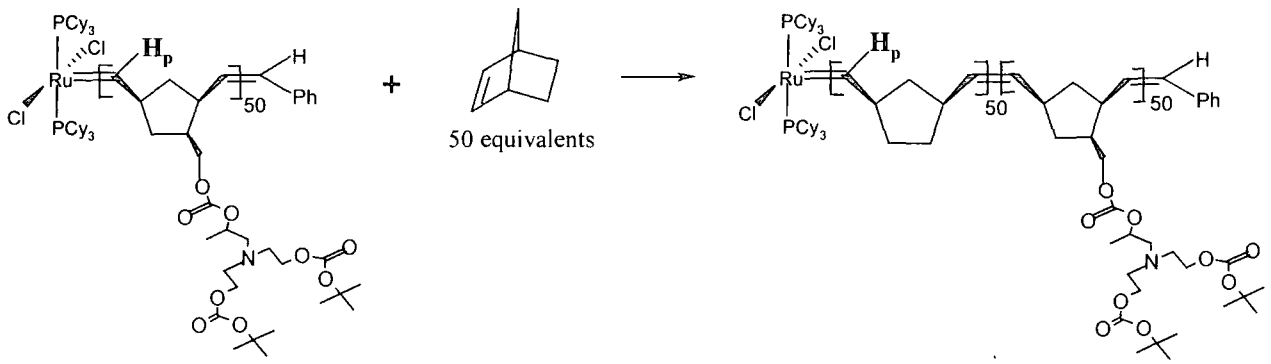

Figure 3.7 Addition of 50 molar equivalents of norbornene to the polymerisation mixture containing 50 molar equivalents of **DMPCB1M** *in chloroform-d to produce a diblock copolymer (only head insertion of monomer is shown)*

3.3.2 The Preparative Scale Polymerisation of DMPCB1M (50 molar equivalents)

A 1g-scale polymerisation using 50 molar equivalents of **DMPCB1M** was performed. The dendronised monomer and initiator were stirred overnight in dichloromethane and the reaction was terminated by addition of ethyl vinyl ether. The mixture was precipitated using methanol and dried in the oven resulting in a brown glass-like solid polymer.

3.3.3 The Characterisation of Polymers obtained from the Polymerisation of DMPCB1M

The GPC characterisation results are shown in *Table 3.1.* For the 20 and 50 molar ratio systems, it can be deduced that there is a reasonable correlation between the calculated and found molecular weight values. The polydispersity index of both systems is low, which indicates that a well-defined living polymerisation has occurred. In the diblock copolymer system, it can be seen that there is a poor correlation between the calculated and found molecular weight values and that the PDI of the system is high. The reason for this poor correlation is due to the fact that in the polymerisation of norbornene, the rate of propagation is much greater than the rate of initiation, not every living **DMPCB1M** chain will initiate a norbornene, which leads to high molecular weight systems having a broad PDI.

Table 3.1 GPC characterisation results for the three varying polymer systems obtained from the polymerisation of **DMPCB1M**

Molar ratio of dendronised monomer : initiator	M_n calculated	M_n found	Polydispersity Index (PDI)
20 to 1	10,773	10,400	1.15
50 to 1	25,650	18,500	1.12
50 : 50 norbornene : to 1	30,350	65,000	1.96

The glass transition temperature (T_g) of the polymers synthesised from both the 50 molar equivalents of **DMPCB1M** and the diblock copolymer systems were measured using differential scanning calorimetry (DSC). The samples were heated from –180°C to 180°C at a rate of 10°C per minute, cooled at a rate of 50°C per minute and heated a second time through the same temperature range at 10°C per minute. The value of T_g was taken as the midpoint of the inflection from the second heating run. It was found that the T_g of the 50 molar equivalent product (3°C) was essentially the same as that of the diblock copolymer product (5°C). The T_g of polynorbornene is 35°C and there is no transition at this point in the block copolymer. This indicates that the glass transition process in these materials is dominated by the side chain, an observation consistent with earlier studies of polynorbornene-g-polystyrene copolymers,[2] and probably indicates that there is no phase segregation in the diblock copolymer.

3.4 The NMR Scale Polymerisations of a Di-Substituted First Generation Polycarbonate Dendronised Monomer (DMPCB1D)

The NMR scale polymerisations of **DMPCB1D** at varying monomer to initiator molar ratios have been investigated. In particular, ROMP reactions at a molar ratio of 10, 20 and 60 to 1 (monomer to initiator) were performed. Analysis of the ^{1}H NMR spectrum of the 10:1 molar ratio system in chloroform-d after 1 hour showed that all of the initiator had reacted as there was no signal present at approximately 20 ppm and a small amount of the monomer remained as there was a small signal present at approximately 6.01 ppm arising from the monomer's vinylic hydrogens. However, analysis of the ^{1}H NMR spectrum of the polymerisation mixture after 1 day revealed that all of the monomer had reacted, as there was no signal remaining.

For both the 20:1 and 60:1 molar ratio systems, it was again found that all of the initiator had reacted after 1 hour and that approximately 1 day was required for all of the monomer to react. From these reactions, it could therefore be deduced that in the case of the polymerisation of a first generation di-substituted polycarbonate dendronised monomer, the rate of propagation is slower than the rate of initiation and hence the former is the rate determining step. We can speculate that the reason for the decrease in the rate of propagation in going from the mono-substituted dendronised monomer system to the di-substituted system is due to increased steric constraint. In the polymerisation of the di-substituted dendronised monomer, the increased occurrence of dendrons along the polymer backbone makes it more difficult for the incoming monomer to bind to the propagating ruthenium alkylidene species. Due to the pathway of the incoming di-substituted monomer being more hindered, the monomer preferentially reacts with the less hindered ruthenium alkylidene of the initiator. This observation leads to the speculation that in the polymerisation of the mono-substituted monomer the smaller of the propagating alkylidene signals is due to insertion of monomer with the dendron close to the metal centre (head insertion) and the larger peak arises from the species with the dendron further away (tail insertion).

3.4.1 The NMR Scale Synthesis of a Di-Block Copolymer containing DMPCB1D and Norbornene

In the case of the 20:1 molar ratio system containing **DMPCB1D**, 20 equivalents of norbornene were added to the polymerisation mixture in order to determine whether the system had remained living. When norbornene was added to the polymerisation mixture, the signals corresponding to the hydrogen of the propagating alkylidene, $\mathbf{H_p}$, shifted from a broad signal at 18.98 ppm to two sharp signals at 18.76 and 18.74 ppm, which are indicative of living polynorbornene.

3.4.2 The Characterisation of Polymers obtained from the Polymerisation of DMPCB1D

The GPC results for the polymers obtained from the polymerisation of **DMPCB1D** at varying molar ratios are shown in *Table 3.2*. For the 10:1 molar ratio system, it can be seen that there is a good correlation between the calculated and found molecular weight values and that the PDI of the system (1.09) is low, which is indicative of a well-defined living system. For the diblock copolymer system

containing 20 molar equivalents of both **DMPCB1D** and norbornene, there appears to be a good correlation between the calculated and found molecular weight values. However, it can be seen from the GPC trace that there is a high molecular weight shoulder present, which has the effect of increasing the polydispersity of the system to 1.51, *Figure 3.8 (a)*. This high molecular weight shoulder stems from the very high rate of norbornene propagation. With the 60:1 molar ratio system, the correlation between M_n calculated and M_n found is only fair and the polydispersity of the system (1.34) is again slightly raised. These findings stem from the high molecular weight 'bump' present in the GPC trace, for which we have no good explanation, *Figure 3.8 (b)*.

Table 3.2 GPC characterisation results for the three varying polymer systems obtained from the polymerisation of **DMPCB1D**

Molar ratio of dendronised monomer : initiator	M_n calculated	M_n found	Polydispersity Index (PDI)	Tg(°C)
10 to 1	9,330	9,130	1.09	1
20 : 20 norbornene : to 1	20,545	19,900	1.51	2
60 to 1	58,784	48,000	1.34	1

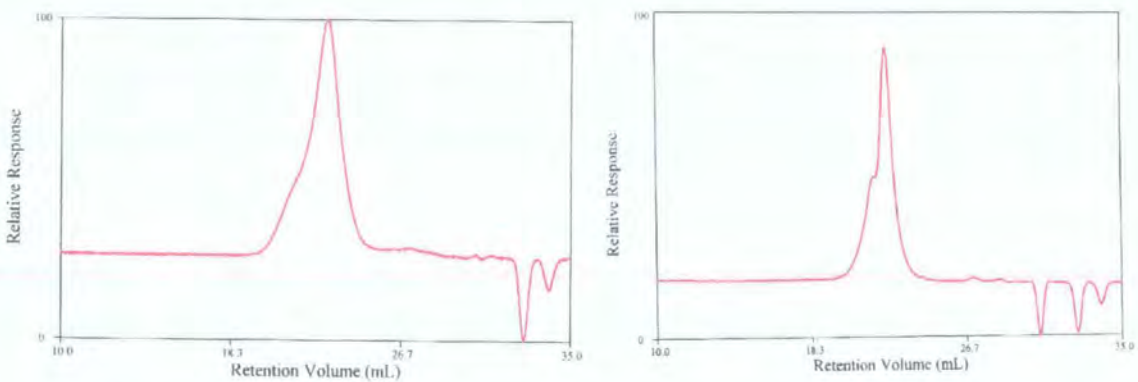

Figure 3.8 a) GPC trace of a diblock copolymer containing 20 equivalents of **DMPCB1D** *and 20 equivalents of norbornene (left trace) b) GPC trace of the polymerisation of a 60:1 molar ratio of* **DMPCB1D** *(right trace)*

The glass transition temperatures (T_g) of the homopolymers of **DMPCB1D** at a molar ratio of 10 and 60:1 to initiator were found to be approximately the same

(~1°C) and it was also found that the addition of 20 molar equivalents of norbornene to the polymerisation system did not affect the T_g value. The T_g of the first generation di-substituted monomer was found to be –12°C. These observations suggest that, as in the case of poly(**DMPCB1M**), the glass transition process is dominated by the dendritic side chain and no evidence for the polynorbornene backbone relaxation could be observed. Since the monomer T_g is 13°C lower than that of the polymer, it appears that polymerisation crowds the side chains resulting in a reduction of freedom of movement and a consequent increase in T_g.

3.5 The NMR Scale Polymerisations of a Di-Substituted Second Generation Polycarbonate Dendronised Monomer (DMPCB2D)

Two NMR scale polymerisations using **DMPCB2D** have been investigated at a molar ratio of 20 and 25 to 1 (monomer to initiator), using 0.254 g and 0.318 g of dendronised monomer respectively. The first polymerisation was performed using a 25:1 molar ratio of monomer and it was found from analysis of the ^{1}H NMR spectrum that the rate of initiation was greater than the rate of propagation. In particular, it was found that the initiator had fully reacted after approximately one day, but the di-substituted dendronised monomer took approximately one week to react fully. The slower rate of propagation results from the increased steric bulk of the di-substituted second generation dendrons, which makes it much more difficult for the incoming dendronised monomer to react with the propagating ruthenium alkylidene species. Therefore, the dendronised monomer preferentially reacts with the ruthenium alkylidene of the initiator and hence the rate of initiation is greater than the rate of propagation.

Due to the large number of synthetic steps required to synthesise **DMPCB2D** and the overall low yield of the final product, it was difficult to obtain sufficient quantities of material in order to polymerise the dendronised monomer at high molar ratios to initiator. As a result of this, when a second batch of **DMPCB2D** was synthesised, it was found that there was only enough material to perform a polymerisation reaction at a molar ratio of 20:1. One of the aims of the project was to perform polymerisations at a high monomer to initiator molar ratio using successive generations of dendronised monomers in order to examine the impact of the steric demands of the substituent on the polymerisation. It was anticipated that at a certain polymer chain length, the polymerisation would stop because the incoming monomer

would be unable to react with the propagating ruthenium alkylidene species, which would be buried in the polymer conformation. Unfortunately, this proved impossible to determine, as an insufficient amount of dendronised monomer was synthesised. However, it can be postulated that the molar ratio of monomer to initiator would not have to be increased greatly from the previously studied 25:1 molar ratio system, as the rate of propagation was already very slow in this instance.

The polymerisation of the 20:1 molar ratio system agreed with the findings from the 25:1 system in that the rate of initiation was greater than the rate of propagation and approximately 1 week was required for all of the second generation dendronised monomer to react.

3.5.1 The NMR Scale Synthesis of a Di-Block Copolymer containing DMPCB2D and a Norbornene Derivative

In the case of the 25:1 molar ratio system containing **DMPCB2D**, 10 equivalents of dimethylnorbornene-5-*exo*, 6-*exo*-dicarboxylate were added to the polymerisation mixture in order to determine whether the system had remained living. When the substituted norbornene derivative was added to the polymerisation mixture, the signals corresponding to the hydrogen of the propagating alkylidene, $\mathbf{H_p}$, shifted from 18.99 and 18.69 ppm to 18.59 and 18.37 ppm, see *Figure 3.9*. This observed shift in the chemical shift of the propagating signals proved that the system was indeed living and that a diblock copolymer had been synthesised.

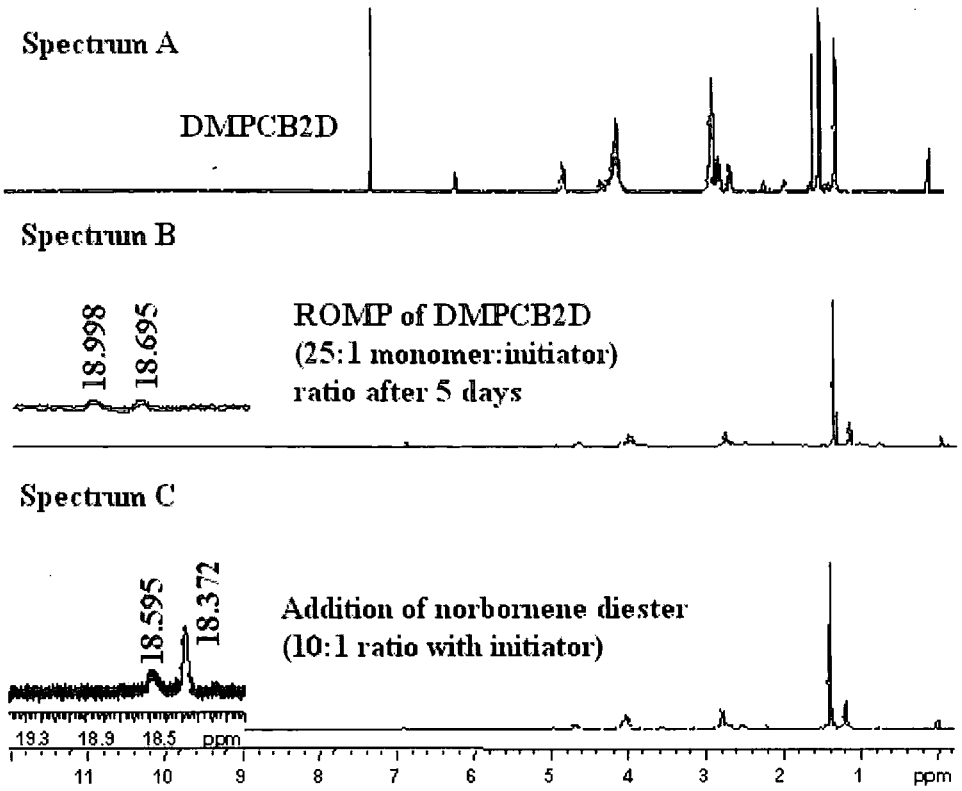

Figure 3.9 ^{1}H NMR spectra of **DMPCB2D** *in chloroform-d (Spectrum A), the living ROMP of* **DMPCB2D** *at a molar ratio of* 25:1 *in chloroform-d after 5 days (Spectrum B) and the formation of a diblock copolymer via the addition of* 10 *molar equivalents of* dimethylnorbornene-5-*exo*, 6-*exo*-dicarboxylate *(Spectrum C)*

3.5.2 The Characterisation of Polymers obtained from the Polymerisation of DMPCB2D

The GPC trace for the product of the polymerisation of 20 molar equivalents of **DMPCB2D** is shown in *Figure 3.10.* As can be seen, a well-defined polymerisation has occurred, as the peak is symmetrical. It was found that the PDI of the polymer was 1.09. The molecular weight of the polymer was found to be 17,300 Da, which was not in good agreement with the expected value of 41,800 Da. This poor correlation is thought to be due to the fact that the mass per unit length of the dendronised polymer obtained from the polymerisation of a second generation dendronised monomer is much larger than the calibration standard polystyrene.[3] Therefore, the true molar mass should indeed be higher than the molar mass indicated by GPC. However, a stiffening of the polymer chain due to the sterically demanding

dendrons can lead to an increased hydrodynamic volume, causing the molar mass obtained from GPC measurements to be larger than the actual molar mass. It has recently been suggested that third generation dendrons along the polymer backbone are required to fully stiffen the polymer chain, see *Figure 3.11*.[4] As second generation dendrons are being used in this instance, the polymer backbone has probably not stiffened fully and therefore, it is not surprising that the larger mass per unit length of the dendronised polymer as compared to the polystyrene standard is the dominant effect in the molar mass value measured by GPC.

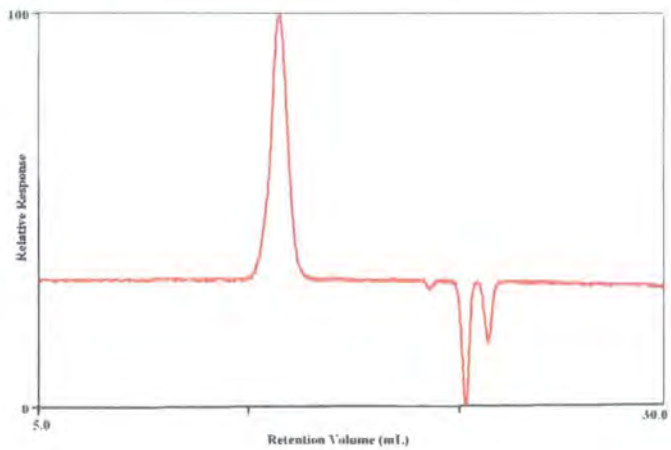

Figure 3.10 GPC trace of the polymerisation of a 20:1 *molar ratio of* **DMPCB2D**

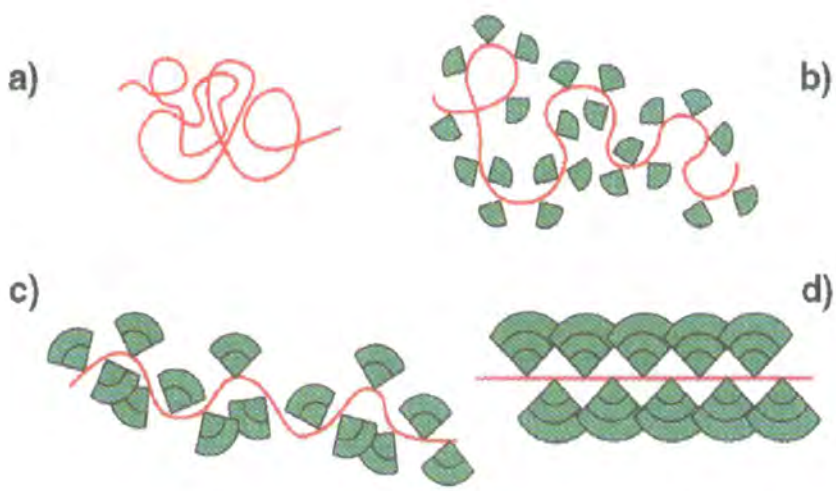

Figure 3.11 The effect of increasing dendron size on the stretching of the polymer backbone: a) a coiled polymer with no dendrons attached; b) dendrons of the first generation attached; c) dendrons of the second generation attached d) a linear polymer containing third generation dendrons attached

The T_g of the polymer obtained from the polymerisation of 20 molar equivalents of **DMPCB2D** was found to be –15°C, which is the same value found for the T_g of the monomer, clearly the side chain is dominating the glass transition process, as in earlier examples. In this case, there is no increase in T_g in going from monomer to a polymer of DP 20, which is surprising and contrasts with the situation for monomers bearing first generation dendrons where an increase in T_g of 13°C was observed on going from monomer to polymer. This suggests that the extent of dendron crowding is the same in the monomer as in the polymer in this case, which is surprising if true. Clearly, the factors controlling T_g are subtle.

The GPC trace for the di-block copolymer synthesised from the polymerisation of **DMPCB2D,** at a 25:1 molar ratio system, and 10 equivalents of dimethylnorbornene-5-*exo*, 6-*exo*-dicarboxylate is shown in *Figure 3.12.* The large, unsymmetrical peak (peak **A**) has a molecular weight of approximately 25,000 Da. This peak is thought to represent the diblock copolymer product, as the high molecular shoulder present is indicative of the fast rate of norbornene propagation. The next signal at approximately 2,500 Da (peak **B**), which represents about 10% of the overall sample, was initially thought to represent unreacted second generation dendronised monomer. However, this seems unlikely, as ^{1}H NMR spectroscopy clearly showed that all of the monomer had reacted. The two remaining low molecular weight signals (peak **C** and peak **D**) have to be ascribed to some degradative side reaction or to the presence of impurities. As the second generation dendronised monomer was found to be pure by a number of characterisation methods prior to polymerisation and there were no low molecular weight signals seen in the polymerisation of 20 molar equivalents of **DMPCB2D**, *Figure 3.10,* the author can only speculate that the three lower molecular weight signals in the GPC trace are a result of degradative side reactions occurring after the addition of the norbornene derivative to the polymerisation system.

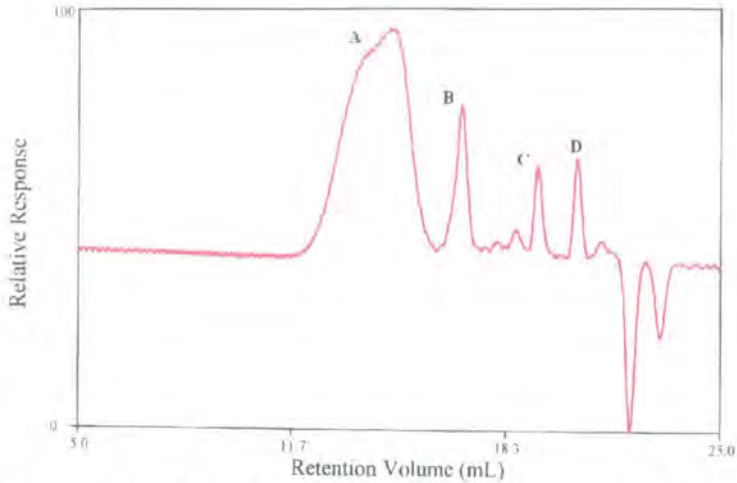

Figure 3.12 GPC trace of a diblock copolymer system containing 25 *equivalents of* **DMPCB2D** *and* 10 *equivalents of* dimethylnorbornene-*5-exo, 6-exo*-dicarboxylate

3.6 Attempted NMR Scale Polymerisations of Di-substituted Second Generation Polyurethane Dendronised Monomers

The ROMP of two di-substituted second generation polyurethane dendronised monomers, **DMPUB2D** and **DMPUH2D**, containing t-butyl and 4-heptyl terminal groups, respectively, has been attempted. ^{1}H NMR spectroscopy was used to monitor the polymerisation of **DMPUB2D** at a molar ratio of 20:1 monomer: initiator. It was found after 1 hour, that a signal was present corresponding to the hydrogen attached to the ruthenium carbene of the initiator, $\mathbf{H_a}$, at ~19.98 ppm, but that there were no signals present corresponding to the hydrogen from a propagating ruthenium alkylidene species, $\mathbf{H_p}$. A spectrum of the reaction mixture was obtained after one day, which indicated that there were still no propagating species present due to the absence of a signal in the region between 18.5 and 19.5 ppm. Interestingly however, it was found that the initiator signal had disappeared too, indicating that the initiator had decomposed. After two days, the situation had not changed, as there were no initiator or propagating signals present in the spectrum of the mixture. A GPC trace of the mixture was obtained, which showed that only dendronised monomer and some relatively low molecular weight impurities were present in the mixture and that no polymer had formed.

The polymerisation of **DMPUH2D**, containing di-substituted second generation polyurethane dendrons with 4-heptyl terminal groups, at a molar ratio of 20:1 (monomer: initiator) was attempted. This polymerisation showed the same characteristics as the polymerisation of **DMPUB2D**, in that the initiator signal

disappeared after approximately one day and there were never any propagating signals present in the spectrum.

A series of experiments was then performed in order to determine the reason why the polymerisations failed. A ^{1}H NMR spectrum of the chloroform-d used in the experiments was obtained prior to the reactions and from the spectrum, it could be deduced that the chloroform was pure. The ^{1}H NMR spectrum of the initiator indicated that there were no impurities present and several other colleagues in the laboratory had also successfully used this batch of initiator.

In order to deduce whether the polyurethane dendrons of **DMPUB2D** or **DMPUH2D** had any effect on the decomposition of the initiator, a third generation polyurethane dendron, provided by Dr Stoddart,[5] was added to the same batch of initiator in chloroform-d and the mixture was monitored by ^{1}H NMR spectroscopy. After several days, it was found that the initiator signal was still present and no significant decomposition had occurred. This suggests that polyurethane linkages are compatible with the ruthenium benzylidene initiator used in this study, which is in agreement with work reported in the literature that suggests the initiator is stable in the presence of this type of functional group.[6]

Due to extensive H-bonding within the polyurethane dendron structure, it was postulated that by-products and solvents might be tightly held within the structure. In particular, it was thought that imidazole, which is a by-product of CDI reactions used in the synthesis of the dendronised monomers, could strongly H-bond to the dendrons within the structure, making it extremely difficult to separate. In order to determine whether the presence of imidazole would cause the initiator to decompose, 10 molar equivalents of imidazole were added to initiator in chloroform-d and the reaction was monitored by ^{1}H NMR spectroscopy. After 1 hour, it could be seen that the initiator signal had totally disappeared and that a doublet at approximately 20.47 ppm was present. ^{31}P NMR spectroscopy was used to determine whether the new signal represented a new initiator or propagating species. If a new initiator had formed from the ligand exchange reaction of imidazole with the ruthenium benzylidene initiator, tricyclohexylphosphine would be liberated, the presence of which could be determined by ^{31}P NMR spectroscopy. However, the signals from the ^{31}P NMR spectrum of the reaction mixture in chloroform-d did not coincide with the signals from the free phosphine ^{31}P NMR spectrum, hence the presence of a new initiator species was not confirmed using this method. A small substituted norbornene

monomer, dimethylnorbornene-5-*exo*, 6-*exo*-dicarboxylate, was then added to the reaction mixture, in order to deduce whether the new doublet at 20.47 ppm shifted or disappeared, which would give an indication as to the type of species the signal represented. By analysis of the ^{1}H NMR spectrum, it was found that the doublet at approximately 20.47 ppm did not shift after the addition of the small monomer and no new signals appeared. On this evidence, it could be deduced that there were no new initiator or propagating species formed from the reaction of imidazole with the ruthenium benzylidene initiator as the polymerisation of the small substituted norbornene monomer would have resulted in the disappearance or chemical shift change of the doublet at 20.47 ppm. Therefore, as the addition of imidazole caused a new doublet to form, which was not observed in the ^{1}H NMR spectrum of the attempted polymerisations of **DMPUH2D** and **DMPUB2D**, it could be concluded that imidazole was *not* to blame for the decomposition of the initiator. The species represented by the doublet at 20.47 ppm could not be explained.

Another possible explanation for the failed polymerisations was that an impurity existed in both the dendronised monomers, which had the effect of destroying the initiator within 1 day. When **DMPUB2D** was synthesised, the purity of the monomer was analysed by a number of methods, see section 2.5.5. The GPC trace indicated that two low molecular weight species were present in the sample at low concentration. Also, both electro spray and MALDI-TOF mass spectrometry were unable to detect the molecular ion. The decomposition of the initiator as a result of the impurities detected by GPC is a possibility, but this cannot be proven as the small amount of **DMPUB2D** synthesised was all consumed in the attempted polymerisation. In the case of **DMPUH2D**, there were no apparent impurities by GPC and the MALDI-TOF mass spectrum showed the presence of signals at 2415 and 2437 Da, corresponding to $[M]^+$ and $[M+Na]^+$, respectively. There was a slight inaccuracy in molecular weight as determined by electro spray mass spectrometry, but this could have been due to the instrument's calibration being slightly out. It is therefore difficult to suggest that impurities in **DMPUH2D** resulted in the failure of the attempted polymerisation of the dendronised monomer. Urethane substituted monomers were expected to undergo polymerisation with this most tolerant of available ROMP initiators. Consequently, the author is unable to account for the surprising failure of attempts to effect the ROMP of **DMPUB2D** and **DMPUH2D** using the Grubbs initiator.

3.7 Conclusions

The NMR scale ROMP reactions of a mono- and di-substituted first generation polycarbonate dendronised monomer along with a di-substituted second generation polycarbonate dendronised monomer, using varying ratios of monomer to initiator, have been performed successfully. It was found that the polymerisations were well-defined and that di-block copolymer products could be obtained due to the living nature of the systems. The attempted ROMP of polyurethane di-substituted second generation dendronised monomers containing two different terminal groups was unsuccessful. The polymers obtained from the ROMP of the polycarbonate dendronised monomers were analysed by Atomic Force Microscopy (AFM), the details of which are described in chapter 4 along with molecular modelling studies carried out on the polycarbonate systems.

3.8 References

1. Ivin, K. J; Mol, J. C. *Olefin Metathesis and Metathesis Polymerisation*, Academic Press: London, **1997**.

2. Rizmi, A. C. M; Khosravi, E.; Feast, W. J; Mohsin, M. A; Johnson, A. F. *Polymer* **1998**, *39*, 6605.

3. Rabe, J. P.; Schlüter, A. D. *Angew. Chem. Int. Ed.* **2000**, *39*, 864.

4. Zhang, A.; Shu, L.; Bo, Z.; Schlüter, A. D. *Macromol. Chem. Phys.* **2003**, *204*, 328.

5. Stoddart, A. Synthesis, Characterisation and Properties of Novel Dendrimers *Ph.D. Thesis, University of Durham*, **2002**.

6. Bielawski, C. W.; Grubbs, R. H. *Angew. Chem. Int. Ed.* **2000**, *39*, 16.

Chapter 4

Molecular modelling and AFM studies

4.1 Introduction

This chapter describes the results of molecular modelling studies performed using the CAChe® 3.2 program, designed by Oxford Molecular, together with results of Atomic Force Microscopy (AFM) studies performed using a scanning probe microscope MultiMode Nanoscope IIIa (Digital Instruments, Santa Barbara, CA). In particular, molecular modelling studies were carried out on the di-substituted second generation polycarbonate dendronised monomer, **DMPCB2D**, and on poly(**DMPCB2D**) up to a degree of polymerisation of 16. AFM measurements were carried out on a polymer sample synthesised from the polymerisation of 20 molar equivalents of **DMPCB2D** and the images obtained will be presented and discussed in the light of the modelling studies.

4.2 Background to Molecular Modelling using CAChe

CAChe for Windows is a computer-aided molecular design (CAMD) modelling tool for Microsoft Windows operating systems. It enables the user to draw and model molecules and perform calculations on a molecule to discover molecular properties and energy values. These calculations, or experiments, are performed by carrying out computations, which apply equations from classical mechanics and quantum mechanics to a molecule. The molecular mechanics calculation calculates the total steric energy of the molecule by combining the strain energies of bonds, angles, dihedrals and non-bonded interactions such as van der Waals and electrostatic interactions. The results of these calculations can be displayed in a variety of ways, one of which involves a three-dimensional energy graph viewed simultaneously alongside a series of low-energy conformations of the structure, this procedure will be illustrated later in this chapter.

As an example of the steps in the optimisation experiment, consider the case of propane shown overleaf, *Figure 4.1*. In the example, the C-C-C bond angle was varied and the computed steric energy dropped from 13.3 kcal/mol in the initial

strained conformation to a minimised value of 1.5 kcal/mol in the relaxed conformation.

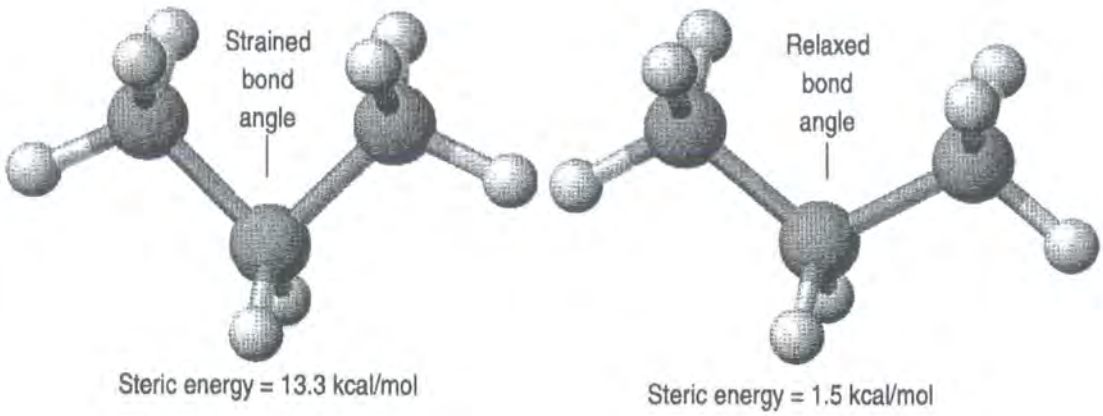

Figure 4.1 Optimisation experiment performed by CAChe to lower the steric energy of a molecule of propane

Using the CAChe program also provides the user with a three dimensional modelling tool that aids in the visualisation of the structure and by rotating and examining a model of a molecule, a new perspective can be gained. Three-dimensional ball and stick models, space-filling models, and colour coded shaded surfaces are some of the many useful features that can be used in the visualisation of the structure.

4.2.1 Performing Experiments with CAChe

The first process in running an experiment in CAChe for Windows is to build the desired molecule in a chemical sample file and view it from different perspectives by moving it around the screen, rotating it in three dimensions, and scaling it. A computation can then be run on CAChe to generate the desired data for the properties of the molecule that are of interest. An example of the type of experiment that would be carried out on a molecule is a Mechanics computational application experiment. Mechanics optimises molecular geometry using classical molecular mechanics. The experiment finds an optimum geometry by systematically moving all the atoms in a chemical sample until the net force acting on each atom approaches zero. Mechanics then generates files containing the computed structural details, and alters the structure of the molecule in the chemical file to correspond to the calculated optimum

geometry. In effect, the operator draws the molecular structure using conventional bond connectivities and multiplicities, and the computer program is then operated to optimise the geometry of the molecule by minimising the energy as a function of the structure.

Once the experiments have finished, a series of low-energy conformations of the molecule and the corresponding point on a potential energy graph can be viewed simultaneously. When the point in the energy graph is moved to a region of higher or lower potential energy, the geometry of the molecule changes and its conformation at that particular energy can be viewed.

4.3 Obtaining the Minimum Energy Conformations of DMPCB2D

In order to obtain minimum energy conformations of **DMPCB2D**, calculations using the MM3 force field first introduced by Allinger[1] were performed on the dendronised monomer in which sections of the molecule were considered to maintain their minimised geometry while single bond sequences were allowed to vary their dihedral angles so as to minimise the total energy. The first step of the procedure was to highlight the bonds whose dihedral angles were being energy minimised in the dendronised monomer, *Figure 4.2 a)*. As can be seen, the dihedral angle between the (–CH-CH-CH_2-O)- bonds of the norbornene monomer and the dendron was highlighted, (*1), as was the dihedral angle between the (-CH_2-N-CH_2-CH)- bonds of the dendron itself, (*2), *Figure 4.2 b)*. Calculations were performed on these dihedral angles, all symmetry equivalent structures being included in the calculation, as it is thought that they would be important in determining the overall minimum energy conformations of **DMPCB2D**. In the CAChe program, the Define Geometry Label option was selected, which performed a search between the various limits for the selected dihedral angles. In particular, a sequence of molecular mechanics minimisation calculations was performed for each of the dihedral angles, which involved calculations between pre-determined angle ranges. The Optimised Conformation Map experiment was then selected, which generates a potential energy map of conformations determined by the geometry search labels for each dihedral angle highlighted in the sample. Therefore, each point on the potential energy map corresponds to a particular conformer of **DMPCB2D**, the structure of which has been optimised.

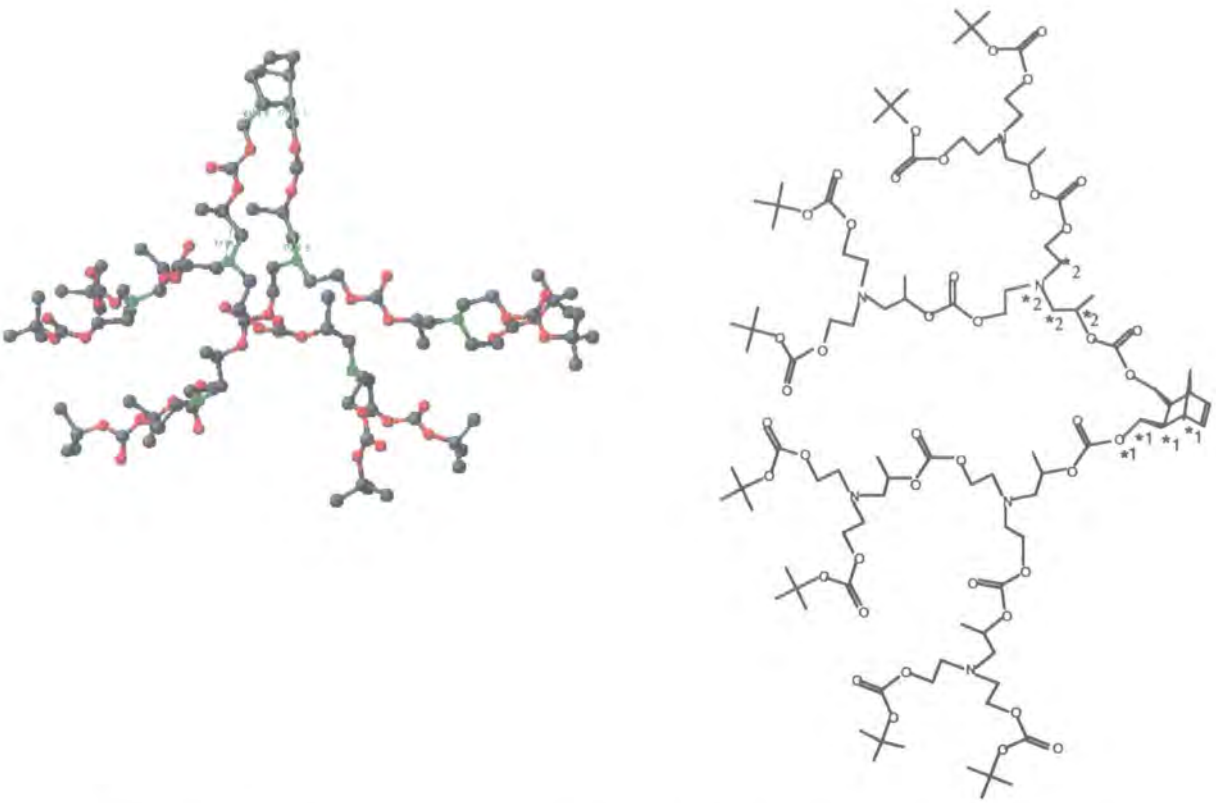

Figure 4.2 a) The varied dihedral angles (solid green lines) of **DMPCB2D** *as seen in the CAChe program (carbon = grey, oxygen = red, nitrogen = green, hydrogens omitted for clarity) (left) and b) the structure of* **DMPCB2D** *indicating the two dihedral angles selected for calculation (*1 and *2) (right)*

The optimised map experiment results are shown in *Figure 4.3*. As can be seen, there is an optimised energy graph (*Figure 4.3 left*) with a small sphere present at a particular point on the graph, which represents the energy of the corresponding conformation of **DMPCB2D** shown in *Figure 4.3 right*. The sphere can be moved to a new point on the energy graph, which has the effect of changing the molecular conformation of the dendronised monomer. In the case of *Figure 4.3*, the overall energy of the monomer is fairly low (approximately 158 kcal/mol) and this is reflected in the structure of the molecule as the dendrons are not interfering with each other in a manner which would cause an increase in repulsion energy between the two dendrons. The space filling structure of the molecule gives a better indication of the distance between the dendrons in this conformation, *Figure 4.4*. As can be seen, a slight space exists between the two dendrons even though they are well packed together. This packing, along with any attractive forces that exist between the two

dendrons (there are no H-bonding possibilities between the polycarbonate dendrons), probably leads to the overall low potential energy of this conformer.

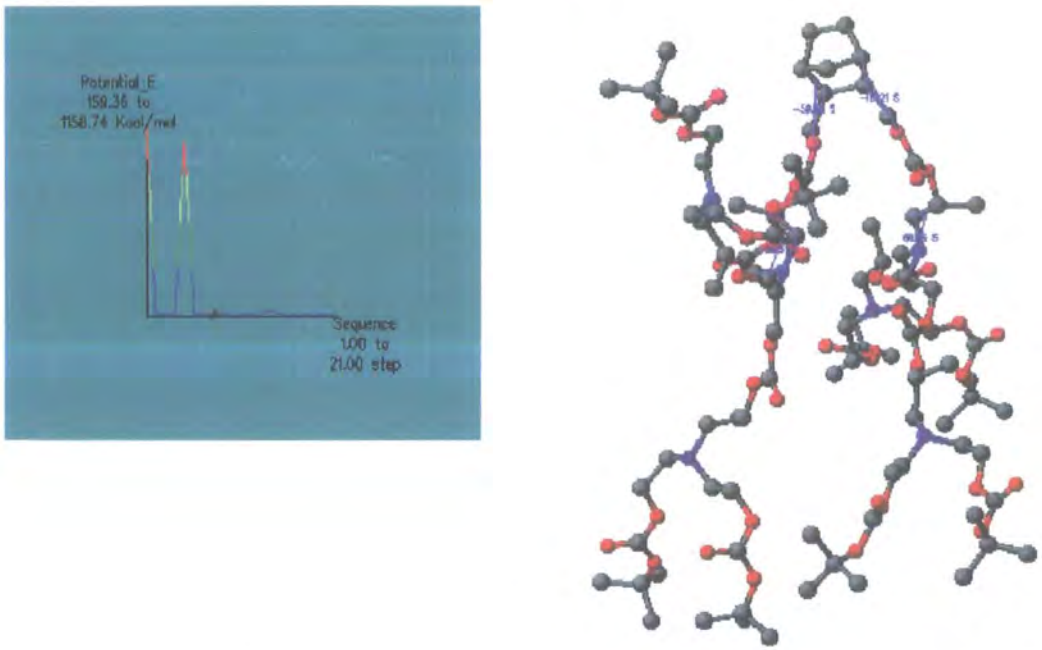

Figure 4.3 a) The potential energy curve calculated from an optimised map experiment (left) and b) the conformation of **DMPCB2D** *corresponding to the point of the sphere on the energy curve (carbon = grey, oxygen = red, nitrogen = blue) (right)*

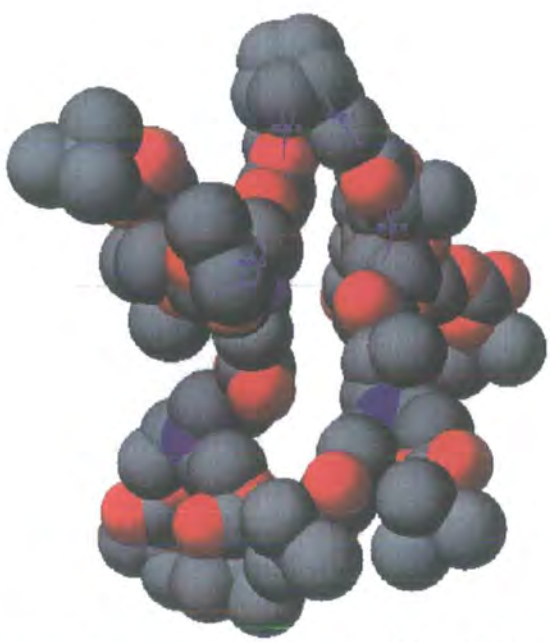

Figure 4.4 A low potential energy conformer of **DMPCB2D** *shown via space filling (carbon = grey, oxygen = red, nitrogen = blue)*

When the small sphere was moved to a high potential energy point on the curve, it could be deduced that the dendrons were interfering with each other in the corresponding conformation of **DMPCB2D**, leading to a high repulsion energy, *Figure 4.5.*

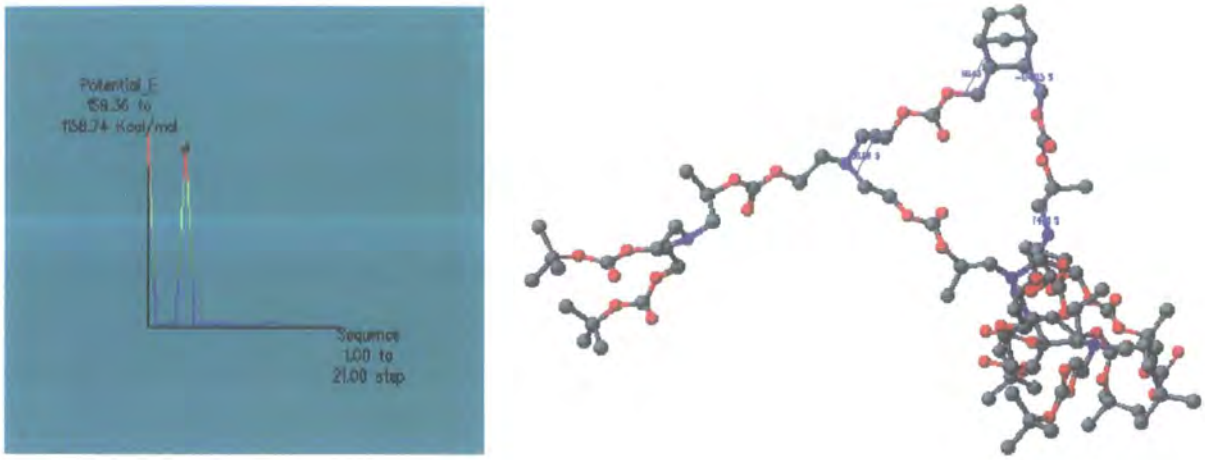

Figure 4.5 a) The potential energy curve with the sphere at a high potential energy point (left) b) the conformation of **DMPCB2D** *corresponding to the point of the sphere along the energy curve (carbon = grey, oxygen = red, nitrogen = blue) (right)*

The space filling structure of the conformer of **DMPCB2D** at this particular point on the energy curve is shown in *Figure 4.6.*

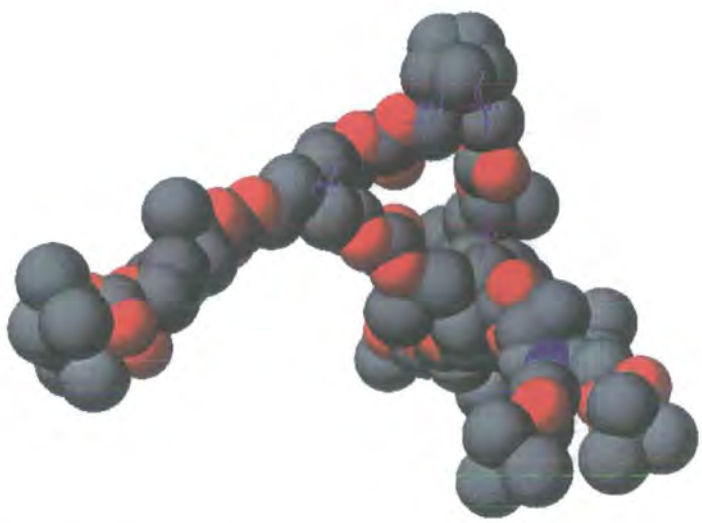

Figure 4.6 A high potential energy conformer of **DMPCB2D** *shown via space filling (carbon = grey, oxygen = red, nitrogen = blue)*

As can be seen, one arm of a dendron is interfering with the other dendron leading to a high repulsion energy, which has the effect of increasing the overall potential energy of the conformer.

When a calculation was performed, which included a third dihedral angle near to the periphery of the dendrons, *Figure 4.7*, a total of approximately seven minimum energy conformations of **DMPCB2D** were established from the lowest values on the potential energy curve.

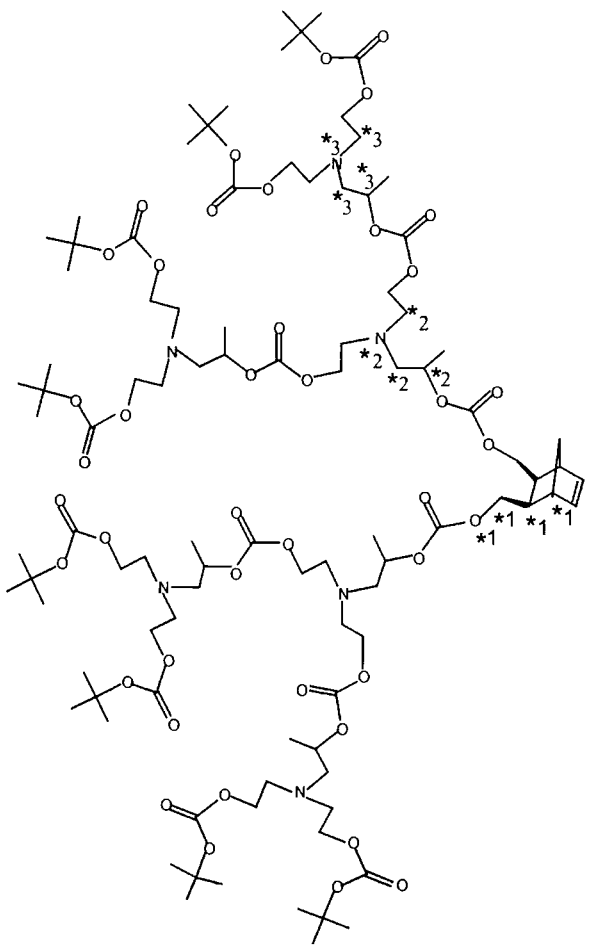

Figure 4.7 Structure of **DMPCB2D** *showing the three dihedral angles (*1, *2, *3) used in the dihedral angle effect calculations*

Two of the lowest energy conformers of **DMPCB2D**, which had potential energies of 141.8 kcal/mol and 144.5 kcal/mol, respectively, are shown in *Figure 4.8.* Both the ball and stick and space filling structures are shown for each conformer.

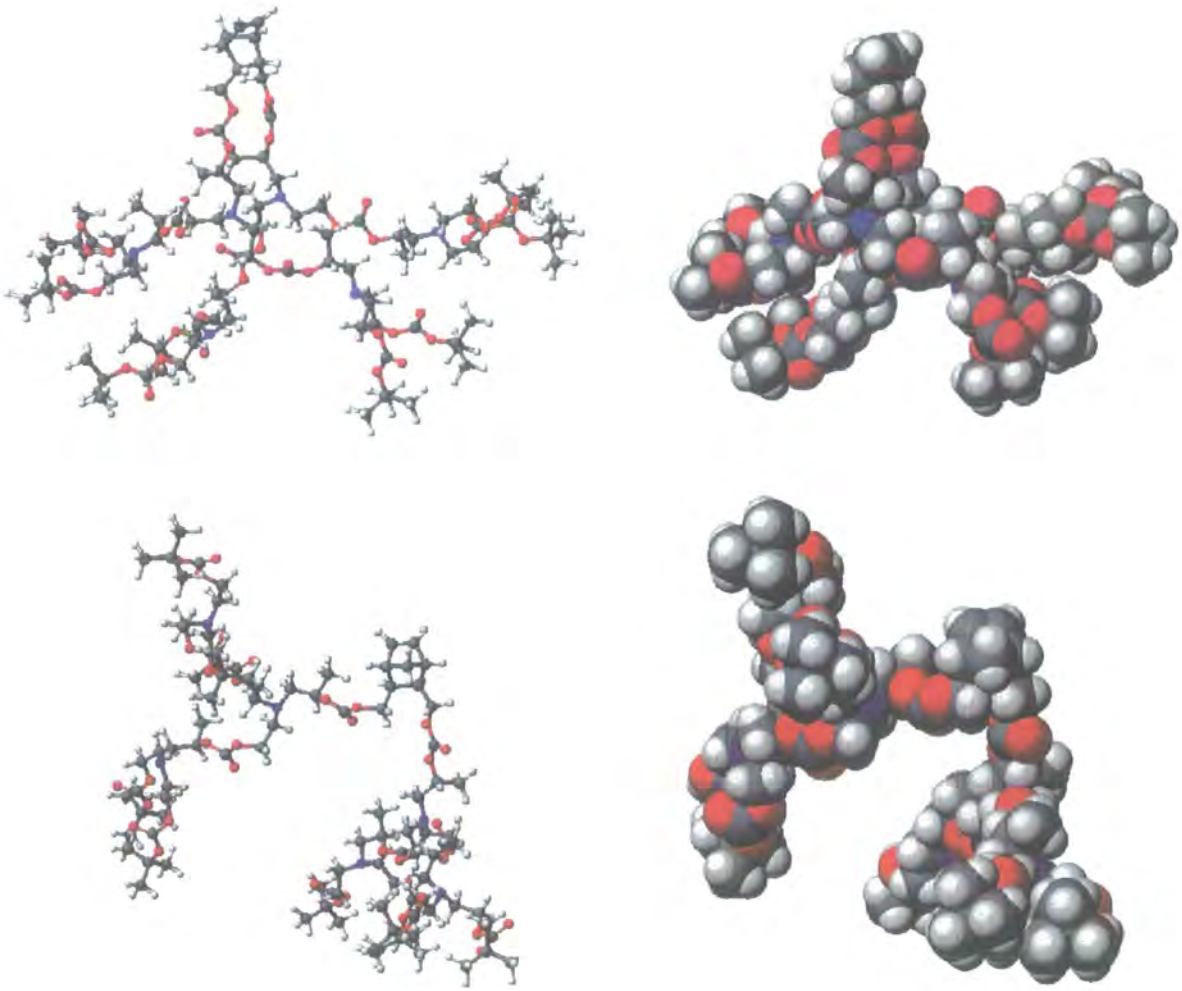

Figure 4.8 a) Top left, ball and stick and, top right, space filling representation of a conformer with a potential energy of 141.8 kcal/mol and b) bottom left, and bottom right, representations of a conformer with a potential energy of 144.5 kcal/mol (carbon = dark grey, oxygen = red, nitrogen = blue, hydrogen = grey)

As can be seen, in the conformer with the potential energy of 141.8 kcal/mol, the two dendrons are tightly packed together, which is especially noticeable in the space filling structure shown in the top right of *Figure 4.8*. There is no H-bonding possible between the dendrons in these polycarbonate dendronised monomers, hence the reason for the potential energy value of the conformer being low must be due to a combination of the close packing of the dendrons and any attractive forces that exist between the dendrons. Due to the existence of a small space between the two

dendrons, the repulsion energy should be very low. In the case of the conformer with the potential energy of 144.5 kcal/mol, it can be seen that the dendrons are far apart from each other and hence, there should be no repulsion energy between the two dendrons, which gives the overall low potential energy of the structure. In both structures, the positions of the atoms within the dendrons themselves have been optimised to reduce the net force acting on each atom.

4.4 Constructing Polymers using CAChe

By performing the dihedral angle calculations on **DMPCB2D**, an indication of the approximate minimum energy conformation of the molecule was established. However, the conformation of the polymer at various degrees of polymerisation was required in order to deduce, by approximation, the shape of the structure when the monomer units combine. The reason why the polymer structures are only an approximation is due to the fact that it would have been too time consuming to take into consideration the effects of cis/trans double bond isomerisation along the polymer backbone, which is typically 20/80, in polymerisations using Grubbs' ruthenium benzylidene initiator. Also, when combining the monomers, it was assumed that the conformation of each dendronised unit was identical, which in reality is unlikely to be the case as the dendrons will be in constant motion. Nonetheless, it was thought that approximations in the size and shape of the polymer structures might aid in the visualisation of the polymers via AFM imaging.

Using the seven minimum energy conformations of **DMPCB2D** approximated by the dihedral angle effect calculations, two, four and eight repeat units of each conformer were built using the CAChe program. A calculation was then performed on each of the structures at every repeat unit length to determine the optimised structures and hence the overall potential energy of the structures, the results of which can be seen in *Table 4.1*.

Table 4.1 The potential energy of various repeat units of **DMPCB2D**

Conformer number of **DMPCB2D**	Potential energy of conformer (kcal/mol)	16 DP (kcal/mol)	8DP (kcal/mol)	4DP (kcal/mol)	2DP (kcal/mol)
1	141.8		6,707	2,536	240.4
2	152.5		5,343	1,474	268.6
3	148.8		1,661	503	264.1
4	144.5	5,205	1,280	436	234.9
5	145.1		4,535	708	247.1
6	147.6		12,957	2,372	242.6
7	148.3	10,099	2,243	479	251.2

As can be seen, the potential energies of the structures containing two repeat units are roughly the same for each of the seven conformers. It is only after combining the dendronised monomer four times that marked differences appear in the overall potential energies of the structures, e.g. conformer 4 when combined to a DP of 4 has the lowest potential energy of 436 kcal/mol, whereas conformer 1, which had the lowest potential energy of all the conformers, has the highest potential energy for all the tetramers of 2,536 kcal/mol. The reason for this marked difference between the two structures is due to the packing efficiency of the dendrons when the monomer units combine. It appears that when the dendrons are far apart from each other as in the case of conformer 4, a more efficient packing of the dendrons takes place when the monomer units combine, *Figure 4.9 (left)*. This can be seen from the structure, as the dendron arms do not seem to be too entangled with each other. This is obviously not the case for the tetramer derived from conformer 1, where the result of the dendrons being close together in the original conformer results in a poor packing of monomer units, which leads to the structure having a high potential energy, *Figure 4.9 (right)*. It can be noted from this structure that the dendron arms appear to be highly entangled with each other, which has the effect of increasing the overall potential energy of the structure.

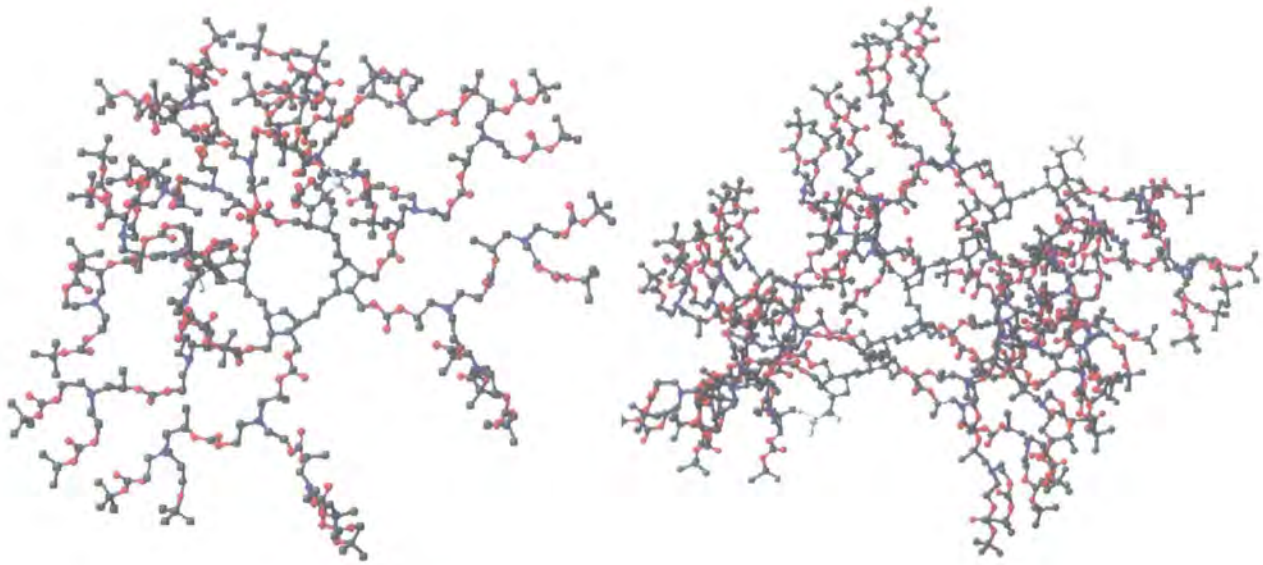

Figure 4.9 The structures corresponding to 4DP of conformer 4 (left) and conformer 1 (right) (carbon = grey, oxygen = red, nitrogen = blue, hydrogens have been omitted for clarity)

As can be seen from *Table 4.1*, conformer 4 at a degree of polymerisation of 8 has the lowest potential energy of 1,280 kcal/mol, the structure of which can be seen in *Figure 4.10.* The structure at this degree of polymerisation is now very crowded and as such, there is virtually no space between the dendrons of the monomer units. This is an energy minimised structure and hence it can be assumed that the structure prefers to be tightly packed in this ball-shaped manner. The shape of the structure at this degree of polymerisation agrees with work previously reported, which suggests at low DP, dendronised polymers prefer to adopt a spherical conformation.[2,3,4] The steric impact of the dendrons on the overall structure can only now be fully appreciated and this clearly provides an explanation to the slow rate of propagation in the polymerisation of the second generation dendronised monomer, **DMPCB2D**, as incoming monomer must find it increasingly difficult to react with the reactive chain end of the polymer, especially when this reactive end is most likely to be found in the centre of the propagating structure.

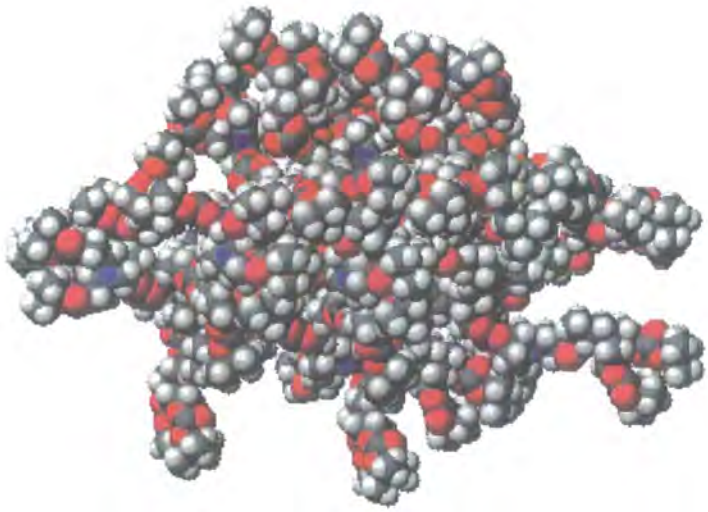

Figure 4.10 Structure corresponding to 8DP of conformer 4 (carbon = grey, oxygen = red, nitrogen = blue)

The computer calculations at a degree of polymerisation of 8 were very time consuming and as a result of this, it was decided to only perform calculations for a degree of polymerisation of 16 on three of the lowest potential energy structures derived from conformers 3, 4 and 7. As can be seen from *Table 4.1*, the structure of conformer 4 at a degree of polymerisation of 16 has the lowest potential energy (5,205 kcal/mol), the value of which is approximately half that of the potential energy of structure 7 at the same degree of polymerisation. A structure of conformer 3 at a degree of polymerisation of 16 could not be determined, as the computer package in this instance did not have the capacity to deal with all the parameters involved in the calculation.

The optimised structure that CAChe calculated for conformer 4 at a degree of polymerisation of 16 is shown in *Figure 4.11*. It was found that the end-to-end distance of the structure was approximately 10 nm (97 Ångstroms) and the cross-section distance was approximately 4 nm (42 Ångstroms). From this, a very rough indication as to the size and shape of poly(**DMPCB2D**), which was synthesised from a polymerisation reaction at a 20:1 molar ratio of dendronised monomer (chapter 3, section 3.5), can be obtained. The effect of increasing the degree of polymerisation can be seen from this figure, as the structure is becoming more sterically constrained with increasing polymer chain length. From viewing this structure, it is not surprising that the polymerisation of 20 molar equivalents of **DMPCB2D** required approximately 1 week to reach completion, as unreacted monomer would have found

it increasingly difficult to enter the structure and react with the chain end of the polymer. It can also be seen that the polymer structure is now more stretched compared to the structure with a DP of 8, which correlates quite well with previous work, which suggested that the polymer structure prefers to adopt more of a cylindrical conformation with increasing DP.[2,3,4]

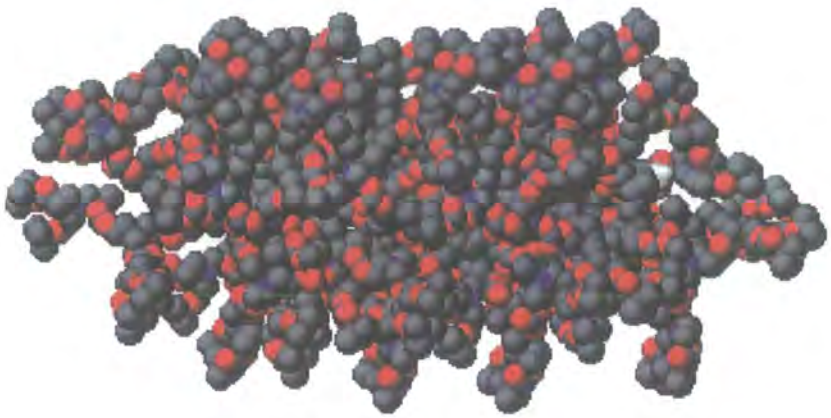

Figure 4.11 Structure corresponding to 16DP of conformer 4 (carbon = grey, oxygen = red, nitrogen = blue, hydrogens have been omitted for clarity)

It must be remembered that the structures calculated by the CAChe program are only approximations. The possibility exists that the dendronised monomer synthesised experimentally exhibits conformations in solution that are close to that of the 7 lowest potential energy structures calculated by the CAChe program. However, as has been mentioned, the polymer structures calculated by the CAChe program are, at best, rough approximations due to the fact that cis/trans double bond isomerisation effects along the backbone and all the possible combinations of the various conformations that the monomers probably exhibit could not be taken into consideration during the calculations because of limitations of computing capacity and time.

In conclusion, these molecular modelling computations suggest that low DP oligomers of **DMPCB2D** have an approximately spherical shape, which tends towards a cylindrical shape as DP increases; this conclusion is in agreement with earlier measurements on related but different systems, where a polymer was synthesised containing second generation polybenzyl ether dendrons along the backbone.[4]

4.5 Background to Atomic Force Microscopy (AFM) Imaging

The scanning probe microscope MultiMode^{TM} Nanoscope IV (MM-SPM) produced by Digital Instruments was used to perform AFM imaging only on polymers derived from di-substituted second generation polycarbonate dendronised monomers due to time constraints. Multiple SPM modes are available via the MultiMode microscope, including contact and TappingMode AFM and Scanning Tunnelling Microscopy (STM).[5]

A picture of an SPM is shown in *Figure 4.12*. A laser beam is reflected off the end of the tip of a cantilever and onto a mirror, which reflects the beam onto a photodetector, where even the smallest movements are detected, *Figure 4.13*. As the tip traces various surface features, its upward and downward movement shifts the beam between the upper and lower photodiode components, creating voltage differences, which are electronically rendered into height information. This change of position of the tip is read by a feedback loop that can increase or decrease the voltage to a Z piezo crystal, which controls the movement of the tip and from this, the laser beam can be restored to its original position in the centre of the photodiode array.

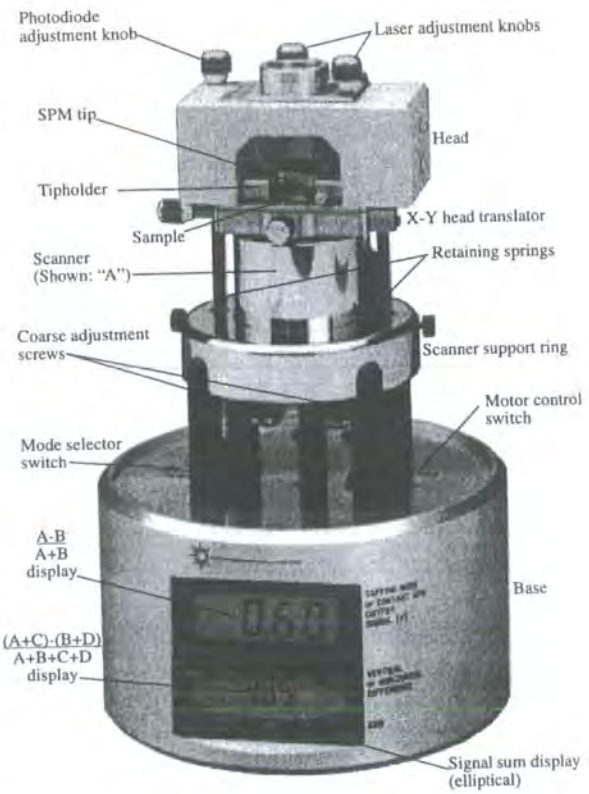

Figure 4.12 Picture of a MultiMode SPM

When the tip is scanning a flat portion of the sample surface left-to-right, the laser beam stays at the centre of the photodiode array, as in **A** of *Figure 4.13*. However, if the tip encounters a raised feature of the sample, the cantilever is pushed up and the laser beam is deflected onto the A portion of the photodiode array, which causes its voltage to increase while portion B's decreases, as seen in **B**. This voltage difference is sensed by the feedback electronics, which drops the voltage to the Z piezo crystal. As a result of this, the Z piezo retracts and the tip is pushed up until the laser recentres on the photodiode array, see **C**. The opposite is true when the tip encounters a dip in the sample topology; portion B's voltage increases, the piezo crystal extends to counter this and the tip is pushed down so that the laser beam recentres on the photodiode array, see **D** and **E**, *Figure 4.13*.

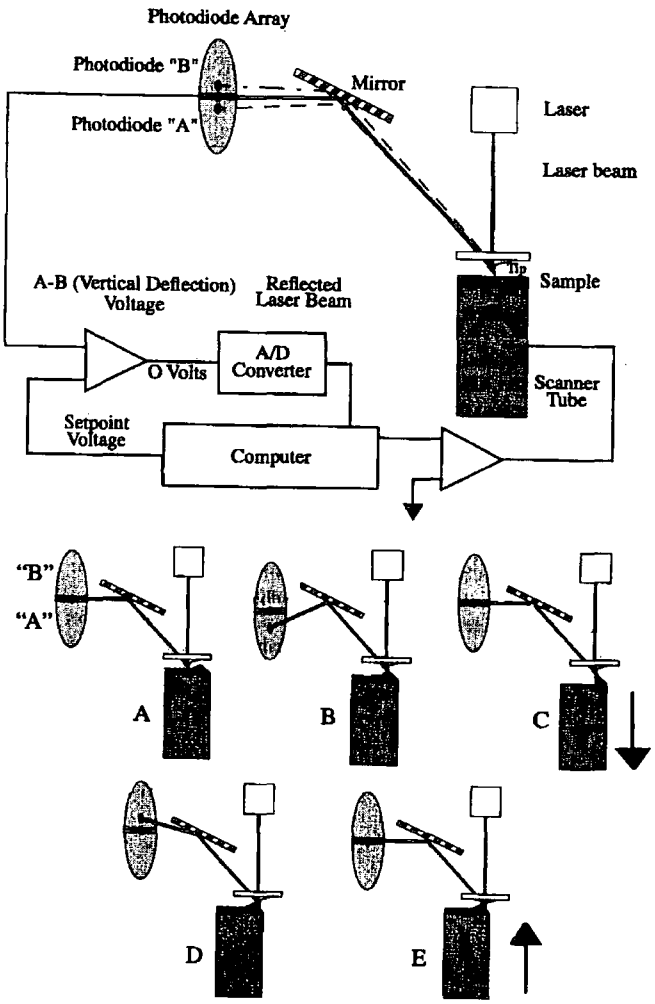

Figure 4.13 Use of a feedback loop to adjust the laser spot to its original position

The tip is attached to a flexible cantilever probe, which extends from a rigid substrate, *Figure 4.14*. In contact AFM, the cantilever's flexibility acts as a nanometric spring, allowing the tip to slide across the sample surface to measure the surface forces. The type of tip used is a silicon nitride tip, which exhibits excellent flexibility and can be produced in a variety of sizes and coatings, allowing the user to match them to the sample being imaged. However, one characteristic of these tips is that they are easily trapped within a microscopic layer of condensed atmospheric water vapour on the sample surface, which leads to a surface tension effect that exerts considerable force at the probe's atomically sharp tip. This is not too much of a problem with harder samples, but is frequently enough to deform softer samples. The polymer samples synthesised from the polymerisation of 20 molar equivalents of **DMPCB2D** were found to be relatively soft in nature and hence the imaging of the samples by contact AFM was unsuccessful as the tip constantly became trapped. Therefore, it was decided to use TappingMode AFM to obtain images of the polymer materials synthesised in this work. In TappingMode, a stiff crystal silicon probe is oscillated at its resonant frequency, which gives the tip sufficient energy to break free of surface tension forces. The sample surface is in close proximity to the cantilever and as such, the tip only touches the surface at the lowest point of its oscillation. The probe is considerably stiffer than silicon nitride, making it more brittle and less forgiving and hence care had to be taken when analysing samples.

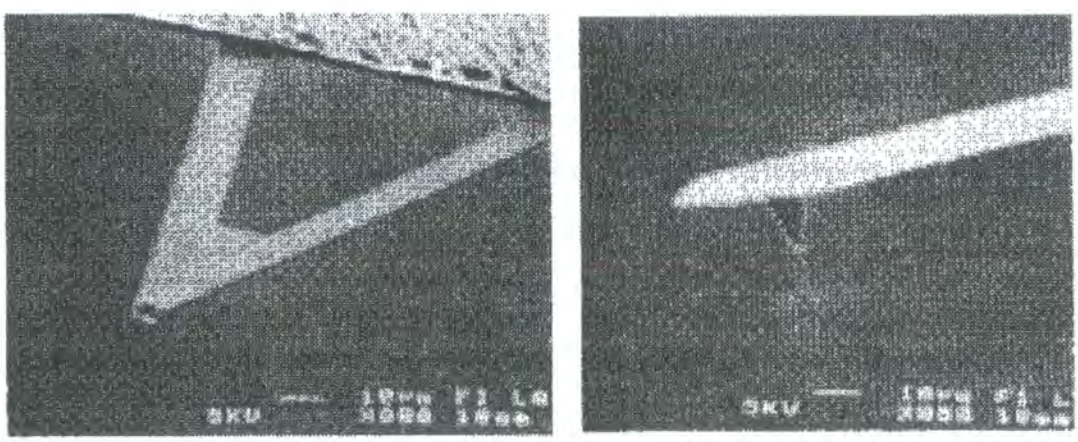

Figure 4.14 A contact AFM silicon nitride tip attached to the end of a triangular flexible cantilever which is fixed to a rigid substrate (left) and a TappingMode AFM crystal silicon tip attached to a vibrating cantilever at a constant amplitude (right)

In order to control tip-sample interactions and obtain images, the feedback system must be optimised for each new sample. This can be accomplished by adjusting various gains in the SPM's feedback circuit. The type and intensity of the tips responses to the sample can be modelled in terms of three types of feedback: proportional, integral and LookAhead gain. The object is to assign a setpoint value corresponding to a certain amount of tip-sample force, and then adjust the gains to track the surface as closely as possible while maintaining the setpoint. In TappingMode, the amplitude of the oscillating tip determines the setpoint – as the setpoint decreases, the amplitude decreases and the tip-sample forces increase. Proportional gain means that something is done proportionally in response to something else, e.g., if the tip becomes too close or too far away from the sample, the voltage of the crystal is altered in order to compensate. When the proportional gain is high, the voltage of the crystal needs to be changed more frequently to keep the tip at a suitable distance from the sample. Integral gain feedback is used to reduce total error by addressing error over a longer time period. This tends to smooth out the short term, fluctuating effects of proportional gain while narrowing the error closer to the setpoint value. LookAhead gain keeps the tip within the proper height from the sample and takes advantage of regular surface features by using previous lines to anticipate future lines and hence, it is extremely useful on regular surfaces and less so on random surfaces.

4.6 Sample Preparation and Laser Alignment

Two-sided adhesive tape was initially placed on a 15 mm diameter steel sample disk. A small wafer thin section of either silicon or highly ordered pyrolytic graphite (HOPG) substrate was then placed very carefully on top of the adhesive using tweezers, making sure that no damage was done to the substrate surface. The desired concentration of the polymer sample in dichloromethane was then prepared. A drop of the solution was either added directly onto the substrate and allowed to evaporate, or spin-coated onto the substrate. The steel disk containing the polymer sample was placed on top of the scanner tube in the SPM, which contained an internal magnet to hold the sample in place. A single crystal silicon probe tip was very carefully slotted into the tipholder's groove and the tipholder was placed inside the SPM head and clamped into position making sure that it did not touch the sample. The laser was aligned by removing the head of the SPM and then by observing light

patterns reflected or diffracted from the surface of the cantilever onto a piece of paper, *Figure 4.15*. This was achieved by first of all locating the laser spot on the substrate and by moving the spot along the Y-axis to locate the centre of the cantilever. Finally, the laser spot was adjusted to the end of the cantilever. In the TappingMode, a mirror lever to the rear of the head and the photodiode adjustment knob were used to maximise the signal displayed on the bar graph and minimise the top/bottom differential signal shown in the lower LCD display. In practise this laser alignment involves direct visual observation confirmed by the patterns referred to above.

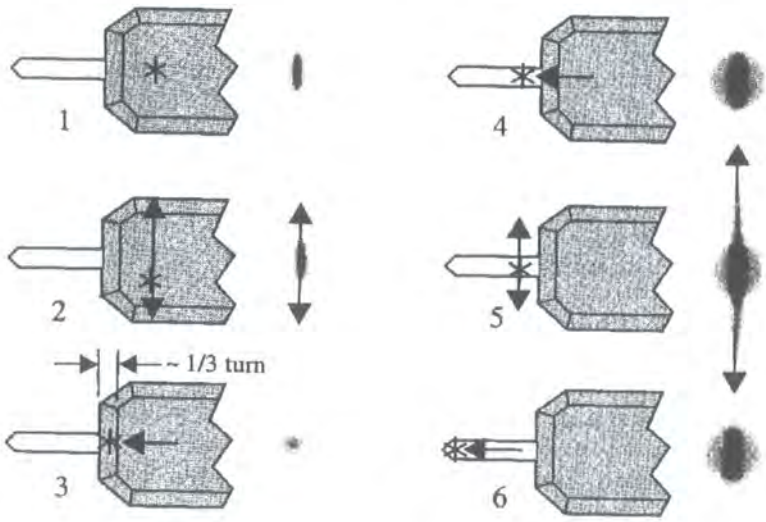

Figure 4.15 Procedure for aligning silicon cantilevers by observing the light patterns on a piece of paper: 1) locate beam on substrate; 2) find centre of substrate; 3-5) find centre of cantilever; 6) move beam to the end of cantilever

4.7 Obtaining AFM Images

It was found, as has been reported,[6] that the visualisation of samples on substrates by AFM is highly dependent on an optimal sample preparation. Key factors, which can be the difference between success and failure in obtaining images, are the choice of substrate, the concentration of the applied solution and the thermal annealing of the sample.

In initial attempts to obtain images, a silicon wafer was used as the substrate and the concentration of the polymer sample in dichloromethane ranged from 0.01 mg/mL to 0.0025 mg/mL. A very low concentration of sample was used as it had been reported that when the solution concentration is too high, the AFM can only

observe traces of ordered structures.[6] Both spin coating of the sample, which involves placing a droplet of the dilute polymer solution onto the substrate and then spinning the substrate at 2000rpm for 20 seconds, and allowing the solvent from the droplet to evaporate from the static silicon wafer were attempted. The thermal annealing of samples at 120°C for two hours and annealing at room temperature were also performed. Despite the range of conditions employed in the search for the visualisation of samples, no AFM images were obtained when a silicon wafer was used as the substrate. A possible reason why no images were obtained could be that the interactions between the sample and the substrate were insufficient for the sample to adhere to the silicon, as it has been reported that strong interactions can in some instances lead to clearer images.[6]

The substrate was then changed to highly ordered pyrolytic graphite (HOPG), as it had been reported in the literature that the use of graphite leads to a strong interaction between the surface lattice of the graphite and any n-alkyl groups contained within the sample. Despite an absence of n-alkyl groups in poly(**DMPCB2D**), it was thought that the polymer sample may bind more strongly to the surface lattice, which would aid in the provision of images. The concentration of the polymer sample in dichloromethane ranged from 0.01 mg/mL to 0.001 mg/mL and sample solutions were both spin coated and allowed to evaporated from the static HOPG. It was found that when the samples were spin coated onto the HOPG, AFM images were obtained for each of the different polymer solution concentrations. The AFM images for samples of poly(**DMPCB2D**) at a concentration in DCM of 0.01 and 0.0025 mg/mL are shown in *Figure 4.16.*

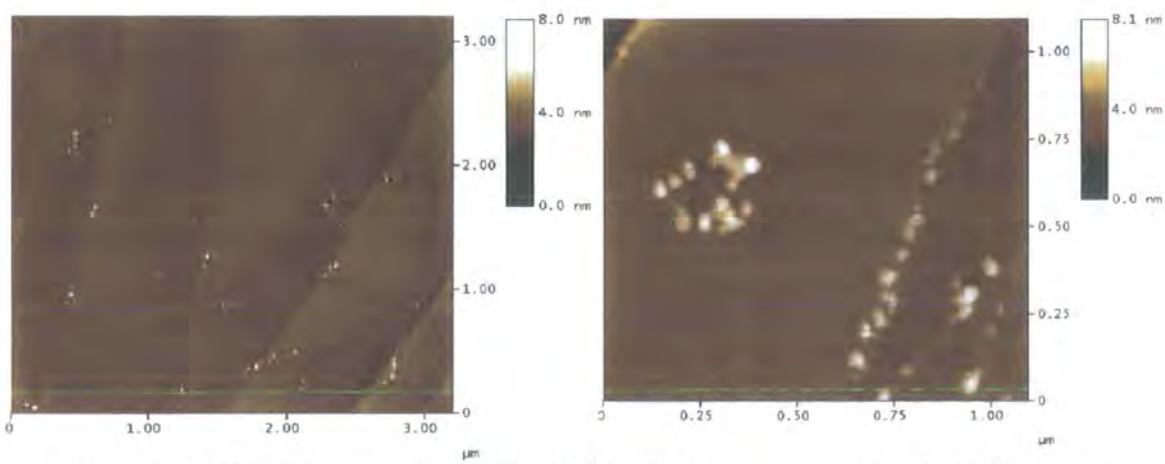

Figure 4.16 AFM images of poly(**DMPCB2D**) *at a concentration in DCM of 0.01(left) and 0.0025 mg/mL (right)*

From the AFM image of poly(DMPCB2D) at a concentration in DCM of 0.01 mg/mL, *Figure 4.16 (left)*, it can be seen that there are discrete yellow structures present with dimensions of approximately 30-50 nm diameter by 5-8 nm thickness. The dark brown background represents the HOPG and the ridges that run along the image are due to layers of the graphite stacked on top of each other. It can be seen that the clusters are predominantly found along the lines of the graphite where two layers meet and that there are only a few clusters present on the flat graphite surface. In spin coating, a droplet of the polymer solution travels very quickly from the centre of the HOPG to the edge of the disk. By viewing the images, it is thought that the interaction between the sample and the substrate is weak, as it appears that the graphite ridges are the only barrier stopping the sample from travelling directly off the disk, as may have been the case with the molecularly smooth silicon substrate. However, it was surprisingly found that no AFM images could be obtained when a droplet of the sample solution at various concentrations was placed onto the graphite, with the solvent being allowed to evaporate.

From the image of poly(**DMPCB2D**) at a concentration in DCM of 0.0025 mg/mL, it can again be seen that there are discrete structures present with dimensions of approximately 30-50 nm diameter by 5-8 nm thickness, *Figure 4.16 (right)*. The structures are mostly found along the ridges of the graphite, but there is one large cluster present on the flat graphite surface. The sizes of the structures in the two AFM images are at least a factor of three greater than that predicted by the computer modelling studies, where the dimensions of the polymer at 16 DP were calculated to be approximately 10 nm diameter by 4 nm thickness and the shape was close to being cylindrical in nature. The reason for this observed discrepancy in size is due to the fact that when performing calculations, the computer modelling package could not be programmed to take into consideration structure-solvent or structure-substrate interactions and hence the dimensions of the polymer calculated correspond to an isolated molecule in the vacuum. However, when attempting to obtain AFM images of the sample, the sample is initially dissolved at high dilution in a solvent and then placed on top of a substrate and hence such interactions are very important in determining the final conformation of the polymer when the images are being obtained. It is believed that when dichloromethane, which is a good solvent for poly(**DMPCB2D**), is added to the polymer sample, the polymer chains adopt a random coil configuration and as such, the dendrons are not as tightly packed as the

molecular modelling would suggest. It can be seen from the area of HOPG displayed in *Figure 4.17*, that when the majority of the solvent has evaporated from the sample on the substrate, the sample is spread out across the substrate and its shape resembles that of a pancake. The pancake shape is thought to arise from both the structure/solvent interactions and structure/substrate interactions, making the polymer spread out across the substrate. It is thought that each pancake on the AFM image represents *one* dendronised polymer backbone and that dimensions of 30-40 nm diameter by 3-6 nm thickness gives a more accurate representation as to the size of the polymer when it is interacting with the substrate after evaporation of a good solvent, where it probably existed as a random coil. Structure-substrate interactions include intra- and intermolecular forces as well as interfacial forces.[7] The latter includes a rather short range van der Waals type force on the nanometer scale, which is due to different dielectric properties of the two adjacent phases. This force is always attractive, and therefore favours a high molecular segment density at the interface.

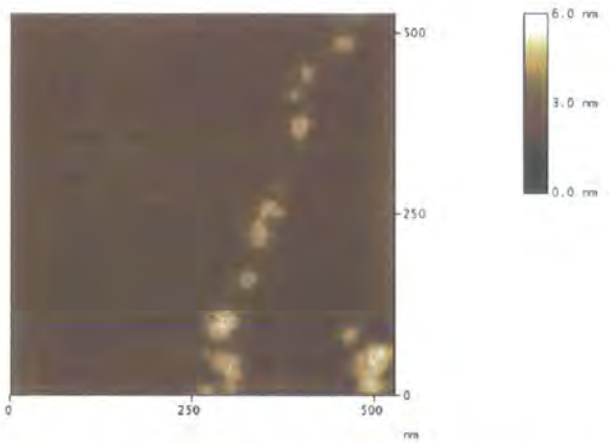

Figure 4.17 Enlarged image of poly(**DMPCB2D**) *at a concentration in DCM of 0.0025 mg/mL*

As can be seen from *Figure 4.17*, the images are not too well resolved. This could be due to the fact that the ordering in the part of the sample nearest the substrate is, as expected, the strongest. The substrate/sample interactions gradually diminish as the distance from the surface increases resulting in a loss in the degree of ordering in the parts of the sample more distant from the surface. Therefore, when the sample being analysed consists of several different zones of entangled dendron it is understandable that the image viewed from the AFM tip is not that well resolved.

The AFM images for samples of poly(**DMPCB2D**) at a concentration in DCM of 0.005 and 0.001 mg/mL are shown in *Figure 4.18.*

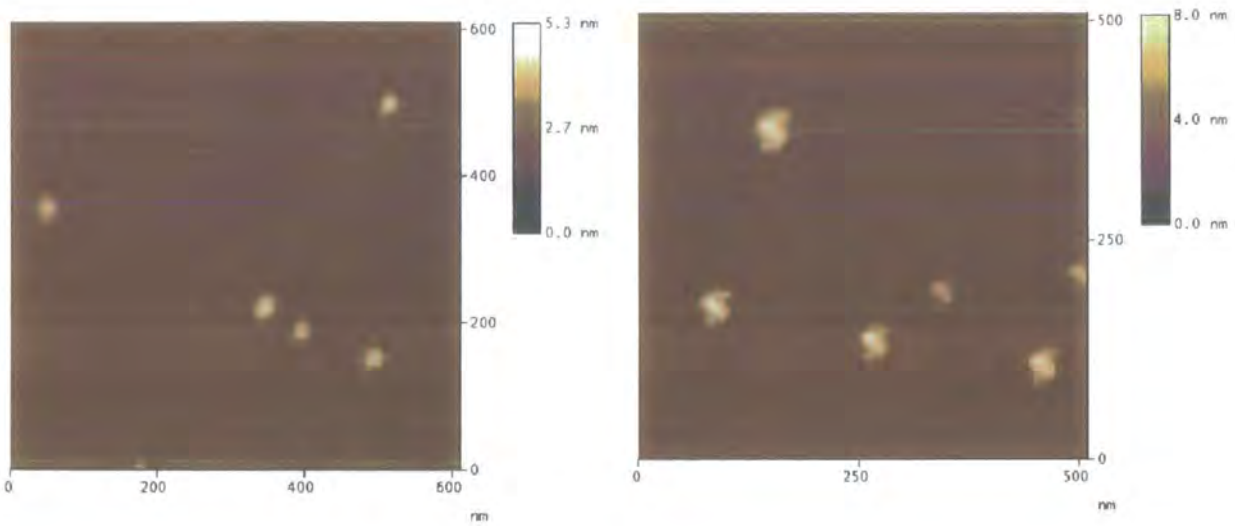

Figure 4.18 AFM images of poly(**DMPCB2D**) *at a concentration in DCM of 0.005 (left) and 0.001 mg/mL (right)*

From the AFM image of poly(**DMPCB2D**) at a concentration in DCM of 0.005 mg/mL, *Figure 4.18 (left)*, it can be seen that there are discrete yellow structures present with dimensions of approximately 40-50 nm diameter by 3-5 nm thickness. It can be seen that the number of structures in this 600 x 600 nm image is fairly low. However, no correlation was found between the concentration of the polymer samples and the number of structures present within the AFM images, as can be seen from the number of structures in the image resulting from a solution concentration of 0.001 mg/mL, *Figure 4.18 (right)*. In this image, the structures again have dimensions of approximately 40-50 nm diameter by 6-8 nm thickness. By analysing each image, it can be deduced that there is a fairly narrow distribution in sizes between the structures. This suggests that each structure indeed only represents one polymer chain because if clusters had formed, there would have been a greater probability of observing a broader distribution of structure sizes. This narrow distribution is consistent with a well-defined living polymerisation where most of the chain lengths tend to be similar and correlates with the GPC trace of the polymer, which had a computated PDI of 1.09 (chapter 3, section 3.5.2). By measuring the dimensions of each structure in the images, it could be seen that the diameters of the set of structures

varied in the ranges 39 ± 8 nm and 38 ± 5 nm for *Figure 4.18 left* and *right*, respectively.

Thermal annealing of the samples was also performed at 120°C for several hours as it had been reported in the literature that annealing leads to more efficient packing of samples on the graphite.[6] However, it was found that only poor images of the samples were obtained after they had been annealed and hence the procedure was not continued.

In conclusion, AFM images of poly(**DMPCB2D**) produced in a reaction using a 20:1 monomer: initiator ratio were obtained and it was found that discrete structures with approximate dimensions of 30-50 nm diameter by 3-6 nm thickness were present on the substrate. It is thought that each individual structure represents *one* dendronised polymer chain that is spread across the graphite substrate, as there is a fairly narrow distribution of sizes and the thickness corresponds approximately to the cross section of the polymer chain, suggesting that a random coil in solution has flattened into a pancake on the surface.

4.8 Conclusions

Molecular modelling studies have been performed using the CAChe program, which estimates the conformation of the monomers/polymers in the vacuum. It was found that low DP oligomers of **DMPCB2D** had an approximately spherical shape, which tended towards cylindrical as the DP increased. One particular conformation of monomer combined to form lower potential energy polymer structures than the combination of any of the other conformers. The polymer at a DP of 16 was found to have a roughly cylindrical shape with dimensions of approximately 10 nm diameter by 4 nm thickness. AFM images were also obtained using a scanning probe microscope MultiMode™ Nanoscope IV. Optimising the imaging conditions proved vital and experimentally tricky and time-consuming; it was found that a very dilute polymer solution using the spin coating technique and the use of highly ordered pyrolytic graphite as substrate were required to obtain images. The structures were found to be pancake shaped with dimensions of between 30-50 nm diameter and 3-6 nm thickness, which was approximately a factor of 3 greater than the dimensions calculated by molecular modelling. This discrepancy in size is thought to arise from the effect that structure-solvent and structure-substrate interactions have on the overall shape of the dendronised polymer when imaging by AFM. It is therefore apparent

that the two sets of data from the molecular modelling and AFM studies cannot be directly compared due to the conditions under which the molecules are examined being very different.

4.9 References

1. Allinger, N. L. *J. Am. Chem. Soc.* **1977**, *122*, 3783.

2. Rabe, J. P.; Schlüter, A. D. *Angew. Chem. Int. Ed.* **2000**, *39*, 864.

3. Frey, H. *Angew. Chem. Int. Ed.* **1998**, *37*, 2193.

4. Percec, V.; Schlueter, D. *Macromolecules* **1997**, *30*, 5783.

5. *MultiMode SPM Instruction Manual*, Version 4.31ce, Digital Instruments Metrology Group.

6. Percec, V.; Holerca, M. N.; Maganov, S. N.; Ungar, G.; Yeardley, D. J. P.; Duan, H.; Hudson, S. D. *Biomacromolecules* **2001**, *2*, 706.

7. Israelachvili, J. N. *Intermolecular and Surface Forces*, Academic Press, London, **1985**.

Chapter 5

Experimental

5.1 General Information

5.1.1 Chemicals

Starting materials were purchased from Aldrich, Lancaster and Raylo Chemicals, Canada (CDI) and used without further purification. The toluene used as solvent for the reactions was analytical grade and was used as received. All reactions were performed under an atmosphere of nitrogen, unless stated otherwise. Silica gel used for column chromatography was supplied from Aldrich (70-270 mesh, 60Å) or Fluorochem (40-63u, 60Å). For preparative gel permeation chromatography, BioBeads ®, S-X1 Beads purchased from Bio-Rad were used.

5.1.2 Characterisation

Elemental Analysis

Elemental analysis data was obtained from an Exeter Analyser CE-440, through the Chemistry Departmental Service.

NMR Spectroscopy

NMR spectra were recorded using either a Varian Mercury-200 (^{1}H at 200 MHz and ^{13}C at 50.2 MHz), a Bruker AM-250 (^{1}H at 250.1 MHz and ^{13}C at 62.9 MHz), a Varian Unity-300 (^{1}H at 299.9 MHz and ^{13}C at 75.4 MHz), a Varian Mercury-400 (^{1}H at 400 MHz and ^{13}C at 100 MHz) or a Varian Inova-500 (^{1}H at 500 MHz and ^{13}C at 125 MHz). Deuterated solvents were used as supplied from Aldrich ($CDCl_3$) and Cambridge Isotope Laboratories (CD_3OD, $(CD_3)_2CO$, $(CD_3)_2SO$). Chemical shifts (δ) are reported in parts per million (ppm) with respect to an internal reference of tetramethylsilane (TMS) using residual solvent signals as secondary references.

Mass Spectrometry

For gas chromatography, an electro spray Micromass Autospec instrument was used.

The MALDI-TOF mass spectrometer used was an Applied Biosystems Voyager-DE STR MALDI-TOF. The sample preparation and other details were as follows: the matrix used was trans-3-indole acrylic acid and the concentration of the matrix solution (in THF) was 10 mg/mL. The concentrations of the dendritic solutions (in THF) varied in the range of 1 mg/mL to 3 mg/mL. Initially, the matrix solution was deposited on the slide, followed by the dendritic solution. The MALDI-TOF (Voyager) mass spectra were obtained in reflection mode using polyethylene oxide (Polymer Labs) as external calibrants. Some spectra were obtained in linear mode for comparison.

Gel Permeation Chromatography (GPC)

Analysis by GPC was achieved using tetrahydrofuran (THF) as eluent using a flow rate of 1 mL/min at 30°C. Columns comprised of 2 x 'mixed B' columns containing PL-gel beads. The columns were calibrated with polystyrene standards (Polymer Labs) and samples analysed using conventional calibration with all data collected from a refractive index detector.

Glove Box

The type of Glove Box used was an MBraun MB150B-G model containing a PLC-controlled Combi-Analyser. Polymerisation samples were prepared and sealed in an NMR tube inside the box, which operates under a nitrogen atmosphere.

5.2 Procedures for the Synthesis of Norbornene Monomer Derivatives

5.2.1 Synthesis of Norbornene-5-*exo/endo*-carboxylic acid

Norbornene-5-*exo/endo*-carboxylic acid was prepared following the published route.[1,2] Dicyclopentadiene (198 g, 1.5 mol) and acrylic acid (324 g, 4.5 mol) and two spatulas of hydroquinone (ca. 3g) were placed in a 2 L stainless steel autoclave equipped with an overhead stirrer and a thermocouple to measure the internal temperature. The temperature was set at 160°C and this temperature was reached

after 110 minutes. The reaction proceeded for two hours during which the exothermicity of the reaction raised the temperature to 200°C. The mixture was then allowed to cool to room temperature overnight. The crude product was obtained as a yellowish viscous liquid with some white solid and gel also present around the stirrer and base of the autoclave. The crude product was distilled under vacuum to remove excess acrylic acid and the product fraction was obtained as a mixture of *exo* and *endo* norbornene-5-carboxylic acids (ratio 52/48 *exo/endo* as determined by ^{1}H NMR spectroscopy), bp=87°C/0.07 mbar (187 g, 35.8%), Lit[1] bp 132-134°C/7 Torr. The spectroscopic parameters were in full agreement with the literature values.[2] ^{13}C NMR (50MHz, $CDCl_3$) δ 183.09 (***exo* C_8**), 181.58 (*endo* C_8), 138.35 (***exo* $C_{2/3}$**), 138.14 (***exo* $C_{2/3}$**), 135.94 (*endo* $C_{2/3}$), 132.66 (*endo* $C_{2/3}$), 49.95 (*endo* C_7), 46.91 (***exo* $C_{1/4}$**), 46.60 (***exo* C_7**), 45.92 (*endo* $C_{1/4}$), 43.52 (*endo* C_5), 43.37 (***exo* C_5**), 42.77 (***exo* $C_{1/4}$**), 41.88 (*endo* $C_{1/4}$), 30.54 (***exo* C_6**), 29.33 (*endo* C_6). ^{1}H NMR (200MHz, $CDCl_3$) δ 11.25 (broad s, 2H, ***exo*** and *endo* –COOH), 6.2, 6.02 (dd, J=5.6Hz, J=3Hz, 2H, *endo* $H_{2/3}$), 6.13 (m, 2H, ***exo* $H_{2/3}$**), 3.22 (broad s, 1H, *endo* $H_{1/4}$), 3.1 (broad s, 1H, ***exo* $H_{1/4}$**), 2.99 (m, 1H, *endo* H_5), 2.92 (broad s, 2H, *endo* $H_{1/4}$, ***exo* $H_{1/4}$**), 2.24 (m, 1H, ***exo* H_5**), 1.98 (m, 1H, ***exo* H_{6exo}**), 1.92 (dd, 1H, *endo* H_{6exo}), 1.5 (broad d, 1H, ***exo* $H_{7/7'}$**), 1.44-1.20 (m, 5H, ***exo* $H_{7/7'}$**(1), *endo* $H_{7/7'}$(2), ***exo* H_{6endo}** (1) and *endo* H_{6endo}(1)). *m/z* (ES MS) 138 [M^+].

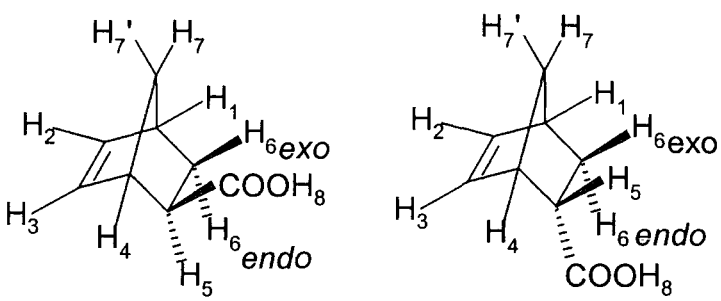

Assignment of hydrogen atoms

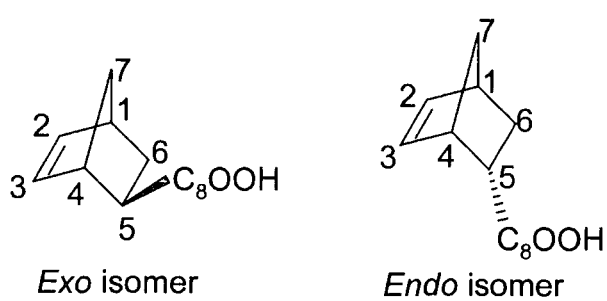

Assignment of carbon atoms

5.2.2 Isolation of Norbornene-5-*exo*-carboxylic acid

Norbornene-5-*exo*-carboxylic acid was prepared following the published route.[2,3,4] Crude norbornene-5-*exo/endo*-carboxylic acid (85 g, 0.621 mol) was placed in a separating funnel (2 L) and neutralised with a 26% sodium hydroxide solution (52 g in 200 mL of water). Sodium bicarbonate (500 mL, 90 g in 1 L) was added in two equal batches. The mixture was shaken thoroughly and aqueous I_2/KI solution (430 mL, prepared by dissolving 254 g of I_2 in 1 L of water containing 508 g of KI) was added in portions with shaking until the resulting mixture remained the colour of the I_2/KI solution, i.e. purple. The solution was shaken every ten minutes for 1 hour. The iodolactone of the *endo* acid precipitated as a dark viscous oil and was separated using a glass wool plug in a funnel, the oil remained on and above the plug. The remaining clear brown aqueous layer was acidified with sulphuric acid (170 mL, prepared by adding 40 mL 1.8M H_2SO_4 to 200 mL of water) resulting in the monomer precipitating as a pale brown oil. Ether (200 mL) was added to extract the monomer and the aqueous layer was further extracted with ether (3 x 250 mL). The combined ether extracts were washed with a solution of $Na_2S_2O_3$ (400 mL, prepared by adding 223.2 g to 1 L of water) and dried over $MgSO_4$. After filtration, the solvent was removed and the resultant solid was recrystallised from hexane four times to give norbornene-5-*exo*-carboxylic acid as a yellowish solid (34 g, 77% recovery of *exo* from the original *endo/exo* mixture). Found C, 66.43; H, 6.98%. $C_8H_{10}O_2$ requires C, 69.54; H, 7.30%, the low carbon analysis result was attributed to the hygroscopic nature of the acid, which was very difficult to dry. The spectroscopic parameters were in full agreement with the literature values.[2] ^{13}C NMR (75MHz, $CDCl_3$) δ 183.22 (C_8), 138.46 (C_2), 136.05 (C_3), 47.04 ($C_{1/4}$), 46.73 (C_7), 43.52 (C_5), 42.01 ($C_{1/4}$), 30.67 (C_6). ^1H NMR (300MHz, $CDCl_3$) δ 11.42 (s, 1H, COOH), 6.17 (m, 1H, $H_{2,3}$), 6.15 (m, 1H, $H_{2,3}$), 3.14 (broad s, 1H, $H_{1,4}$), 2.96 (broad s, 1H, $H_{1,4}$), 2.29 (m, 1H, H_5), 1.96 (m, 1H, H_{6exo}), 1.56 (m, 1H, $H_{7/7'}$), 1.41 (m, 1H, $H_{7/7'}$), 1.43-1.40 (m, 1H, H_{6endo}). *m/z* (ES MS) 138 [M^+].

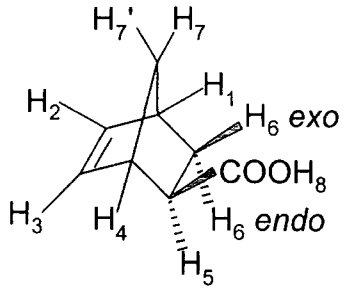

Assignment of hydrogen atoms

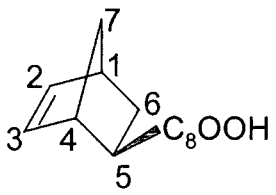

Assignment of carbon atoms

5.2.3 Synthesis of Norbornene-5-*exo*-methanol

Norbornene-5-*exo*-methanol was prepared following the published route.[5] Norbornene-5-*exo*-carboxylic acid (20 g) was dissolved in 100 mL of sodium-dried ether and added drop wise over a period of two hours to a two-neck 1 L flask cooled in ice and containing 15.1 g of lithium aluminium hydride in 200 mL of sodium dried ether. The mixture was stirred overnight at room temperature and then refluxed for 1.5 hours. The residual hydride in the reaction flask was destroyed by slow addition of 65 mL of water to the ice cold mixture. The white-grey precipitate of $Al(OH)_3$ formed, was dissolved by addition of 200 mL (20%) HCl solution and 40 mL (36%) HCl solution. The residual undissolved white-grey precipitate was finally dissolved by addition of 37 mL of concentrated hydrochloric acid in three portions. Stirring was continued for 30 minutes. This gave a clear two-phase system; an ether layer and an aqueous layer with some dispersed precipitates. The ether layer was separated using a separating funnel, and the aqueous layer together with the dispersants were extracted with ether (4 x 100 mL). The ether extracts were combined and washed with a 10% aqueous NaOH solution and water. The ether extract was then dried over magnesium sulphate. After filtration, ether was removed under reduced pressure and the residue was distilled at 44°C, 0.3Torr (Lit[5] bp:101-101.5/7Torr), to yield norbornene-5-*exo*-methanol as a clear liquid (14.8 g, 74%). Found C, 75.06; H, 9.60%. $C_8H_{12}O$ requires C, 77.38; H, 9.74%, the low carbon analysis result was attributed to the hydroscopic nature of the compound, which was very difficult to dry. The spectroscopic parameters were in full agreement with the literature values.[5] ^{13}C NMR (75 MHz, $CDCl_3$) δ 137.05 (C_2), 136.74 (C_3), 67.72 (C_8), 45.23 (C_7), 43.54 ($C_{1/4}$), 42.11 (C_5), 41.79 ($C_{1/4}$), 29.81 (C_6). ^1H NMR (300 MHz, $CDCl_3$) δ 6.06 (dd,

J=5.6Hz, J=2.7Hz, 2H, *exo* $H_{2/3}$), 3.67 (dd, J=10.5Hz, J=6.3Hz, 1H, $H_{8a/8b}$), 3.51 (dd, J=10.5Hz, J=8.7Hz, 1H, $H_{8a/8b}$), 2.8 (broad s, 1H, $H_{1/4}$), 2.74 (broad s, 1H, $H_{1/4}$), 1.92 (broad s, 1H, -OH), 1.6 (m, 1H, H_5), 1.31-1.2 (m, 3H, $H_{7/7'}$ and H_{6endo}), 1.1 (pseudo dt, J=11.4Hz, J=3.8Hz, 1H, H_{6exo}). *m/z* (ES MS) 124 [M^+].

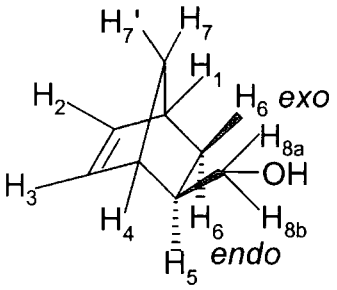

Assignment of hydrogen

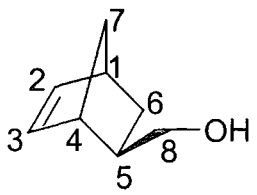

Assignment of carbon atoms

5.2.4 Synthesis of Norbornene-*exo*-5, 6-dicarboxylic anhydride

Norbornene-*exo*-5, 6-dicarboxylic anhydride was prepared following the published route.[6] Maleic anhydride (91.67 g, 0.93 mol) and 1,2-dichlorobenzene (100 mL) were placed in a 3-neck, round bottom flask (500 mL) fitted with a condenser, thermometer and dropping funnel. The colour of the clear solution at this stage was brown. The mixture was stirred and heated to 178°C. Dicyclopentadiene (75 mL, 73.65 g, 0.56 mol) was added to the flask via the dropping funnel over a period of 90 minutes, which turned the solution a dirty dark brown colour. The mixture was heated to reflux for 6 hours (maximum temperature due to exotherm 195°C). The solution was then cooled overnight. The resultant brown solid was recovered by filtration and recrystallised eight times from acetone to give norbornene-*exo*-5, 6-dicarboxylic anhydride as transparent lath like crystals (12.07 g, 7.2%). Found C, 65.65; H, 4.86%. $C_9H_8O_3$ requires C, 65.85; H, 4.91%. The spectroscopic parameters were in full agreement with the literature values.[6,7] ^{13}C NMR (63MHz, C_3D_6O) δ 173.26 (s, $C_{8,9}$), 138.97 (s, $C_{2,3}$), 50.03 (s, $C_{5,6}$), 47.65 (s, $C_{1,4}$), 44.86 (s, C_7). ^1H NMR (250MHz, C_3D_6O) δ 6.38 (m, 2H, $H_{2,3}$), 3.35 (m, 2H, $H_{1,4}$), 3.13 (m, 2H, $H_{5,6}$), ABq δ_A 1.6, δ_B 1.4, J_{AB} =10.25Hz, 2H, $H_{7/7'}$. *m/z* (ES MS) 164 [M^+].

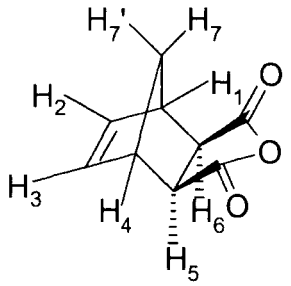

Assignment of hydrogen atoms

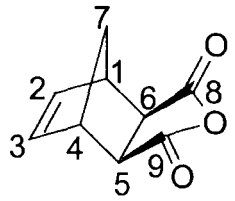

Assignment of carbon atoms

5.2.5 Synthesis of Norbornene-5-*exo*, 6-*exo*-dicarboxylic acid

Norbornene-5-*exo*, 6-*exo*-dicarboxylic acid was prepared following the published route.[6] Norbornene-*exo*-5, 6-dicarboxylic anhydride (12.07 g, 72 mmol) and distilled water (160 mL) were placed in a one neck round bottom flask (250 mL) fitted with a condenser and a stirrer bar. The mixture was heated to reflux for 2 hours to give a clear, colourless solution, which was allowed to cool overnight. The solid formed was recovered by filtration from the solution and dried *in vacuo* to give norbornene-5-*exo*, 6-*exo*-dicarboxylic acid as colourless crystals (8.58 g, 71%). Found C, 57.08; H, 5.65%. $C_9H_{10}O_4$ requires C, 59.34; H, 5.53%, the low carbon analysis result was attributed to the hydroscopic nature of the compound, which was very difficult to dry. The spectroscopic parameters were in full agreement with the literature values.[6] ^{13}C NMR (63MHz, C_3D_6O) δ 174.47 ($C_{8,9}$), 138.23 ($C_{2,3}$), 47.06 ($C_{1,4}$), 45.92 ($C_{5,6}$), 45.26 (C_7). ^1H NMR (250MHz, C_3D_6O) δ 6.24 (m, 2H, $H_{2,3}$), 3.01 (m, 2H, $H_{1,4}$), 2.59 (m, 2H, $H_{5,6}$), ABq δ_A 2.18, δ_B 1.37, J_{AB} =8.6Hz, 2H, $H_{7/7'}$. *m/z* (ES MS) 182 [M^+].

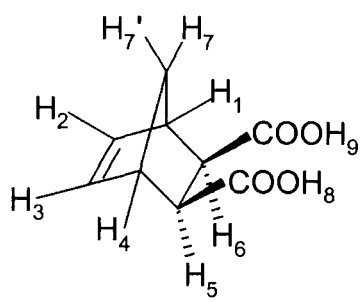

Assignment of hydrogen atoms

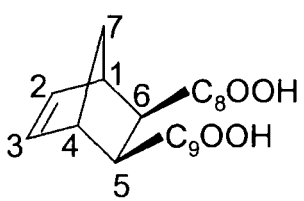

Assignment of carbon atoms

5.2.6 Synthesis of Norbornene-5-*exo*, 6-*exo*-dimethanol

Norbornene-5-*exo*, 6-*exo*-dimethanol was prepared by following an amended version of the procedure used in the reduction of norbornene-5-*exo*-carboxylic acid.[5] Norbornene-5-*exo*, 6-*exo*-dicarboxylic acid (8.4 g) was dissolved in 100 mL of sodium-dried ether and this solution was added drop wise over a period of two hours to a two-neck 1 L flask containing 12 g of lithium aluminium hydride in 200 mL of sodium dried ether. The flask was cooled in ice. The mixture was then stirred overnight at room temperature and refluxed for 1.5 hours. The flask was cooled in ice and the residual hydride in the reaction flask was destroyed by slow addition of 65 mL of water. The white-grey precipitate of $Al(OH)_3$ formed, was dissolved by addition of 200 mL (20%) HCl solution and 40 mL (36%) HCl solution. The residual undissolved white-grey precipitate was finally dissolved by addition of 37 mL of concentrated hydrochloric acid in three portions. Stirring was continued for 30 minutes. This gave a clear two-phase system; an ether layer and an aqueous layer containing some dispersed precipitates. The ether layer was separated and the aqueous layer together with the dispersants was extracted with ether (4 x 100 mL). The ether extracts were combined and washed with a 10% aqueous NaOH solution and water. The ether extract was then dried over magnesium sulphate. After filtration, ether was removed under reduced pressure and the residue was distilled (105°C, 0.25Torr) to give norbornene-5-*exo*, 6-*exo*-dimethanol as a clear liquid (2.79 g, 32.5%). Found C, 69.54; H, 9.18%. Calculated for $C_9H_{14}O_2$ C, 70.10; H, 9.15%. ^{13}C NMR (75MHz, C_3D_6O) δ 137.82 ($C_{2,3}$), 65.32 (C_8), 46.14 (C_7), 44.24 ($C_{1,4}$), 43.82 ($C_{5,6}$). ^1H NMR (300MHz, C_3D_6O) δ 6.18 (m, 2H, $H_{2,3}$), 3.76 (m, 4H, $H_{8a,8b}$), 3.51 (bs, 2H, -OH), 2.53 (bs, 2H, $H_{1,4}$), 1.85 (m, 2H, $H_{5,6}$), ABq δ_A 1.39, δ_B 1.09, J_{AB} =9Hz, 2H, $H_{7/7'}$. *m/z* (ES MS) 66 [C_5H_6, M^+ - $C_4H_8O_2$].

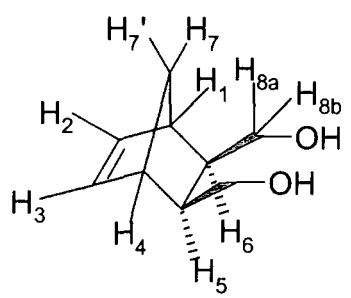

Assignment of hydrogen atoms

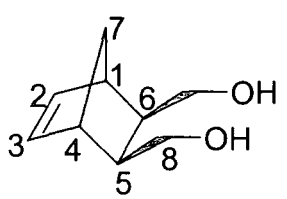

Assignment of carbon atoms

5.2.7 Synthesis of Norbornene-5-*exo*, 6-*exo*-dicarbonyl chloride

Norbornene-5-*exo*, 6-*exo*-dicarbonyl chloride was prepared following the published route.[8] Norbornene-5-*exo*, 6-*exo*-dicarboxylic acid (28.7 g, 0.158 mol) and oxalyl chloride (100 g, 0.788 mol) were placed in a 500 mL round bottom flask fitted with a reflux condenser and a drying tube. The evolution of gas started immediately and once it had subsided, the mixture was refluxed (85°C) for 3 hours from an oil bath. The excess oxalyl chloride was removed *in vacuo* (in fumehood) and the residue distilled to give pure norbornene-5-*exo*, 6-*exo*-dicarbonyl chloride as a white solid (23.3 g, 68%). Found C, 48.87; H, 3.10; Cl, 32.04%. $C_9H_8Cl_2O_2$ requires C, 49.34; H, 3.68; Cl, 32.37%. The spectroscopic parameters were in full agreement with the literature values.[8] ^{13}C NMR (75MHz, C_3D_6O) δ 172.21 ($C_{8,9}$), 138.37 ($C_{2,3}$), 49.21 (C_7), 47.28 ($C_{1,4}$), 44.54 ($C_{5,6}$). ^1H NMR (300MHz, C_3D_6O) δ 6.37 (m, 2H, $H_{2,3}$), 3.35 (m, 2H, $H_{1,4}$), 3.13 (m, 2H, $H_{5,6}$), 1.62, 1.42 (m, 2H, $H_{7,7'}$).

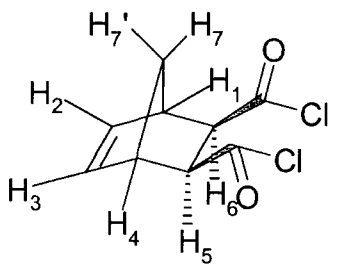

Assignment of hydrogen atoms

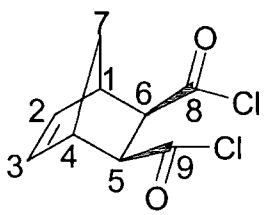

Assignment of carbon atoms

5.3 Procedures for the Synthesis of the First and Second Generation Polycarbonate Dendrons

5.3.1 Compounds of the Zeroth and First Generation

Note: For the key to the name codes of the polycarbonate dendrons, see chapter 2, section 2.4.1 and the bookmark card.

5.3.1.1 Synthesis of BG0IM

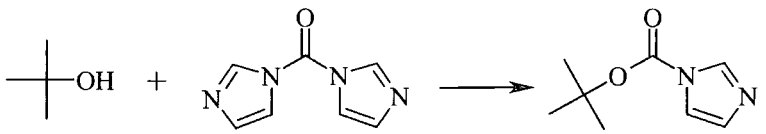

BG0IM

BG0IM was prepared following the published route.[9] *t*-Butanol (52.92 g, 0.714 mol) and toluene (200 mL) were stirred in a round bottom flask fitted with a reflux condenser. CDI (57.88 g, 0.357 mol) was added and the reaction mixture was heated at 60°C for 4 hours. The solvent was removed *in vacuo* and the oil obtained was redissolved in CH_2Cl_2 (250 mL). The organic phase was washed with water (3 x 250 mL), dried over $MgSO_4$ and, after filtration, the solvent was removed *in vacuo*. The product was vacuum dried to give **BG0IM** as a white crystalline solid (54.39 g, 90%). Found C, 56.70; H, 7.08; N, 16.34%. $C_8H_{12}N_2O_2$ requires C, 57.13; H, 7.19; N, 16.66%. The spectroscopic parameters were in full agreement with the literature values.[9] ^{13}C NMR (62.9 MHz, $CDCl_3$) δ 147.1, 137.04, 130.23, 117.06, 85.32, 27.85. ^1H NMR (250 MHz, $CDCl_3$) δ 8.08 (s, 1H), 7.38 (s, 1H), 7.04 (s, 1H), 1.63 (s, 9H). *m/z* (ES MS) 168 $[M]^+$.

5.3.1.2 Synthesis of BG1OH

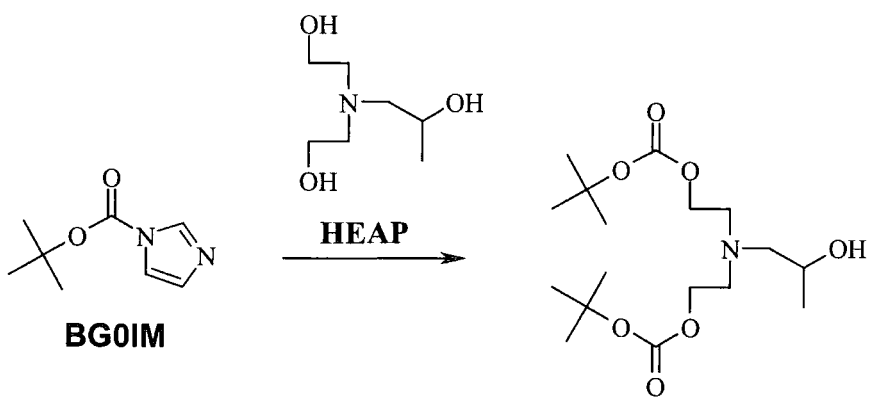

BG0IM **HEAP** **BG1OH**

BG1OH was prepared following the published route.[9] **HEAP** (11.47 g, 0.07 mol) was added to a solution of **BG0IM** (24.864 g, 0.148 mol) in toluene (80 mL) containing approximately 50 mg of KOH. The mixture was stirred and heated at

80°C for 3 days. The reaction mixture was analysed by ^{1}H NMR spectroscopy, which indicated that there was no **BG0IM** remaining. The reaction mixture was concentrated *in vacuo* and redissolved in CH_2Cl_2 (250 mL). The organic phase was subsequently washed with water (3 x 250 mL), dried over $MgSO_4$ and, after filtration, the solvent was removed *in vacuo*. The yellow oil was purified by column chromatography (silica gel, eluting with EtOAc:C_6H_{14} 1:1) and dried under vacuum to give **BG1OH** as a colourless oil (11.71 g, 46%). Found C, 55.62; H, 9.14; N, 3.65%. $C_{17}H_{33}NO_7$ requires C, 56.18; H, 9.15; N, 3.85%. The spectroscopic parameters were in full agreement with the literature values.[9] ^{13}C NMR (62.9 MHz, $CDCl_3$) δ 153.5, 82.2, 64.4, 63.7, 63.1, 53.3, 27.7, 19.6. ^{1}H NMR (250 MHz, $CDCl_3$) δ 4.12 (m, 4H), 3.70 (m, 1H), 3.30 (s, br, $CH_2CH(OH)CH_3$), 2.91 (dt, J=14.25Hz, J=6.25Hz, 2H), 2.81 (dt, J=14.1Hz, J=5.4Hz, 2H), 2.62 (dd, J=13Hz, J=2.8Hz, 1H), 2.32 (dd, J=13Hz, J=10.4Hz, 1H), 1.47 (s, 18H), 1.10 (d, J=6Hz, 3H). *m/z* (ES MS) 364 $[M+H]^+$.

5.3.1.3 Synthesis of BG1IM

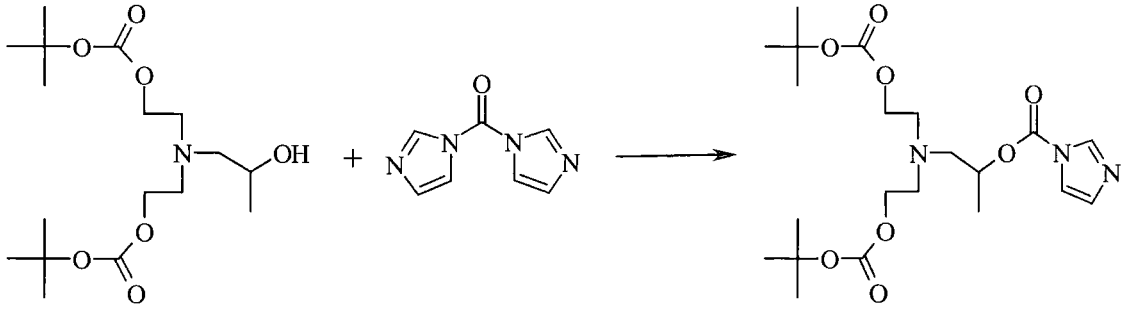

BG1OH **BG1IM**

BG1IM was prepared following the published route.[9] CDI (4.15 g, 25.6 mmol) and **BG1OH** (4.65 g, 12.8 mmol) were stirred together at 65°C for 4 hours in a 2-neck 250 mL flask containing 100 mL of dry toluene and some KOH (approximately 50 mg). After which, analysis of the ^{1}H NMR spectrum of the reaction mixture showed that the reaction had gone to completion, as there was no evidence of **BG1OH**. The toluene was removed *in vacuo* and dichloromethane (250 mL) was added to the mixture. The organic layer was washed with water (3 x 250 mL), dried over $MgSO_4$ and, after filtration, concentrated *in vacuo*. The product was dried under vacuum for 1 day, to give **BG1IM** as a colourless oil (5.67 g, 97%). Found C, 54.5; H, 7.7; N, 9.91%. $C_{21}H_{35}N_3O_8$ requires C, 55.13; H, 7.71; N, 9.18%. The spectroscopic

parameters were in full agreement with the literature values.[9] ^{13}C NMR (63MHz, $CDCl_3$) δ 153.39, 148.5, 138.98, 130.51, 117.08, 82.09, 74.27, 64.69, 59.56, 53.5, 27.69, 17.77. ^{1}H NMR (250MHz, $CDCl_3$) δ 8.12 (s, 1H), 7.41 (s, 1H), 7.04 (s, 1H), 5.15 (m, 1H), 4.07 (m, 4H), 2.86 (m, 4H), 2.78, 2.76 (dd, J=14.1Hz, J=5.1Hz, 2H), 1.45 (s, br, 18H), 1.38 (d, J=6.5Hz, 3H). *m/z* (ES MS) 457 [M^+].

5.3.2 Compounds of the Second Generation

5.3.2.1 Synthesis of BG2OH

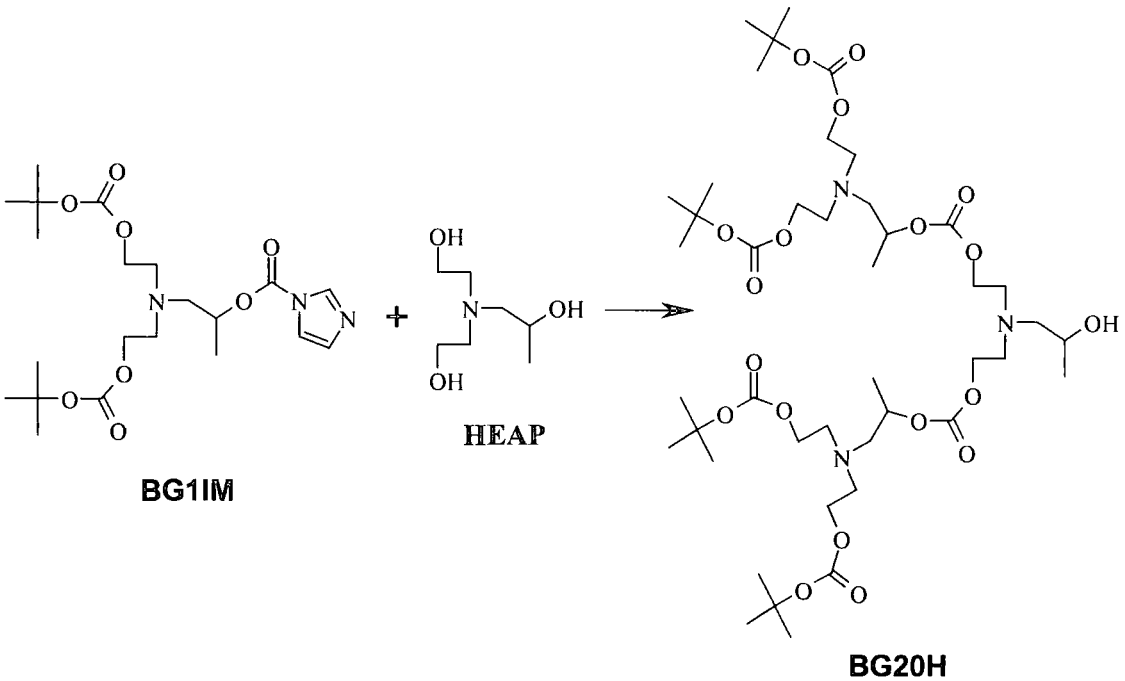

BG2OH was prepared following the published route.[9] **HEAP** (2.38 g, 14.6 mmol) was added to a stirred solution of **BG1IM** (13.36 g, 29.23 mmol) in toluene (75 mL). A catalytic amount of KOH was added and the mixture was stirred at 75°C for 5 days. Analysis of the ^{1}H NMR spectrum of the reaction mixture showed that the reaction had gone to completion. The reaction mixture was concentrated *in vacuo* and redissolved in CH_2Cl_2 (250 mL). The organic phase was subsequently washed with water (3 x 250 mL), dried over $MgSO_4$ and, after filtration, the solvent was removed *in vacuo*. The yellow oil was purified initially by column chromatography (silica gel, eluting with EtOAc:C_6H_{14} 1:1) and then by several Biobeads columns eluting with toluene to form **BG2OH** as a colourless oil (4.5 g, 33%). Found C, 54.59; H, 8.72; N,

4.53%. $C_{43}H_{79}N_3O_{19}$ requires, C, 54.82; H, 8.45; N, 4.46%. The spectroscopic parameters were in full agreement with the literature values.[9] ^{13}C NMR (100 MHz, $CDCl_3$) δ 156.3, 155.0, 82.6, 74.8, 66.9, 66.3, 66.1, 64.1, 61.0, 54.9, 54.8, 28.1, 20.8, 18.3. ^1H NMR (400 MHz, $CDCl_3$) δ 4.72 (m, 2H), 4.02 (m, 8H), 4.14 (m, 4H), 3.63 (m, 1H), 2.92 (m, 4H), 2.85 (m, 10H), 2.75, 2.64 (dd, J=13.6Hz, 6.0Hz, 2H), 2.33 (m, 2H), 1.41 (s, 36H), 1.19 (d, J=6.4Hz, 6H), 1.04 (d, J=6.4Hz, 3H). *m/z* (ES MS) 942.5 $[M+H]^+$, 964.4 $[M+Na]^+$. GPC; M_w = 1,250 PDI 1.00.

5.3.2.2 Synthesis of BG2IM

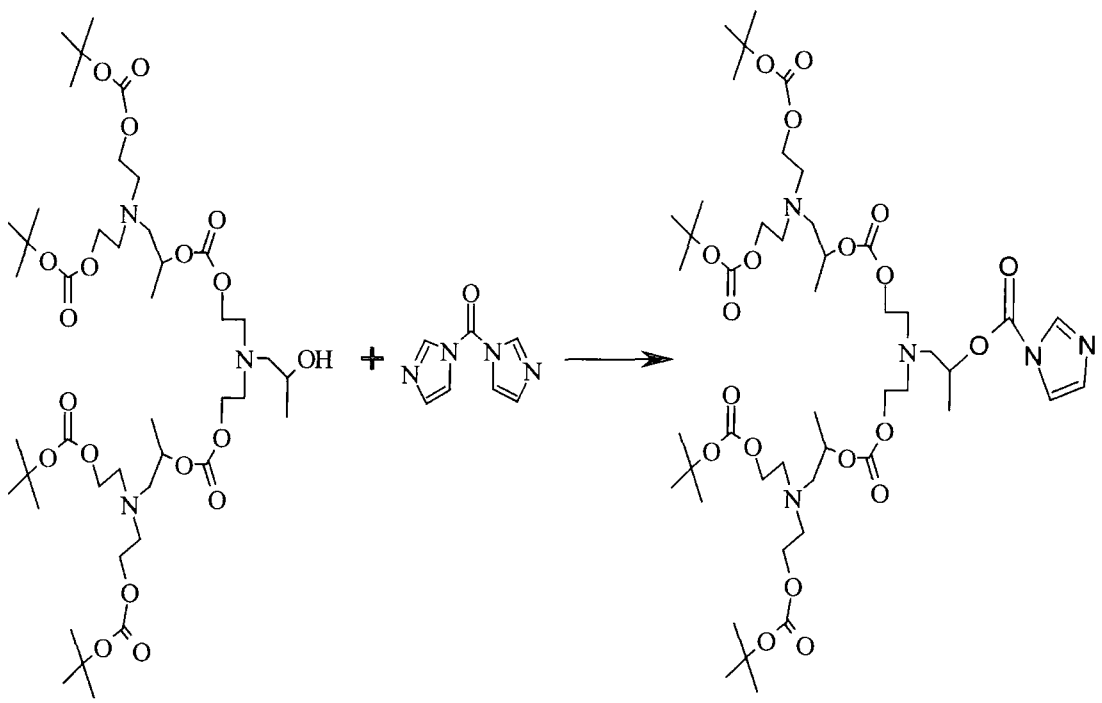

BG2IM was prepared following the published route.[9] CDI (3.72 g, 22.8 mmol) was added to a round bottom flask containing **BG2OH** (10.754 g, 11.40 mmol) and a catalytic amount of KOH in 200 mL of toluene. The mixture was heated at 70°C for 4 hours. Subsequently, the reaction mixture was analysed by ^1H NMR spectroscopy, which indicated that there was no **BG2OH** remaining. The reaction mixture was concentrated *in vacuo* and redissolved in CH_2Cl_2 (250 mL). The organic phase was subsequently washed with water (3 x 250 mL), dried over $MgSO_4$ and, after filtration, the solvent was removed *in vacuo*. This resulted in **BG2IM** as a yellowy product (11.5 g, 97%). Found C, 53.97; H, 7.80; N, 6.94%. $C_{47}H_{81}N_5O_{20}$ requires C, 54.48; H, 7.88; N, 6.76%. The spectroscopic parameters were in full agreement with the

literature values.[9] ^{13}C NMR (125 MHz, $CDCl_3$) δ 154.67, 153.45, 148.29, 137.13, 130.59, 117.15, 81.93, 74.19, 73.55, 65.53, 64.88, 59.88, 59.67, 59.58, 53.57, 27.76, 17.92, 17.81. ^1H NMR (500 MHz, $CDCl_3$) δ 8.16 (s, 1H), 7.42 (s, 1H), 7.08 (s, 1H), 5.18 (m, 1H), 4.79 (m, 2H), 4.09 (m, 8H), 4.09 (m, 4H), 2.86 (m, 8H), 2.86 (m, 4H), 2.79 (m, 4H), 2.61 (m, 2H), 1.48 (s, 36H), 1.38 (d, J=6.5Hz, 3H), 1.24 (m, 6H). *m/z* (ES MS) 1036.6 $[M]^+$, 1059.6 $[M+Na]^+$.

5.4 Procedures for the Synthesis of Polycarbonate Dendronised Monomers

Note: For the key to the name codes of all the dendronised monomers, see chapter 2, section 2.5.1 and the bookmark card.

5.4.1 Synthesis of DMPCB1M

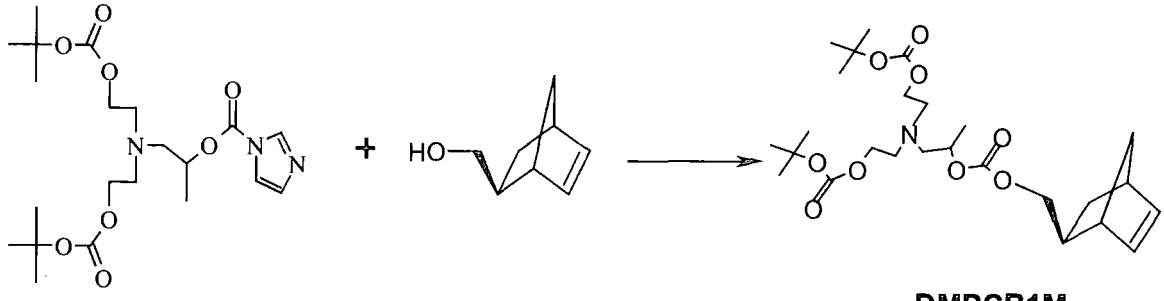

BG1IM **DMPCB1M**

Norbornene-5-*exo*-methanol (1.46 g, 11.7 mmol) and **BG1IM** (5.39 g, 11.7 mmol) were placed in a 2-neck 250 mL flask containing 100 mL of dry toluene and approximately 50 mg of KOH. The mixture was purged with nitrogen and stirred at 95°C for three days. Analysis of the ^1H NMR spectrum of the reaction mixture showed that the reaction had gone to completion as there was no **BG1IM** remaining. The toluene was removed *in vacuo* and dichloromethane (250 mL) was added to the mixture. The organic layer was then washed with water (3 x 250 mL), dried over $MgSO_4$ and, after filtration, concentrated *in vacuo*. Purification by column chromatography (silica gel, eluting with EtOAc:C_6H_{14} 1:4) gave **DMPCB1M** as a colourless oil (4 g, 66%). Found C, 60.41; H, 8.13; N, 2.21%. Calculated for $C_{26}H_{43}NO_9$ C, 60.80; H, 8.44; N, 2.73%. ^{13}C NMR (63 MHz, $CDCl_3$) δ 154.84, 153.42, 136.85, 136.2, 81.95, 73.21, 71.83, 64.85, 59.70, 53.48, 44.89, 43.48, 41.54, 37.95, 29.40, 27.74, 17.98. ^1H NMR (500 MHz, $CDCl_3$) δ 6.01 (m, 2H), 4.75 (m, 1H), 4.15-3.96 (m, 2H), 4.04 (m, 4H), 2.79 (broad s, 4H), 2.78-2.64 (m, 2H), 2.72-

2.59 (m, 2H), 1.72 (broad s, 1H), 1.58- 1.32 (broad s, 2H), 1.40 (broad s, 18H), 1.3-1.11 (m, 2H), 1.21 (dd, 3H). *m/z* (ES MS) 513 [M+H]$^+$.

5.4.2 Synthesis of DMPCB1D

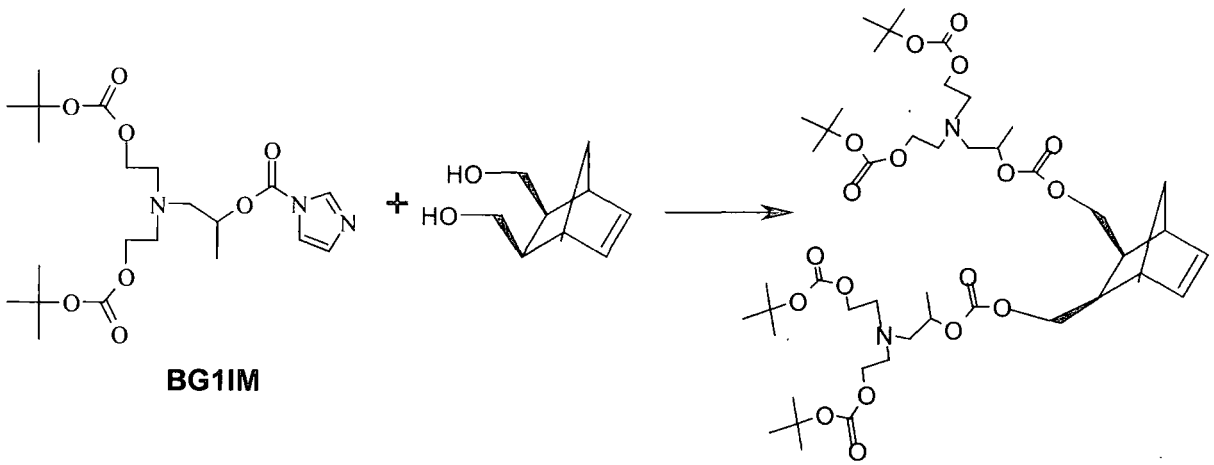

BG1IM **DMPCB1D**

Norbornene-5-*exo*, 6-*exo*-dimethanol (3.3 g, 21.6 mmol) and **BG1IM** (20.14 g, 21.6 mmol) were placed in a 2-neck 250 mL flask containing 80 mL of dry toluene and approximately 50 mg of KOH. The mixture was stirred at 90°C for five days. Analysis of the ^{1}H NMR spectrum of the reaction mixture showed that the reaction had gone to completion, as there was no **BG1IM** remaining. The toluene was removed *in vacuo* and dichloromethane (250 mL) was added to the mixture. The organic layer was then washed with water (3 x 250 mL), dried over $MgSO_4$ and, after filtration, concentrated *in vacuo*. Purification by column chromatography (silica gel, eluting with EtOAc:C_6H_{14} 1:1.5) gave **DMPCB1D** as a colourless oil (8.79 g, 44%). Found C, 57.53; H, 8.15; N, 2.66%. Calculated for $C_{45}H_{76}N_2O_{18}$ C, 57.92; H, 8.21; N, 3.00%. ^{13}C NMR (125 MHz, $CDCl_3$) δ 154.91, 153.69, 137.48, 82.22, 73.72, 68.90, 65.11, 59.94, 53.78, 44.81, 42.64, 40.01, 28.01, 18.25. ^{1}H NMR (500 MHz, $CDCl_3$) δ 6.15 (s, 2H), 4.78 (m, 2H), 4.28 (m, 2H), 4.11 (m, 8H), 4.01 (m, 2H), 2.86 (m, 8H), 2.84, 2.62 (m, 4H), 1.92, 1.4 (m, 4H), 1.47 (s, 36H), 1.26 (m, 6H), 1.1 (d, J=6Hz, 2H). *m/z* (ES MS) 933.6 [M$^+$]. *m/z* (MALDI-TOF (Kratos) MS 934 [M+H]$^+$, 956 [M+Na]$^+$. GPC; M_w = 1,070 PDI 1.01.

5.4.3 Synthesis of DMPCB2D

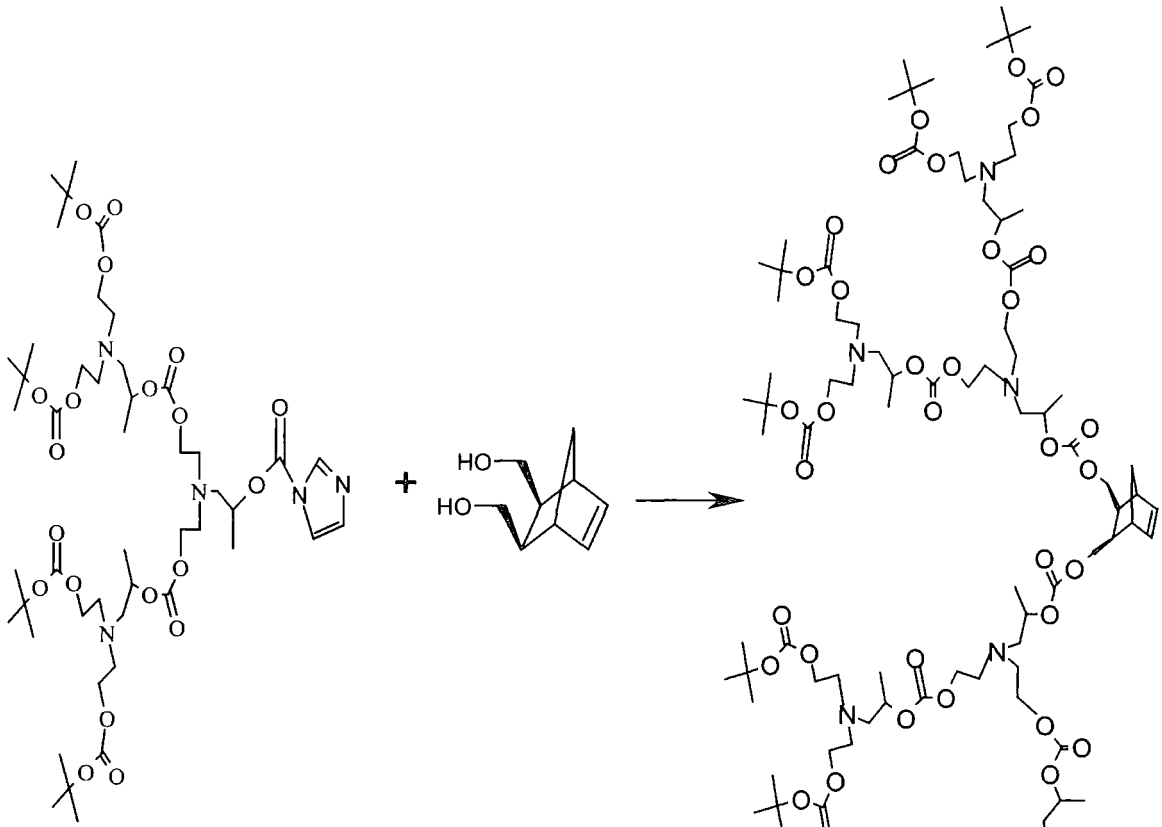

BG2IM **DMPCB2D**

BG2IM (2 g, 1.93 mmol) was added to a stirred solution of norbornene-5-*exo*, 6-*exo*-dimethanol (0.149 g, 0.965 mmol) in toluene (30 mL). A catalytic amount of KOH was added (approximately 50 mg) and the mixture was stirred at 75°C for 7 days. Analysis of the ^{1}H NMR spectrum of the reaction mixture showed that the reaction had gone to completion, as there was no **BG2IM** remaining. The reaction mixture was concentrated *in vacuo* and redissolved in CH_2Cl_2 (250 mL). The organic phase was subsequently washed with water (3 x 250 mL), dried over $MgSO_4$ and, after filtration, the solvent was removed *in vacuo*. The viscous yellow oil was purified initially by column chromatography (silica gel, eluting with EtOAc:C_6H_{14} 1:1) and then by several Biobeads columns eluting with toluene to form **DMPCB2D** as a colourless oil (0.489 g, 24%). Found C, 55.75; H, 8.10; N, 3.86%. Calculated for $C_{97}H_{168}N_6O_{42}$ C, 55.73; H, 8.10; N, 4.02%. ^{13}C NMR (125 MHz, $CDCl_3$) δ 154.93,

153.69, 137.43, 82.19, 73.66, 65.94, 65.88, 65.10, 59.85, 53.77, 44.81, 43.91, 40.01, 28.01, 18.23, 1.27. ^{1}H NMR (500 MHz, $CDCl_3$) δ 6.19 (s, 2H), 4.79 (m, 4H), 4.29 (m, 2H), 4.09 (m, 16H), 4.09 (m, 8H), 2.86 (m, 16H), 2.83 (m, 8H), 2.80 (m, 8H), 2.61 (m, 4H), 1.92 (s, 2H), 1.64 (m, 2H), 1.56 (s, 4H), 1.47 (m, 72H), 1.38 (m, 6H), 1.3 (m, 2H), 1.27 (m, 12H). *m/z* (MALDI-TOF (Kratos) MS 2090.5 [M^+]. GPC; M_w = 2,150 PDI 1.14.

5.5 Procedures for the Synthesis of Second Generation Polyurethane Dendrons and Dendronised Monomers

5.5.1 Synthesis of HG2IM (U)

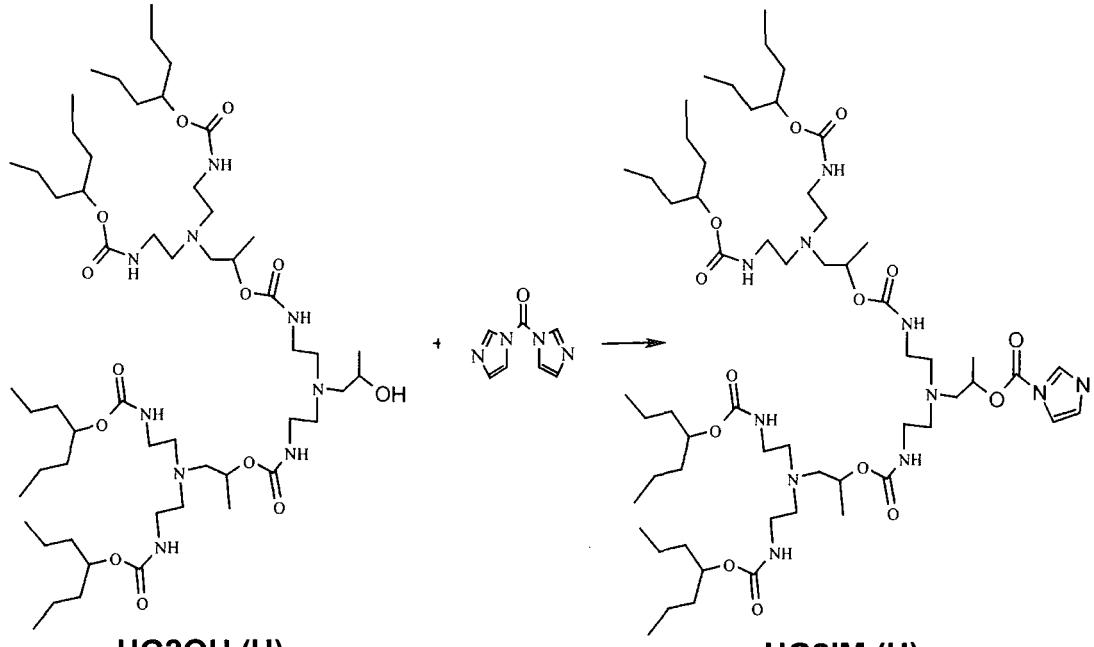

CDI (0.89 g, 5.43 mmol) was added to a round bottom flask containing **HG2OH (U)** (2.75 g, 2.49 mmol) and a catalytic amount of KOH (approximately 50 mg) in 150 mL of toluene. The mixture was heated at 70°C for 5 hours. Analysis of the ^{1}H NMR spectrum of the reaction mixture showed that the reaction had gone to completion, as there was no **HG2OH (U)** remaining. The reaction mixture was concentrated *in vacuo* and redissolved in CH_2Cl_2 (250 mL). The organic phase was subsequently washed with water (3 x 250 mL), dried over $MgSO_4$ and, after filtration, the solvent was removed *in vacuo*. This resulted in **HG2IM (U)** as a clear viscous product (2.13 g, 71%). Found C, 57.64; H, 9.12; N, 12.13%. Calculated for

$C_{59}H_{111}N_{11}O_{14}$ C, 59.12; H, 9.33; N, 12.85%, the low carbon analysis result was attributed to the hygroscopic nature of the compound, which was very difficult to dry. ^{1}H NMR (400 MHz, $CDCl_3$) δ 8.16 (s, 1H), 7.42 (s, 1H), 7.07 (s, 1H), 5.30 (s, br, 4NH), 5.21 (m, 2H), 4.87 (s, br, 2NH), 4.75 (m, 4H), 3.28 (m, 1H), 3.28-3.09 (m, 12H), 2.68-2.42 (m, 18H),1.54-1.47 (m, 16H), 1.30-1.41 (m, 16H), 1.29 (m, 3H), 1.19 (d, J=6.4Hz, 6H), 0.92 (t, J=7.2Hz, 24H). *m/z* (ES MS) 1221.8 $[M+Na]^+$.

5.5.2 Synthesis of DMPUH2D

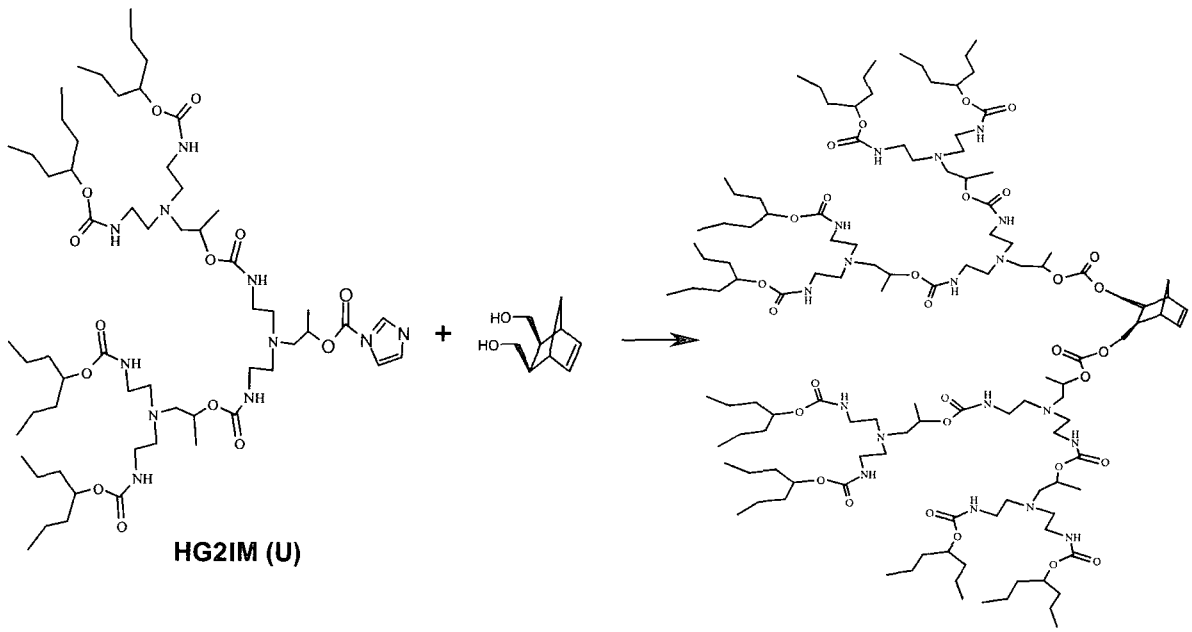

HG2IM (U) **DMPUH2D**

HG2IM (U) (2.1 g, 1.752 mmol) was added to a stirred solution of norbornene-5-*exo*, 6-*exo*-dimethanol (0.135 g, 0.876 mmol) in toluene (150 mL). A catalytic amount of KOH (approximately 50 mg) was added and the mixture was stirred at 80°C for 7 days. Analysis of the ^{1}H NMR spectrum of the reaction mixture showed that the reaction had gone to completion as there was no **HG2IM (U)** remaining. The reaction mixture was concentrated *in vacuo* and redissolved in CH_2Cl_2 (250 mL). The organic phase was subsequently washed with water (3 x 250 mL), dried over $MgSO_4$ and, after filtration, the solvent was removed *in vacuo*. The viscous yellow oil was purified initially by flash chromatography (silica gel, eluting with EtOAc:C_6H_{14} 1:1) and then via a Biobeads column eluting with toluene, to form **DMPUH2D** as a colourless viscous oil (0.214 g, 10.1%). Found C, 59.09; H, 9.37; N, 10.87%. Calculated for $C_{121}H_{228}N_{18}O_{30}$ C, 60.17; H, 9.52; N, 10.44%, the low carbon analysis

result was attributed to the hygroscopic nature of the compound, which was very difficult to dry. ^{13}C NMR (75 MHz, CD_3OD) δ 159.89, 159.53, 150.78, 137.28, 135.07, 129.77, 76.58, 76.00, 73.82, 71.55, 61.82, 56.46, 52.44, 40.89, 38.78, 20.51, 19.9, 19.47, 15.37. ^1H NMR (400 MHz, C_3D_6O) δ 6.42, 6.21, 4.9-4.7, 3.78, 3.3-3.1, 2.75-2.45, 2.08, 1.6-1.3, 1.1, 0.92-0.88. *m/z* (MALDI TOF (Kratos) MS 2415 $[M]^+$, 2437 $[M+Na]^+$. GPC; M_n = 2,550 PDI 1.00.

5.5.3 Synthesis of BG2IM (U)

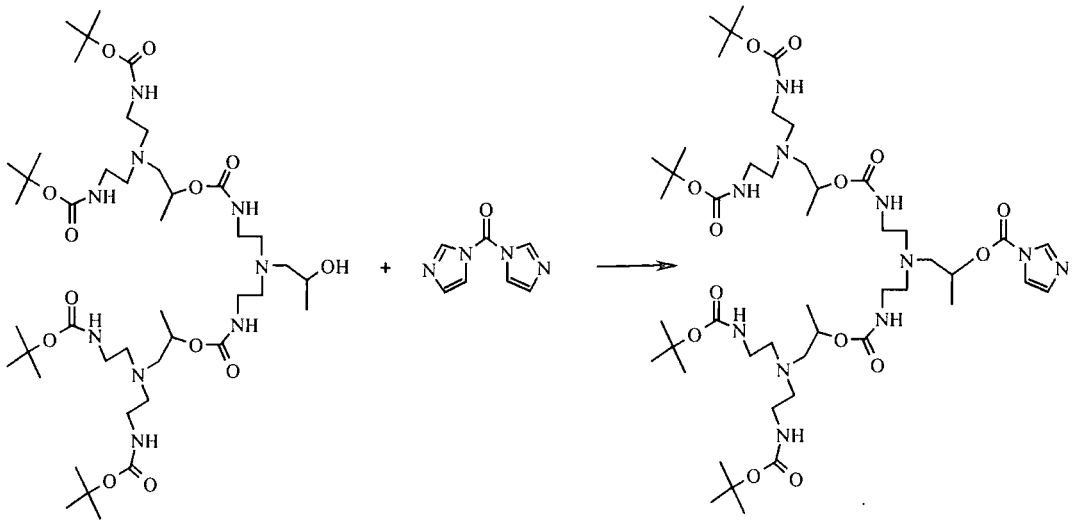

BG2OH (U) **BG2IM (U)**

CDI (0.97 g, 5.94 mmol) was added to a round bottom flask containing **BG2OH (U)** (2.78 g, 2.97 mmol) and a catalytic amount of KOH (approximately 50 mg) in 100 mL of toluene. The mixture was heated at 70°C for 5 hours. Analysis of the ^1H NMR spectrum of the reaction mixture showed that the reaction had gone to completion, as there was no **BG2OH (U)** remaining. The reaction mixture was concentrated *in vacuo* and redissolved in CH_2Cl_2 (250 mL). The organic phase was subsequently washed with water (3 x 250 mL), dried over $MgSO_4$ and, after filtration, the solvent was removed *in vacuo*. This resulted in **BG2IM (U)** as a yellowy viscous product (2.37 g, 78%). Found C, 55.06; H, 8.56; N, 13.78%. Calculated for $C_{47}H_{87}N_{11}O_{14}$ C, 54.79; H, 8.51; N, 14.95%. ^{13}C NMR (75 MHz, C_3D_6O) δ 156.92, 156.44, 137.51, 130.74, 117.71, 78.09, 75.00, 69.29, 60.31, 59.98, 55.16, 54.85, 50.11, 39.24, 39.07, 34.61, 18.49, 17.79. ^1H NMR (400 MHz, C_3D_6O) δ 8.19 (s, 1H), 7.58 (s, 1H), 7.02 (s, 1H), 6.24 (s, br, 2H, O(CO)N*H*CH_2), 6.02 (s, br, 4H $C(CH_3)_3O(CO)N$*H*CH_2), 5.21(m, 1H), 4.82 (m, 2H), 3.09-3.2 (m, 12H), 2.82 (m, 4H),

2.55-2.62 (m, 12H), 2.49 (m, 2H), 1.42 (s, 36H), 1.38 (3H), 1.19 (d, J=6.5Hz, 6H). *m/z* (ES MS) 1030.8 $[M]^+$, 1053.7 $[M+Na]^+$.

5.5.4 Synthesis of DMPUB2D

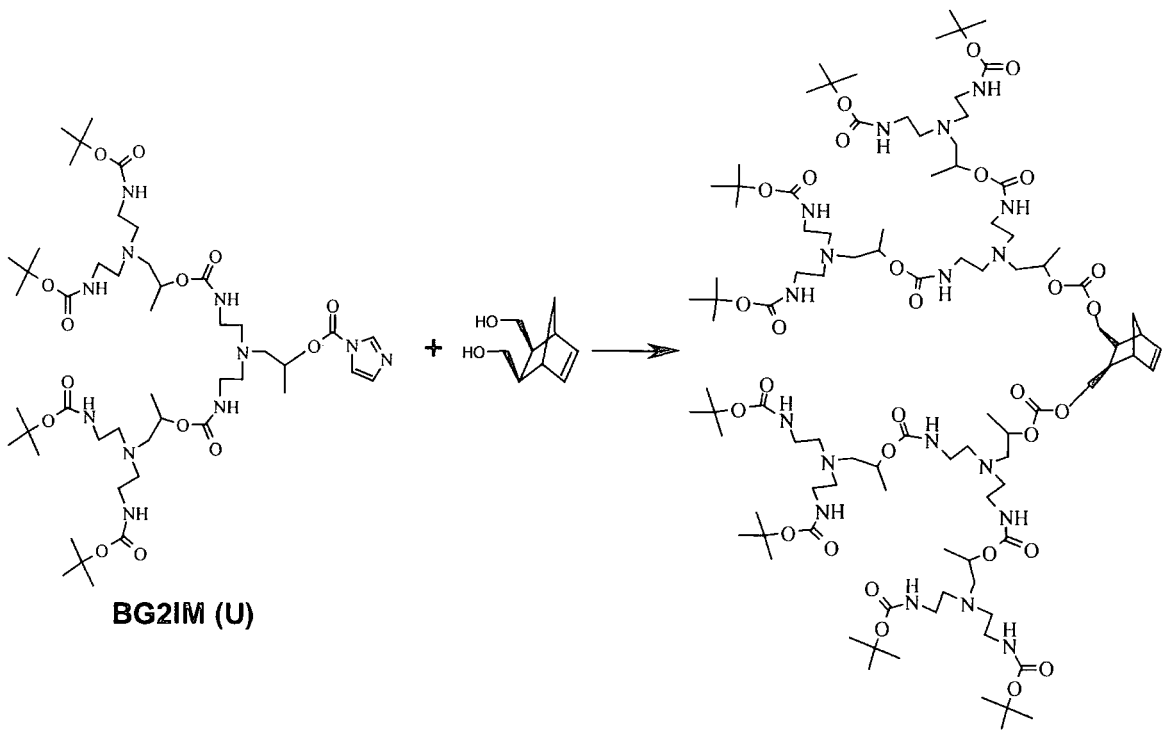

BG2IM (U) (2.1 g, 1.752 mmol) was added to a stirred solution of norbornene-5-*exo*, 6-*exo*-dimethanol (0.135 g, 0.876 mmol) in toluene (150 mL). A catalytic amount of KOH was added and the mixture was stirred at 80°C for 7 days. Analysis of the ^1H NMR spectrum of the reaction mixture showed that the reaction had gone to completion, as there was no **BG2IM (U)** remaining. The reaction mixture was concentrated *in vacuo* and redissolved in CH_2Cl_2 (250 mL). The organic phase was subsequently washed with water (3 x 250 mL), dried over $MgSO_4$ and, after filtration, the solvent was removed *in vacuo*. The viscous yellow oil was purified initially by flash chromatography (silica gel, eluting with EtOAc:C_6H_{14} 1:1) and then via a Biobeads column, eluting with toluene to form **DMPUB2D** as a colourless viscous oil (0.19 g, 8.4%). Found C, 55.52; H, 8.75; N, 12.70%. Calculated for $C_{97}H_{180}N_{18}O_{30}$ C, 56.05; H, 8.73; N, 12.13%. ^1H NMR (400 MHz, $CDCl_3$) δ 6.70 (m, 4 NH), 6.4 (s, br, 8 NH), 6.2 (s, br, 2H), 4.85 (s), 3.72 (m), 3.25-3.05, 2.7-2.44, 2.32, 2.21, 1.84, 1.56-1.36, 1.24-1.16. GPC; M_n = 1,960 PDI 1.00.

5.5.5 Synthesis of BHG1IM (U)

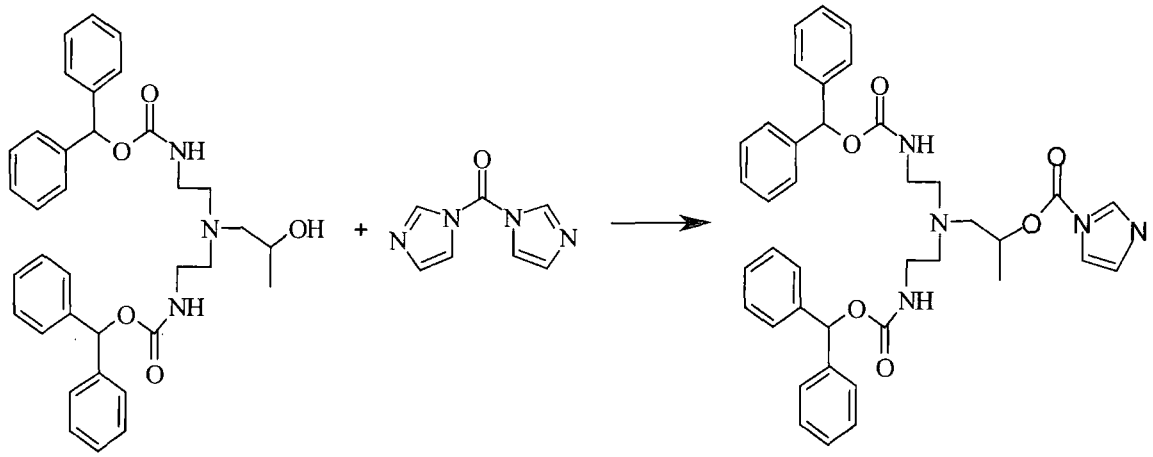

BHG1OH (U) **BHG1IM (U)**

CDI (6.88 g, 42.15 mmol) was added to a stirred solution of **BHG1OH (U)** (12.26 g, 21.08 mmol) in toluene (75 mL). A catalytic amount of KOH (approximately 50 mg) was added and the mixture was heated at 75°C for 5 hours. Analysis of the ^{1}H NMR spectrum of the reaction mixture showed that the reaction had gone to completion, as there was no **BHG1OH (U)** remaining. The reaction mixture was concentrated *in vacuo* and redissolved in CH_2Cl_2 (250 mL). The organic phase was subsequently washed with water (3 x 250 mL), dried over $MgSO_4$ and, after filtration, the solvent was removed *in vacuo*. The solid material was purified by column chromatography (silica gel, eluting with EtOAc:C_6H_{14} 5:1) to form **BHG1IM (U)** as a yellow glassy product (6.74 g, 47%). Found C, 68.46; H, 5.94; N, 11.80%. Calculated for $C_{39}H_{41}O_6N_5$ C, 69.32; H, 6.12; N, 10.36%, the low carbon analysis result was attributed to the hygroscopic nature of the compound, which was very difficult to dry. ^{13}C NMR (75 MHz, $CDCl_3$) δ 156.28, 148.83, 140.91, 137.31, 131.04, 128.72, 128.06, 127.24, 117.34, 75.01, 74.28, 59.81, 54.62, 39.24, 18.21. ^{1}H NMR (300 MHz, $CDCl_3$) δ 8.04 (s, 1H), 7.36 (s, 1H), 7.26 (m, 20H), 6.95 (s, 1H), 6.74 (s, 2H), 5.41 (s, br, 2H, O(CO)N*H*CH_2), 5.11 (m, 1H), 3.09-3.21 (m, 4H), 2.64-2.73 (m, 2H), 2.57 (m, 4H), 1.23 (d, J=6.6Hz, 3H). *m/z* (ES MS) 698.2 $[M+Na]^+$. GPC; M_n = 590 PDI 1.00.

5.6 Procedures for the Synthesis of First Generation Polyamide Dendrons and a Dendronised Monomer

5.6.1 Synthesis of 5-nitroisophthaloyl dichloride

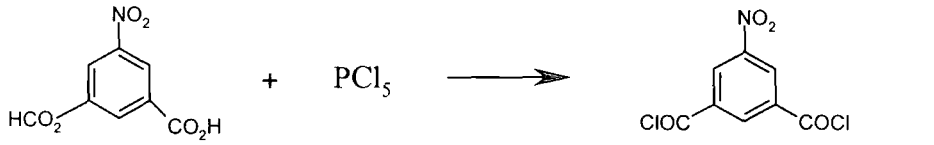

5-nitroisophthaloyl dichloride

5-Nitroisophthaloyl dichloride was prepared following the published route.[10] A 2 L, 3 neck flask was fitted with a reflux condenser attached to a scrubbing tower in which dilute sodium hydroxide solution was circulated, 5-nitroisophthalic acid (100 g, 0.47 mol) and phosphorus pentachloride (200 g, 0.96 mol) were then added. The mixture was gently warmed on a water bath resulting in a homogeneous yellow solution forming with the, at times, vigorous evolution of a gas. The mixture was heated to 90°C for 5 hours. The mixture was cooled overnight and the phosphorus oxychloride formed was removed *in vacuo*. An off white residue was obtained which was recrystallised from petroleum ether (40-60°C) to give 5-nitroisophthaloyl dichloride as white needles, m.pt 66-68°C (74.2 g, 63.12%), Lit[11] m.pt 67-68°C. Found C, 38.78; H, 1.21; N, 5.56; Cl, 28.70%. $C_8H_3Cl_2NO_4$ requires C, 38.74; H, 1.22; N, 5.65; Cl, 28.59%. The spectroscopic parameters were in full agreement with the literature values.[10] ^{13}C NMR (100 MHz, $CDCl_3$) δ 165.88, 149.11, 137.69, 136.26, 131.14. ^1H NMR (300 MHz, $CDCl_3$) δ 9.23 (d, J=1.5Hz, 2H), 9.12 (t, J=1.5Hz,1H). *m/z* (ES MS) 272.1 $[M+Na]^+$. GPC; M_n = 200 PDI 1.05.

5.6.2 Synthesis of [3]-NO_2

Note: For the key to the name codes of the polyamide dendrons, see chapter 2, section 2.4.5 and the bookmark card.

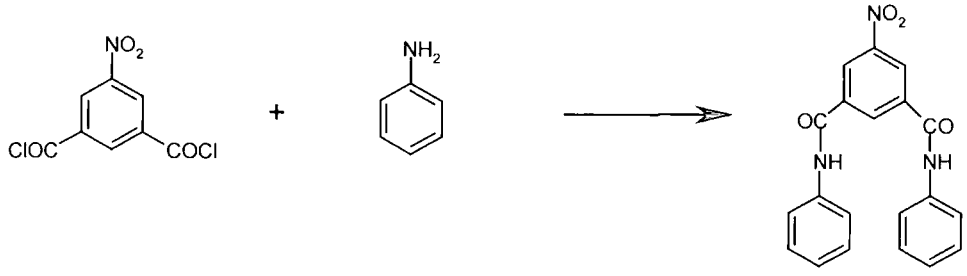

[3]-NO_2

[3]-NO_2 was prepared following the published route.[10] A 500 mL 2 neck round bottom flask fitted with a reflux condenser was charged with aniline (30.66 g, 0.33 mol) and dry pyridine (150 mL). The contents of the flask were stirred and the flask was cooled in ice. 5-Nitroisophthaloyl dichloride (40.88 g, 0.17 mol) was added in small portions over 30 minutes and stirred for 2 hours. The mixture was slowly heated to reflux and maintained at reflux for 5 hours, then cooled. Most of the excess pyridine was removed *in vacuo*, and the resulting yellow solid was poured into 1 L of water. The yellow solid formed was filtered off and dissolved in approximately 1.5 L of acetone. The clear yellow solution was then added dropwise to several litres of water. A white fluffy solid precipitated which was filtered off and dried (52.9 g, 89%) and identified as **[3]-NO_2**. Found C, 66.26; H, 4.10; N, 11.60%. $C_{20}H_{15}N_3O_4$ requires C, 66.48; H, 4.18; N, 11.63%. The spectroscopic parameters were in full agreement with the literature values.[10] ^{13}C NMR (75 MHz, d-DMSO) δ 162.89, 147.89, 138.60, 136.61, 133.11, 128.82, 125.09, 124.36, 120.63. ^{1}H NMR (300 MHz, d-DMSO) δ 10.75 (s, 2H), 8.96 (m, 3H), 7.82 (d, J=7.6Hz, 4H), 7.41 (t, J=7.6Hz, 4H), 7.16 (t, J=7.6Hz, 2H). GPC; M_n = 290 PDI 1.03.

5.6.3 Synthesis of [3]-NH_2

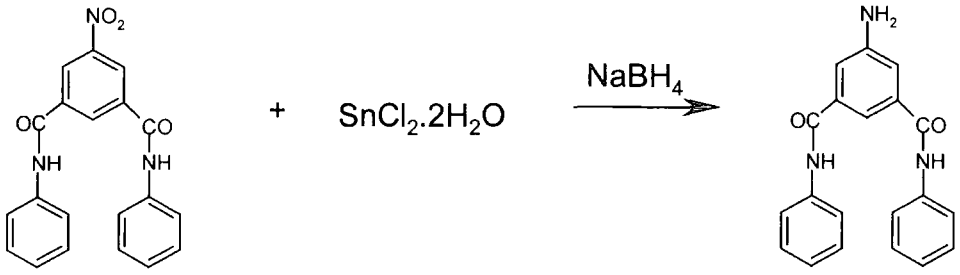

[3]-NO_2 **[3]-NH_2**

[3]-NH_2 was prepared following the published route.[10] A 2 L 3 neck round bottom flask fitted with a reflux condenser was charged with **[3]-NO_2** (52.9 g, 0.15 mol), tin chloride dihydrate (167.7 g, 0.74 mol) and ethanol (1 L). The suspension formed was heated to reflux with stirring. A suspension of sodium borohydride (3.18 g, 0.084 mol) in ethanol (300 mL) was added dropwise via a pressure equalising dropping funnel over approximately 30 minutes. The mixture was stirred at reflux for a further 5 hours during which time a yellow solution formed. The solution was cooled and ethanolic potassium hydroxide was added to the solution until the mixture became alkaline. A fine white precipitate of tin salts were formed which was removed by filtration and the ethanol was removed *in vacuo*. The resultant solid was dissolved in DMF and the precipitates that formed were removed by filtration. Evaporation of the solvent produced a dark orange solid (13.74 g, 28%), which was identified as **[3]-NH_2**. Found C, 72.20; H, 5.34; N, 12.10%. $C_{20}H_{17}N_3O_2$ requires C, 72.49; H, 5.17; N, 12.68%. The spectroscopic parameters were in full agreement with the literature values.[10] ^{13}C NMR (50 MHz, d-DMSO) δ 165.97, 148.95, 139.25, 136.17, 128.62, 123.60, 120.28, 115.71, 113.93. ^{1}H NMR (300 MHz, d-DMSO) δ 10.24 (s, 2H), 7.78 (d, J=7.7Hz, 4H), 7.61 (s, 1H), 7.35 (t, J=7.7Hz, 4H), 7.26 (s, 2H), 7.09 (t, J=7.7Hz, 2H), 5.61 (s, 2H). GPC; M_n = 220 PDI 1.05.

5.6.4 Synthesis of [7]-NO_2

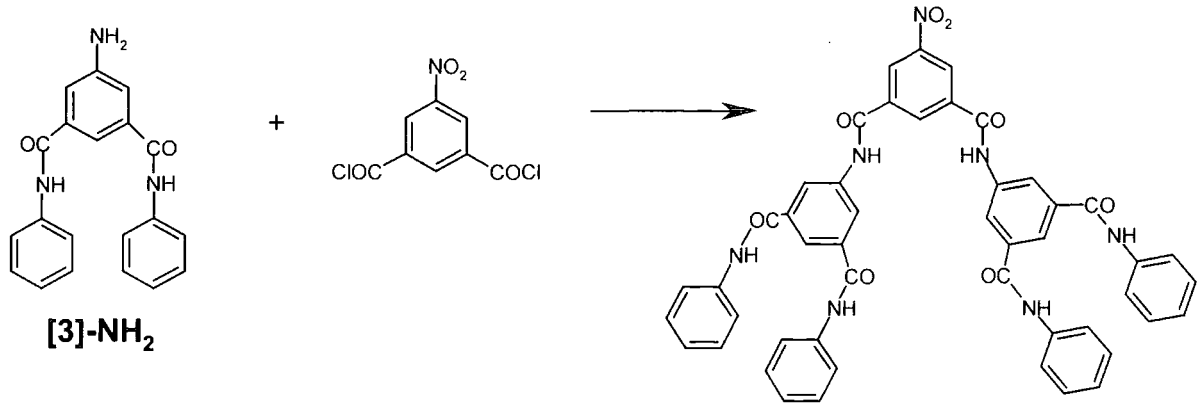

[3]-NH_2 **[7]-NO_2**

[7]-NO_2 was prepared following the published route.[10] A 250 mL 2-neck round bottom flask fitted with a condenser was charged with **[3]-NH_2** (13.28 g, 40.08 mmol) and freshly dried pyridine (100 mL) and stirred to give a brown solution, which was cooled to 5°C. 5-Nitroisophthaloyl dichloride (4.73 g, 19.08 mmol) was added in three portions over 15 minutes. The mixture was stirred with cooling for 2 hours, warmed to room temperature and stirred for a further two hours, and then slowly heated to reflux for 6 hours. The mixture was cooled, and a small amount of pyridinium hydrochloride was removed by filtration. The pyridine was removed *in vacuo* and the resultant syrup was precipitated into water to yield a light brown solid, which was dried. Impurities were then dissolved in methanol, leaving pure **[7]-NO_2**, which was recovered by filtration. This process was repeated several times to yield **[7]-NO_2** as a dark brown solid (3.43 g, 21.5%). Found C, 66.60; H, 4.40; N, 10.75%. $C_{48}H_{35}N_7O_8$ requires C, 68.81; H, 11.70; N, 4.21%, the low carbon analysis result was attributed to the hydroscopic nature of the compound, which was very difficult to dry. The spectroscopic parameters were in full agreement with the literature values.[10] ^{13}C NMR (125 MHz, d-DMSO) δ 165.02, 163.08, 148.05, 139.10, 139.03, 136.13, 135.95, 133.42, 128.75, 125.46, 123.92, 122.78, 122.26, 120.38. ^1H NMR (400 MHz, d-DMSO) δ 11.17 (s, 2H), 10.52 (s, 4H), 9.15 (s, 1H), 9.13 (s, 2H), 8.61 (s, 4H), 8.37 (s, 2H), 7.82 (d, J=7.8Hz, 8H), 7.39 (t, J=7.8Hz, 8H), 7.14 (t, J=7.8Hz, 4H). *m/z* (ES MS) 835.7 [M^+]. GPC; M_n = 720 PDI 1.06.

5.6.5 Synthesis of [7]-NH_2

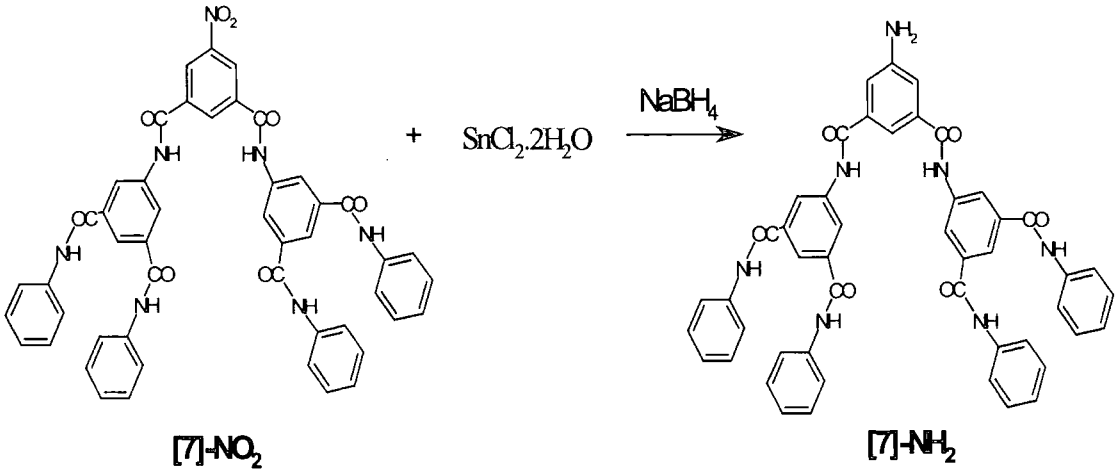

[7]-NH_2 was prepared following the published route.[10] A 1 L 3-neck round bottom flask fitted with a condenser was charged with **[7]-NO_2** (3.43 g, 4.09 mmol), tin chloride dihydrate (4.67 g, 20.72 mmol) and ethanol (400 mL). The suspension that formed was heated to reflux with stirring. A suspension of sodium borohydride (0.07 g, 1.88 mmol) in ethanol (20 mL) was added dropwise via a pressure equalising dropping funnel over approximately 5 minutes. The mixture was refluxed for a further 5 hours. The mixture was cooled and the precipitate that formed was recovered by filtration and dried. The solid was added to a dilute sodium hydroxide solution to obtain **[7]-NH_2** (2.62 g, 79%). Found C, 67.4; H, 4.67; N, 10.63%. $C_{48}H_{37}N_7O_6$ requires C, 71.36; H, 4.62; N, 12.14%, the low carbon and nitrogen analyses results were attributed to the hygroscopic nature of the compound, which was very difficult to dry. The spectroscopic parameters were in full agreement with the literature values.[10]. ^{13}C NMR (125 MHz, d-DMSO) δ 166.18, 165.20, 149.17, 139.67, 139.07, 135.87, 135.68, 128.74, 123.86, 122.48, 121.62, 120.35, 116.01, 114.03. ^1H NMR (500 MHz, d-DMSO) δ 10.69 (s, 2H), 10.49 (s, 4H), 8.57 (s, 4H), 8.27 (s, 2H), 7.81 (d, J=7.5Hz, 8H), 7.38 (t, J=7.5Hz, 8H), 7.13 (t, J=7.5Hz, 4H), 5.71 (2H). *m/z* (ES MS) 807.2 $[M+H]^+$. GPC; M_w = 730 PDI 1.05.

5.6.6 Attempted synthesis of DMPAP1D

Note: For the key to the name code of the polyamide dendronised monomer, see chapter 2, section 2.5.1 and the bookmark card.

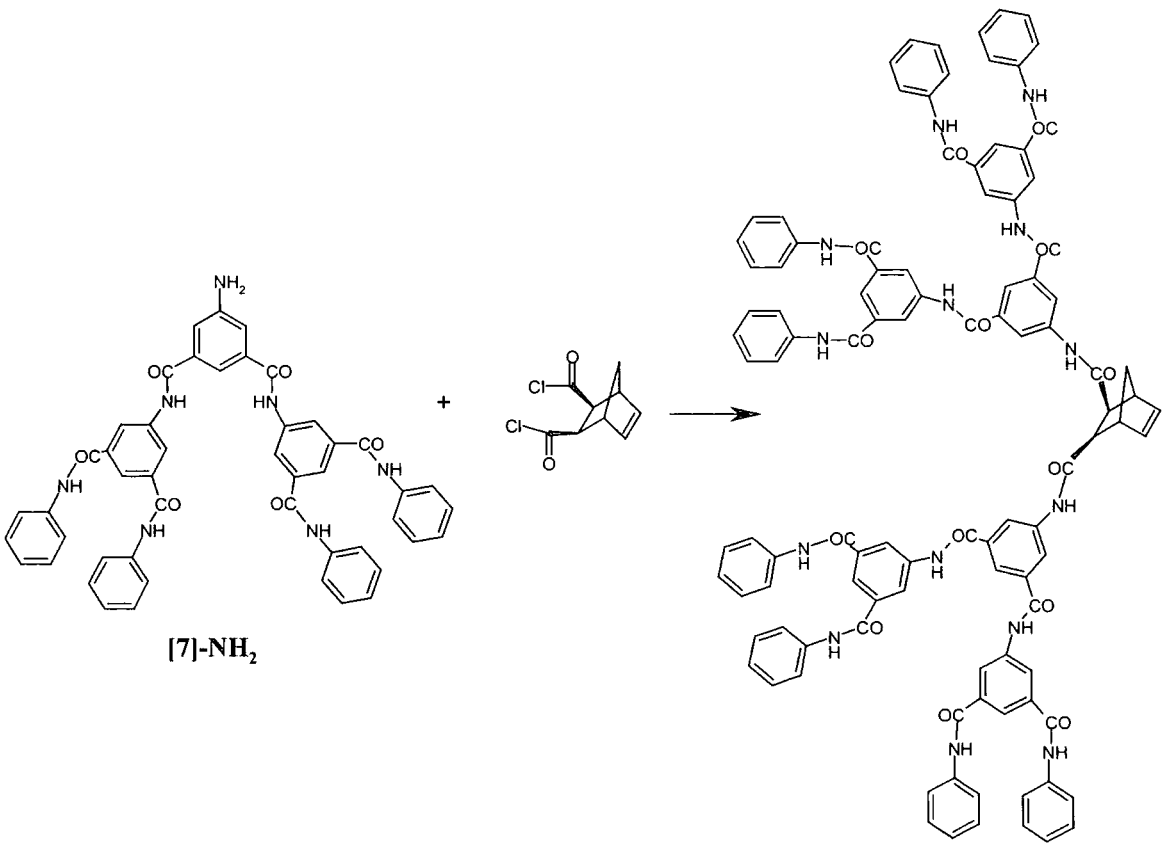

[7]-NH_2

DMPAP1D

[7]-NH_2 (1.93 g, 2.39 mmol) was added to a stirred solution of norbornene-5-*exo*, 6-*exo*-dicarbonyl chloride (0.26 g, 1.19 mmol) in tetrahydrofuran (50 mL). Pyridine (0.2 g, 2.39 mmol) was added and the mixture was stirred at 60°C for 2 days. Analysis of the ^{1}H NMR spectrum showed that there was still a small amount of **[7]-NH_2** remaining. The crude reaction mixture was washed with 10% HCl solution several times and subsequently dried. The remaining material was purified by successive flash chromatography columns, eluting with tetrahydrofuran/hexane at a 2:1 ratio, producing mainly an intramolecular condensation product (0.19 g, 9%), rather than the anticipated product (see chapter 2, section 5.7). Found C, 67.92; H, 5.44; N, 8.95%. Calculated for $C_{57}H_{43}N_7O_8$ C, 71.76; H, 4.54; N, 10.28%, the low carbon and nitrogen analyses results were attributed to the hygroscopic nature of the compound, which was very difficult to dry. The ^{1}H NMR spectroscopic parameters, coupled with 2D COSY, were in agreement with the formation of the intramolecular

condensation product, see diagram below. ^{1}H NMR (400 MHz, DMSO) δ 10.92 (s, 2H), 10.47 (s, 4H), 8.79 (s, 1H), 8.55 (s, 4H), 8.3 (s, 2H), 8.16 (s, 2H), 7.8 (d, J=7.2Hz, 8H), 7.37 (t, J=7.6Hz, 8H), 7.11 (t, J=7.6Hz, 4H), 6.39 (t, J=1.8Hz, 2H), 3.30 (s, 2H), 2.95 (s, 2H), 1.55 (s, 2H). *m/z* (MALDI TOF (Kratos) MS 977.25 $[M+Na]^+$, 993.21 $[M+K]^+$ corresponding to the intramolecular product below.

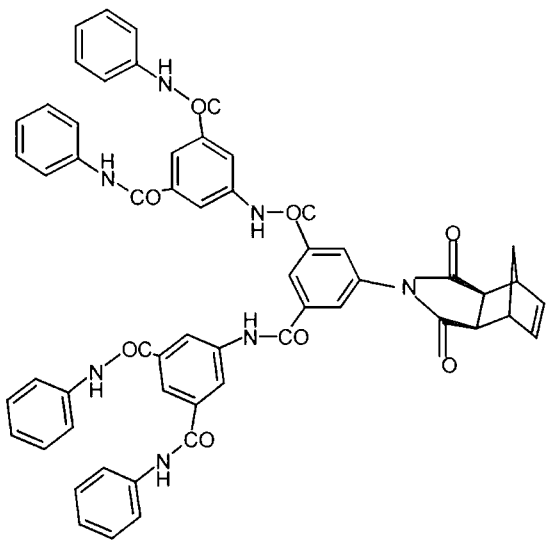

Intramolecular condensation product formed in the attempted synthesis of **DMPAP1D**

5.7 Synthesis of Ruthenium Benzylidene Initiator

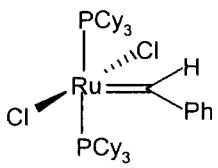

Ruthenium benzylidene initiator

Ruthenium benzylidene initiator was prepared following the published route.[12] Benzaldehyde tosylhydrazone (10 g, 0.012 mol) and benzyltriethylammonium chloride (1.5 g, 6.6 mmol) were added to a 1 L flask containing hexane (75 mL), toluene (15 mL), a stirrer bar and a reflux condenser. An aqueous 15-weight % NaOH solution (300 mL) was added to the mixture, which was heated at 70°C for 2 hours. After this time, the aqueous phase was clear and colourless and the organic phase was dark red. The mixture was then poured into a 1 L separating funnel, half filled with ice, and shaken until all of the ice had melted. The aqueous phase was

discarded and the ice-water wash was repeated. The organic phase was then dried over sodium sulphate and degassed with nitrogen. The resultant phenyldiazomethane solution was stored overnight at –50°C.

Dichloromethane (500 mL) was added to a 1 L 3-neck flask equipped with a stirrer bar and inlet adapter for nitrogen. $(PPh_3)_3$ $RuCl_2$ (14 g) was added under nitrogen. The brown solid was dissolved with stirring and the solution was cooled to –50°C. The cooled (0°C) phenyldiazomethane solution was then added via polyethylene cannula to the solution of $(PPh_3)_3RuCl_2$ over a period of 10 to 15 minutes. Once the addition was complete, the solution was warmed to –20°C and tricyclohexylphosphine was added via solid addition funnel over 5 to 10 minutes. The mixture was warmed to room temperature. Most of the solvent was then removed under vacuum to leave a thick dark slurry. To this mixture, degassed methanol was added (the flask was filled) to precipitate the catalyst. The solids were recovered by filtration on a medium fritted funnel in air and washed with methanol (3 x 300 mL) followed by acetone (3 x 200 mL). The solid residue was dried under vacuum. The final solid was purple in colour and was relatively pure >90%. The catalyst was further purified by dissolution in degassed methylene chloride followed by filtration through celite. Most of the solvent was removed under vacuum and the catalyst was precipitated by addition of methanol. The precipitated catalyst was isolated by filtration in air and washed with methanol. ^{1}H NMR (400 MHz, CD_2Cl_2) δ 20.02 (s, Ru=CH), 8.44 (d, o-H of C_6H_5), 7.59 (t, p-H of C_6H_5), 7.37 (t, m-H of C_6H_5), 2.62-2.58, 1.77-1.67, 1.46-1.39, 1.25-1.16 (all m, $P(C_6H_{11})_3$). ^{13}C NMR (125 MHz, CD_2Cl_2) δ 294.03, 153.02, 131.14, 129.49, 129.27, 32.41, 29.98, 28.21, 26.89.

5.8 A Typical NMR Scale Polymerisation

Ruthenium benzylidene initiator (10 mg, 0.012 mmol) and **DMPCB1M** (0.312 g, 50 molar equivalents) were dissolved in d-chloroform (500 µl and 300 µl, respectively) in separate sample vials in the Glove Box. The dendronised monomer solution was then transferred drop-wise to the initiator solution and the mixture was stirred for 5 minutes. The solution was transferred into a screw cap NMR tube, taken out of the Glove Box and analysed by ^{1}H NMR spectroscopy. After analysis, the polymerisation mixture was reacted with ether vinyl ether to terminate the

polymerisation and left to stand for 5 minutes with periodic shaking. The polymerisation mixture was then added drop wise to methanol (10 fold excess) to precipitate the polymer. A cycle of decanting and washing with methanol was repeated several times and the polymer was finally recovered by filtration or using a centrifuge prior to drying in a vacuum oven at 30°C overnight.

5.9 Preparative Scale Polymerisation

Ruthenium benzylidene initiator (32.05 mg, 0.039 mmol) was dissolved in dichloromethane (2 mL) in a sample vial and placed in a 50 mL single neck round bottom flask. **DMPCB1M** (1 g, 50 molar equivalents) was dissolved in dichloromethane (3 mL) and added to the initiator solution in three equal portions at 5-10 minute intervals under vigorous stirring. After the addition was complete, the mixture was stirred overnight. The reaction was terminated by adding an excess of ethyl vinyl ether. The mixture was precipitated by pouring into methanol (10 fold excess). The methanol was then decanted; the precipitate was washed with excess methanol, and dried in a vacuum oven at 30°C. Finally, the polymer was reprecipitated from dichloromethane into methanol and dried in a vacuum oven at 30°C for 3 days to give polymer as a brown glass-like gel.

5.10 References

1. Diels, Alder, *Justus Liebigs Ann. Chem.* **1928**, *460*, 117.

2. Viera, M. P. New Water-Soluble Polymers for Surface Applications *Ph.D. Thesis, University of Durham*, **2000**.

3. Boehme, W. R.; Schipper, E.; Scharpf, W. G.; Nichols, J. *J. Am. Chem. Soc.* **1958**, *80*, 5488.

4. Rondestvedt, C. S. Jr.; Ver Nooy, C. D. *J. Am. Chem. Soc.* **1955**, *77*, 4878.

5. Berson, J. A.; Remanick, A.; Suzuki, S.; Reynolds-Warnhoff, P.; Willner, D. *J. Am. Chem. Soc.* **1961**, *83*, 3986.

6. Megson, J. L. The Synthesis and Characterisation of Water Soluble Polymers and Biomimetic Applications *Ph.D. Thesis, University of Durham*, **2001**.

7. Canonne, P.; Belanger, D.; Lemay, G. *J. Org. Chem.* **1982**, *47*, 3953.

8. Rizmi, M. Synthesis, Characterisation and Properties of Some Well-Defined Comb Graft Co-Polymers *Ph.D. Thesis, University of Durham*, **1997**.

9. Stoddart, A. Synthesis, Characterisation and Properties of Novel Dendrimers *Ph.D. Thesis, University of Durham*, **2002**.

10. Parker, D. Some Approaches to the Synthesis of Dendritic Polyamides *M.Sc. Thesis, University of Durham*, **1991**.

11. Mensour, E. S. M. E.; Kandid, S. H.; Soliman, M. E. M.; Ibrahim, M. *Polym. Int.*, **1992**, *29*, 61.

12. Schwab, P.; Grubbs R. H.; Ziller, J. W. *J. Am. Chem. Soc.* **1996**, *118*, 100.

Chapter 6

Conclusions and Future Work

6.1 Conclusions

A series of dendronised monomers of different generations possessing different chemical structures has been synthesised using the selectivity of the coupling agent 1,1'-carbonyl diimidazole (CDI). In particular, mono- and di-substituted first generation polycarbonate dendronised monomers have been synthesised and fully characterised, along with a di-substituted second generation polycarbonate dendronised monomer. Two di-substituted second generation polyurethane dendronised monomers containing t-butyl and 4-heptyl terminal groups were also successfully synthesised. However, the synthesis of a first generation polyamide dendronised monomer containing phenyl terminal groups was unsuccessful, due to the formation of a stable five membered cyclic diimide intramolecular condensation product.

The NMR scale ROMP reactions of the mono- and di-substituted first generation polycarbonate dendronised monomers along with the di-substituted second generation polycarbonate dendronised monomer, using varying ratios of monomer to initiator, have been performed successfully. It was found that the polymerisations were well-defined and that di-block copolymer products could be obtained due to the living nature of the systems. The attempted ROMP of the polyurethane di-substituted second generation dendronised monomers containing two different terminal groups was unsuccessful, for reasons that are unknown to the author.

Molecular modelling studies have been performed using the CAChe program. In particular, modelling was carried out on the di-substituted second generation polycarbonate dendronised monomer, **DMPCB2D**, and on poly(**DMPCB2D**) up to a degree of polymerisation of 16. It was found that low DP oligomers of **DMPCB2D** had an approximately spherical shape, which tended towards cylindrical as the DP increased. The polymer at a DP of 16 had dimensions of approximately 10 nm by 4 nm. AFM images of poly(**DMPCB2D**) produced in a reaction using a 20:1 monomer: initiator ratio were obtained using a scanning probe microscope MultiMode™ Nanoscope IV. The spin-coating technique and highly ordered pyrolytic graphite as

the substrate were required to obtain images. The structures were found to be pancake shaped with dimensions between 30-50 nm diameter and 3-6 nm thickness. The difference in the shape and size of the structures calculated by the modelling predictions on isolated molecules and that found experimentally by AFM probably arises from the addition of solvent to the sample, which results in the polymer backbone adopting a random coil configuration as compared to the tightly packed structure predicted by modelling and the presence of structure/substrate interactions that could have an effect on the overall configuration of the structure at the HOPG surface.

6.2 Future Work

It is thought that the addition of dichloromethane, which is a relatively good solvent for these systems, resulted in the dendronised polymer adopting a random coil configuration rather than the tightly packed cylindrical shape that the modelling predicted. It may therefore be interesting to vary the type of solvent added to the polymer previous to AFM imaging, in order to see the effects that the solvent has on the overall shape of the polymer. In particular, the addition of a relatively poor solvent to the polymer may result in the polymer retaining more of its tightly packed structure when viewed by AFM. It would then be interesting to compare the dimensions of the polymer when it is in a random-coil configuration as opposed to when the dendrons are tightly packed together resulting in an approximate cylindrical polymer shape.

It may also be interesting to chemically alter the dendron units along the polymer backbone. By attaching long alkyl chains throughout the periphery of the dendrons, it may be possible to obtain a better interaction between the sample and the AFM substrate, which may enhance the resolution of the images.

More detailed computer modelling studies could also be performed on these systems in order to take into consideration the effects of both structure/solvent and structure/sample interactions, which would lead to a better understanding of the influence such interactions have on the overall polymer shape.

Appendix

Contents

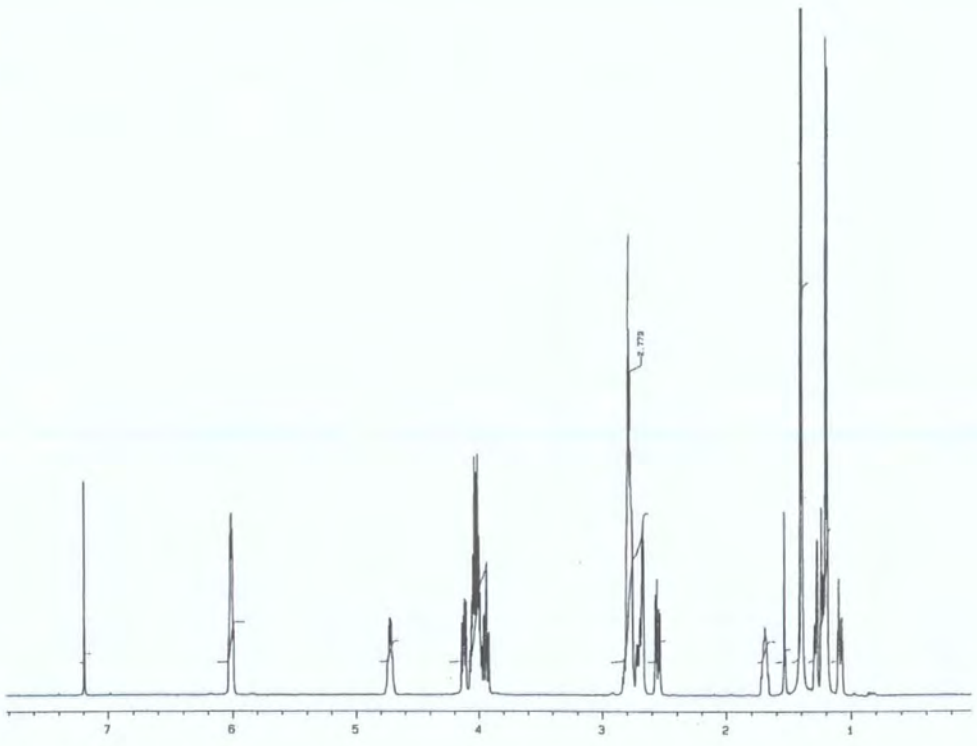

Appendix 1 ^{1}H NMR spectrum of **DMPCB1M**

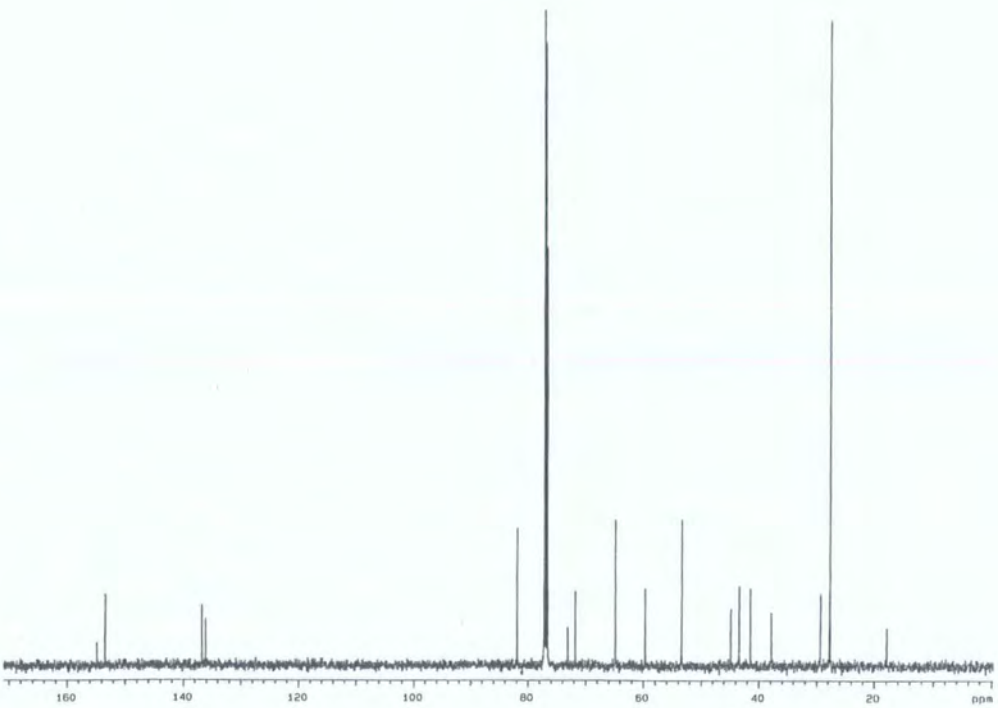

Appendix 2 ^{13}C NMR spectrum of **DMPCB1M**

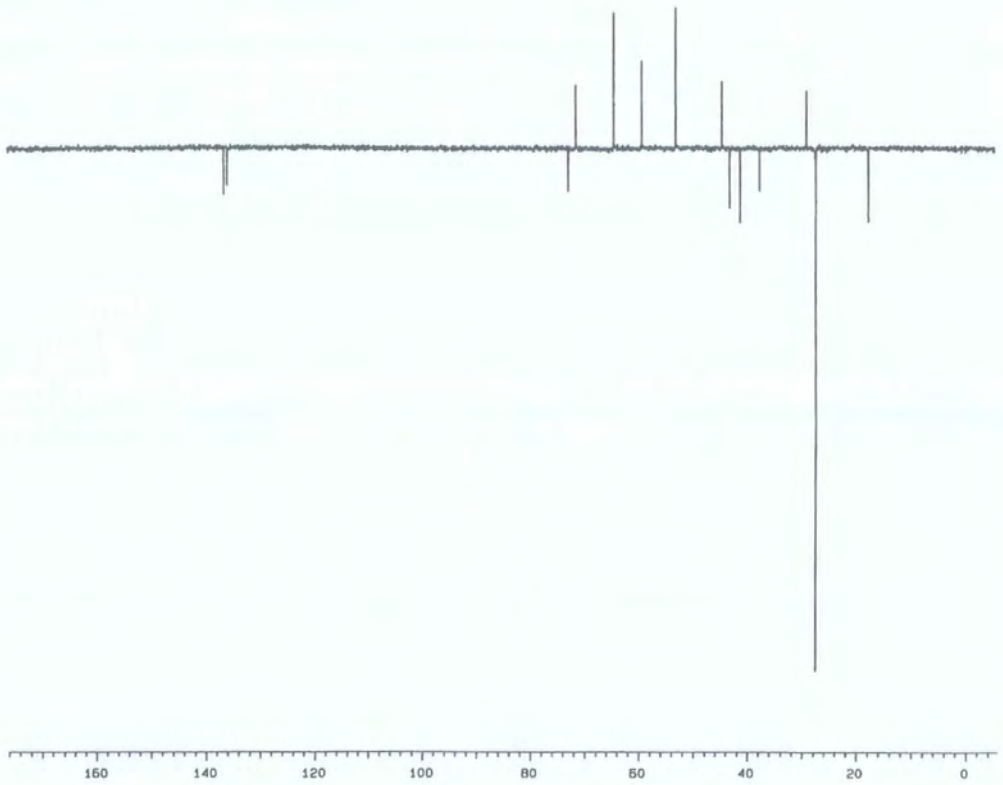

Appendix 3 2D COSY spectrum of **DMPCB1M**

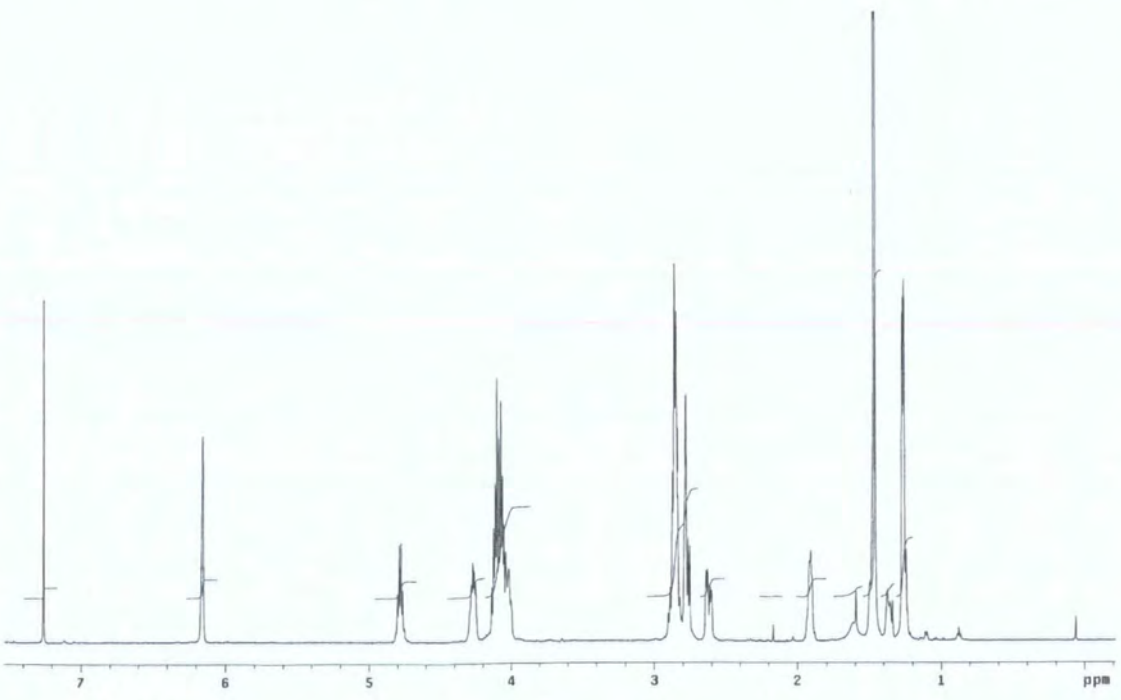

Appendix 4 ^{1}H NMR spectrum of **DMPCB1D**

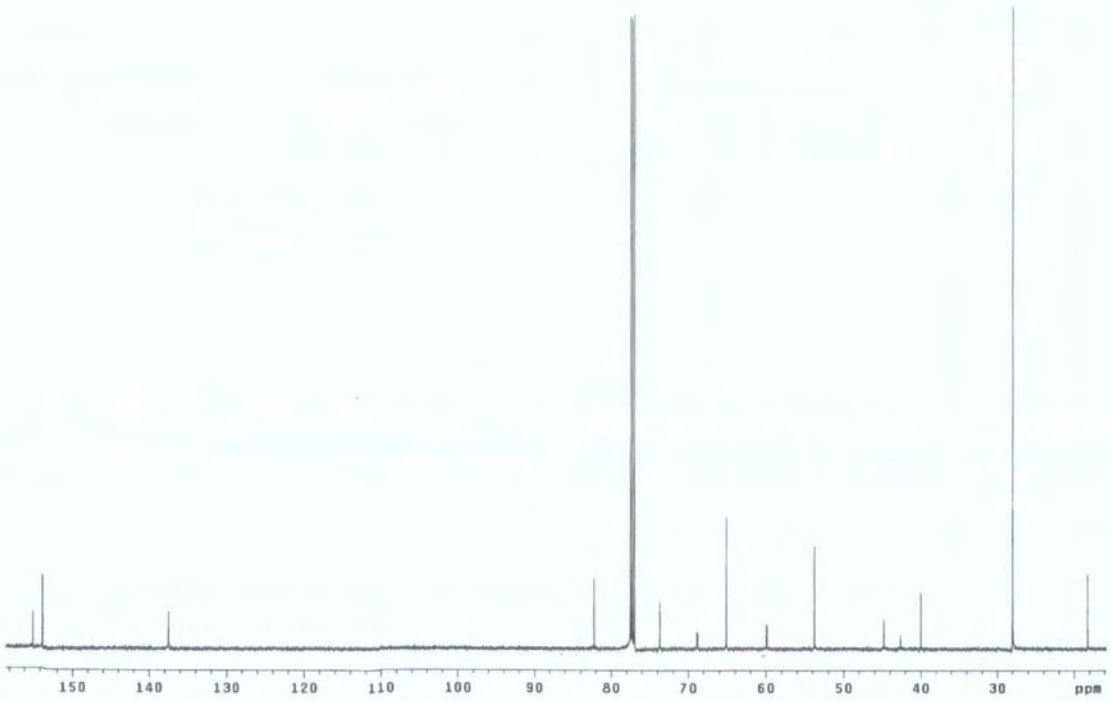

Appendix 5 ^{13}C NMR spectrum of **DMPCB1D**

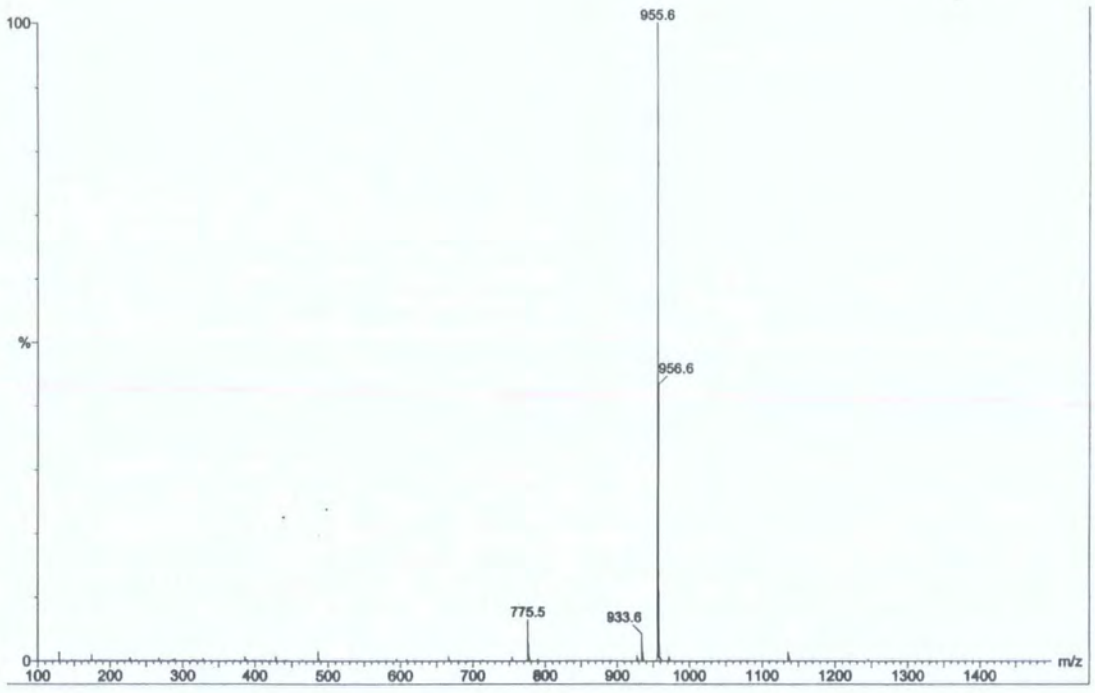

Appendix 6 ES Mass spectrum of **DMPCB1D**